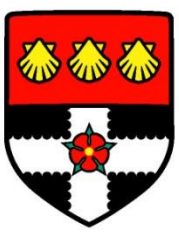

University of Reading

# Spectroscopic Analysis of Roads at Traffic Speed

PhD Chemistry

Department of Chemistry

A thesis submitted in part fulfilment of the degree of Doctor of Philosophy

Hannah Bowden

Supervised by Professors Matthew Almond and Wayne Hayes

February 2019

## Declaration

I confirm that the research presented in this report is my own work and that the use of all materials from other sources has been properly and fully acknowledged.

Hannah Bowden

## Acknowledgements

I would like to thank a number of people for their help and support throughout these three years. Firstly I need to extend a very big thank you to my supervisor Matthew Almond. He has supported me throughout my seven total years at the University of Reading, and every one of my successes I owe to him. Thank you also to Professor Wayne Hayes, Stuart McRobbie and Helen Viner for project supervision and technical advice throughout this project. Thank you to Donald Burton at Highways England for project management and development.

I would also like to thank John Prime and Damien Bateman for advice throughout this work. Thank you also to Phil Parker, James Nichols, Ali Palmer and everyone at the Surrey County Council Highways Lab for lots of help and guidance with the mechanical testing and for accommodating and teaching me the techniques. For help with scanning electron microscopy and asphalt sample cutting thank you to Amanpreet and John Jack.

I need to extend a massive thank you to Tahkur Sing Babra and Oli Balmford for their technical support and expertise. This work would have looked a lot different without their motivating and inspiring presence in the lab and the office.

I dedicate this thesis to Jessi Godleman, the Patsy to my Eddie, it would not exist without her and I am incredibly proud of how she has continued to dedicate herself to her work regardless of life's obstacles. Thank you for the cocktails and shopping in first year, the coffee breaks in second year, and the dinner dates in third year!

Thank you to Sam Burholt and Iain Hopkins for many years of friendship throughout our long time in Reading.

Everyone in the G06/07 office has made the past year so much fun, it has been wonderful working with everyone in there and all the staff in the department throughout my time at the University.

I have been incredibly lucky to have the love and support of my husband Lewis throughout this part of my career. Thank you to him for consistently keeping me sane and grounded.

# Abstract

Currently in the UK road surfaces are monitored visually for defects and signs of failure. However the time between detection of road degradation (e.g cracks and potholes), and complete failure of the road surface is very short. Therefore rejuvenation techniques that may initially be favourable are ineffective and a total resurfacing is the required. It is therefore of interest to be able to predict the condition of the road surface in an attempt to better plan and schedule the rejuvenation techniques and effectively save money, and maintain safer, more comfortable roads.

Road surfaces can fail in many different ways as a result of many different factors. The chemical oxidation of bitumen, the main binding component of asphalt road surfaces, is a major contributor to the age hardening and ultimate failure of the roads.

There is an abundance of research in the literature that has identified the use of infrared spectroscopy as an analytical technique to monitor the oxidation of bitumen and therefore this research looks to explore the feasibility of utilising this technique as a detection method for the oxidation of bitumen within asphalt road surfaces. Diffuse reflectance infrared spectroscopy has been utilised in this project in order to identify any possible oxidation product markers present within the infrared spectra collected.

The project initially involved ageing bitumen artificially and naturally and analysing the changes with Diffuse Reflectance Infrared Fourier Transform (DRIFT) spectroscopy. Once chemical oxidation markers had been identified the project then focused upon the artificial and natural ageing of asphalt. The same chemical markers were identified and quantified with regards to the solar exposure. Mechanical testing of bitumen and asphalt has also been carried out in order to compare the chemical changes to standardised physical property changes that correspond to deterioration of the bitumen.

The project also develops a method for analysis of real road surfaces outside of the laboratory. A trolley has been built in order to support a handheld spectrometer close to the surface for data collection. A number of different roads have been analysed in this way.

This report will outline the results obtained from these experiments and the data analysis. The recommendations and future work are also included within this report.

# Abbreviations

TRL – Transport Research Laboratory

HRA – Hot Rolled Asphalt

SMA – Stone Mastic Asphalt

W/CMA – Warm/Cold Mix Asphalt

SARA – Saturates, Aromatics, Resins and Asphaltene fractions of bitumen

DSR – Dynamic Shear Rheometer

RTFO test - Rolling Thin Film Oven test

RCAT – Rotating Cylinder Ageing Test

PAV – Pressure Ageing Vessel

E-RTFO test- Extended Rolling Thin Film Oven test

Rpm – Revolutions per minute

UV/Vis light – Ultra violet/Visible light

IR – Infrared

ATR – Attenuated Total Reflectance

FTIR – Fourier Transform Infrared

DRIFT Spectroscopy-Diffuse Reflectance Infrared Fourier Transform Spectroscopy

CAF – Chemical Analysis Facility

SEM – Scanning Electron Microscopy

EDX – Electron Dispersive X-Ray

GPC – Gel Permeation Chromatography

THF-Tetrahydrofuran

BHT – Butylate Hydroxytoluene

DCM-Dichloromethane

TGA – Thermogravimetric Analysis

PDA – Personal Digital Assistant

# Contents

# Chapter 1

This introductory chapter has been separated into two parts. The first part of this chapter provides the reader with an overview of the motivations for this research, with part two considering the procedures and equipment used to carry out the research.

## Part 1-General Introduction

### 1.1 Bitumen and road surfaces

Asphalt pavements are constructed by layering different materials in order to reduce the stress created by vehicle loads on the naturally occurring material beneath the road (subgrade). In general, the materials become more complex and expensive the closer to the road surface they are, starting from graded mixes of unbound aggregate immediately above the subgrade to a carefully designed combination of aggregate sizes coated with bituminous binder at the surface. Figure 1.1 is a photograph of a core collected by TRL which clearly shows the different layers of graded aggregates through a cross section of an asphalt surface.

**Figure 1. 1 Photograph of a core collected by the Transport Research Laboratory**

Simplistically, road surfaces are constructed using three basic components. Bitumen, a viscous mixture of hydrocarbons obtained through the fractional distillation of crude oil, is used within road surfaces as a binding agent along with secondary fillers. The filler can be either crushed mineral carbonate sourced from local quarries or fibres. The addition of the filler increases the adhesion between the bitumen and the aggregates by filling in the voids and holes in the aggregate's surface and also helps to bulk out the bitumen.[1] The binder is then mixed with stone aggregates and then it is ready to be laid. The asphalt mixture is compacted into the smooth, flat road surface that is then ready to be driven on.

Bitumen has many different uses and some examples include waterproofing, sound deadening and security 'anti-climb' paint. Bitumen's main use however is as a binder in road surfaces because of its adhesion and cohesion and also its thermoplastic and visco-elastic properties. Its thermoplastic ability allows it to be heated and mixed with the required aggregates and then cooled into the road surface.[2] It has the ability to act as a viscous liquid, giving the pavement flexibility from traffic stresses; however, it is also solid once cooled, giving it the ability to withstand the traffic loading.

Road surface design can be tailored to make it more suitable for the different kinds of traffic and environment it will be exposed to throughout its surface life. For example a road surface being designed for a motorway will experience a very different set of conditions than the surface roads within a town centre. Factors including traffic speed and intensity, tree cover and drainage will vary for each location.

There are a number of different asphalt types that can be applied to different road surfaces. Some examples include Hot Rolled Asphalt (HRA), Stone Mastic Asphalt (SMA), Warm or Cold Mix Asphalt (W/CMA), and Porous Asphalt. HRA is asphalt that is laid at a high temperature (160 ˚C) and aggregate chippings are rolled into the surface to give the road texture. The high binder content and the high application temperature of this mixture allow the chippings to be embedded well into the surface. HRA is commonly applied to roads that are highly trafficked, major highways or airfields for example. SMA on the other hand has a high stone aggregate content and is mixed and laid to produce a surface with more texture depth than a HRA (0-3 mm). Texture depth is used to describe the deviations from the smooth and planar surface of the compacted road surface. The increased texture depth of the SMA allows for efficient water drainage, and skid resistance on the surface. SMA is resistant to deformation and cracking as a result of the stone skeleton being held together with the

bitumen binder and is therefore suitable for a wider range of highway applications, especially high stress areas such as roundabouts. WMA and CMA have been designed to use emulsifiers and surfactants, as opposed to high temperature, to decrease the viscosity of the bitumen used throughout the asphalt construction. The reduction in temperature means that there is a reduction in fossil fuel consumption and an increase in safety for the construction workers with fewer hazardous emissions from the hot bitumen. Porous asphalt is asphalt that has been designed with a high content of interlocking voids within the structure. This allows large amounts of water to be drained from the surface and is commonly used in car parks and in locations where storm water or high rainfall and poor drainage are issues. The type of bitumen, filler, size of aggregate, void and binder content can all be varied to produce the optimum road surface for the traffic requirements.

Chemically, bitumen is a complex mixture of large hydrocarbons of varying molecular weight, both long chain and aromatic, within which are a number of heteroatoms including oxygen, nitrogen, sulfur and trace amounts of some metals such as vanadium and nickel (7-1590 ppm and 10-139 ppm respectively). [3,4] The exact chemical composition of bitumen is very difficult to determine as a result of the complex and variable structures of the hydrocarbons which can vary between crude oil sources and fracking procedures within refineries.[5] Studies have been conducted to investigate the separation of bitumen molecules into groups dependent upon a specific separation parameter, molecular size or polarity for example. Commonly the bituminous hydrocarbons are separated into general fractions which are commonly termed Saturates, Aromatics, Resins and Asphaltenes which are typically referred to as SARA fractions, see Figure 1.2.[6] The saturated component is made up of non-polar hydrocarbons with saturated carbon atoms such as *n*-alkanes and cycloalkanes. The aromatic component is composed of benzene ring-containing structures and derivatives. The resin fraction consists of components with highly polar end groups and long alkane tails. These end groups are commonly aromatic and naphthenic rings, often containing heteroatoms such as sulfur, oxygen and nitrogen. The resin, aromatic and saturated fractions are commonly referred to as the 'Maltenes'.[7] Finally, asphaltenes which are *n*-heptane insoluble,[8] can be described as large, highly polar molecules made from condensed aromatic and naphthenic rings which also can contain heteroatoms.[9] When separated into these fractions the Saturates fraction is a yellow oil, the Aromatic fraction is a viscous liquid, the Resins are a highly viscous, brown semi-solid and the Asphaltene component is a dark-brown/black solid.[10]

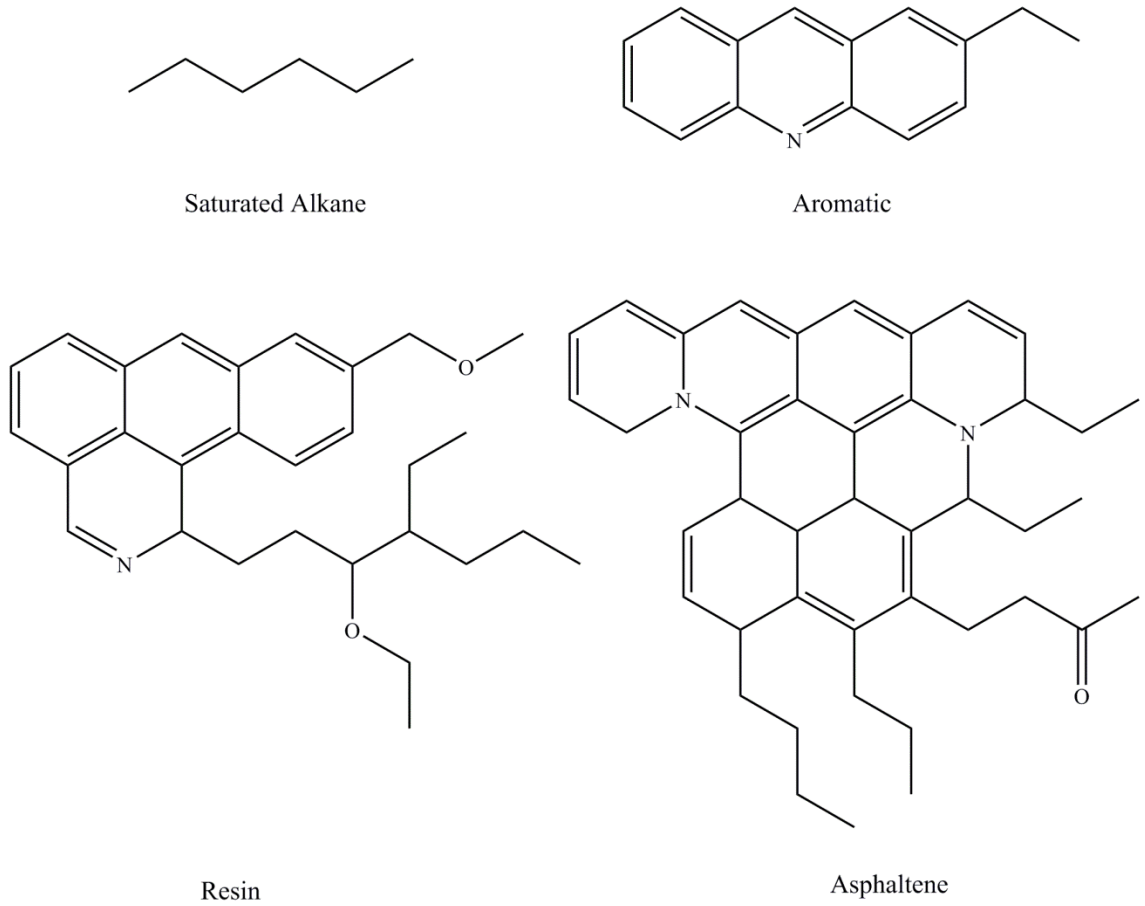


**Figure 1. 2 Example chemical structures of the four different fractions possible in the composition of bitumen[6]**

The highly aromatic nature of the asphaltenes gives them an almost planar molecular structure. As a result of the high electron density of these compounds they are able to exhibit some π-π stacking within the bitumen composition. The formation of the 'graphite' like stacks of asphaltene molecules can develop into micelle-like structures. These micelles are said to be dispersed into the oily maltene component. The polarity of the asphaltene micelles is stabilised by the resins in this oily medium. This describes the 'Yen model of asphaltene microstructure'[11] and can be used to describe the differences in viscosity of bitumen. When the asphaltene micelles are well dispersed, the viscosity is low; however, when the asphaltenes align even further and there is interaction between micelles, or when the asphaltenes become more condensed as a result of higher temperatures during distillation of the bitumen, there is an increase in bitumen viscosity.[7,12]

It is questionable whether the separation of fractions into groups is a reliable method for analysing the chemical composition of bitumen as the separation suggests that there are defined groups into which the molecules fit. Redelius *et al.*[3] suggested that there is a continuum of molecular sizes and polarities as opposed to defined cut off points for the

named groups. The variation of the time and temperatures used throughout the refining process of fractional distillation gives every bitumen source a unique chemical composition. The presence of the heteroatoms such as oxygen, sulfur, vanadium and nickel also vary greatly between crude oil sources around the world allowing for different properties of the bitumen.[13] The chemical composition of the bitumen can greatly affect the properties of the bitumen, including the elasticity, viscosity and durability therefore it is important to ensure that bitumen with the appropriate properties is selected for the road type being designed.

The design of the road surface must be optimised to find a balance between initial road costs and length of expected service life. The longer the road surface is in service before any rejuvenation or resurfacing is required, the better value for money the road becomes. Asphalt road surfaces are known to fail in a number of different ways making them unsafe and uncomfortable for road users. Pavement design, extensive bitumen and asphalt analysis and predictive ageing are all essential in order to prevent or reduce the effects of the asphalt road failure.

### *1.1.1 Road surface failure*

There are many different factors that contribute to the degradation of a pavement making the pavement performance very difficult to predict. Factors such as the weather, the bitumen adhesion and cohesion, temperature fluctuations, pavement design, construction and compaction processes, and traffic loading and intensity,[14] all vary greatly between each road that is constructed.

As bitumen ages it loses its elastic properties and becomes more brittle. This reduces the road's ability to withstand the traffic-induced stresses and strains and leads to localised failures in the pavement structure. These failures include fretting, rutting, cracking (fatigue and low temperature), and permanent deformation.

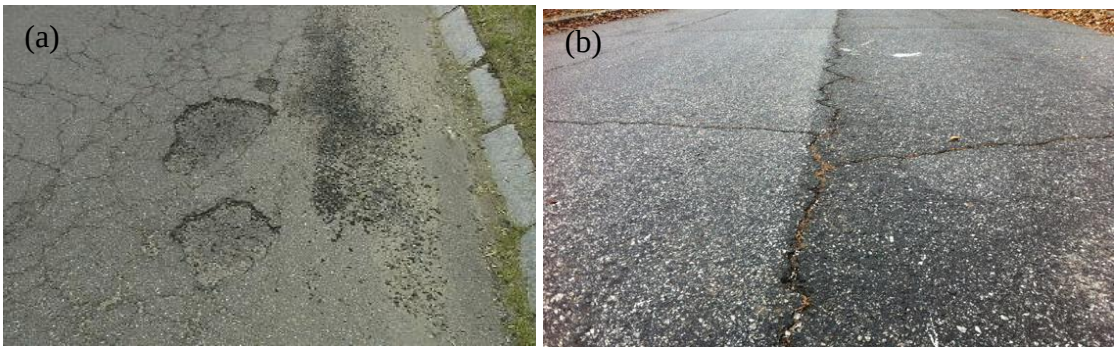


**Figure 1. 3 Photographs of examples of (a) fretting and (b) transverse and longitudinal cracking within a road surface**

Fretting, or ravelling, is the progressive loss of surface aggregates from the road, and occurs when there is low cohesion within the bitumen and/or poor adhesion between the bitumen and the aggregate.[2] The mechanical agitation of trafficking can lead to the removal of these poorly-bound aggregates from the surface. Fretting is commonly identified in areas of slow moving traffic, or where traffic is changing direction such as junctions for example. The physical effect of tyre movement in these areas is greater therefore the aggregates are agitated and eventually pulled from the surface. This creates a point of weakness as a result of the loss of aggregates and a pothole is rapidly formed as aggregates are continued to be lost from the surface. Fretting can be caused by a number of different factors: poor compactions during construction, high surface temperatures, slow traffic speed, water ingress or brittle bitumen binder.[14]

Pavement failure due to cracking has two different mechanisms: fatigue and thermal cracking. Fatigue cracking occurs when the surface is exposed to repeatedly high tensile stress and strain at low temperatures. At low temperatures the bitumen is more brittle and therefore less flexible to the repeated loading of trafficking. Thermal cracking occurs when the fluctuations in temperature and humidity are extreme and the binder cannot elastically adapt to the sudden drops in temperature. This is very common in the winter months when the temperatures fluctuate throughout the day and can reach below 0 ˚C. Cracking in the road surface is also encouraged by the embrittlement of the bitumen concrete due to ageing.[15]

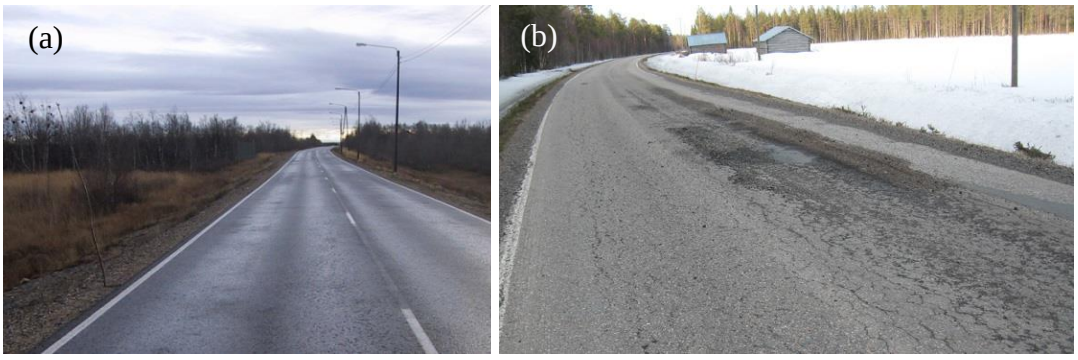


**Figure 1. 4 Photographs of examples of rutting in the wheel path of road surfaces. (a) Shows surface rutting and (b) shows fatigue cracking within a rut. [16]**

Rutting can be described as the formation of surface depressions in the wheel path of the road. Rutting can have two main causes; surface rutting and subgrade rutting. Surface rutting occurs as a result of the surface material failure or mixture and compaction problems throughout construction, and involves the shearing or uplift of the road surface alongside the wheel path. Surface ruts can also be developed when the environmental temperature is high, the bitumen

is less viscous and therefore the asphalt can deform under the weight of heavy vehicles.[2] Subgrade rutting, however, is caused by structural factors within the lower layers that compress the subgrade and as traffic loads pass, the surface layers depress into the road. Rutting is a problem as the depressions in the road surface collect water which presents a safety issue for road users.[17] Subgrade rutting can also lead to fatigue cracking in the ruts, see photograph in Figure 1.4 (b) as the asphalt moves under the poor support from the subgrade.

Many of these failures are exacerbated by physical and environmental factors; however, the condition of the bitumen also has a big effect on the asphalt. The mechanical properties of the bitumen are tested prior to road surface construction and are also monitored throughout the service life of the road in order to appropriately maintain the surface.

### *1.1.2 Mechanical property testing*

As previously mentioned the chemical composition of the bitumen can greatly affect the physical performance of the bitumen. As each bitumen source and refinery process is slightly different all bitumen that is produced from the oil refineries is mechanically tested in order to determine the physical properties it exhibits. This is carried out using standardised tests that are widely used to determine the quality of bitumen. Bitumen is commonly classified in Penetration grades. This is done by analysing the bitumen with the penetration point test, and the upper and lower limit result of this test become the penetration grade of the bitumen. For example a soft bitumen would be labelled a 100/150 penetration grade bitumen with a very high penetration value, whereas a harder bitumen, 40/60, has much lower penetration grade limits.

The penetration point test is a measure of the consistency, hardness and stiffness of the bitumen at ambient temperatures.[18] The specification for the penetration point test can be found in the British Standard EN 1426:2015.[19] It is described as a method for measuring the distance, in tenths of a millimetre ($1/10^{th}$ mm) that a standardised needle with a 100 g loading weight attached, penetrates vertically through a sample of bitumen being held at 25 ˚C in 5 seconds. Figure 1.5 contains a diagrammatic representation of this test. Experimentally it has been found that the distance that the needle travels through the bitumen, defined as the penetration, decreases as the bitumen ages.[20,21] A low penetration point indicates a harder bitumen, and a high penetration point is indicative of a soft bitumen. The penetration grade of the bitumen is used when designing a road surface. For example bitumen with a high penetration point, softer bitumen, will be utilised in a road surface in a colder climate and a

hard bitumen with a low penetration point would be better suited in a hotter climate.[18] A low penetration grade bitumen is also suitable in asphalt roads that are to experience sever trafficking; a hard bitumen in these areas allows a better resistance to deformation from high traffic loads. Softer bitumen is then utilised in minor roads that experience light traffic and are then flexible to the sporadic trafficking.[7]

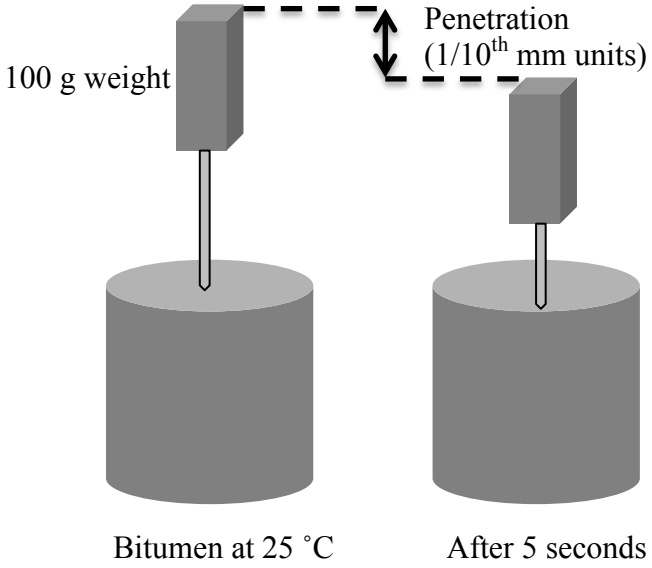


**Figure 1. 5 Diagram of the Penetration point test experiment**

The softening point is another standardised mechanical property test which measures the temperature at which the bitumen reaches a specific consistency and is measured using the Ring and Ball method detailed in the British Standard EN 1427:2015.[22] This is done by heating two discs of bitumen at a constant rate (5˚C per minute) in a liquid bath of either water or glycerol. These two discs each support a steel ball of standardised weight and dimensions and the softening point is the average temperature at which the bitumen allows the ball to fall a distance of 25 ± 0.4 mm. As the bitumen is aged the softening point temperature increases as the binder becomes more viscous at the lower temperatures. Bitumen that has a high softening point is more viscous, is more brittle and therefore more likely to fracture as a result of a loss of cohesion within the road surface. The softening point is also utilised throughout pavement design as it indicates the temperature that the bitumen starts to flow. Therefore, bitumen with a low softening point would not be suitable for a road surface in a country that experiences a hot climate as the bitumen would be too soft for the asphalt to support traffic.[18]

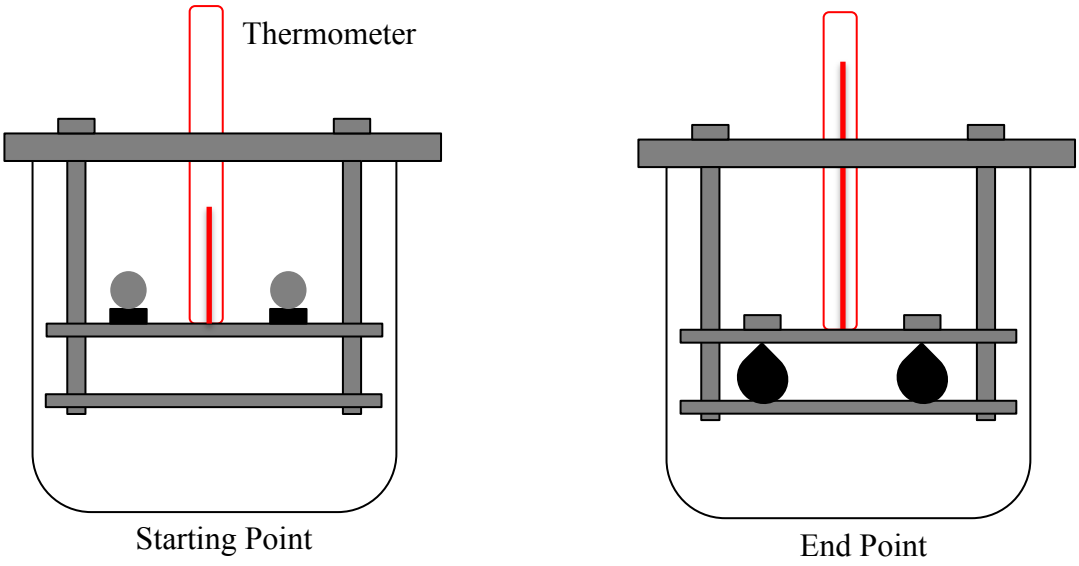


**Figure 1. 6 Diagram representing the softening point experimental starting point and ending point. Two discs of bitumen sit upon a cradle within a bath of water, the temperature of the water bath when the steel balls fall to the bottom of the cradle is the softening point.**

Another mechanical property of the bitumen that is of interest in order to predict the quality of road structure is the cohesion. Cohesion is very important within the binder so as to prevent fretting of the aggregates. The Vialit pendulum test is designed to measure the energy per unit area required to detach a standardised steel cube that has been adhered to a support with a 1 mm thick layer of bitumen. Figure 1.7 shows the experimental starting position; with the bitumen between two steel cubes and the pendulum at its highest point. When the test is started the pendulum is released and the top steel cube is removed from the sample holder. The force required to remove this cube is calculated based upon the swing angle of the pendulum after contact. The test is repeated across a range of temperatures in order to find the temperature at which the cohesion is the highest. Full experimental parameters can be found in the British Standard EN 13588:2008. [23]

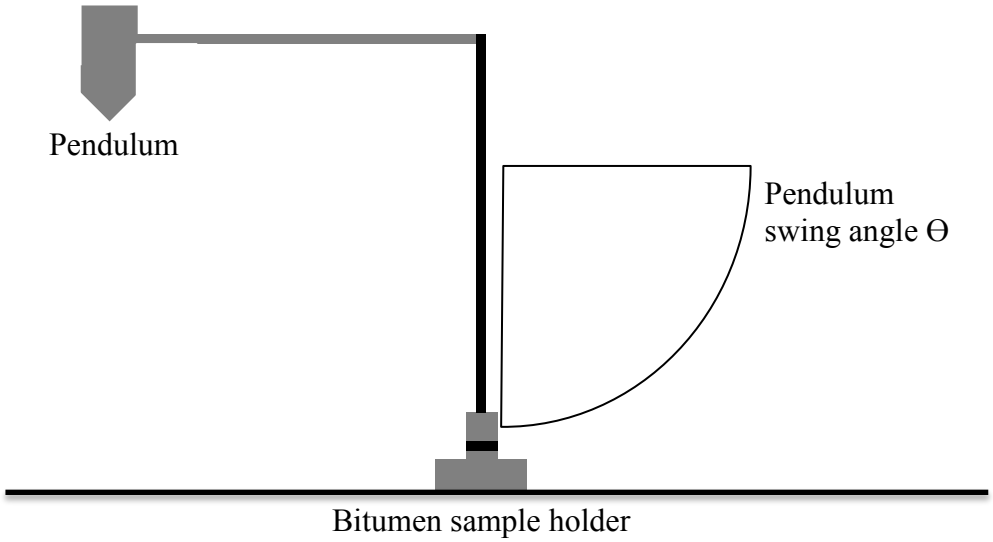


**Figure 1. 7 Diagram displaying a simplistic Vialit Pendulum test set up**

The ductility and the elastic recovery of bitumen can also be measured to determine the elasticity of the bitumen. The ductility test works by pulling apart a sample of bitumen within a standardised specimen holder. The sample is pulled to a specific distance at a set speed and then is cut in the centre. The distance that the two halves retreat back is used to determine the elastic recovery of the bitumen. This recovery distance decreases as the sample ages as the elasticity decreases.

These tests have been around for many years and as technology advances more precise mechanical test methods are becoming more widely used. The Dynamic Shear Rheometer (DSR) is currently being researched for use as a technique for measuring the rheological properties of bitumen. A thin disc of bitumen is pressed between two circular discs of which the bottom is static and the top can oscillate creating a shear action. This experiment allows the complex modulus (G*), the phase angle (δ) and the storage (G`) and loss modulus (G``) to be calculated. The complex modulus is the bitumen's ability to resist deformation when repeatedly sheared whereas the phase angle is the offset between the elastic and viscous response of the material. Bitumen is a visco-elastic material therefore can act as an elastic solid or a viscous liquid. A high phase angle and a low modulus means that the bitumen is acting more as a viscous liquid, and is able to flow, meaning the asphalt would be more susceptible to rutting. By contrast a low phase angle and a high modulus means the bitumen is brittle and could lead to cracking.[24] There is not yet a standardised method for the analysis of bitumen using DSR; however, the utilisation of this technique is being researched. [6,25,26,27,28]

Once the road surface has been laid the condition of the road throughout its surface life is mainly monitored visually. This presents a problem as the time between visual detection of a defect and the complete failure of the road surface is very short. The rapid development of potholes from fretting is an example of this rapid failure mechanism. The aforementioned mechanical tests are used while the road is in service, so that analysts can test the condition of the bitumen throughout its surface life and to monitor any changes to the road. To carry out these tests a core must be collected from the road. The bitumen is then recovered from this slab *via* a binder recovery process. The asphalt core is broken down into smaller chunks and the bitumen is dissolved in dichloromethane and separated from the aggregates and filler *via* filtration and centrifuge separation. This method has been standardised in the British Standard EN 13074 2:2011.[29] The solvent is evaporated from the bitumen with a rotary evaporator and the bitumen is ready for the penetration point, softening point and the Vialit pendulum test.

Changes within the mechanical property test results for the bitumen in the road surface can be an indicator of the road's potential for failure. This process of mechanical testing of asphalt, however, is very time consuming, expensive and requires man-power and road closures to collect cores. Therefore it is not ideal. It is of interest to be able to predict the way that the bitumen will behave in service, prior to laying the road to assist the initial road surface design. There are a number of standardised tests that have been developed that artificially age the bitumen allowing analysts to better understand the ageing behaviour of bitumen.

### *1.1.3 Enhanced ageing*

Bitumen ageing occurs in two stages. The first is short-term ageing and occurs while the bitumen is in transit to the road site. Here the bitumen is kept at high temperatures to prevent the bitumen from solidifying. Chemical ageing is predominant within this stage and consists of oxidation of the bitumen. The second is long-term ageing and occurs after the road has been laid. This ageing mechanism is slower and is affected by external factors including temperature cycles, rain water, UV light exposure and the physical effects of trafficking. Both types of ageing affect the properties of the bitumen over time. Enhanced ageing tests have been developed that allow analysts to predict the effects of ageing, in a much shorter time and are used to accelerate the mechanical and chemical degradation that that bitumen experiences in service by using extremes in temperature or pressure. The tests that are used commonly within the industry include the Rolling Thin Film Oven (RTFO) test, the Rotating Cylinder Ageing test (RCAT) and the Pressure Ageing Vessel (PAV).

The RTFO test involves heating bitumen at 163 ˚C for 75 minutes with exposure to continuous air flow.[30] This test reasonably replicates the short-term, oxidative ageing that the bitumen experiences while it is in transit from the supplier to the road site.[1] Figure 1.8 contains photographs of the RTFO at the Transport Research Laboratory (TRL).

**Figure 1. 8 Photograph of the Rolling Thin Film Oven at the Transport Research Laboratory, Crowthorne House, UK**

Within unpublished works at TRL, Gershkoff *et al.*[31] extended the RTFO test to 225 minutes in order to develop a test which replicates long-term ageing. Changes in mechanical properties similar to those from bitumen that has been aged in service for 3 years were reported. A 56 % decrease in penetration point and a 21 % increase in softening point of bitumen were recorded in this work.

The RCAT test can be used to replicate short and long-term ageing and it has been standardised in the British Standard EN 15323:2007.[32,33] The RCAT involves heating a cylindrical vessel containing the bitumen sample. The short-term ageing experiment is carried out at 163 ˚C for 4 hours with an air flow rate of 4 L/min and a rotation rate of 5 rpm. This is then followed by the long-term ageing experiment which uses a 90 ˚C oven temperature for 140 hours with a flow rate of 4.5 L/min and rotation of 1 rpm.

The PAV test is sometimes used to replicate the long-term ageing of bitumen in service however, as a result of the complexity of the in-service ageing, the data collected from the PAV testing is used to compare bitumen rather than for predictive ageing.[10] The experiment is standardised and runs for 20 hours at temperatures of 90, 100 or 110˚C dependent upon the grade of bitumen being tested, and the pressure is increased to 2.1 MPa within the oven.[34] The PAV test details have been standardised and published within the British Standard EN 14769:2012.[35]

The effect of UV ageing on bitumen has been very widely researched in recent years and has been identified as a contributing factor in the oxidation of bitumen in road surfaces. Intense UV light exposure has been investigated as an enhanced ageing technique with mixed results as there is no standard method for predicting this type of ageing.[36] There are a number of parameters that can be altered by researchers while developing a UV ageing method including the UV light intensity and energy and the temperature of the experiment. The literature sees a wide range of different parameters being used, some examples include an intensity range from 0.77-100 W/m$^2$,[37,38,39] with very variable UV energy values including 3.08 W [40] and 500 W.[41] These published experiments have also all been carried out at different temperatures ranging between 40-80 ˚C.

Yi-Qiu *et al.*[42] have carried out a thermal and UV ageing comparison on four different bitumen types. The RTFO test was used for the thermal ageing and UV radiation equipment outlined by Tan *et al.*[43] was used to UV age the bitumen samples. The samples were held at 73 ˚C for 9 hours, which they equated to 5 months natural ageing in Tibet, China. A 42% decrease in penetration point and a 22% increase in the softening point were reported after the UV ageing. The UV ageing also significantly increased the asphaltene content in the bitumen.

Zeng *et al.*[36] have looked into the effect of varying temperature on the UV ageing mechanism. They identified that when UV light is coupled with a temperature of 70 ˚C there is accelerated oxidation and volatilisation of the bitumen. Therefore to identify the effects of UV light alone the experiment must be carried out at a temperature below 50 ˚C.

The effect of UV light has generally been omitted from standardisation as the effect is localised on the surface layers of the asphalt and bitumen.[44,45] However as some failure mechanisms can propagate from the surface, it seems reasonable to investigate the effect of UV light on asphalt ageing.

The aforementioned tests have been designed for the ageing of bitumen alone. There is a lack of standardised tests that reliably age asphalt. This is because there are such a large number of unpredictable factors that can affect the road while in service and there is no one factor alone that initiates failure. Weathering chambers have been utilised within the literature to attempt to include this major influencer into the methodology.[46,47] These chambers take into account the temperature cycling, humidity and UV light exposure of natural weather conditions.

It must be stated that the ageing mechanisms that the bitumen experiences in-service are vastly different to the mechanisms that are identified *via* these enhanced ageing tests, but a

change in mechanical properties can be measured that may correlate to a specific time of service life and therefore allow for the prediction of the ageing behaviour.[48]

Bitumen embrittlement is a major contributor to the failure of road surfaces and the oxidation of bitumen has been widely researched and has been linked to bitumen embrittlement.

## 1.2 Bitumen oxidation and analysis

Many researchers have attempted to find the main cause for bitumen age hardening and there are some contradictory results that have been published over the years. Asphaltenes are the highly aromatic, high molecular weight compounds within the bitumen composition and an increase in asphaltene content has been linked to an increase in viscosity. [49] The increase in oxygen contained within the bitumen composition has also been linked to an increase in viscosity and it is likely that a combination of these effects contributes to the age hardening of bitumen.

When discussing bitumen, oxidation refers to the addition of oxygen to a compound. Very simply this usually involves the reaction of oxygen with an unsaturated hydrocarbon. Oxygen is an oxidising agent meaning it can remove electrons from a molecule. Unsaturated hydrocarbons containing groups, such as C=C or aromatic rings, are electron rich and therefore can react rapidly with oxygen.

Benzyl carbons attached to lower molecular weight, aromatic resins are also susceptible to oxidation. Ketone functional groups are formed upon oxidation of these carbons. Petersen *et al.*,[50] state that the ketone functional group formation creates an increase in polarity which causes an agglomeration of the strongly interacting molecules which leads to an increase in viscosity of the overall composition. Polar and hydrogen bonding are possible interactions that can occur between these newly polar, oxygen containing molecules. The introduction of highly electronegative oxygen will withdraw electrons within the carbonyl bonds and create charged dipoles upon the oxygen and carbon atoms involved in the bond. These dipoles can then attract atoms with the opposite charge and create a weak, electrostatic, intermolecular bond.

Once the polarity becomes sufficiently high, the intermolecular forces increase and there is a reduction in the mobility of the molecules. If the molecules become insufficiently mobile, the bitumen can no longer withstand the mechanical stress of trafficking and cracks and fractures develop.[20]

Bitumen ageing can be split into four groups: short-term, long-term, chemical and physical. The short-term ageing occurs while the bitumen is in-transit to the road. This involves high temperatures and exposure to oxygen, and is mainly chemical ageing. Chemical ageing involves the chemical alteration of the bitumen composition through oxidation. [51] This is an irreversible process. The long-term ageing occurs throughout the life-span of the road surface. Once the road is laid the bitumen cools and is exposed to a number of external factors. The temperatures experienced by the bitumen are much lower than in transit and short term ageing, and any oxidation is normally UV initiated. The bitumen can experience physical ageing at these lower temperatures which involves the molecular structuring and arrangement of the molecules within the bitumen.[52]

Petersen *et al.*[53] describe a mechanism for the short-term and long-term oxidative ageing of the bitumen. The conditions for the two types of ageing are very different as previously mentioned; therefore the oxidation mechanisms are understandably different. During the short-term ageing the bitumen experiences high temperatures and exposure to oxygen. These conditions allow a 'spurt' reaction to occur within the unsaturated bitumen. The published spurt reaction mechanisms have been reproduced below. 'Asp' represents a highly interacting, asphaltene compound and 'R' represents a weakly interacting molecule, such as a lower molecular weight saturated hydrocarbon.

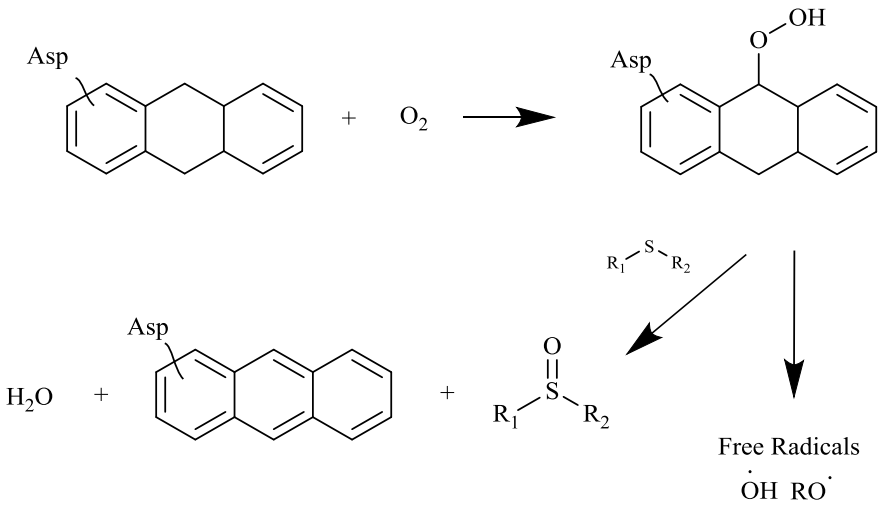


**Figure 1. 9 Spurt reaction scheme between molecular oxygen and aromatic structures within asphaltenes.[53]**

The spurt reaction involves the reaction of unsaturated groups with molecular oxygen to produce peroxide groups. These peroxides can then either decompose to form free radicals, or react further with alkyl or aryl-alkyl sulfides to form sulfoxide groups. The free radicals are reactive species and can initiate further reactions. In the reaction scheme outlined above

(Figure 1.9) the central, strained, non-planar ring is aromatised as a result of the decomposition of the peroxide group. This increase in aromaticity makes the molecule more planar and these new unsaturated bonds add electron density to the system. The change in molecular structure allows the molecule to undergo more intramolecular bonding through this highly electron rich π-network and therefore the viscosity of the bitumen is increased. Some work in the literature has stated that these, high molecular weight, aromatic asphaltenes are the main contributing factor to bitumen age hardening.[42,54,55]

Once the road surface has been laid the conditions change and the oxidation slows. Petersen *et al.*[53] describe a slower oxidation reaction mechanism which requires a free radical initiator.

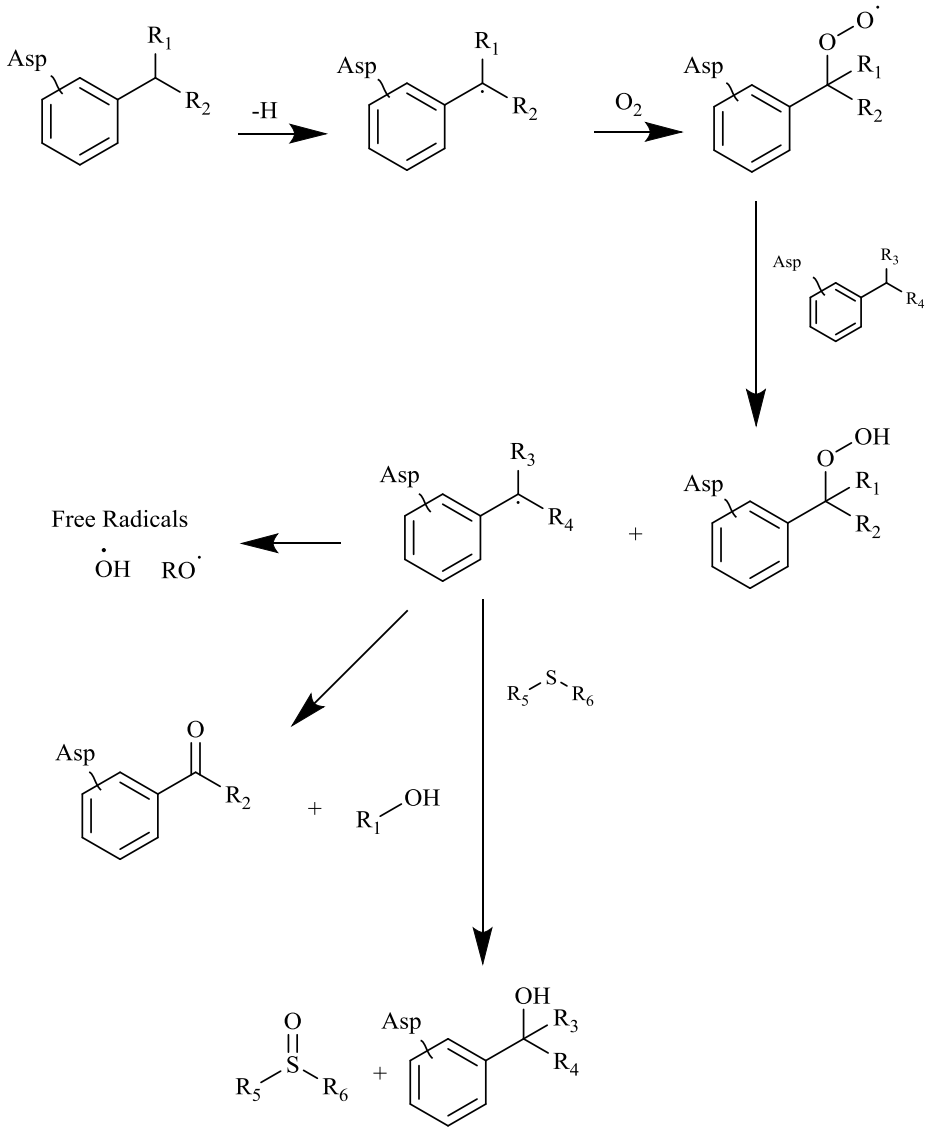


**Figure 1. 10 Long-term, slow oxidative ageing reaction mechanism of asphaltenes in bitumen[53]**

In the above mechanism (Figure 1.10), hydrogen is readily removed from a benzyl carbon to form a free radical carbon. This can react with molecular oxygen to form a peroxide group.

The peroxide group can decompose, as seen before in the spurt reaction (Figure 1.9), however, there are some differences as a result of the lower energy of the reaction. Three different compound types are formed upon the decomposition; ketones (C=O), sulfoxides (S=O) and alcohols (O-H). The direction of the decomposition is governed by the bitumen's chemical composition; sulfur content, the temperature and oxygen availability. The increased polarity as a result of the increased oxygen content within the composition allows a greater number of intermolecular interactions that can occur between molecules therefore, increasing viscosity.

Oxidation reactions require an initiator to provide enough energy to the molecules in order to break and form new bonds. Within the short-term, spurt reaction, the high temperature can provide this energy, however within long-term ageing the slow oxidation mechanism requires an oxidising initiator to enhance the reaction. Some examples of possible oxidising agents that may have the power and the opportunity to enhance the oxidisation of bitumen within asphalt road surfaces are singlet oxygen and hydroxyl radicals.

Singlet oxygen is an excited state of molecular oxygen in which the two valence electrons are spin paired within the π* antibonding orbital. The molecular orbital diagram in Figure 1.11 outlines the differences between singlet oxygen and the triplet ground state configuration.

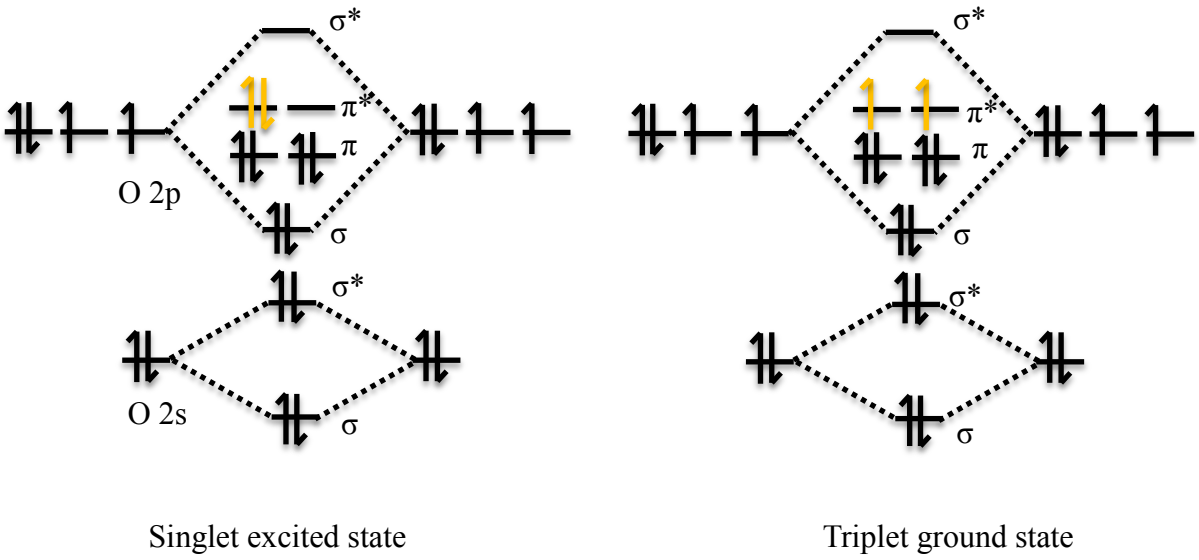


**Figure 1. 11 Molecular Orbital Diagram of the singlet and triplet states of molecular oxygen**

This excited state of molecular oxygen can be formed in the atmosphere by irradiating ozone with UV light of a short wavelength.[56] It is commonly formed in organic chemistry *via* the photosensitisation of oxygen in the presence of UV light and a highly aromatic dye such as

Rose Bengal or Methylene Blue. A photosensitiser is a molecule that is capable of absorbing a photon of light and can then pass this energy onto molecular oxygen to form the excited singlet oxygen.[57] The photosensitiser must be capable of absorbing light in the UV-Visible wavelength range (190-750 nm) and commonly contains a large delocalised π system. These properties are all consistent with the asphaltene compounds within bitumen; therefore it could be the case that the large aromatic compounds of the highly absorbing bitumen are acting as sensitizers for the photosensitisation of molecular oxygen.

As singlet oxygen is highly electrophilic it has the capacity to react with electron rich unsaturated hydrocarbons. There are a number of different reactions that singlet oxygen is known to initiate that could be occurring within the bitumen, including the 'ene' reaction, Diels-Alder 4+2 cycloaddition, 2+2 cyclo-addition and the oxidation of heteroatoms such as sulfur.[58] Examples of these reaction schemes can be found in Figure 1.12.

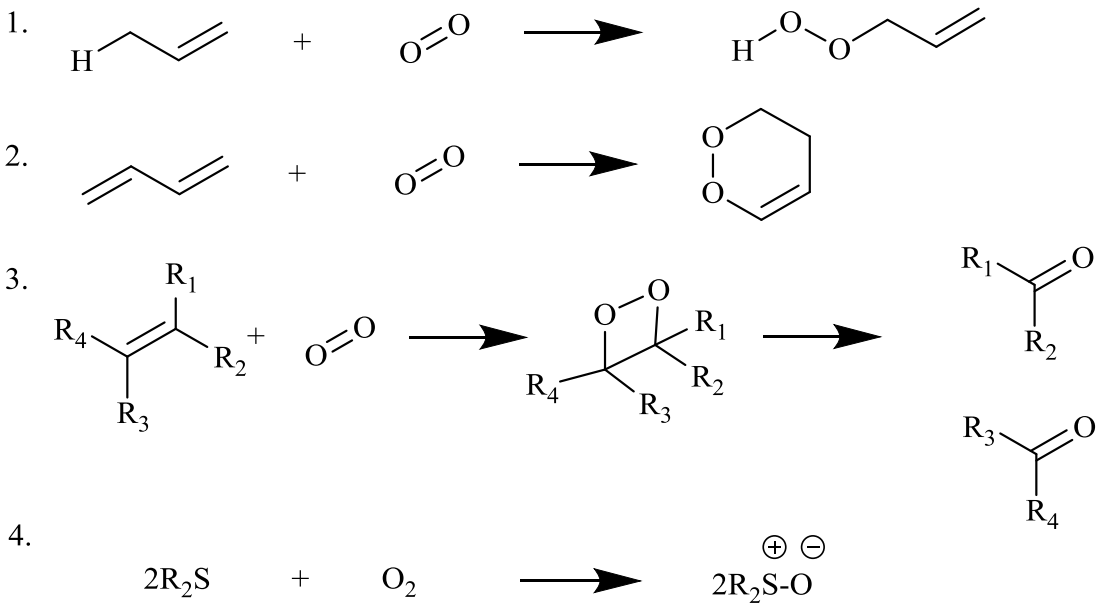


**Figure 1.12 Example reaction schemes that can occur between singlet oxygen and unsaturated and aromatic hydrocarbons and sulfur containing compounds. 1. Ene reaction. 2. Diel-Alder 4+2 cycloaddition. 3. 2+2**

The 'ene' reaction involves forming a peroxide group from unsaturated alkenes and singlet oxygen. These have been seen to decompose to a number of different oxygen containing compounds in the spurt and slow reactions outlined above.[53]

Diels-Alder reactions can occur between diene functional groups and singlet oxygen to produce endo-peroxides. This 4+2 cycloaddition with singlet oxygen produces an endo-peroxide with an O-O functional group.

The third mechanism scheme presented in Figure 1.12 is the 2+2 cyclo addition of singlet oxygen to an alkene. This produces a 4-membered ring which is quite unstable, and decomposes to two carbonyl functional groups. These carbonyl bonds are detectable with IR and can be monitored throughout the oxidation of the bitumen.

The final scheme is that of the oxidation of sulfur containing compounds which can readily form S-O single bonds with a dipole.[59] When in conjunction with an unsaturated system, such as asphaltenes and resins, this bond can form an S=O double bond through resonance.

As mentioned previously bitumen oxidation is greatly affected by access to oxygen, the bitumen source, the aggregates and the void content of the asphalt, the temperature and also UV light exposure. Alongside producing the singlet oxygen required for the previously mentioned reactions, UV light exposure can also assist in the production of hydroxyl radicals which can act as oxidising agents for bitumen.

Hydroxyl radicals are formed as part of the decomposition of hydro-peroxides; however, they can also be formed as a result of UV light interacting with ozone in the atmosphere. This reaction creates highly reactive O atoms and molecular oxygen. These O atoms are then able to react with water to form 2 hydroxyl radicals (Figure 1.13).[60] The production of hydroxyl radicals in this way is known to occur within the atmosphere and is responsible for the 'cleaning' of the atmosphere of greenhouse gases including methane.[61]

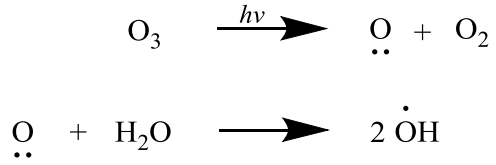


**Figure 1. 13 Formation of hydroxyl radicals *via* the reaction between ozone, UV light and water**

The reactive hydroxyl radical can react with unsaturated hydrocarbons to form oxidation products.[62] The reaction scheme in Figure 1.14 outlines a reaction between a hydroxyl radical and an aromatic ring.

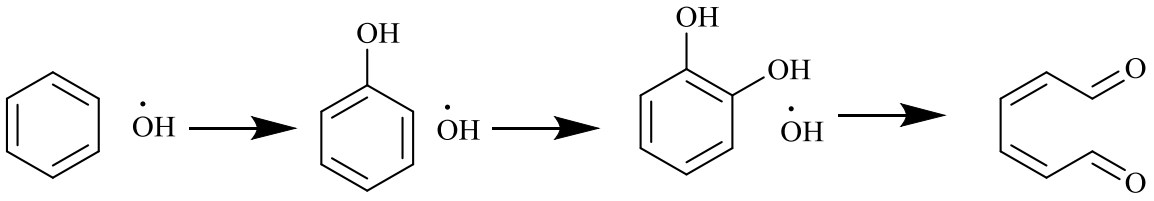


**Figure 1. 14 Example reaction scheme between hydroxyl radicals and aromatic ring structures.[62]**

Aromatic rings are a part of the bitumen composition therefore the reaction scheme shown in Figure 1.14 is a viable route for carbonyl bond formation upon oxidation. One of the limiting factors is the presence of the hydroxyl radicals within the bitumen. As a result of rainfall there can be liquid water or water vapour present on the surface of the asphalt and in the atmosphere, and this could provide the bitumen with a source of the hydroxyl radicals required for this reaction upon UV irradiation.

The presence of moisture upon the asphalt surface can greatly enhance the severity of failures such as cracks, rutting and fretting that have already established. It is well researched that water causes a decrease in cohesion within the bitumen itself but there is also a reduction in adhesion between the bitumen and the aggregate stones. [63,64] A reduction in the cohesion and adhesion means that the aggregates are more easily lost from the surface, leading to fretting. Noguera *et al.*[65] have published results that suggest that the presence of water can produce oxidative changes within the bitumen. Within the research asphalt was aged in water and after 12 months of being submerged an increase in asphaltenes content was measured, alongside a 26 % decrease in penetration point, an 8 % increase in softening point and a 20 % increase in viscosity (measured at 60 ˚C). Similar research papers have identified the oxidative effect of water on bitumen and asphalt.[66,67] Water can also cause damage to an asphalt road surface by the action of 'freeze-thaw' during the cold winter months. In this case the water present within the voids of the asphalt freezes and expands as the temperature drops. This expansion leads to cracks as the bitumen is cold and brittle. As the temperature increases the ice melts and the asphalt structure is weaker.

The oxidation of bitumen has many different causes and can be occur *via* a number of different mechanisms. Measurement of the formation of oxidation products formed within the bitumen upon oxidation, including the carbonyl, C-O, sulfoxide and alcohol functional groups, can be carried out using Infrared spectroscopy.

### *1.2.1 Infrared spectroscopy for the analysis of bitumen oxidation*

Infrared (IR) spectroscopy is a very well-known and widely used analytical technique. The most commonly adopted design for the IR spectrometer is the Michelson interferometer.[68] Very simply, this type of spectrometer works by shining a beam of light from an infrared laser source, through a beam splitter to two sets of mirrors. One of these mirrors is moving, causing an interference pattern in the recombined infrared light beam, dependent upon the moving mirror's position. This beam is then transferred to the sample and then a detector. A Fourier transform is carried out and an infrared spectrum is produced.

There are many different detection methods for infrared spectroscopy including Attenuated Total Reflectance, Diffuse Reflectance, Angle Grazing and Non-Dispersive IR analysis. These adaptations to the spectrometer allow a very diverse array of samples to be analysed. IR spectrometers can be portable allowing measurements to be taken outside of a laboratory for applications such as coating monitoring for aeroplanes and Formula 1 car tyres, archaeological dig site analysis or quality control throughout food production.[69,70,71]

Infrared spectroscopy works by irradiating a sample with infrared light between 800 nm and 1 mm wavelength range (12500-10 $cm^{-1}$), and measuring how much of this light is absorbed by the sample. This wavelength range include the near, mid and far infrared light regions of the electromagnetic spectrum, however, commonly only the mid infrared wavelength range is utilised between (4000-400 $cm^{-1}$). Infrared active vibrations within a molecule lead to absorption of the infrared light at specific wavelengths. Infrared active vibrations are those which experience a change in dipole moment while vibrating. These normally involve hetero-atomic bonds in which there is a difference in electronegativity between the atoms. The simplest IR active vibration is that of a heteronuclear diatomic molecule where the bond between the atoms can stretch leading to IR absorption. When considering triatomic or polyatomic molecules the bonds can stretch symmetrically and asymmetrically, and bending modes are also observed.

Infrared active vibrations have a natural 'resonant' vibrating frequency and when the sample is irradiated with light that has a frequency that matches this, IR light is absorbed, and the amplitude of the vibration is increased. The resonant frequency is dependent on the reduced mass of the atoms involved in a vibration and on the force constants of the bonds joining the atoms together. For a diatomic molecule, assuming harmonic vibration, this may be expressed by Equation 1.1 where c is the speed of light (m $s^{-1}$), f is the force constant (kg $m^{-1}s^{-1}$), and μ

is the reduced mass (kg). [72] A harmonic oscillator can be used to describe a system that is oscillating with a restoring force that is equal in magnitude but opposite in direction to the displacement from the system's starting position.

$$\tilde{\nu} = \frac{1}{2\pi c}\sqrt{\frac{f}{\mu}}$$

**Equation 1. 1 Calculation of circular frequency in wavenumbers, of a diatomic molecule with force constant f, and reduced mass μ**

Thus it is often possible to assign absorbance bands in an IR spectrum to a specific functional group present in the samples.

This approach has been used to identify oxygen containing functional groups within bitumen after ageing to prove the presence of oxidation products. Many researchers have identified groups such as the carbonyl (C=O), carbon-oxygen single bond (C-O), alcohol (O-H) and sulfoxide (S=O) absorbance bands present in oxidised bitumen. [73,74,75,76]

**The Beer-Lambert Law states that absorbance is directly proportional to concentration at a constant path length. This link is shown in Equation 1. 2 Beer-Lambert Law**

where A is the absorbance, $\varepsilon$ is the molar extinction coefficient ($dm^3\ mol^{-1}\ cm^{-1}$), c is the concentration ($mol\ dm^{-3}$) and l is the path length of the light (cm).

$$A = \varepsilon \cdot c \cdot l$$

**Equation 1. 2 Beer-Lambert Law**

The molar extinction coefficient is a measure of how strongly a molecule can absorb light of a given frequency. It is possible to quantify the concentration of molecules within a sample based upon the Beer-Lambert relationship. This can be done by preparing a set of calibration samples with known concentrations of a specific compound or functional group. The calibration curve of the absorbance band area *vs.* concentration, for example, could then be used to interpolate an unknown sample's concentration. This methodology works extremely well within UV/vis spectroscopy, and IR spectroscopy of simple compounds, however there is a lot more variability within IR spectroscopy, where spectra are typically more complex with overlapping absorbance bands, therefore this is sometimes less reliable.

In the case of bitumen oxidation, absorbance bands that correspond to the oxidation products have been successfully quantified by integrating the area underneath the band.[77,78,79] This can be carried out very simply in modern FTIR software which allows two or four base pairs to be

selected. The base pairs can be used to indicate to the software the position of the baseline for the integration. The software will then integrate the area between the base pairs and display this to the analyst.

Some researchers have calculated indices to better understand the chemical changes occurring as the bitumen oxidises. Indices are calculated ratios of absorbance bands and can be used to more reliably compare spectra without the need for normalisation of the data. Niritha *et al.*[80] identified the carbonyl (1678-1725 $cm^{-1}$), sulfoxide (1010-1043 $cm^{-1}$), aliphatic (1350-1510 $cm^{-1}$), aromatic (1535-1625 $cm^{-1}$) and long chain (715-733 $cm^{-1}$) absorbance band areas as areas of interest. Within the report each index was calculated by dividing the absorbance band area by the sum of all of the absorbance bands. This paper reported an increase in the carbonyl and sulfoxide index of unmodified bitumen after ageing in the RTFO test. Lopes *et al.*[47] calculated the carbonyl and sulfoxide indices by dividing the absorbance band areas underneath the carbonyl (1750-1650 $cm^{-1}$) and sulfoxide (1045-1020 $cm^{-1}$) absorbance bands by the area underneath the C-$H_2$ and C-$H_3$ (1500-1325 $cm^{-1}$) absorbance band. The calculated indices were both seen to increase after the bitumen samples had been thermally aged at 180 ˚C for 24 hours.

It would be extremely difficult to use this quantification to calculate actual concentrations of these groups within the bitumen composition. The initial bitumen structure is unknown and different between every source, meaning that the exact oxidation mechanism is unknown. Therefore the data calculated from the spectra collected can only be compared in order to determine a *change* in the functional group quantities rather than give a definite indication of the exact concentration.

A large amount of the work referenced here has been carried out using ATR-FTIR on raw bitumen. ATR is a detection method that requires close contact between the ATR crystal and the sample. This is very easy to obtain when analysing bitumen as it is a very malleable and soft semi-solid. The incident light beam travels through the ATR crystal and is reflected from at least one of the internal surfaces to form an evanescent wave. This wave then travels to the sample where is penetrates between 0.5-2 μm.[81] The light then travels back into the crystal where it can then pass through to the detector and interferometer and the signal is converted into a spectrum. The signal to noise ratio of spectra collected in this way is very good, with well resolved absorbance bands. See diagram in Figure 1.15 (a).

Asphalt, however, is a combination of bitumen and hard aggregates and therefore has a rough surface and close contact with an ATR crystal is difficult which leads to poor quality spectra being collected. Therefore a non-contact detection method is required for asphalt analysis.

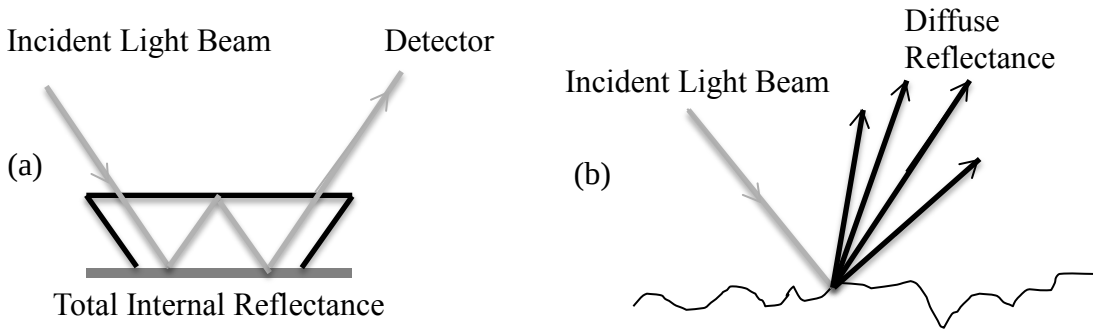


**Figure 1. 15 Diagram of the total internal reflectance within an ATR spectroscopy crystal (a) and the diffuse reflectance of light from a rough surface (b)**

Diffuse reflectance infrared Fourier transform (DRIFT) spectroscopy is a non-contact detection method that works by collecting light that is diffusely scattered from the rough sample surface. The incident light interacts with the sample and is then scattered at angles that are not equal to the incident angle. See diagram in Figure 1.15 (b). The angles of the scattering are dependent upon the wavelength of the light and the size properties of the surface particles. The diffuse reflectance detector has the ability to detect this scattered light and, after a Fourier transform, an infrared spectrum is produced. Specular reflectance on the other hand, is another form of reflection which occurs when a smooth, shiny surface is irradiated with a beam of light. The light is then reflected from the surface at an angle that is equal to the incident angle.

As a result of the increased path length that the light has to travel to the reflectance detector there is a reduction in signal to noise ratio for reflectance measurements. This can make DRIFT spectra more difficult to interpret. The spectra obtained from asphalt samples are likely to be a mixture of diffuse and specular reflectance as bitumen is shiny and the aggregates are rough. As such the reflectance spectra of a sample like asphalt can be difficult to interpret where it appears that some absorbance bands have negative intensities and some are positive.

The reflectance of light is related to the refractive index of the sample. The refractive index of the sample changes depending upon the wavelength of light being used.[82] Therefore, it is possible that the sample will experience a change in refractive index along an absorbance

band, with a maximum absorbance at a high wavenumber and a minimum at a lower wavenumber.

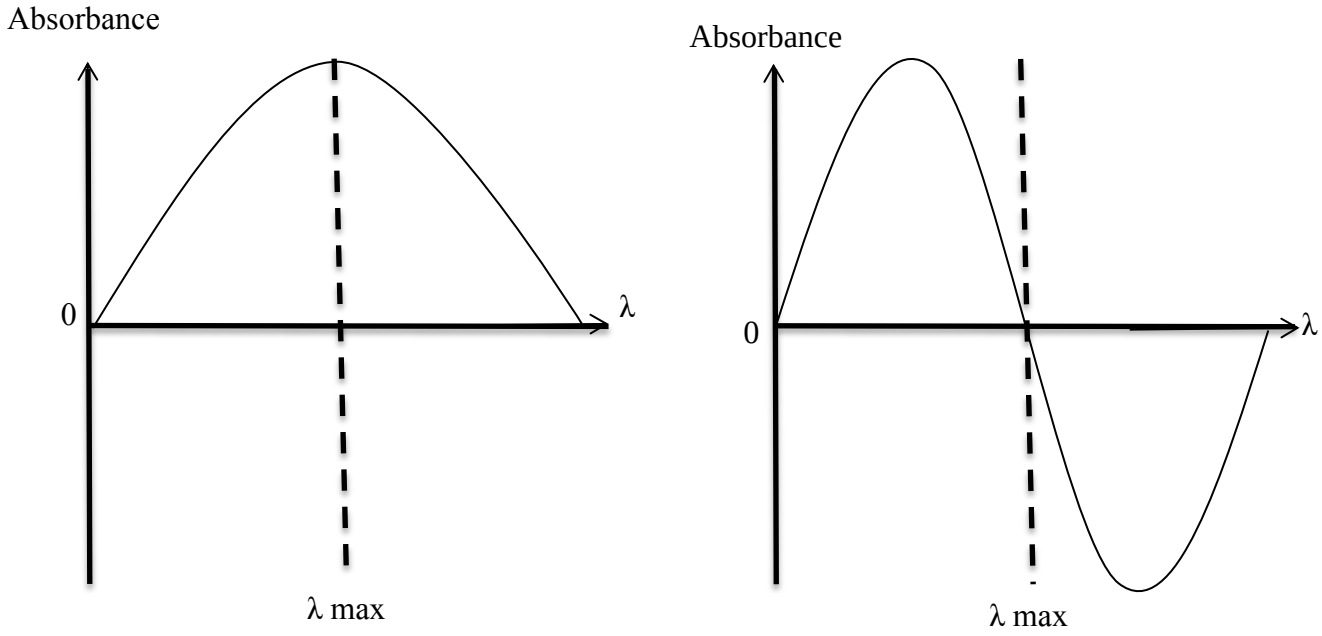


**Figure 1. 16 Diagrammatic representation of a normal absorbance band and a first derivative graphical curve with λmax at the 0 position.**

This gives the absorbance band a first derivative characteristic with the expected $\lambda_{max}$ for the absorbance of the functional group, at the centre of this band (Figure 1.16). [83]

### *1.2.2 Experimental aims*

The overall aim for this project is to develop the use of infrared spectroscopy for a traffic speed detection of asphalt road surfaces, and to determine if this technique can predict failure prior to visual detection of a defect. In this case the use of Diffuse Reflectance Infrared Fourier Transform (DRIFT) spectroscopy has been investigated with a number of different samples that have been aged artificially and naturally.

As asphalt is a mixture of raw bitumen, filler and aggregates of different mineral types, it is beneficial to reduce the number of external components that may affect the infrared spectrum of the sample in the first instance. Once any chemical and physical changes have been identified within the raw bitumen, DRIFT spectroscopy can then be applied to asphalt samples, which are more complex.

This project aims to answer the following research questions;

- Can oxidation product functional groups be detected and assigned using ATR and DRIFT spectra from the surface of raw bitumen that has been aged artificially and with natural conditions?
    - Can these changes be appropriately quantified?
    - Do these chemical changes correspond to mechanical property changes within the bitumen?
- Can DRIFT spectroscopy be used to analyse asphalt, and to determine the chemical changes in the surface after artificial and natural ageing experiments?
    - After recovery of the bitumen from these aged asphalt samples, is there a change in the mechanical properties?
- To ascertain if it is possible to utilise a DRIFT system to analyse road surfaces in real time
    - What will the issues be for developing DRIFT spectroscopy into a traffic speed detection method?

# Part 2-Sample preparation and experimental parameters

40/60 penetration grade bitumen has been used for the testing in this project. Samples for the bitumen were prepared by heating the bulk bitumen sample at 150 ˚C for approximately 1 hour until the bitumen was viscous enough to pour. Aluminium tins were used to hold the bitumen, and approximately 150 g was decanted into each tin ready for the different ageing experiments. The bitumen was allowed to cool before it was subjected to any ageing.

Asphalt samples have been manufactured using a 10 mm stone mastic asphalt (SMA) purchased from United Asphalt. Stone mastic asphalt is hard, durable asphalt used widely within Europe as it is resistant to deformation. The samples were compacted into 200 x 200 x 50 mm slabs using a wooden mould shown in Figure 1.17. The samples have been made according to the parameters outlined in the British Standard EN 13108-1:2006.[84]


**Figure 1. 17 Photographs of the asphalt samples being created at the Transport Research Laboratory (TRL).**

The enhanced ageing experiments outlined in the following chapters have been carried out using the Rolling Thin Film Oven test and ultra-violet light exposure.

The RTFO test was carried out by following the British Standard EN 12607-1, 1999, [30] using a MATEST Rolling Thin Film oven at TRL.

A UV light chamber was built as part of this project at TRL which contains 8 Sylvia UV black lights that omit broad-band UV light with a maximum output at 368 nm. The chamber was held at 60 ˚C in order to enhance the ageing of the samples. Figure 1.18 is a photograph of the UV chamber.

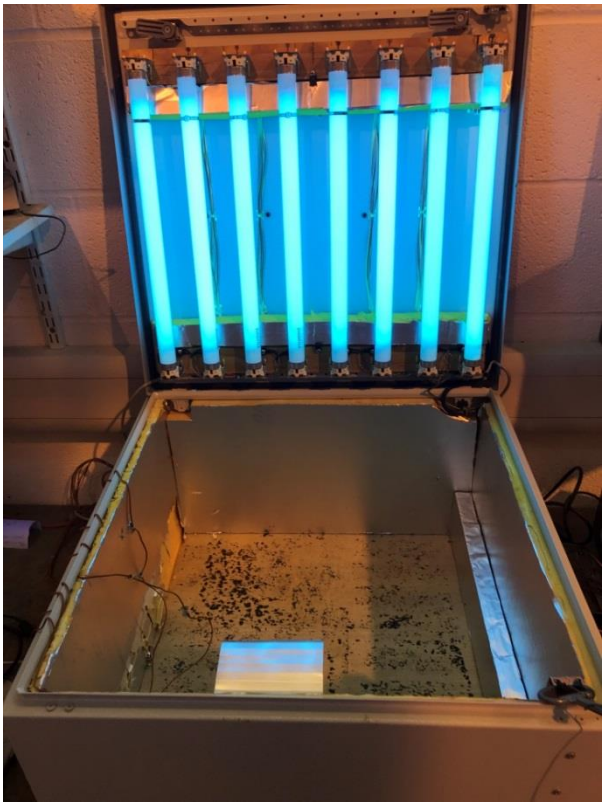

**Figure 1. 18 Photograph of UV chamber manufactured at the Transport Research Laboratory, Crowthorne, UK**

Natural ageing of bitumen and asphalt samples has also been carried out. The samples were placed onto the roof of TRL headquarters, Crowthorne House. A weather station was created at TRL which measures temperature (˚C), UV light exposure ($W/m^2$), rainfall (mm), wind speed ($m\ s^{-1}$) and direction, pressure (mBar) and relative humidity (%), every 15 minutes for 24 hours.

**Figure 1. 19 Photograph of the weather station on the roof of Crowthorne House**

The mechanical properties of the bitumen were measured using the penetration point, the softening point and the Vialit pendulum test. The mechanical test methods have been carried out using the British Standards- BSEN 1426:2015, BSEN 1427:2015, and BSEN 13588:2008, respectively, and will be explained in full in Chapter 3.

The spectroscopic analysis was carried out using a handheld Agilent Technologies ExoScan 4100 FTIR spectrometer. The ExoScan has the capacity to measure in both ATR and diffuse reflectance modes using separate detection attachments.[85]


**Figure 1. 20 Photograph of the ExoScan 4100 handheld spectrometer (a), with ATR (b) and Diffuse Reflectance (c) detection attachments**

This spectrometer has been chosen so that the data collection can be carried out in the laboratory and also outside of the lab with the same machine. This removes any possibility for machine variability to be a factor in the different sample spectra collected.

### *1.2.3 Infrared microscopic analysis*

Infrared spectroscopy can be coupled with a microscope imaging system to create a technique called IR microscopy. This allows an analyst to visualise the sample being analysed and record microscope images of the surface of the sample. These images can be used to specifically select the area required for a point infrared spectrum and it can also be used to create ChemiMaps. ChemiMaps are created by selecting an area of the sample surface and collecting an IR spectrum in each pixel of this image. The spectrum in each pixel can then be viewed and the ChemiMap can be altered to enhance areas that contain spectra with a high absorbance at a specific wavenumber of interest. This technique allows for chemical differentiation within a sample to be carried out.

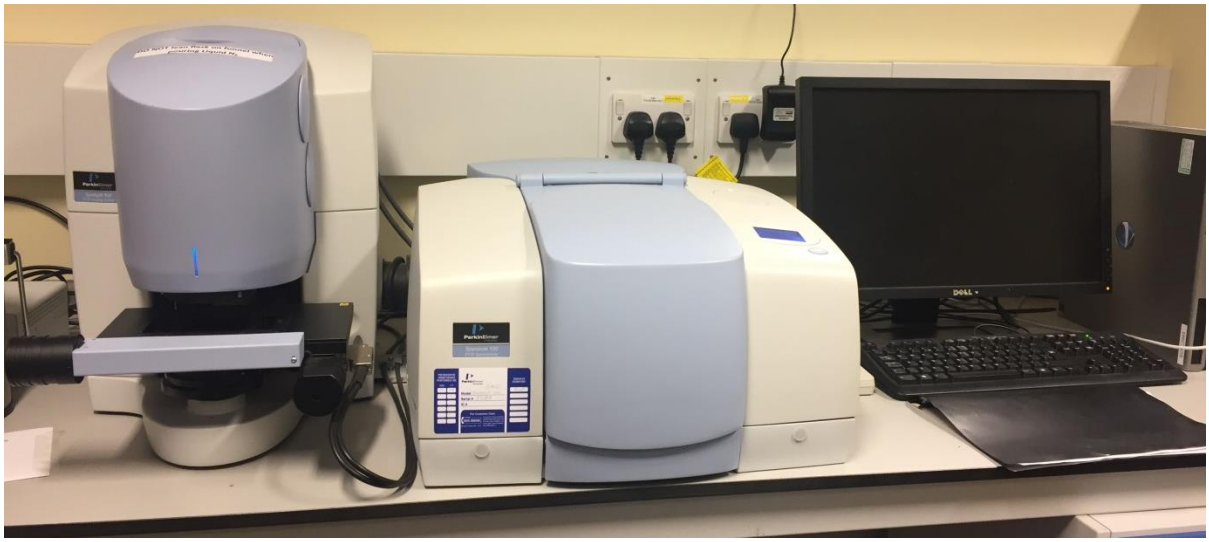

**Figure 1. 21 Photograph of the Perkin Elmer Spectrum 100 with a Spotlight 100 imaging microscope system attachment located in the Chemical Analysis Facility (CAF) at the University of Reading**

The Infrared microscopy was carried out using a Perkin Elmer Spectrum 100 FTIR with a Spotlight 100 microscope imaging system.

### *1.2.4 Scanning Electron Microscopy Elemental analysis*

Scanning electron microscopy (SEM) was utilised in the research to explore further changes seen to occur on the surface of the aged bitumen and asphalt samples upon ageing using visual imaging. This allows for any microscopic physical changes to the surface of the samples to be visualised. The facility of the scanning electron microscope for elemental analysis using the EDX (Energy Dispersive X-Ray) analysis attachment has also been utilised in this project to determine which elements (atoms) are present within the bitumen and asphalt. These elements can vary depending upon the oil source, the refinery and the quarry source for the aggregates and fillers. Thus it is important to know something of the elemental composition of the samples being studied.

Within a SEM an electron gun produces electrons which are accelerated at a voltage between 1-30 KeV, towards a sample, through condenser and objective lenses. The electron beam penetrates the sample to a depth of approx. 1 μm and this interaction with the sample causes elastic collisions which produce scattered electrons. There are two types of scattered electrons that are used to produce the image of the sample; secondary and backscattered electrons. Secondary electrons are those that are scattered from the surface of the sample whereas backscattered electrons are those that have been scattered from deeper layers in the sample and are a result of multiple elastic collisions.[86]

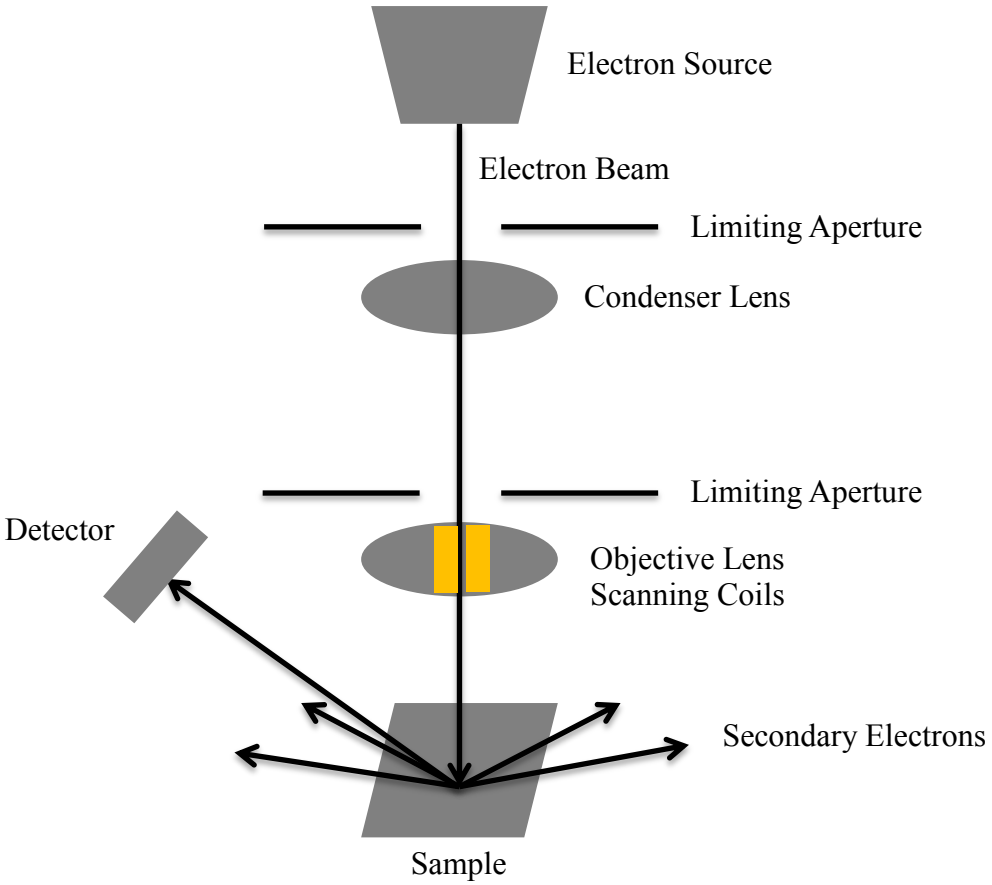


**Figure 1. 22 A simplified diagram representing the internal working of a scanning electron microscope**

It is also possible to use SEM for elemental analysis of samples. The intense electron beam can eject electrons from the atoms on the surface of the sample being analysed. These electrons can be removed from inner electron orbitals which leaves a 'hole' in the electron structure of the atom. The outer orbital electrons then fall to fill these holes and upon doing so they release an X-ray with energy that is equivalent to the energy gap between the orbitals. These quantum levels are different for each different elemental atom therefore it is possible to determine which electronic transition has occurred based on the energy of the X-rays detected, and therefore to determine which elements are present in the sample.[87]

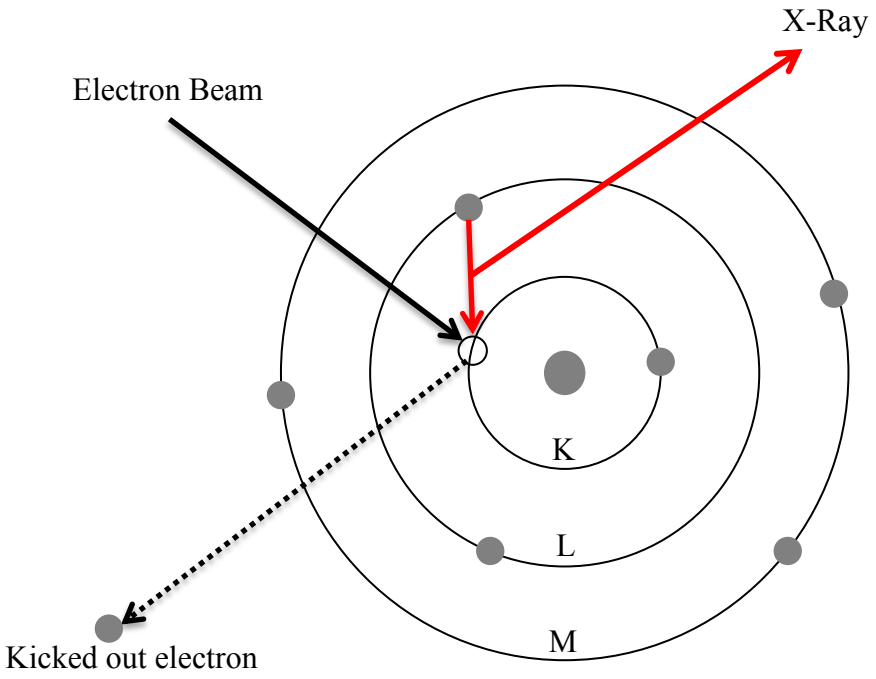


**Figure 1. 23 Diagram representing the elemental x-ray detection elemental analysis spectroscopy**

The scanning electron microscopy experiments were carried out using a low vacuum Oxford Instruments Scanning Electron Microscope with an X-Sight attachment, running INCA software for elemental analysis. The pressure within the sample chamber was set to 0.68 Torr.

### *1.2.5 Gel Permeation Chromatography*

Gel Permeation Chromatography is a chromatographic technique that can be used to separate mixtures of molecules based upon their molecular size. The GPC column consists of a porous-particle packed column and the sample solution is carried though the column *via* a liquid mobile phase. The GPC column is composed of a packing material that has been made with a variety of different pore sizes within its structure. The larger molecules do not interact with these pores and therefore elute rapidly through the column. By contrast the smaller molecules can interact with the pores and they have a longer path length through the column and therefore have a longer retention time.[88] When analysing bitumen *via* GPC, the size of the hydrocarbon molecules can be related to their molecular weight.

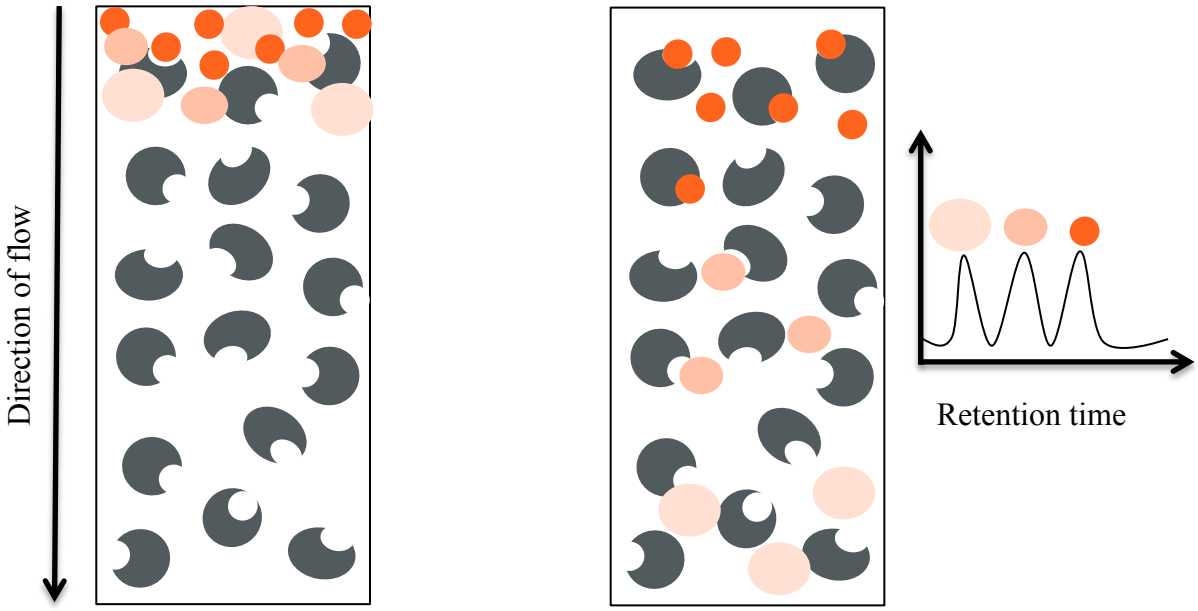


**Figure 1. 24 Diagram to represent the size exclusion separation that occurs within gel permeation chromatography columns with an example of the chromatograph produced**

Details about the molecular weight distribution within the sample mixtures can be calculated from the chromatogram produced.[89] The number average molecular weight ($M_n$) is the average molecular weight of a chain based on the number of different weights in the mixture, Equation 1.3. The weight average molecular weight ($M_w$) is the average molecular weight, taking into account to weight of the molecules.[90] This is commonly higher than the number average molecular weight as the larger molecules have a bigger impact on the average, skewing the $M_w$ to a higher value, Equation 1.4. The polydispersity index is the ratio of the weight average to number average molecular masses, Equation 1.5.

$$M_n = \frac{\sum M_i \cdot N_i}{\sum N_i}$$

**Equation 1. 3 Number average molecular weight calculation[91]**

$$M_w = \frac{\sum M_i^2 \cdot N_i}{\sum M_i N_i}$$

**Equation 1. 4 Weight average molecular weight calculation**

$$Đ = \frac{M_w}{M_n}$$

**Equation 1. 5 Polydispersity calculation from the number and weight average molecular masses[92]**

Gel Permeation Chromatography was carried out at the University of Reading using an Agilent Technologies 1260 Infinity systems fitted with a polystyrene column. Bitumen

samples were dissolved in Tetrahydrofuran (THF) (2 mg/mL), filtered and then run through the GPC with a flow rate of 4 mL/min. The molecules were then detected using a refractive index detector. This works by detecting a change in the refractive index of the sample compared to a reference of the blank solvent. When a molecule enters the refractometer it diffracts the light and this change is detected.

# References


[1] J. Reed and D. Whiteoak, *The Shell Bitumen Handbook*, Shell UK Oil Products Limited, 2003.

[2] Mastering bitumen for better roads and innovative application, Road-construction bitumen characteristics-1-generalities, École des Ponts ParisTech, https://www.coursera.org/lecture/mastering-bitumen/11-road-construction-bitumens-characteristics-1-generalities-S3ttR, ACCESSED 27.08.2018, 16:03.

[3] P. Redelius and H. Soenen, Relation between bitumen chemistry and performance, Fuel, **140**, 2015, 34-43.

[4] www.bitumeninstitute.org/wp-content/uploads/IS230_3edition.pdf, ACCESSED 25.01.16

[5] A. Kebritchi, A. Jalali-Arani and A. A. Roghanizad, Rheological behaviour and properties of bitumen modified with polymeric coated precipitated calcium carbonate, *Constr. Build, Mater.,* **25,** 2011, 2875-2882.

[6] X. Lu and U. Isacsson, Effect of ageing on bitumen chemistry and rheology, *Const. Build. Mater.,* **16,** 2002, 15-22.

[7] J. C. Nicholls, *Asphalt Surfacings, A guide to asphalt surfacings and treatments used for the surface course of road pavements*, E & FN SPON, London, 1998.

[8] S. Rudyk, Relationships between SARA fractions of conventional oil, heavy oil, natural bitumen and residues, *Fuel*, **216,** 2018, 330-340.

[9] Asphaltenes and Waxes, SPE international, http://petrowiki.org/Asphaltenes_and_waxes, ACCESSED 23.09.2018.

[10] Mastering bitumen for better roads and innovative applications, Road-construstion bitumens characteristics-4-ageing, https://www.coursera.org/lecture/mastering-bitumen/14-road-construction-bitumens-characteristics-4-ageing-xmJOU, ACCESSED 27.07.2018, 16:17.

[11] O. C. Mullins, Modified Yen Model, *Energy and Fuels*, **24** (4), 2010, DOI: 10.1021/ef900975e

[12] Mastering bitumen for better roads and innovative applications, Composition of bitumen, École des ParisTech, https://www.coursera.org/lecture/mastering-bitumen/10-composition-of-bitumen-y2T4y, ACCESSED 28.07.2018, 14:29.

[13] J. A Wess, L. D. Olsen and M. H. Sweeney, Concise International Chemical Assessment Document 59, (Asphalt Bitumen), *World Health Organisation*, 2005.

[14] L. Francken, *Bituminous Bitumens and Mixes*, E&FN SPON, London, 1998.

[15] M. Elkashed, R. C. Williams and E. Cochran, Investigation of fatigue and thermal cracking behaviour of rejuvenated reclaimed asphalt pavement binders and mixtures, *Int. J. Fatigue,* **108,** 2018, 90-95.

[16] Roadex Network, Permanent deformation rutting classification, E-Learning lesion 3.1-Why rutting classification is needed, http://www.roadex.org/e-learning/lessons/permanent-deformation/permanent-deformation-rutting-classification/, ACCESSED 28.07.2018, 08:29.

[17] Pavement Interactive Webpage-Rutting. www.pavementinteractive.org/article/Rutting/ ACCESSED 29.05.2018 13:47.

[18] Mastering bitumen for better roads and innovative applications, École des Ponts ParisTech, Road Construction bitumen characteristics-2-Penetratability and softening point, https://www.coursera.org/lecture/mastering-bitumen/12-road-construction-bitumens-characteristics-2-penetrability-softening-point-dmMqA, ACCESSED 28.07.2018, 09:21.

[19] British Standard EN 1426:2015, Bitumen and bituminous binders- Determination of needle penetration.

[20] D. Mastrofini and M. Scarsella, Application of Rheology to the evaluation of Bitumen Ageing, Fuel, 79 (9), 2000, 1005-1015.

[21] S. A. Nabavi-Amri, A. Haghighi and M. M. Norouzi, Improving the Ageing resistance of bitumen by reduction, Pet. Sci. Technol., 33, 2015, 780-786.

[22] British Standard EN 1427:2015, Bitumen and bituminous binders- Determination of the softening point- Ring and Ball method.

[23] British Standard EN 13588:2008, Bitumen and bituminous binders- Determination of cohesion of bituminous binders with pendulum test.

[24] Mastering bitumen for better roads and innovative applications, École des Ponts ParisTech, Rheology of bitumens video, https://www.coursera.org/lecture/mastering-bitumen/17-rheology-of-bitumens-8J4Ji, ACCESSED 27.07.2018, 14:06.

[25] S.Saoula, K. Soudani, S. Haddadi, M. E. Munoz, A. Santamaria, Analysis of the rheological behaviour of bitumen and predicting the risk of permanent deformation of asphalt, *Materials Sciences and Applications,* **4,** 2013, 312-318.

[26] X. Li, A. Zofka, M. Marasteanu and T. R. Clyne, Evaluation of field ageing effects on asphalt binder properties, *Road Mater. Pavement*, EATA, 2006, 57-73.

[27] A. Kebritchi, A. Jalali-Arani and A. A. Roghanizad, Rheological behaviour and properties of bitumen modified with polymeric coated precipitated calcium carbonate, *Constr. Build, Mater.,* **25,** 2011, 2875-2882.

[28] B. Sengoz, L. Bagayogo, J. Oner and A. Topal, Investigation of rheological properties of transparent bitumen, *Constru. Build. Mater.,* **154,** 2017, 1105-1111.

[29] British Standard EN 13074 2:2011, Bitumen and bituminous binders- Recovery of binder from bituminous emulsion or cut-back or fluxed bituminous binders. Stabilisation after recovery by evaporation.

[30] British Standard, EN. 12607-1: Bitumen and bituminous binders- Determination of the resistance to hardening under the influence of heat and air, RTFOT method. (2007) British Standards Institution.

[31] D. Gershkoff, A38 Pervious Mecadax Trial 1984: Binder Rheology before and after artificial hardening, Transport and Road Research Laboratory, Dept. Transport, Unpublished Work, 1984.

[32] A. Verhasselt, "Long-term ageing – Simulation by RCAT ageing tests". 9th International Conference on Asphalt Pavements, Conference proceedings in PDF format - vol.1, paper 1: 1-2 (16 p.), Copenhagen, August 17-22, 2002.

[33] British Standard EN 15323:2007, Bitumen and bituminous binders-Accelerated long-term ageing/ conditioning by the rotating cylinder method (RCAT).

[34] ASTM International, Designation: D6521-13, Standard Practice for accelerated ageing of asphalt binder using a pressure ageing vessel (PAV), 2016.

[35] British Standard EN 14769:2012, Bitumen and bituminous binders -Accellerated long-term Ageing conditioning by a Pressure Ageing Vessel (PAV).

[36] W. Zeng, S. Wu, J. Wen and Z. Chen, The temperature effects in ageing index of asphalt during UV ageing process, *Constr. Build Mater.,* **93,**2015, 1125-1131.

[37] F. Durrieu, F. Farcas, V. Mouillet, The influence of UV ageing of a styrene/butadiene/styrene modified bitumen: comparison between laboratory and on site ageing, *Fuel,* **86,** 2007, 1446-1451.

[38] Z. G. Feng, J. Y. Yu, H. L. Zhang, D. L. Kuang and L. H. Xue, Effect of ultraviolet ageing on rheology, chemistry and morphology of ultraviolet absorber modified bitumen, *Mater. Struct.,* **46,** 2013, 1123-1132.

[39] X. Lui, S. Wu, L. Pang, Y. Xiao and P. Pan, Fatigue properties of layered double hydroxides modified asphalt and its mixture, *Adv. Mater. Sci. Eng.*, 2014.

[40] F. Ye, J. Yang and P. Huang, Performance of modified asphalt ageing under ultraviolet radiation. In: Pavement Mechanics and Performance-GeoShanghai International Conference, 2006.

[41] J. Y. Yu, P. C. Feng, H. L. Zhang and S. P. Wu, Effect on organo-montmorillonite on ageing properties of asphalt, *Constr. Build Mater.*, **23,** 2009, 2636-2640.

[42] T. Yi-Qui, W. Jia-Ni, F. Zhong-Liang and Z. Xing-Ye, Influence and mechanism of ultraviolet ageing on bitumen performance, 26th Southern African Transport Conference, Pretoria South Africa, 2007, 726-735.

[43] Y. Tan, F. Zhongliang, Z. Xiingye et al., The evaluation method study of the anti-ultraviolet ageing ability of asphalt, *Science Paper Online*, 2003.

[44] V. Mouillet, F. Farcas and S. Besson, Ageing by UV radiation of an elastomer modified bitumen, *Fuel*, **87,** 2008, 2408-2419.

[45] V. C. F. Lins, M. F. A. S. Araujo, M. I. Yoshida, V. P. Fessaz, D. M Andrada and F. S. Lameiras, Photodegradation of hot mix asphalt, *Fuel*, **87,** 2008, 3254-3261.

[46] M. F. A. Araujo, V.C.F. Lins, and V. M. D. Pasa, Effect of ageing on porosity of hot mix asphalt, *Brazilian Journal of Petroleum and Gas*, **5,** 2011, 11-18.

[47] M. Lopes, D. Zhao, E. Chailleux, M. Kane, T. Gabet, C. Petiteau and J. Soares, Characterisation of ageing processes on the asphalt mixture surface, *Road Mater. Pavement*, **15(3),** 2014, 477-487.

[48] Y. Hachiya, K. Nomura and J. Shen, Accelerated Ageing tests for bitumen concretes, 6th RILEM Symposium, PTEBM'03, Zurich, 2003.

[49] J. C. Petersen, Chemical composition of asphalt as related to asphalt durability-state of the art, *TRB*, **999,** 1984, 13-30.

[50]J. C. Petersen, P. M. Harnsberger and R. E. Robertson, Factors affecting the oxidation and age hardending kinetics of asphalt and the relative effects of oxidation products on viscosity, *Preprints, Division of Fuel Chemistry, ACS*, **41(4),** 1986, 1232-1244.

[51] S.A. Nabavi-Amri, A. H. Asl, and M. M. Norouzi, Improving the ageing resistance of bitumen by reduction, *Pet. Sci. Technol.*, **33,** 2015, 780-786.

[52] Y. R. Kim and J. H. Lee, Evaluation of the effect of ageing on mechanical and fatigue properties of sand asphalt mixtures, *KSCE J. Civ. Eng.*, **7,** 2003, 389-398.

[53] J. C. Petersen and R. Glaser, Asphalt oxidative mechanisms and the role of oxidation products on age hardening revisited, *Road Mater. Pavement,* **12,** 2011, 795-819.

[54] J. Minglin, Y. Junhe, F. Anzu and S. Meiren, Analysis of ageing behaviour of South Korea 70 asphalt. Part 1. Changes of component and property, *Coal Conversion ,* **24,** 2001, 92-95 .

[55] J. C. Petersen, Asphalt oxidation-An overview including a new model for oxidation proposing that physiochemical factors dominate oxidation kinetics, *Fuel,* **11,** 1993, 57-58.

[56] R. M. Harrison, *Pollution: Causes, Effects & Control,* Royal Society of Chemistry, Cambridge, 1990.

[57] M. C. DeRosa and R. J. Crutchley, Photosensitised singlet oxygen and its applications, *Coordin. Chem. Rev.,* **233-234,** 2002, 351-371.

[58] C. S. Foote, Mechanisms of addition of singlet oxygen to olefins and other substrates, *Pure Appl. Chem.* **27(4)**, 1971.

[59] C. S. Foote and J. W. Peters, Chemistry of singlet oxygen. XIV. Reactive intermediate in sulphide photooxidation, *J. Am. Chem. Soc.,* **93**(15), 1971, 3795-3796.

[60] S. Li, J. Matthews and A. Sinha, Atmospheric hydroxyl radical production from electronically excited $NO_2$ and $H_2O$, *Science*, **319** (5870), 2008, 165-1660.

[61] Forster, P., V. Ramaswamy, P. Artaxo, T. Berntsen, R. Betts, D.W. Fahey, J. Haywood, J. Lean, D.C. Lowe, G. Myhre, J. Nganga, R. Prinn, G. Raga, M. Schulz and R. Van Dorland, 2007: Changes in Atmospheric Constituents and in Radiative Forcing. In: Climate Change 2007: The Physical Science Basis. Contribution of Working Group I to the Fourth Assessment Report of the Intergovernmental Panel on Climate Change [Solomon, S., D. Qin, M. Manning, Z. Chen, M. Marquis, K.B. Averyt, M.Tignor and H.L. Miller (eds.)]. Cambridge University Press, Cambridge, United Kingdom and New York, NY, USA.

[62] Solarchem Environmental Systems, The UV/ Oxidation handbook, http://infohouse.p2ric.org/ref/27/26568.pdf, ACCESSED 11.06.2018, 10:15.

[63] J. Zhang, A. K. Apeagyei, G. D. Airey and J. R. A. Grenfell, Influence of aggregate mineralogical composition on water resistance of aggregate-bitumen adhesion, *Int. J. Adhe. Adhe.,* **62**, 2015, 45-54.

[64] J. Zhang, A. K. Apeagyei, H. Grenfell and G. D. Airey, Experimental study of moisture sensitivity of aggregate-bitumen bonding strength using a new pull-off test, in the *8th RILEM International Symposium on Testing and Characterisation of Sustainable and Innovative Bituminous Materials,* RILEM Bookseries 11, DOI 10.1007/978-94-017-7342-3_58.

[65] J. A. H. Noguera, H. A. R. Quintana and W. D. F. Gomez, The influence of water on the oxidation of asphalt cements, *Const. Build. Mater.*, **71,** 2014, 451-455.

[66] J.G. Geng, H. Li, W.G. Li, Aging characteristic of styrene-butadiene-styrene modified asphalt under thermal-humidity conditions, *Int. J. Pavement Res. Technol*. **7** (5) (2014) 376–380.

[67] Q. Wang, S. Li, X. Wu, S. Wang and C. Ouyang, Weather ageing resistance of different rubber modified asphalts, *Constr. Build Mater.*, **106,** 2016, 443-448.

[68] B. Stuart, B. George and P. McIntyre, *Modern Infrared Spectroscopy*, John Wiley and Sons, Chichester, 1996.

[69] S. Richard and P. T. Leung, Identification and evaluation of coatings using handheld FTIR, *Agilent Technologies Inc*, *Publ.* 5990-8075EN, 2011.

[70] A. Rein and F. Higgins, At site rock and mineral analysis measurement using a handheld Agilent FTIR analyser, *Agilent Technologies Inc, Publ*, 5990-7794EN, 2011.

[71] A. Rein, FTIR analysis provides rabid QA/QC and authentication of food ingredients prior to processing, *Agilent Technologies Inc., Publ.*, 5991-1246 EN, 2012.

[72] K. Nakamoto, *Infrared and Raman Spectra of inorganic and coordination compounds*, John Wiley and Sons, New York, USA, 1986.

[73] S. M. Dorrence, F. A. Barbour and J. C. Petersen, Direct evidence of ketones in oxidized asphalts, *Analytical Chemistry*, **46,** 1974, 2242-2244.

[74] J. C. Petersen, Quantitative method using differential infrared spectrometry for determination of the compound types absorbing in the carbonyl region in asphalts, *Analytical Chemistry*, **47,** 1975, 112-117.

[75] H. Plancher, E. L. Green and J. C. Petersen, reduction of oxidative hardening of asphalts by treatment with hydrated lime: a mechanistic study, *Proc., Association of asphalt paving technologist*, **45,** 1976, 1-24.

[76] J. C. Petersen and H. Plancher, Quantification determination of carboxylic acids by selective chemical reactions and differential infrared spectrometry, *Analytical Chemistry*, **53,** 1981, 786-789.

[77] M. Lui, M. A. Ferry, R. R. Davison, C. J Glover and J. A. Bullin, Oxygen uptake as correlated to carbonyl growth in aged asphalts and asphalt Corbett fractions, *Ind. Eng. Chem. Res*, **37,** 1998, 4669-4674.

[78] R. Karlsson, and U. Isacsson, Investigations on bitumen rejuvenator diffusion and structural stability (with discussion), *J., Assoc., Asphalt Pav.,* **72,** 2003, 463-501.

[79] K. Yamaguchi, I. Sasaki and S. Meiarashi, Photodegradation test of asphalt binder using pressed thin film samples, *Can., J., Civ., Eng.,* **32,** 2005, 1166-1169.

[80] M. R. Nivitha, E. Prasad and J. M. Krishnan, Ageing in modified bitumen using FTIR spectroscopy, *Int. J. Pav. Eng.,* 565-577, **17** (7)**,** 2015.

[81] F. M. Mirabella, *Internal Reflection Spectroscopy: Theory and Applications,* Practical Spectroscopy Series, Marcel Dekker Inc, 1992.

[82] Molecular Expressions, Optical Microscopy Primer, Physical of Light and Colour, Interactive tutorial, Refraction of Light, http://micro.magnet.fsu.edu/primer/java/refraction/refractionangles/index.html, ACCESSED 13.07.2018, 09:32.

[83] Perkin Elmer Technical Note, Reflection Measurements in IR spectroscopy, R. Spragg, Perkin Elmer Inc. Seer Green, UK, https://www.perkinelmer.com/CMSResources/Images/44-153348TCH_reflection-Measurements.pdf ACCESSED 30.05.2018 17:12.

[84] British Standard EN 13108-1:2006, Bituminous mixtures, Asphalt Concrete.

[85] Agilent 4100 ExoScan FTIR, Operation Manual, Agilent Technologies, https://www.agilent.com/cs/library/usermanuals/Public/0023-401.pdf, ACCESSED 13.07.2018, 09:56.

[86] A. Khursheed, *Scanning Electron Microscope optics and spectrometers*, World Scientific Publishing Co Pte Ltd, Singapore, 2014, EBOOK ISBN 9789812836687.

[87] R. F. Egerton, *Physical Principlesof Electron Microscopy: An Introduction to TEM, SEM and AEM,* Springer, New York, 2006, EBOOK ISBN 9780387260167.

[88] A. Striegel, W. W. Yau, J. J. Kirkland and D. D. Bly, *Modern Size-Exclusion Liquid Chromatography: Practice of Gel Permeation and Gel Filtration Chromatography,* Wiley, New Jersey, 2009, EBOOK ISBN 9780470442838.

[89] J. W. Nicholson, *The Chemistry of Polymers,* Royal Society of Chemistry, United Kingdom, 2017, ISBN 9781788011143.

[90] Technical Overview, *Polymer Molecular Weight Distribution and Definitions of MW Averages,* Agilent Technologies Inc., USA, 2015, 5990-7890EN, https://www.agilent.com/cs/library/technicaloverviews/Public/5990-7890EN.pdf.

[91] R.J. Young and P.A. Lovell, *Introduction to Polymers*, Taylor & Francis, London, 1991.

[92] R. F. T. Stepto, R. G. Gilbert, M. Hess, A. D. Jenkins, R. G. Jones and P. Kratochvíl, Dispersity in Polymer Science, *Pure Appl. Chem*. **81 (2),** 351–353.

# Chapter 2

## Artificial and natural ageing of bitumen-Infrared spectroscopic analysis

This chapter outlines the experimental procedures and the results obtained from the ageing experiments on raw bitumen. The aim of these experiments was to determine whether Attenuated Total Reflectance (ATR) and Diffuse Reflectance Infrared Fourier Transform (DRIFT) spectroscopy can be utilised to monitor chemical changes that occur upon oxidation of bitumen.

The experimental approach to this project began by ageing raw bitumen and identifying any chemical changes as a result of oxidation. The ageing experiments have been devised to expose raw bitumen to extremely harsh conditions in order to maximise the amount of oxidation within the bitumen and enhance the measureable change in the infrared spectra and physical properties. This will allow the areas of interest within the infrared spectrum that correspond to chemical oxidation to be identified. Once these areas have been highlighted it is possible to look for smaller changes within samples that have been aged less harshly, for example in the case of natural ageing.

The Extended Rolling Thin Film Oven (E-RTFO) test and UV light exposure have been used here as enhanced ageing techniques in order to attempt to mimic the thermal cycling of bitumen when being applied to road surfaces and also the environmental conditions. The results from these artificial ageing tests have also been compared to those measured from naturally aged raw bitumen.

Gel Permeation Chromatographic (GPC) analysis has been carried out on all of the samples in order to assess the molecular weight changes of the molecules within the bitumen composition as the bitumen is aged. Scanning Electron Microscopy (SEM) has been carried out on the test samples in order to visualise the surface structure of the bitumen and to determine whether or not changes in physical microstructure may be related to chemical changes. SEM-EDX analysis was also carried out in order to characterise the elemental composition of the raw bitumen.

## 2.1 Enhanced ageing of bitumen-Extended Rolling Thin Film Oven test

The Rolling Thin Film Oven (RTFO) test is a standardised method (EN, BS 12607-1, 2007)[1] that replicates the oxidative ageing that the bitumen will experience while in transit to the road site.[2] The test involves heating and pouring raw bitumen (35 g) into pre-weighed, standardised glass vessels (64 mm diameter, 140 mm height) and placing them into a carousel in the RTFO. The oven is heated to 163 ˚C and the carousel is rotated at 15 rpm. At the bottom of the oven there is a compressed air inlet which blows compressed air into the glass vessels at a flow rate of 4 L/min. The standardised test length is 75 minutes. For this project the time for the test was extended to 225 minutes, in an attempt to intensify the oxidative ageing, and time point samples were collected every 75 minutes. This modified RTFO test will be referred to as the Extended RTFO (E-RTFO) test and has been replicated from the studies of Gershkoff *et al.* [3] at the Transport Research Laboratory (TRL). Upon removal of the sample from the RTFO the glass vessels were re-weighed and the change in weight of the bitumen was measured.

The bitumen samples at each time point were analysed using the ExoScan 4100 handheld spectrometer with an ATR detector. Three spectra were taken from a sample of bitumen aged for 75, 150 and 225 minutes, and each spectrum is an average of 32 scans at a 4 $cm^{-1}$ resolution.

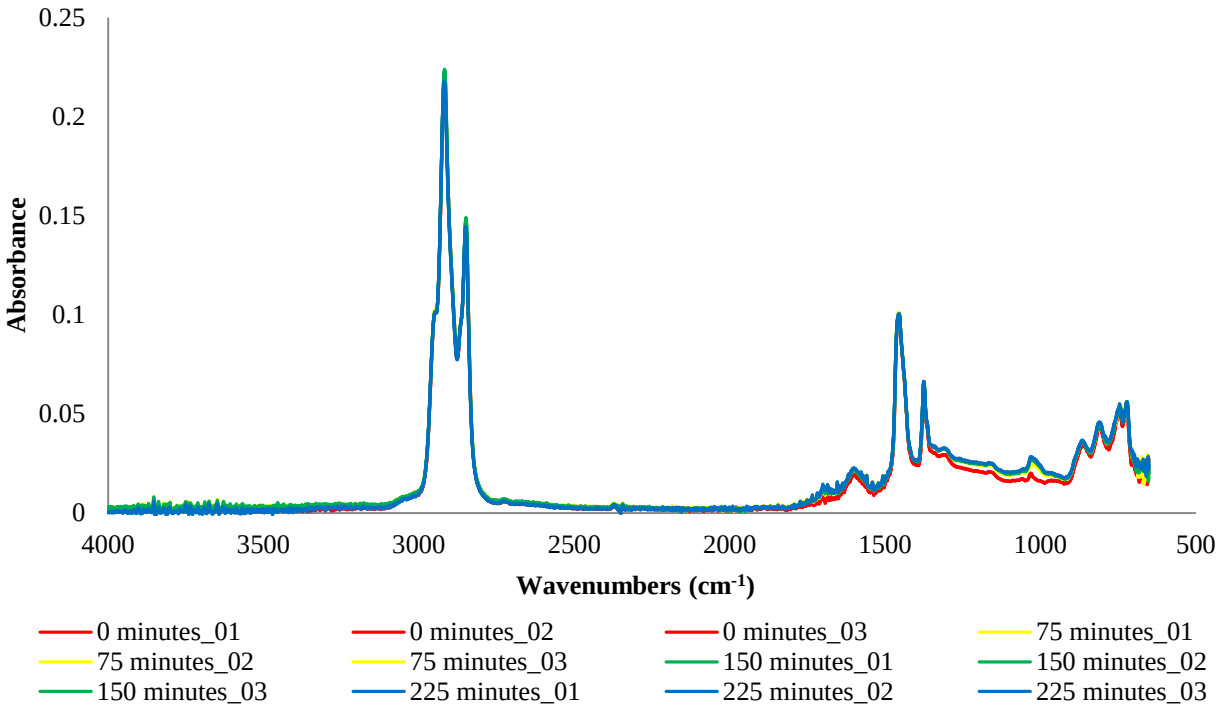


**Figure 2. 1 Full range (4000-680 $cm^{-1}$) ATR-FTIR spectra from the raw bitumen samples that have been aged in the E-RTFO test for 0-225 minutes. Three replicate spectra from each time point sample.**

There are a number of absorbance bands present within Figure 2.1 that can be assigned to the hydrocarbon composition of the bitumen. There are also several key bands that could correspond to oxidation products. Table 2.1 lists the absorbance band frequencies in the spectrum and the bond assignment.

**Table 2. 1 Absorbance bands and their assignments from the ATR-FTIR spectra of the raw bitumen that has been aged in the E-RTFO test, Figure 2.1. [4]**

| Wavenumber ($cm^{-1}$) | Bond Assignment | |
|---|---|---|
| **2920, 2850** | C-H stretch | Hydrocarbon Alkane |
| **1713** | C=O stretch | Carbonyl Oxidation Product |
| **1600** | C=C bend | Aromatic Hydrocarbon |
| **1455, 1375** | C-$H_2$ bend | Hydrocarbon |
| **1170** | C-O | Carboxylic Oxidation Product |
| **1032** | S=O | Sulfoxide Oxidation Product |
| **870, 812** | C-H bending | Aromatic Hydrocarbon |

As bitumen is a mixture of many different length hydrocarbons, with varying degrees of unsaturation and aromaticity, it is as expected that there are a number of C=C and C-H bending and stretching modes identifiable in the IR spectrum. The presence of heteroatoms including oxygen and sulfur can be determined as there are some absorbance bands that correspond to carbonyl and sulfoxide bonds within the spectra in Figure 2.1.

All of the ATR spectra presented in Figure 2.1 contain quite similar features. It is only when focusing on specific areas that it is possible to detect some changes as the samples are aged. Figure 2.2 shows the spectra between the wavenumbers 1900-900 $cm^{-1}$.

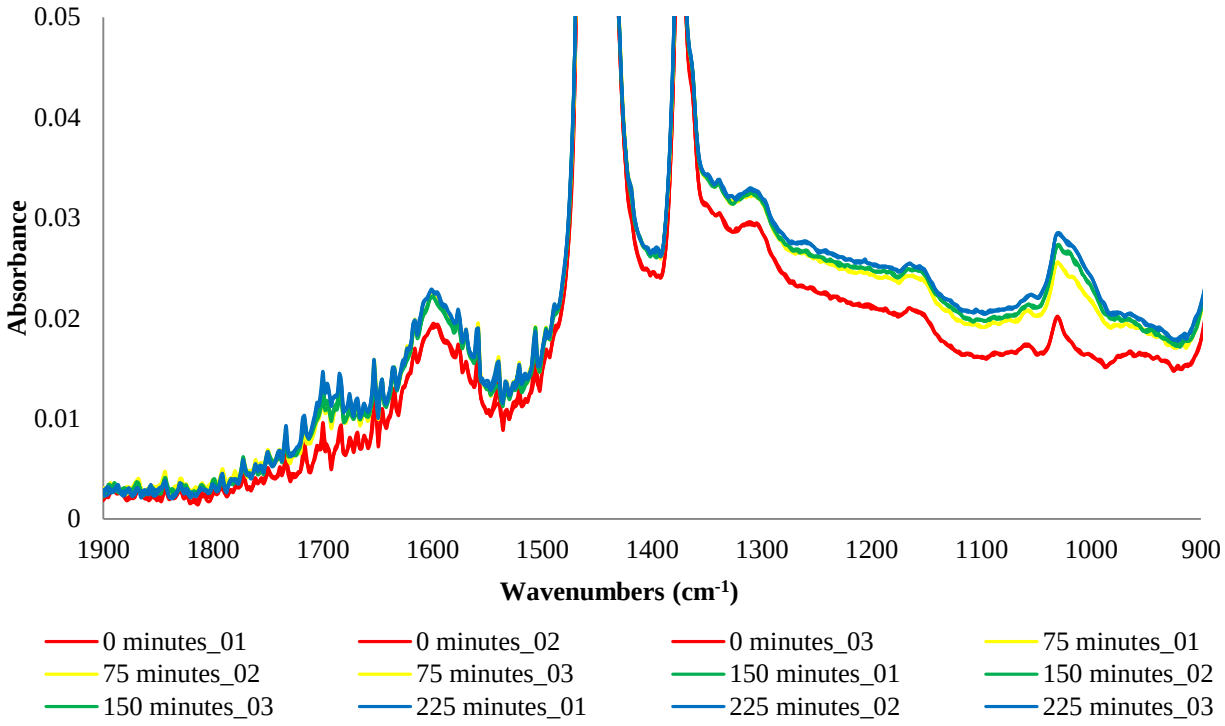


**Figure 2. 2 ATR-FTIR spectra from the raw bitumen samples that have been aged in the E-RTFO test for 0-225 minutes, between the wavenumbers 1900-900 $cm^{-1}$.**

Upon closer inspection of the ATR spectra collected from the raw bitumen (Figure 2.2) it is possible to see a change in absorbance bands arising around 1700, 1600, 1150 and 1030 $cm^{-1}$. These can be assigned to the carbonyl, C=C, C-O and sulfoxide absorbance bands respectively. An increase in these absorbance bands indicates oxidation and also an increase in aromatisation, as predicted by Robertson *et al.* [5] who state that there is an increase in aromaticity and oxygen content within the bitumen composition upon the formation and decomposition of peroxide groups.

The application of the Beer-Lambert law allows the changes in the spectra to be quantified and give an indication of the changes in concentration of the functional groups responsible for

the absorbance bands. This quantification can be done in a number of different ways. Two examples include integrating the area underneath the absorbance band or measuring the absorbance band intensity at a specific wavenumber. It is noteworthy that the actual concentration of these functional groups cannot be calculated reliably with this data, without the use of a calibration curve of some kind. Therefore this analysis provides only a change indicator as opposed to 'real' concentration data.

The average integration has been carried out in this work using the OMNIC software, two base wavenumbers were selected and the baseline was drawn directly between these. The software then integrates the area underneath the absorbance band and this can be recorded.

Figure 2.3 outlines the results of the average integration of the carbonyl (1735-1659 $cm^{-1}$) and sulfoxide (1064-974 $cm^{-1}$) absorbance bands from three spectra from the bitumen aged in the E-RTFO test. The error bars displayed are the 95% limits for the three results, from three spectra from each sample.

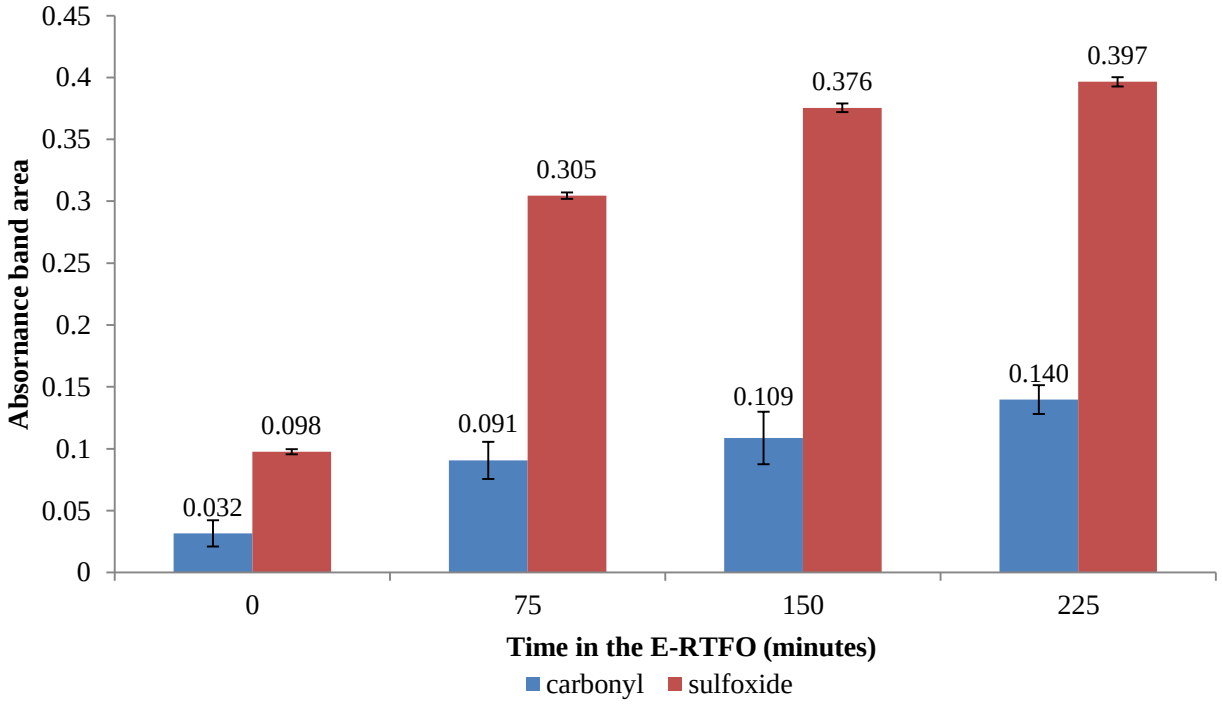


**Figure 2. 3 Integrated carbonyl (1735-1659 $cm^{-1}$) and sulfoxide (1064-974 $cm^{-1}$) absorbance band areas from the ATR-FTIR spectra of the raw bitumen that has been aged in the E-RTFO test between 0-225 minutes**

The integrated absorbance band areas are seen to increase as the time in the E-RTFO test increases for the carbonyl (+314 %) and the sulfoxide (+307 %) absorbance bands. This can correlate to an increase in concentration of the two functional groups within the composition of the bitumen.

An alternative method for quantification is to record the absorbance value at the apex of the absorption band. This has also been carried out here using the OMNIC software, in which a wavenumber can be selected and the software will display the absorbance value measured at this wavenumber. Figure 2.4 outlines the absorbance at 1700 $cm^{-1}$ from the ATR-FTIR spectra presented in Figure 2.2.

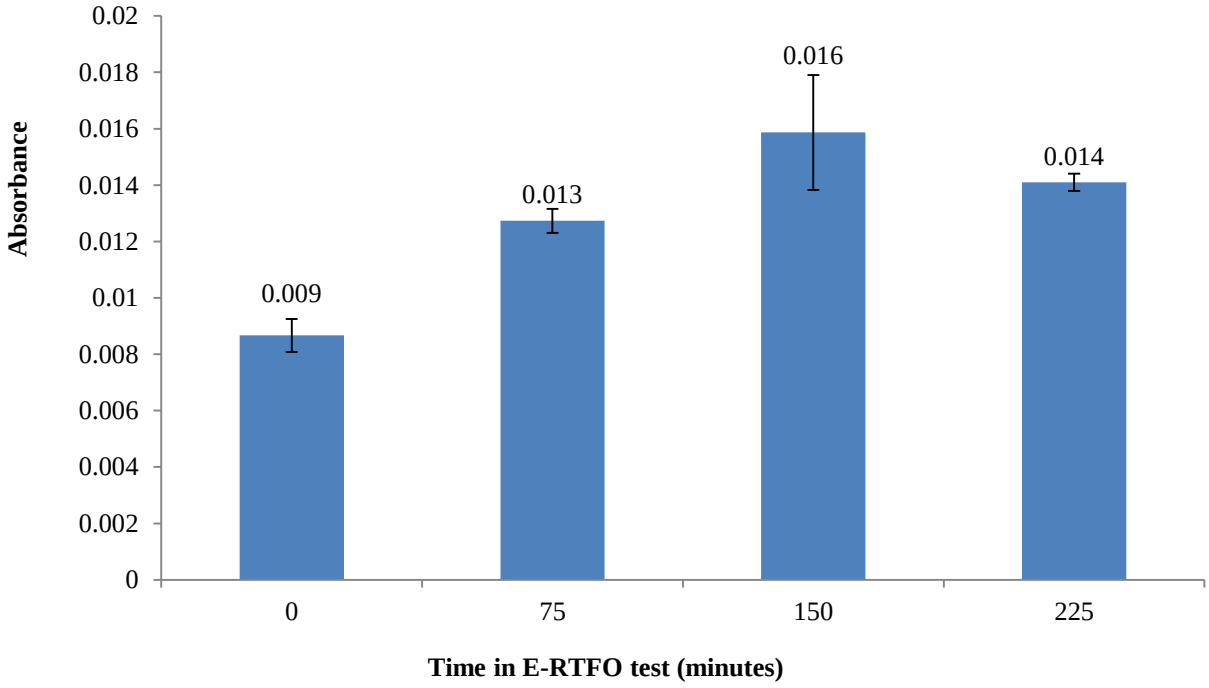


**Figure 2. 4 Absorbance measured at 1700 $cm^{-1}$ from the ATR spectra from the raw bitumen that has been aged in the E-RTFO test for 0-225 minutes**

The absorbance value at 1700 $cm^{-1}$ is seen to increase between 0 to 225 minutes, (55 %). The error bars for the bitumen sample that was aged in the E-RTFO test for 150 minutes is an anomalous results with a large error bar in comparison with the other samples. This suggests that there is not a significant change between the older sample and the result is likely representative of a plateau.

GPC analysis separates the molecules within the bitumen composition based on their molecular weight. GPC has been carried out on the raw bitumen that has been aged in the E-RTFO test in 2 mg/mL concentration solution in THF. Figure 2.5 shows the chromatograms measured by the GPC.

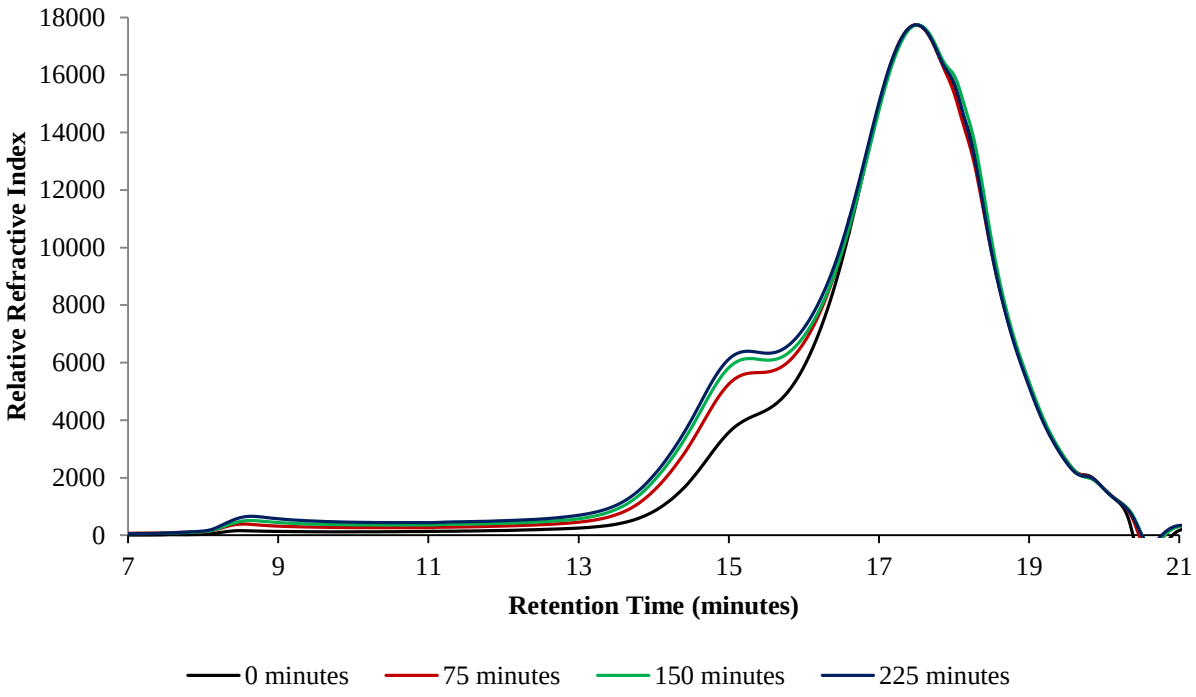


**Figure 2. 5 Gel Permeation Chromatography spectra of the raw bitumen that has been aged in the E-RTFO test for 0-225 minutes**

As the sample moves through the GPC column and is detected by the refractive index detector a peak is measured on the chromatogram. The chromatogram produced by the GPC separation of the bitumen displays a large peak at approximately 17.5 minutes. This corresponds to the bulk of the bitumen molecules eluting through the column and being detected by the refractive index detector. The higher molecular weight molecules elute at a shorter retention time and a shoulder can be seen on this main peak. As the raw bitumen is aged there is an increase in the band at approximately 15 minutes retention time. This indicates that as the bitumen is aged there is an increase in higher molecular weight molecules within the composition. This can be attributed to the increase in oxygen upon formation of carbonyl, carboxylic, sulfoxide and alcohol groups. The high temperatures of the extended rolling thin film oven test (163 ˚C) allow for reactions such as the Spurt reaction described in Chapter 1.[6] The free radicals produced in this Spurt reaction can be used to initiate more oxidation reactions to produce further carbonyl, carboxylic, sulfoxide and alcohol groups.

Table 2. 2 GPC separation results of the raw bitumen samples that have been aged in the E-RTFOT 2.2 contains the molecular parameters measured by the GPC with $M_n$ indicating the number average molecular weight. $M_w$ is weight average molecular weight, and Đ represents the polydispersity index.

**Table 2. 2 GPC separation results of the raw bitumen samples that have been aged in the E-RTFOT**

| Time in E-RTFO test (minutes) | $M_n$ (g $mol^{-1}$) | $M_w$ (g $mol^{-1}$) | Đ |
|---|---|---|---|
| **0** | 640 | 1900 | 2.97 |
| **75** | 680 | 2400 | 3.53 |
| **150** | 680 | 2500 | 3.68 |
| **225** | 710 | 2700 | 3.80 |

The number average molecular weight ($M_n$) increased by 11% after 225 minutes in the RTFO, however; this change is not outside of the error limits of the GPC analyses.[7] This result suggests that there is not a large change in the number of different molecular weight molecules being created which would be the case if the molecule was being broken down and a large number of different molecular sizes were being formed. There was an increase in the weight average molecular weight (by 42%). The weight average molecular weight is affected by the weight of the molecules; therefore the increase $M_w$ indicates that there is an increase in molecular weight of the molecules as a result of the addition of oxygen. The polydispersity index also increased in value with time in the E-RTFO test. The polydispersity index is the ratio of the $M_w/M_n$ and therefore this change confirms that there was an increase in $M_w$ and a lesser increase in $M_n$.

After the glass vessels were removed from the RTFO the weight was recorded so the weight loss could be calculated. The results of these measurements can be found in Table 2.3.

**Table 2. 3 Weight lost from the raw bitumen as the samples were aged in the E-RTFO test**

| Time in the E-RTFO test (minutes) | Weight Loss (g) | % Weight Change |
|---|---|---|
| **0** | - | 0 |
| **75** | 0.2 | 0.08 |
| **150** | 0.2 | 0.08 |
| **225** | 0.3 | 0.1 |

This weight loss recorded was only a 0.1% decrease in weight of the total sample. This is very low, however, the loss of volatiles from bitumen is expected to be low as much of the volatile

material is lost from the crude oil separation and used for other purposes, light solvents, burner oils and lubricating oils for example.[8] After the fractional distillation process is finished there are very few volatiles remaining and therefore a very small weight loss is recorded. Deygout *et al.* [9] have analysed the volatiles released from heated bitumen, trapped in the headspace above the bitumen that is being held within storage tanks with GPC, Flame Ionisation Detection and Mass Spectrometry analysis. A range of carbon chain lengths were detected between $C_5$-$C_{14}$. This gives the volatiles an approximate maximum molecular weight of 198 (based upon a saturated hydrocarbon with the empirical formula $C_{14}H_{30}$). As such, loss of this small amount of volatiles is not expected to affect the GPC results significantly.

Scanning electron microscopy (SEM) was carried out on a sub sample of these raw bitumen samples. These samples were simple to prepare as the bitumen was malleable enough to remove a sub-sample and place onto a carbon SEM stub with a spatula. The samples were not sputter coated prior to analysis as the sample did not present any issues with charging.

The SEM images produces highly magnified (*ca.* 500 ×) images of the surface of the raw bitumen and can therefore be utilised to visualise the microstructure of the surface a sample. The elemental composition of the surface of the sample can be measured using electron dispersive X-ray analysis, (SEM-EDX). The images have been collected in a low vacuum, with a 0.68 Torr internal pressure. The voltage of the electron bean was 12.5 kV.

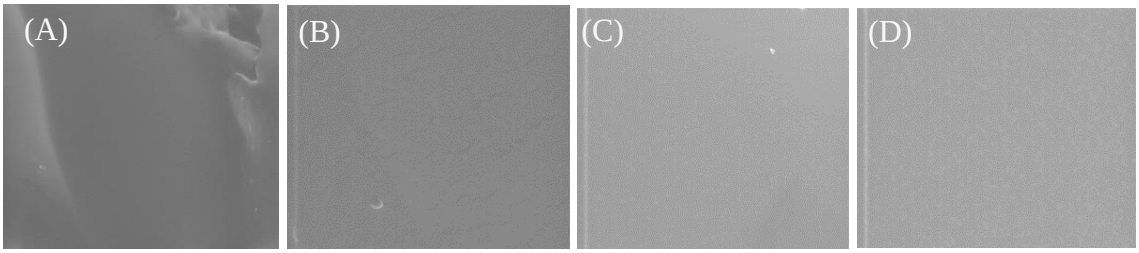


**Figure 2. 6 SEM images from the surface of raw bitumen samples that have been aged in the E-RTFO test for (A) 0 minutes, (B) 75 minutes, (C) 150 minutes and (D) 225 minutes. All images are 530 × magnification.**

The SEM images for the raw bitumen samples reveal very little in the way of structural detail. Bitumen is a smooth and shiny black material to the eye, and under the high magnification of the SEM there is a very smooth microstructure, which is unchanging as the sample ages. Elemental analysis mapping results of the unaged raw bitumen (T0) can be seen in Figure 2.7. Elemental maps highlight the areas where there is an abundance of a specific element present that exceeds an internal threshold value.

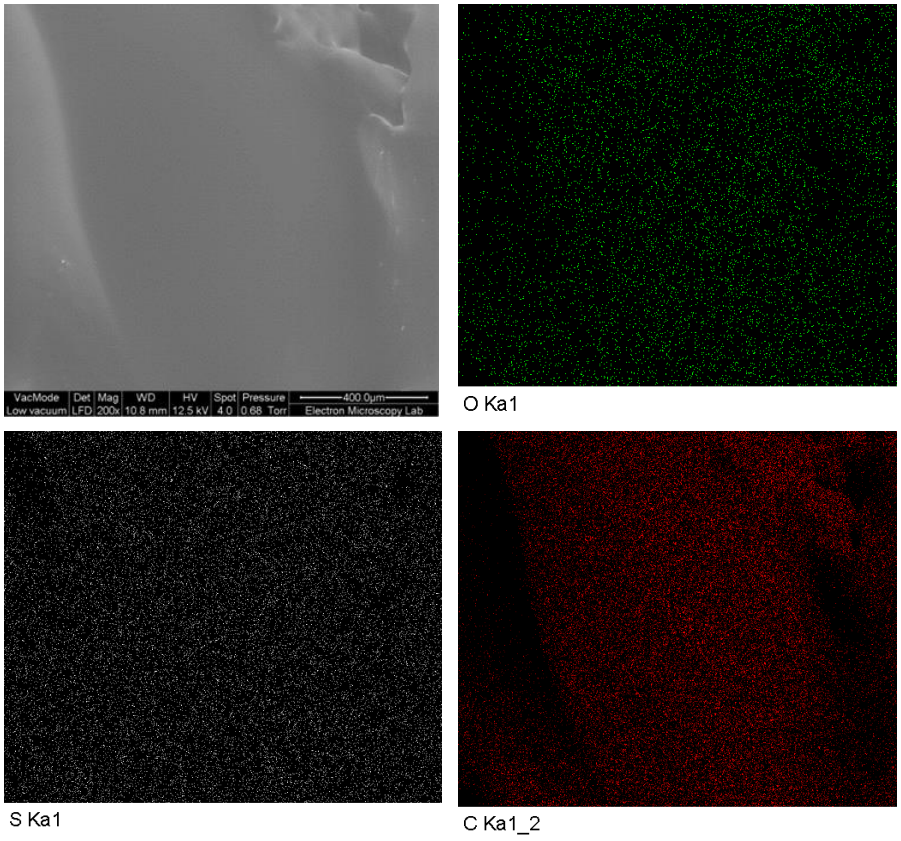


**Figure 2. 7 SEM-EDX image and elemental maps of carbon, oxygen and sulphur from the surface of the raw bitumen that has not been aged (time 0). SEM image is at 200 × magnification.**

It is known that the chemical composition of bitumen is a network of hydrocarbon chains and the elemental analysis confirms that the bulk of the composition is carbon.[8] Hydrogen is not detected *via* SEM-EDX as there are no electron transitions that can occur because hydrogen only has one electron within one orbital. Oxygen has also been detected by the SEM-EDX system. This indicates the presence of oxygen heteroatoms in the composition of the bitumen. These could have been introduced throughout the fractional distillation process which involves high temperatures in order to extract the lighter components of the original crude oil source. The elemental analysis also confirms the presence of sulfur within the composition of the bitumen. This helps to confirm the assignment of the sulfoxide peak within the ATR spectra from the aged bitumen samples, (Figure 2.1 and Figure 2.2). The SEM-EDX software is able to use the intensity and the frequency of X-rays detected from the elemental analysis to quantify the amount of the element present, relative to the others that are detected. This analytical process works well to identify and quantify the presence of heavy elements (metals for example), however, the lighter atoms (Nitrogen is a common example) can be unreliable to quantify.

Oxygen is very difficult to quantify in a reliable manner as the low vacuum is maintained with the help of water vapour in the chamber.[10] Therefore, it would be unreliable to measure the change in the oxygen values measured from the raw bitumen as it is aged.

This analysis has detected the presence of oxidation product absorbance bands in the IR spectra, upon enhanced ageing of the bitumen in the E-RTFO test.

## 2.2 Enhanced ageing of bitumen- Ultra-Violet light

Ultra-Violet (UV) light has been used to age the raw bitumen samples within a UV chamber manufactured at TRL. The bitumen samples were placed into the chamber and exposed to broad band UV light with a maximum at 368 nm, while being held at a temperature of 60 ˚C. This temperature was selected based upon the results published by Yi-Qiu *et al.*,[11] who determined that the combination of thermal and UV energy is the most efficient for oxidation, and is not an uncommon surface temperature for asphalt on a summers day. Samples were removed from the chamber at weekly intervals for a total of 3 weeks. One bitumen sample was placed into the UV chamber as a control at the start of the experiment with a cover so the sample was not exposed to the UV light but did experience the thermal ageing.

It was noted that upon UV ageing a brittle 'skin' was formed on the top of the bitumen sample. This did not occur on the surface of the control bitumen sample therefore this phenomenon can be attributed to the action of the UV light. A visual comparison of the surface of the 3 week UV aged bitumen sample and the unaged bitumen sample is shown in Figure 2.8.

**Figure 2. 8 Photograph of the raw bitumen samples that are unaged (left) and aged for 3 weeks in the UV chamber (right)**

'Skinning' is a term used to describe the formation of this brittle skin on the surface of the bitumen. Skin formation has been attributed to the evaporation of any remaining volatiles

organic compounds and the oxidation of the surface.[12] The skin protects the bulk bitumen from further oxidation while the skin is unbroken. This skinning can occur during heating and storage of bitumen and can be prevented by either blanketing the surface with an inert atmosphere or gently agitating the bitumen, the latter of which is an easier and safer skin prevention method. The development of the rolling thin film oven test was partly to prevent this skin formation during the enhanced ageing testing.[13]

Analysis by ATR-FTIR spectroscopy was attempted in order to study the surface of the UV aged bitumen, however, the hardness of the skin that formed meant that efficient contact between the ATR crystal and the top of the sample was difficult to achieve. Therefore diffuse reflectance infrared Fourier transform (DRIFT) spectroscopy was utilised instead. As mentioned previously this is the desired analysis technique for the analysis of asphalt.

Diffuse reflectance spectra, as mentioned in the introduction of this thesis (Chapter 1), are visually different to the ATR spectra which have a flat baseline and a good signal to noise ratio. DRIFT spectra have a more variable baseline and therefore the DRIFT spectra presented in this report have been normalised at 4000 $cm^{-1}$ to 1 in order to simplify and more readily, visually compare the spectra.

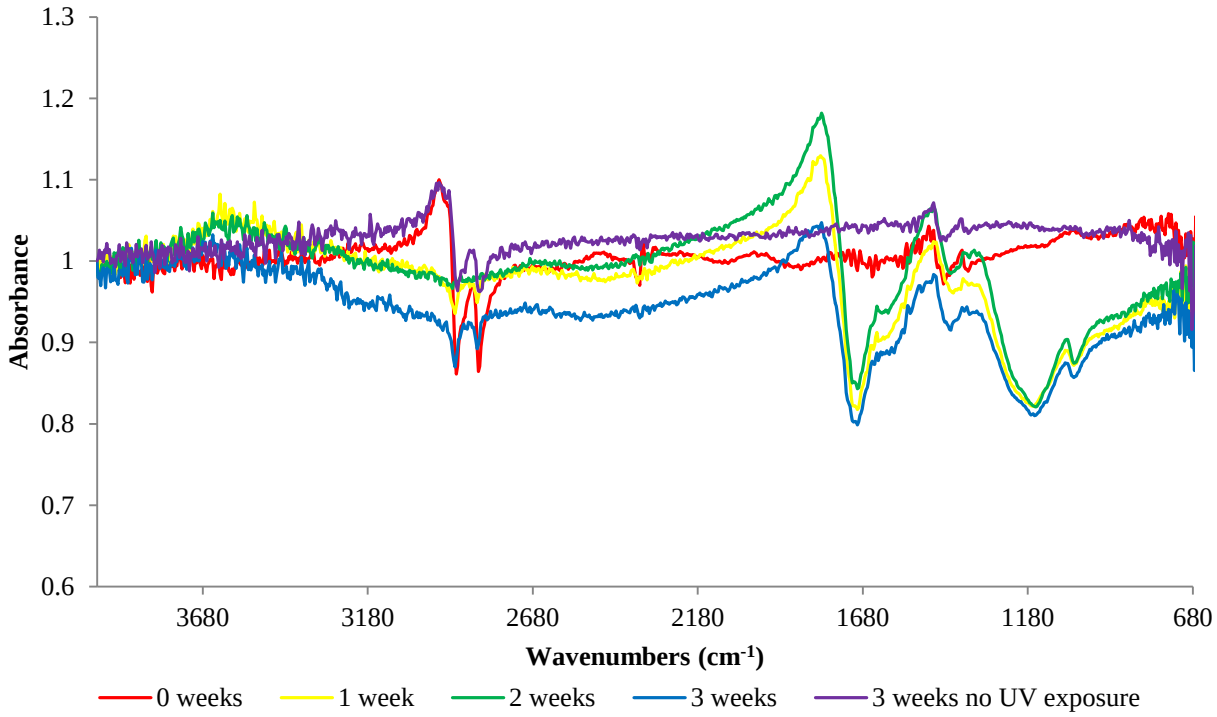


**Figure 2. 9 DRIFT spectra from the surface of the raw bitumen that had been aged in the UV champer for 0, 1, 2 and 3 weeks, with a control sample (purple) that had 3 weeks ageing in the UV chamber with no UV exposure. Spectra are normalised at 4000 $cm^{-1}$.**

Despite the differences in appearance between the ATR and DRIFT spectra it is possible to assign the same absorbance bands seen in the ATR spectrum of the raw bitumen. Table 2.4 outlines the absorbance bands and their positions for the spectra in Figure 2.9. The C-H bending and stretching absorbance bands are very prominent within the spectra of the unaged bitumen (T0_01) and the control sample (T3C_01). Oxidation product absorbance bands can be seen within the spectra from the raw bitumen samples that have been exposed to the UV light for 1, 2 and 3 weeks.

**Table 2. 4 Absorbance bands and their assignments from the DRIFT spectra (Figure 2.9) from the surface of the raw bitumen that has been aged in the UV chamber for 0-3 weeks**

| **Absorbance Band ($cm^{-1}$)** | **Bond Assignment** | |
|---|---|---|
| **2915, 2840** | C-H stretch | Bitumen Hydrocarbon |
| **1770** | C=O stretch | Carbonyl oxidation product |
| **1461, 1364** | C-$H_2$ bend | Bitumen Hydrocarbon |
| **1181** | C-O stretch | Carboxylic oxidation product |
| **1043** | S=O stretch | Sulfoxide oxidation product |

The carbonyl absorbance band is presenting as a first derivative in the aged spectra. First derivative features can arise within reflectance spectra when there is a change in absorbance of the sample as the IR radiation changes frequency.[14] The absorbance is based upon refractive index which is dependent upon the surface structure. The presence of the skin on the surface of the UV exposed bitumen could be the reason for the difference in refractive index compared to the unaged bitumen which has a smooth surface. First derivative absorbance bands can also occur when there is a combination of diffuse reflectance and specular reflectance occurring from the surface. Specular reflectance occurs when the light is reflecting from the surface at an angle that is equal to the incident angle. In the case of the diffuse reflectance detector for the ExoScan 4100, the incident angle is 90 ˚ to the surface and the detector surrounds this. Therefore any specular reflectance will be shone directly back in the direction of the light source and therefore not detected. This could be the reason for the loss of spectral information across a wavenumber range. The 3 week control sample and the unaged samples are the ‘shiniest’ (indicating more specular reflectance as opposed to diffuse reflectance) and there is some spectral information being collected (C-H bending and

stretching modes) therefore it is more likely that the change in refractive index is the reason for the first derivative absorbance band observed in the aged samples.

The C-O absorbance band at 1181 $cm^{-1}$ is very broad within the spectra of the UV exposed bitumen. The broadening of absorbance bands in infrared spectroscopy can be an indication of intramolecular hydrogen bonding. The hydrogen bonding causes a frequency shift of the fundamental bond absorbance to a varying extent depending on the hydrogen bond strength; therefore the absorbance band that is presented is an average of all of these frequency shifts.[15] A very common example of this is the O-H stretch of water molecules. The presence of this hydrogen bonding could be an indicator of the intramolecular bonding that leads to the increase in viscosity of the bitumen. The polar components within the bitumen, including the oxygen containing functional groups formed upon oxidation, are able to interact with other molecules in the bitumen and self-assemble, giving rise to a molecular network that is rigid and highly viscous, much like the skin formation seen here.[5] The sulfoxide absorbance band is presenting as a shoulder on this broad carboxylic absorbance band at 1043 $cm^{-1}$.

It is interesting to note the lack of oxidation product absorbance bands within the 3 week control sample (purple). This sample was placed into the chamber for 3 weeks but was covered from the UV light. As there were no oxidation-product absorbance bands detected within the control sample spectra (Figure 2.9) it can be said that the thermal energy produced by the 60 ˚C chamber temperature is not enough to initiate a measureable amount of oxidation in the bitumen alone. However, the presence of oxidation product functional group absorbance bands can be seen in the DRIFT spectra from the UV exposed bitumen samples therefore confirming that the UV light is an initiator of the oxidation of the bitumen surface. This data corresponds to the result published by Zeng *et al.*[16] who stated that UV light and thermal energy combined are the most efficient conditions for oxidation.

The quantification of absorbance bands has been widely used within the literature for ATR-IR spectroscopy and can reliably be used to detect changes in functional groups. [17,18,19] However, as a result of the increased complexity of the diffuse reflectance nature of DRIFT spectroscopy the reliability of the quantification is under question. An experiment was devised in order to prove the feasibility of utilising diffuse reflectance absorbance band integration as a reliable quantification method. Calcium carbonate was blended with polyethylene glycol (PEG) polymer to form 10 g samples with a range of different amounts of calcium carbonate being added, ranging between 0.5 - 2.5 g. The samples were poured onto

aluminium trays and cooled into a film. The samples were then analysed with the ExoScan 4100 with the diffuse reflectance detection attachment.

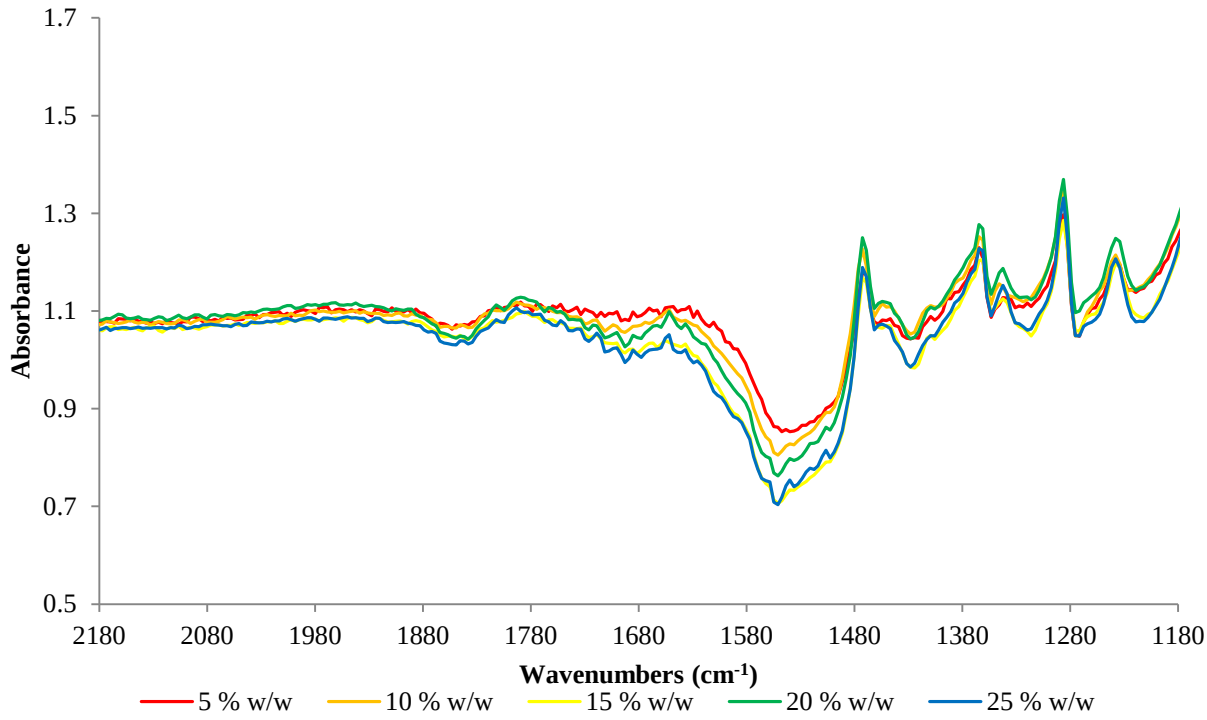


**Figure 2. 10 DRIFT spectra between the wavenumbers 2180-1180 $cm^{-1}$, from the calcium carbonate calibration curve samples between 5%-25% w/w calcium carbonate concentrations in PEG**

The absorbance bands at 1472, 1364, 1286 and 1234 $cm^{-1}$ can be assigned to the C-$H_2$ bonds bending in the PEG polymer. It is possible to see an increase in the absorbance bands at 1692 and 1535 $cm^{-1}$ which correlate to a C=O stretch and the $CO_3^{2-}$ ion fundamental asymmetric stretch, respectively. By integrating the area beneath the carbonyl absorbance band (1692 $cm^{-1}$) it is possible to quantify the increase and determine whether this DRIFT absorbance band follows the Beer Lambert Law.

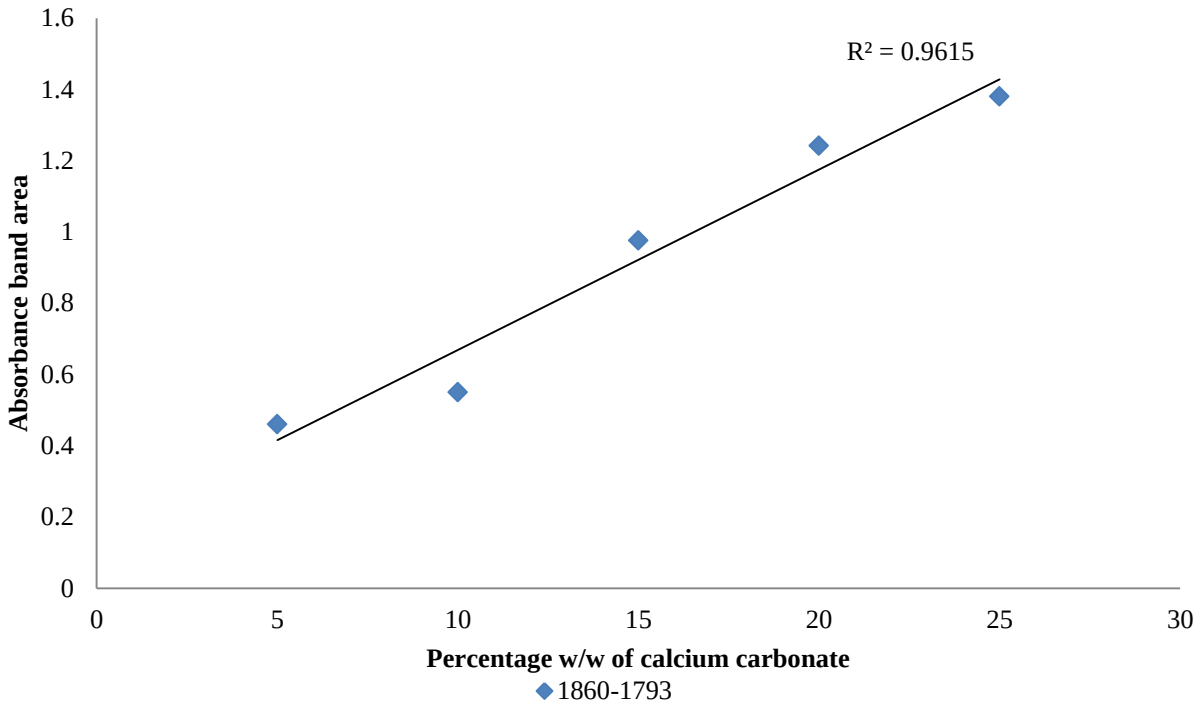


**Figure 2. 11 Calibration curve of calcium carbonate in PEG calculated using the absorbance band area between the wavenumbers 1793-1651 $cm^{-1}$ *vs*. the calcium carbonate concentration**

The linear increase (200%) in the absorbance band area between 0.5 -2.5 mg concentrations confirms that the absorbance band between the wavenumber range 1793-1651 $cm^{-1}$ follows the Beer Lambert law. By taking the absorbance value at the apex of the $CO_3^{2-}$ fundamental absorbance (1692 $cm^{-1}$) it is possible to see a linear relationship as the concentration of calcium carbonate increases.

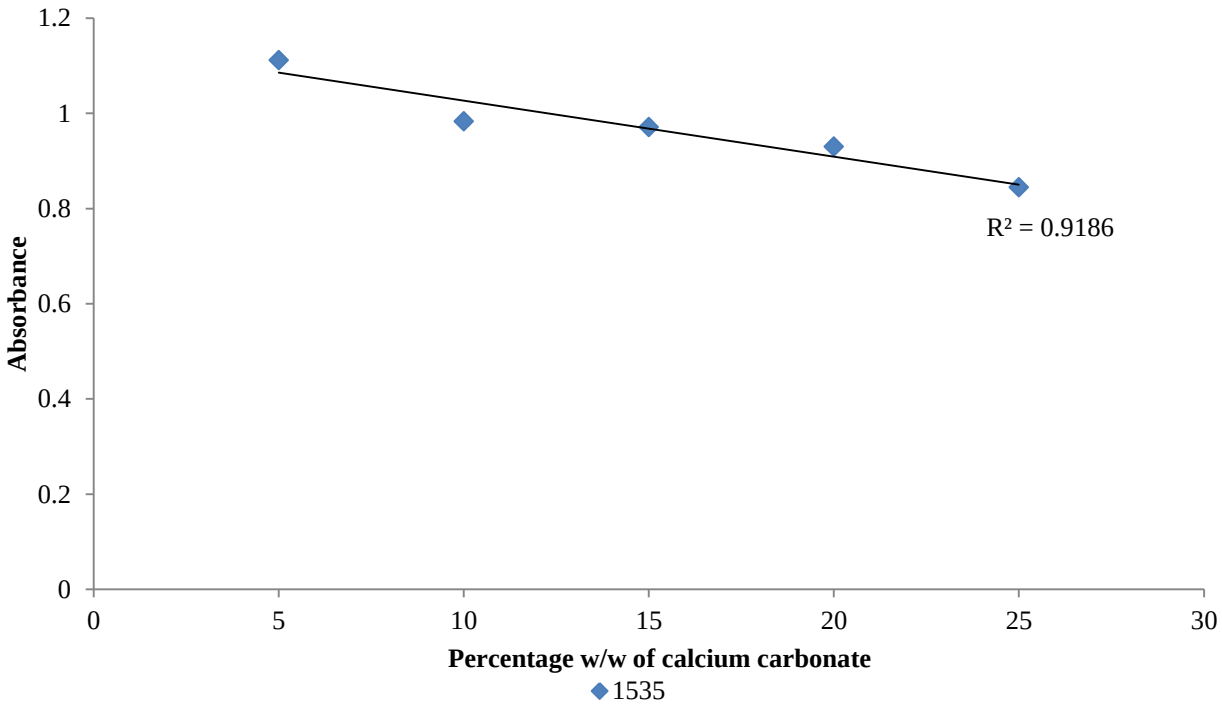


**Figure 2. 12 Calibration curve of the absorbance value measured at 1692 $cm^{-1}$ from the DRIFT spectra of the PEG and carbonate blends vs the concentration of the calcium carbonate**

This apparent decrease in intensity on increase in carbonate concentration initially looks surprising. However as mentioned previously there can be variability between the direction of absorbance bands in diffuse reflectance spectra based upon amounts of diffuse and specular reflectance of the IR light. In this case the asymmetric mode of the $CO_3^{2-}$ ion is presenting as a 'negative' peak. There is a very strong linear trend between concentration and absorbance at 1692 $cm^{-1}$. This gives these quantification methods a level of reliability that can be applied to further DRIFT spectra.

Two absorbance bands were integrated from the DRIFT spectra from the UV aged bitumen, shown in Figure 2.9: the carbonyl (1755-1636 $cm^{-1}$) and the C-O and the sulfoxide bands, which are overlapping and therefore were integrated together (1334-987 $cm^{-1}$). The results of this quantification are shown in Figure 2.13.

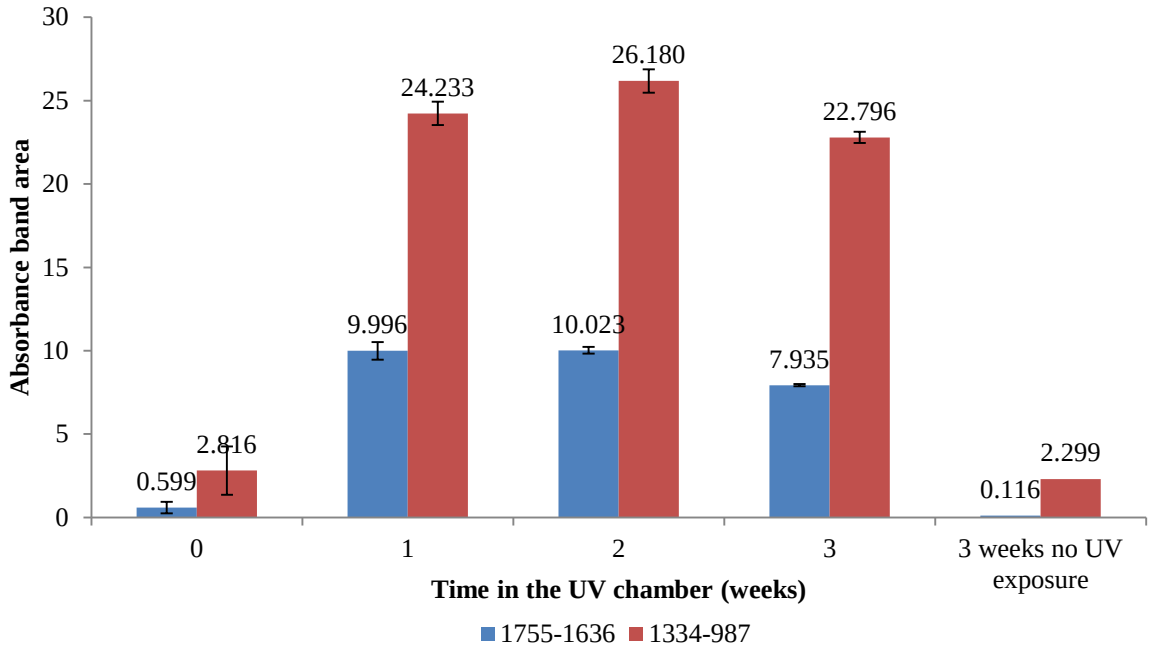


**Figure 2. 13 Average absorbance band area for the carbonyl (1755-1636 $cm^{-1}$) and the carboxylic and sulfoxide (1334-987 $cm^{-1}$) absorbance bands from the DRIFT spectra of the UV aged bitumen**

Both absorbance band areas show a steep increase between 0-1 weeks in the UV chamber. The integrated areas then appear to plateau with a slight decrease. It is interesting to note the similarity between the 0 and the 3 week no UV exposure sample (Figure 2.13). The 3 week control sample did not experience any UV light exposure. This lack of carbonyl absorbance band indicates that the thermal energy transferred to the samples by the 60 ˚C internal temperature of the UV chamber was not as effective at oxidising the bitumen as the combination of the heat and the UV light exposure.

Alongside the absorbance band area integration, the absorbance at 1700 $cm^{-1}$ can be quantified from the spectra in Figure 2.9. As a result of the first derivative nature of this band the absorbance at 1700 $cm^{-1}$ decreased as the absorbance band arises. In this case the *difference* between the absorbance at 1700 $cm^{-1}$ measured in the spectrum of the unaged bitumen and the measured value for the aged bitumen has been calculated and allows for the change in absorbance band intensity to be measured positively. This result can be seen in Figure 2.14.

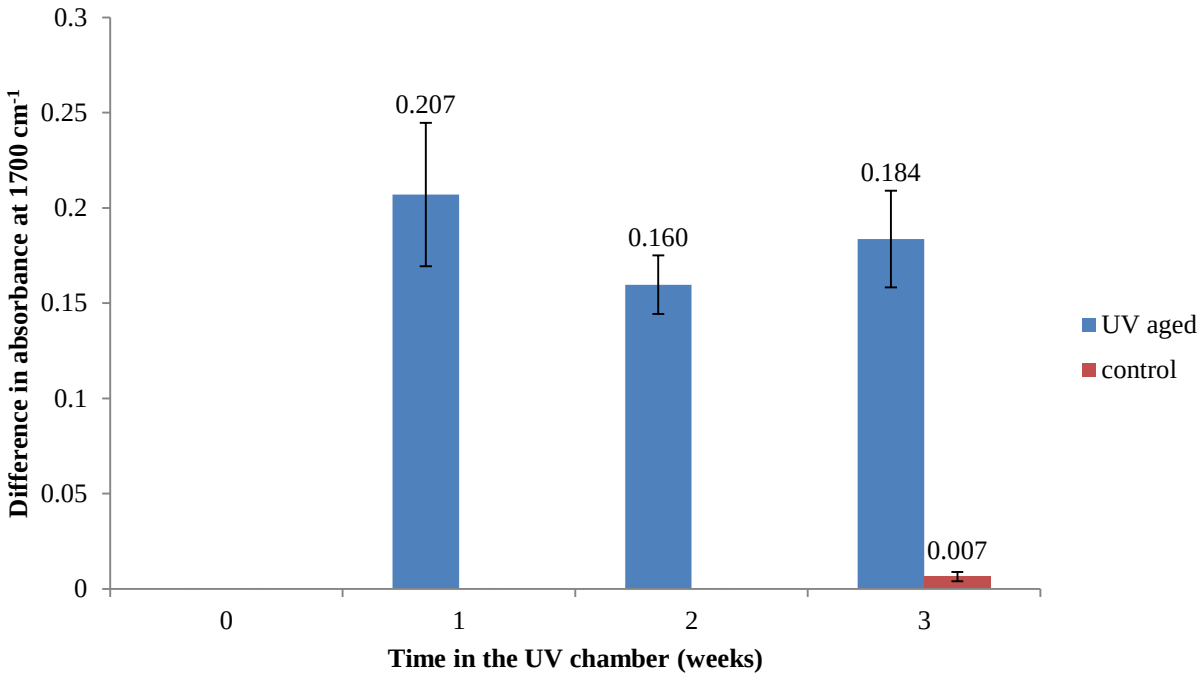


**Figure 2. 14 Difference in absorbance values measured at 1700 $cm^{-1}$ from the DRIFT spectra from the surface of the UV aged bitumen shown in Figure 2.9, compared to the unaged bitumen**

In a similar manner to the ATR spectra of the E-RTFO test bitumen (Chapter 2.1) there is a large change in the absorbance at 1700 $cm^{-1}$ between 0-1 weeks and then a levelling off to a plateau. This suggests that within 1 week in the UV chamber, the surface of the bitumen has become completely oxidised. This could mean that all sites within the bitumen composition that are able to oxidise successfully using the conditions within the UV chamber, have done so within the first week of oxidation.

In order to narrow down the time scale of this surface oxidation, the same UV ageing experiment was carried out, however, the time points that the DRIFT spectra were collected were shortened to hourly and daily intervals. Figure 2.15 contains the DRIFT spectra from the surface of the raw bitumen that has been aged in the UV chamber for up to 336 hours (14 days). At each time point the raw bitumen was removed from the chamber and a DRIFT spectrum was collected from the surface. The bitumen sample was then replaced and the ageing continued.

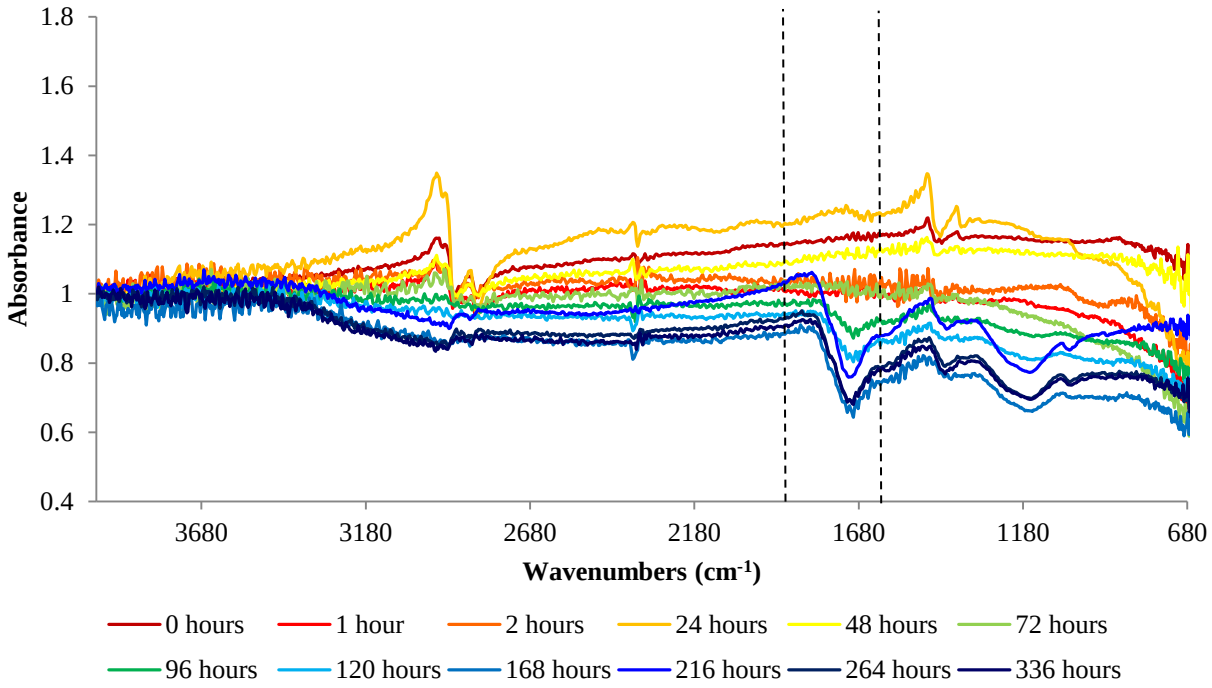


**Figure 2. 15 Normalised DRIFT spectra from the surface of the raw bitumen that has been aged in the UV chamber for 0-2 weeks**

In Figure 2.15 the growth of the first derivative carbonyl absorbance band between the 96 hour (4 days) and the 336 hour (2 weeks) spectra can be observed. Between these points this band is continuously increasing in intensity. This indicates that between 0-72 hours there is an undetectable amount of oxidation occurring and between 72-96 hours, and onwards there is an increase in the amount of carbonyl functional groups present within the surface bitumen composition. This same trend can be seen for the C-O and sulfoxide groups in the lower wavenumber region (1360-1030 $cm^{-1}$) of the spectra also. By integrating the absorbance band areas it is possible to quantify the growth of these absorbance bands. Figure 2.16 shows the results from the integration of the carbonyl (1837-1629 $cm^{-1}$), C-O (1319-1058 $cm^{-1}$) and the alkane C-H (2952-2740 $cm^{-1}$) stretching absorbance bands.

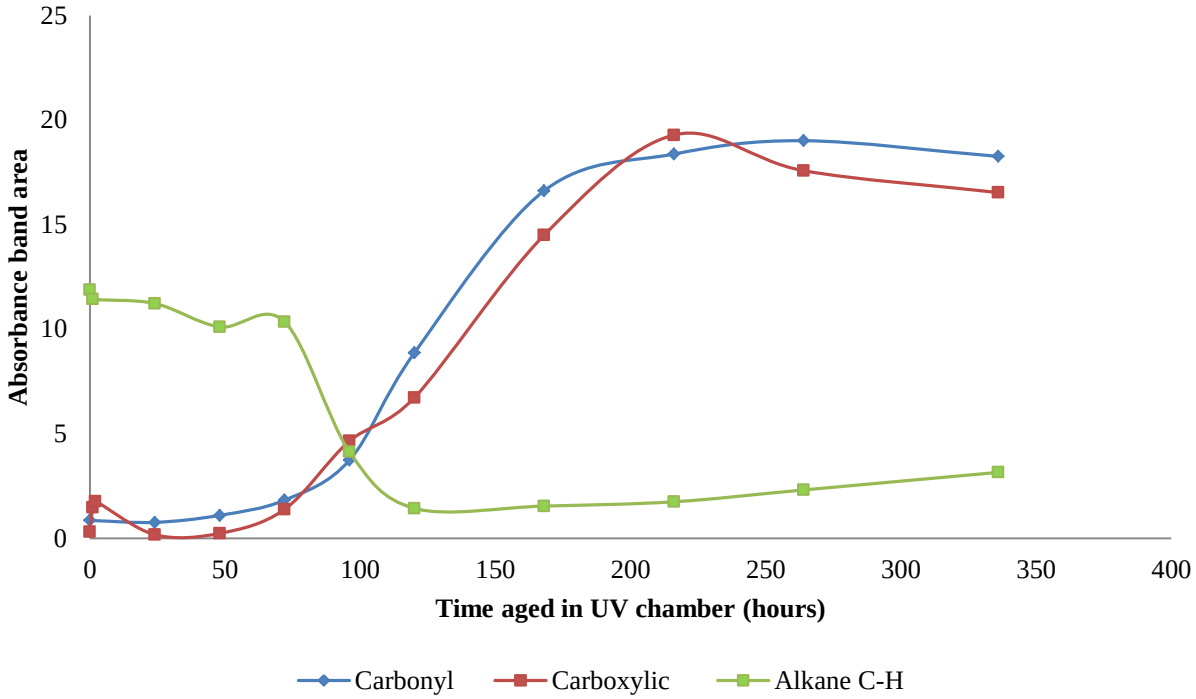


**Figure 2. 16Absorbance bands areas for the carbonyl (1837-1629 $cm^{-1}$), carboxylic (1319-1058 $cm^{-1}$) and alkane C-H (2952-2740 $cm^{-1}$) bands in the DRIFT spectra from the surface of the raw bitumen being aged in the UV chamber for 2 weeks**

The chart in Figure 2.16 clearly indicates that at the 96 hour time point there is a shift in the measured areas. The oxidation product (C=O, C-O) band areas increase and the alkane (C-H) band decreases in area. This group could be reducing in concentration as a result of an increase in oxidation product groups or the band could be reducing in intensity relative to the increasing first derivative band. Petersen *et al.*[6] describe an increase in aromaticity and alkene bonds being produced as a decomposition product of hydroperoxide bonds. This could be another reason for the decrease in alkane C-H absorbance.

The gel permeation chromatography separation results are presented in Figure 2.17.

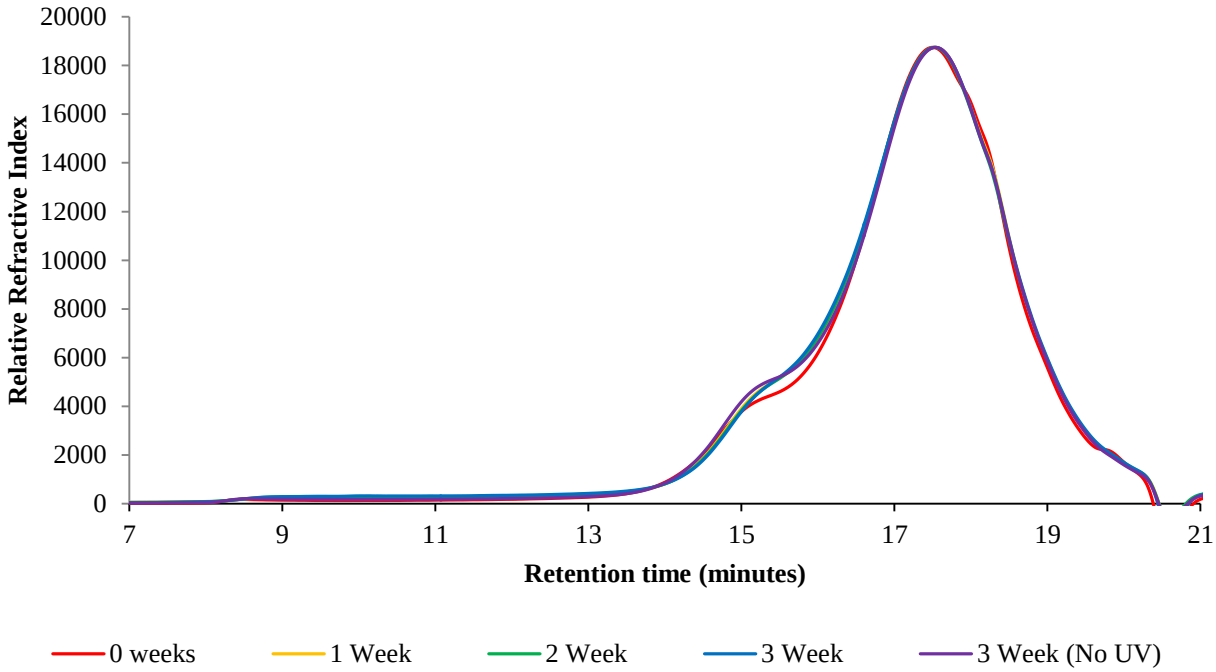


**Figure 2. 17 Gel permeation chromatography results from the raw bitumen that has been aged in the UV chamber for 0-3 weeks**

The GPC result shows a similar chromatogram to those from the E-RTFO test with the biggest peak at a retention time of approximately 17.5 minutes. There is a shoulder on this peak at 15 minutes. There is little change in the size of this shoulder indicating minimal change in the molecular weights of the bitumen. This observation can be clarified by the molecular weight calculations which are outlined in Table 2.5.

**Table 2. 5 GPC separation results of the raw bitumen aged in the UV chamber for 0-3 weeks, including the results from the 3 week without UV exposure sample**

| Time in UV Chamber (weeks) | $M_n$ (g $mol^{-1}$) | $M_w$ (g $mol^{-1}$) | Đ |
|---|---|---|---|
| **0** | 640 | 1900 | 2.97 |
| **1** | 660 | 1800 | 2.72 |
| **2** | 670 | 1800 | 2.69 |
| **3** | 640 | 1800 | 2.81 |
| **3 (no UV)** | 670 | 1800 | 2.69 |

All of the samples analysed show no significant change with respect to the pristine bitumen, outside of the error limits of the GPC, in number average or weight average molecular weight.

This result contradicts the increase in carbonyl absorbance band measured in the DRIFT spectroscopy and shows that the oxidation has only occurred at the surface and the change is not reliably measurable by GPC which is a bulk technique. By contrast the E-RTFO test procedure causes oxidation to the bulk, which has been detected by GPC. The skin has protected the bulk bitumen therefore the oxidation is localised to the surface only. The molecular interactions that are occurring within the oxidised surface, giving the surface a higher viscosity and brittleness, are likely to be broken down when the sample is dissolved into the THF solvent. This would suggest that the increase in viscosity of the UV oxidised surface is a physical property of the bitumen as opposed to the presence of oxygen.

There is a visual difference in the surface of the UV aged bitumen as a result of the brittle skin forming, (see photograph in Figure 2.8). This visual change can be examined in more detail by using SEM. The images shown in Figure 2.18 have been obtained *via* SEM analysis and clearly show this structural difference.

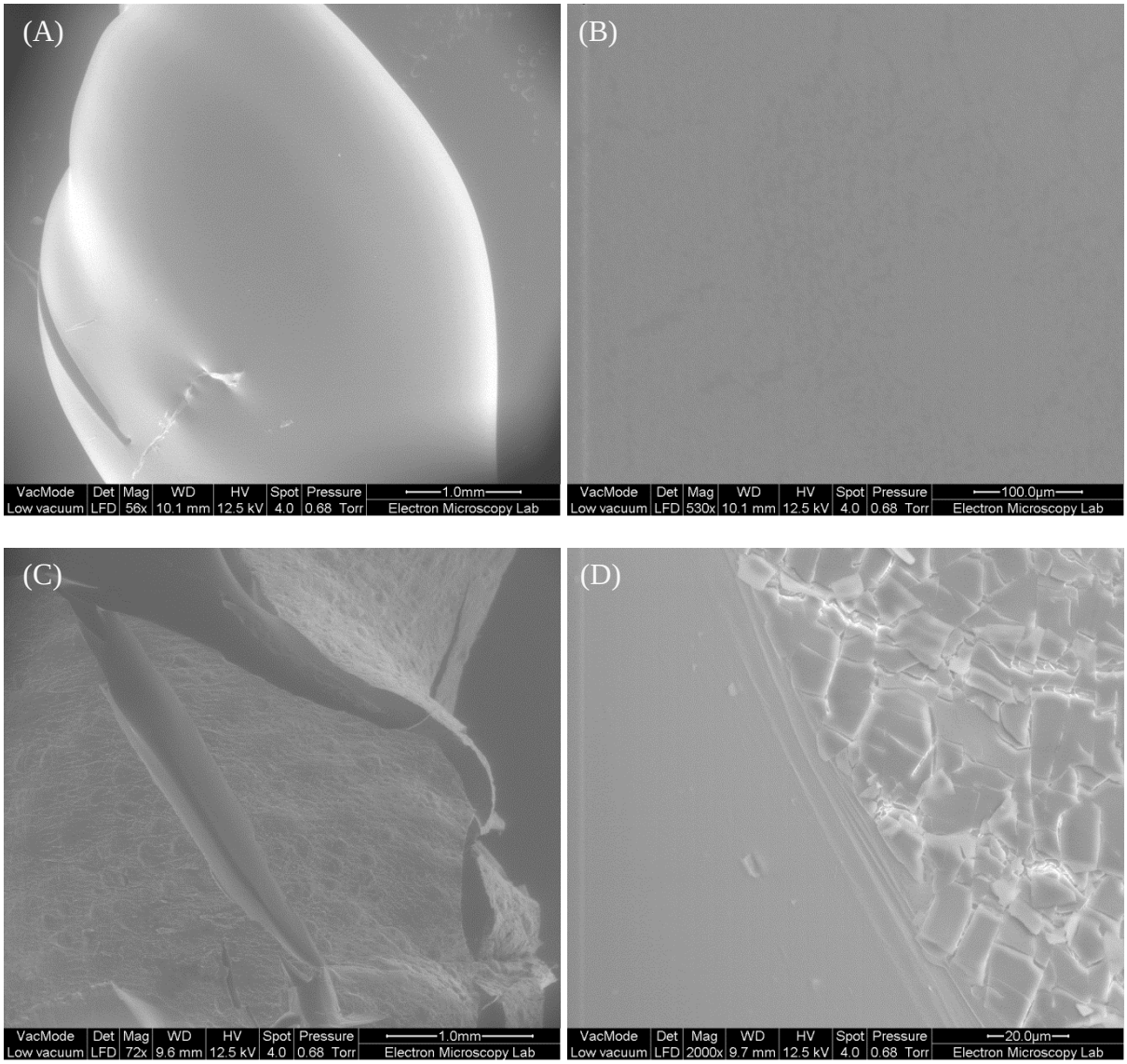


**Figure 2. 18 SEM images from the surface of the raw bitumen that is unaged (A&B), and has been aged in the UV chamber for 3 weeks uncovered (C&D)**

**Table 2. 6 Magnifications of the SEM images shown in Figure 2.18**

| Microscope Image (Figure 2.18) | Magnification (×) |
|---|---|
| **A** | 58 |
| **B** | 530 |
| **C** | 72 |
| **D** | 2000 |

The SEM images (Figure 2.18 A&B) show that the surface unaged bitumen sample has a very similar surface structure to the unaged raw bitumen seen in Figure 2.6 (A). However, the

images obtained from analysis of the UV exposed 3 week aged bitumen (Figure 2.18 C&D) reveal a very different surface structure. The sub-sample of the 3 week UV aged bitumen has fractured from the surface as it was being collected and placed onto the carbon SEM stub (Figure 2.18 C). This is indicative of brittle bitumen. Upon magnification of 2000 × it is possible to see small platelets (*ca.* 20 μm) formed on the surface of the bitumen. There is a very dramatic contrast between the surface of the UV aged bitumen and the bulk of this sample. By studying the region of the sample where fracturing had occurred, it is possible to visualise the difference between the topmost surface of the bitumen, (that was exposed to the UV light) and the bulk (that was not exposed to the UV light but is still part of the same sample). The image in Figure 2.18 D can be used to estimate the depth that the UV light penetrates into the bitumen. The UV light seems to have only had an effect on the surface 5 μm. The image appears to indicate micro-cracking on the surface, possibly as a result of the increased brittleness of the surface.

The formation of the skin upon oxidation is protecting the bulk bitumen from further oxidation. This could be the reason for the lack of chemical change in the GPC results. The surface few micro-meters are oxidised and the bulk bitumen beneath is not affected.

## 2.3 Natural ageing of bitumen

Bitumen samples have been aged naturally in order to determine the extent of oxidation experienced when exposed to natural weather conditions. This is important in order to determine if the DRIFT spectroscopy is sensitive enough to detect any chemical changes occurring within the bitumen that has been exposed to natural conditions, which are much less harsh than the artificial ageing experiments described previously. Raw bitumen samples were prepared in aluminium tins and placed onto the roof of Crowthorne House, UK. The conditions that the bitumen samples were exposed to have been monitored using a weather station. The temperature, rainfall, humidity, UV light exposure and wind speed and direction have been recorded for the duration of the experiment. Samples were removed at weekly intervals and DRIFT spectra were taken at the surface.

**Table 2. 7 Dates that the naturally aged bitumen samples were placed onto and taken off the roof of Crowthorne House**

| Time naturally aged (weeks) | Dates of ageing |
|---|---|
| **1** | 19.04.17-26.04.17 |
| **2** | 19.04.17-03.05.17 |
| **4** | 19.04.17-24.05.17 |

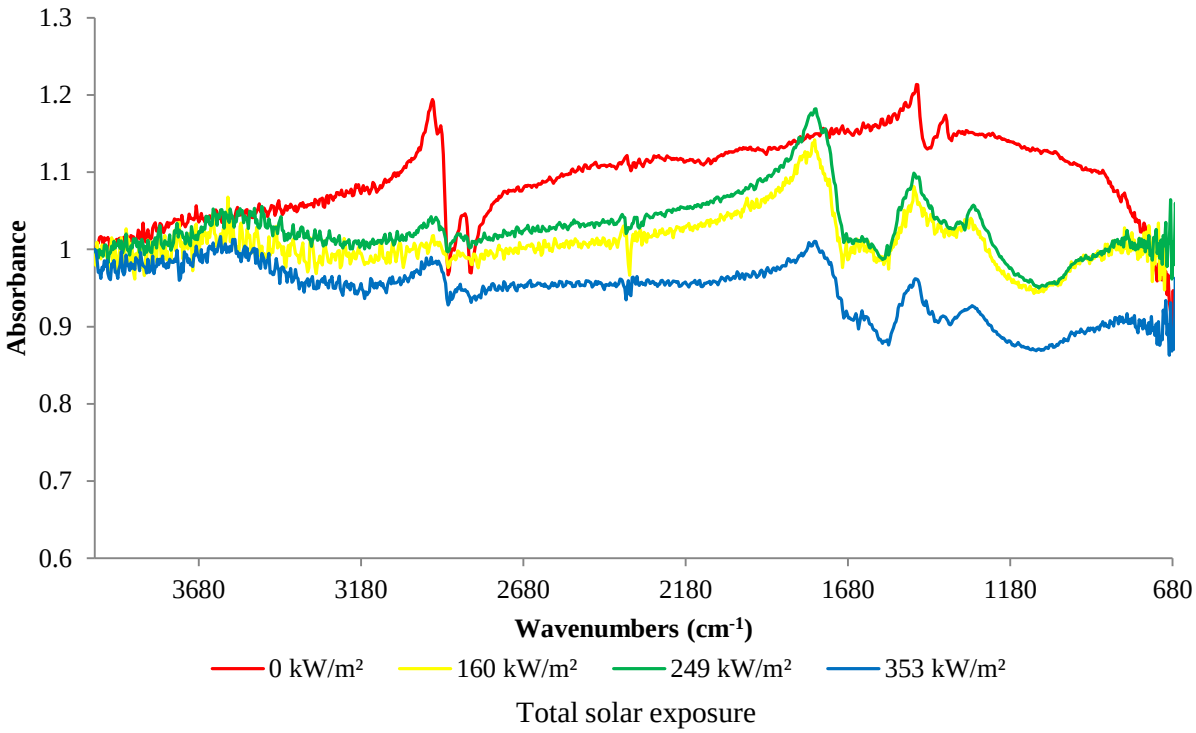


**Figure 2. 19 Normalised DRIFT spectra from the surface of the raw bitumen that has been naturally aged on the roof of Crowthorne House for 0-4 weeks**

The unaged raw bitumen spectrum shows the absorbance bands that correspond to the C-H bonds bending and stretching (2907, 2840 and 1470, 1370 $cm^{-1}$). Upon natural ageing there are absorbance bands arising that correspond to oxidation products. These have been identified and assigned in Table 2.8.

**Table 2. 8 Absorbance bands and their assignments from the DRIFT spectra from the surface of the raw bitumen (Figure 2.19) that has been naturally aged on the roof of Crowthorne House, UK**

| **Absorbance Band ($cm^{-1}$)** | **Bond Assignment** | |
|---|---|---|
| **2911, 2837** | C-H stretch | Bitumen Hydrocarbon |
| **1737** | C=O stretch | Carbonyl oxidation product |
| **1472, 1394** | C-$H_2$ bend | Bitumen Hydrocarbon |
| **1103 (broad)** | C-O, S=O | Carboxylic and sulfoxide oxidation products |

The carbonyl absorbance band appears again as a first derivative, as seen before in the spectra from the UV aged bitumen, (Section 2.2). This suggests that the surface of the naturally aged bitumen is physically similar to that of the UV aged asphalt. A skin was seen to form over the surface of the bitumen as it was naturally aged in a similar manner to the UV aged bitumen. As before changes in refractive index at the surface could be the reason for the first derivative nature of the carbonyl absorbance band. The C-O and the sulfoxide bond absorbance bands are overlapping in Figure 2.19 and a broad absorbance band can be observed between 1323 and 928 $cm^{-1}$. The broad band suggests the presence of hydrogen bonding and intermolecular interactions. This molecular self-assembly could be the reason for the rigid and brittle skin on the surface.[6]

As UV irradiation has been proven to induce changes on the surface of the bitumen it is important to look at the solar exposure that the bitumen has experienced throughout the natural ageing experiment. The solar meter used for this research has recorded the intensity of the UV light in Watts per meter squared (W $m^{-2}$) at 15 minute intervals, 24 hours a day. The total solar exposure experienced by the bitumen samples has been calculated by adding the solar exposure that was recorded by the weather station for the duration of the ageing experiment. The total solar exposure experienced by the naturally aged bitumen samples can be found in Figure 2.20.

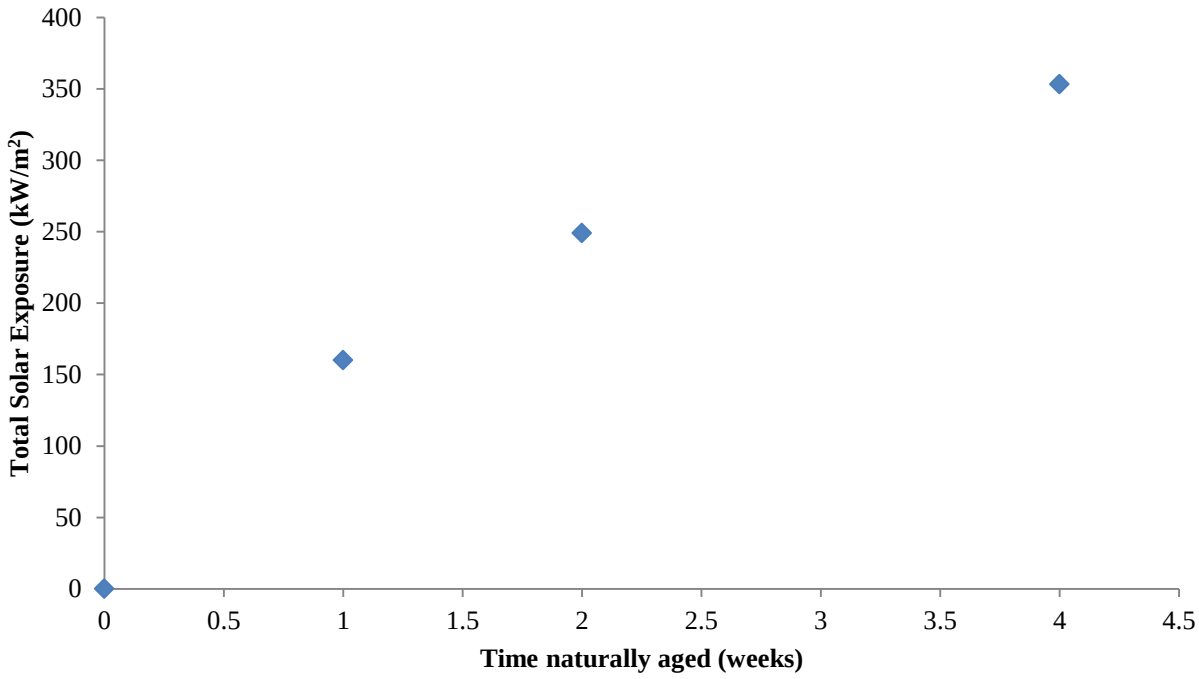


**Figure 2. 20 Total solar exposure experienced by the raw bitumen while on the roof of Crowthorne House, measured by a weather station**

The total solar exposure that the bitumen was exposed to throughout the natural ageing experiment increases as the sample is left on the roof. This is to be expected and should, in theory, lead to a similar, approximately linear increase in the oxidation of the bitumen, as the UV light exposure has been identified as an initiator to the oxidation (Section 2.2).

The quantification of the changes in the carbonyl absorbance band has been carried out by integrating the area underneath the band (1931-1686 $cm^{-1}$) and also by recording the single wavelength analysis at 1700 $cm^{-1}$. The results from this data analysis can be found in Figure 2.21 and Figure 2.22.

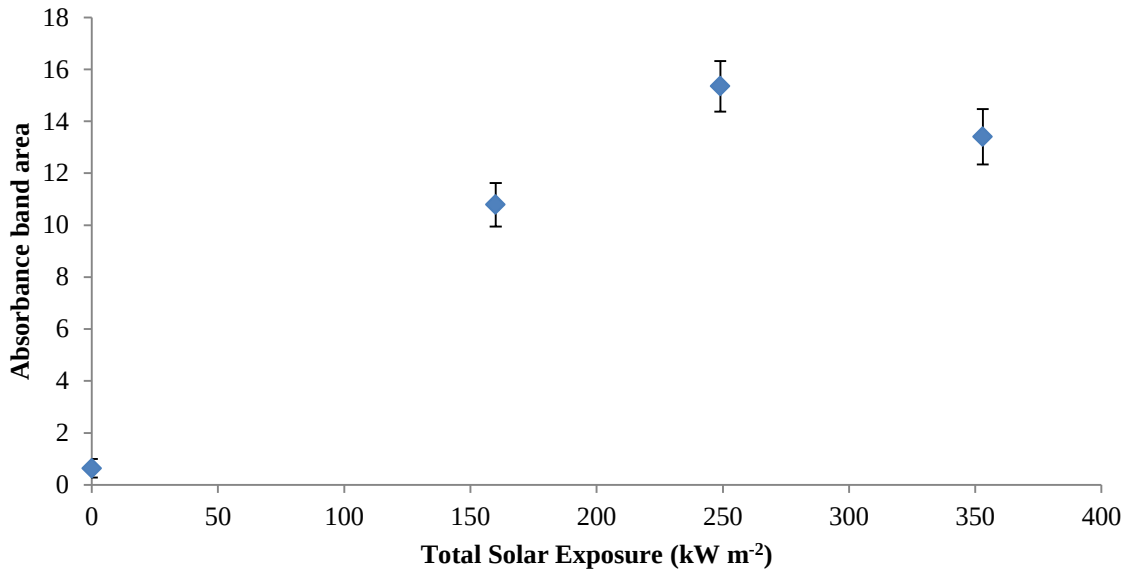


**Figure 2. 21 Absorbance band area (1931-1686 $cm^{-1}$) integration results from the DRIFT spectra from the surface of the bitumen that has been aged naturally on the roof of Crowthorne House.**

The result from the integration of the carbonyl absorbance band (1931-1686 $cm^{-1}$) shows an approximately linear increase between 0-249 kW $m^{-2}$ of solar exposure (0-2 weeks). The absorbance band area then remains approximately constant. The plateau of the absorbance band area suggests that there is complete oxidation of the active sites within the surface of the bitumen, during the first two weeks of exposure.

As the absorbance band at 1700 $cm^{-1}$ (carbonyl) is a negative absorbance band, the absorbance measured at the apex decreases as the samples get older. Therefore the *difference* in the absorbance measured at 1700 $cm^{-1}$ between the unaged and aged sample spectra has been calculated and is plotted in Figure 2.22.

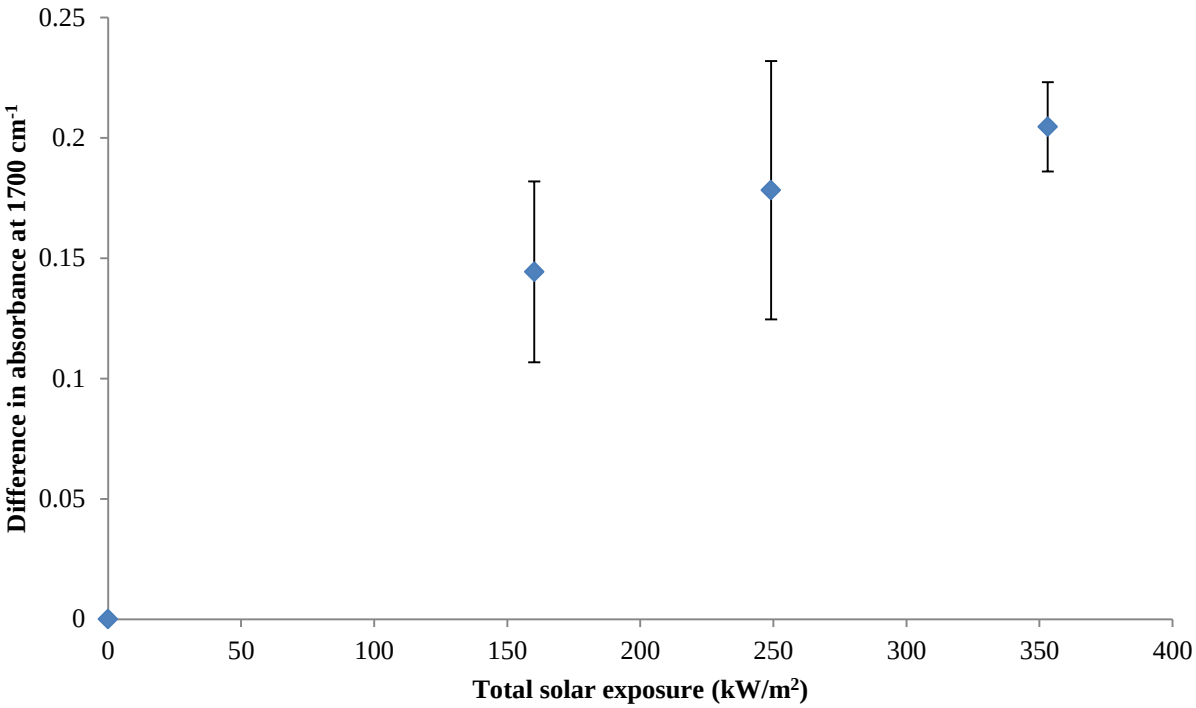


**Figure 2. 22 Difference in absorbance at 1700 $cm^{-1}$ measured from the DRIFT spectra from the surface of the naturally aged raw bitumen, compared to unaged bitumen**

The difference in absorbance value measured at 1700 $cm^{-1}$ shows an increase between 0-1 week natural ageing. The intensities remain constant within experimental error after this time. This is the same trend as measured for the UV aged bitumen (Section 2.2).

Gel Permeation Chromatography has been carried out on a surface sub-sample from the naturally aged raw bitumen samples. These samples were dissolved in THF at a concentration of 2 mg/mL. The chromatograms for the 1 and 4 week naturally aged samples have been plotted in Figure 2.23.

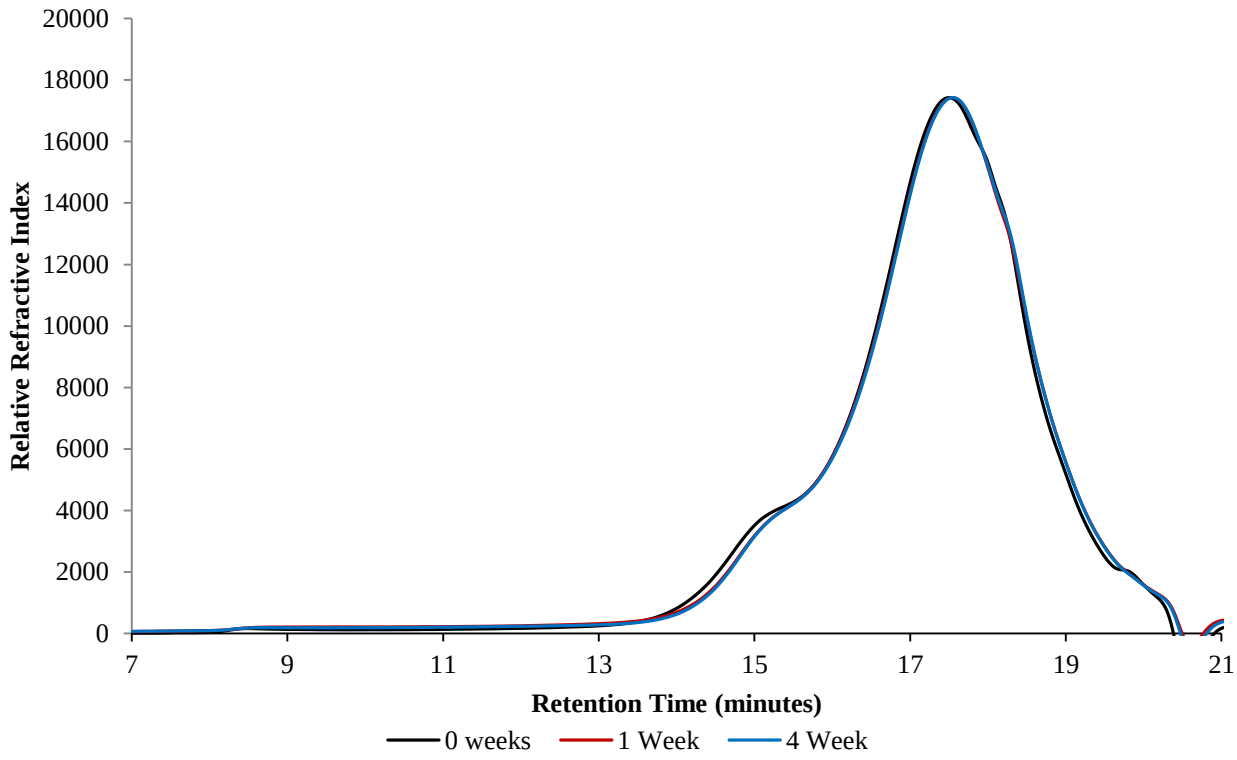


**Figure 2. 23 Gel permeation chromatography results from the raw bitumen that has been aged naturally on the roof of Crowthorne House**

The GPC profile of the naturally aged bitumen (Figure 2.23) shows the same peak at 17.5 minutes with a shoulder at approximately 15 minutes as was seen for the enhanced UV aged samples. Similarly to the UV aged bitumen results there is no significant change seen in the size or shape of these peaks upon natural ageing. Table 2.9 contains the molecular data that quantifies this lack of change.

**Table 2. 9 GPC separation results for the raw bitumen that has been aged naturally on the roof of TRL, Crowthorne**

| Time naturally aged (weeks) | $M_n$ (g/ mol$^{-1}$) | $M_w$ (g mol$^{-1}$) | Đ |
|---|---|---|---|
| **0** | 640 | 1890 | 2.93 |
| **1** | 630 | 1700 | 2.70 |
| **4** | 650 | 1700 | 2.62 |

In agreement with the previous GPC analysis, the results from the GPC separation did not reveal any significant changes relative to the pristine bitumen. The conditions of the natural ageing are considerably less harsh than the E-RTFO test in terms of temperature. The

maximum temperature that the naturally aged samples were exposed to was 27 ˚C, with an average exposure temperature of 10 ˚C.

**Figure 2. 24 Photograph of the surface of unaged (left) and naturally aged (right) bitumen**

After natural ageing there is a change in the surface structure which is similar to that seen in the UV aged bitumen. It is possible to see in Figure 2.24 the evidence of small cracks in the surface revealing the shiny, unaged bitumen below. These features can be seen more clearly by SEM analysis (Figure 2.25).

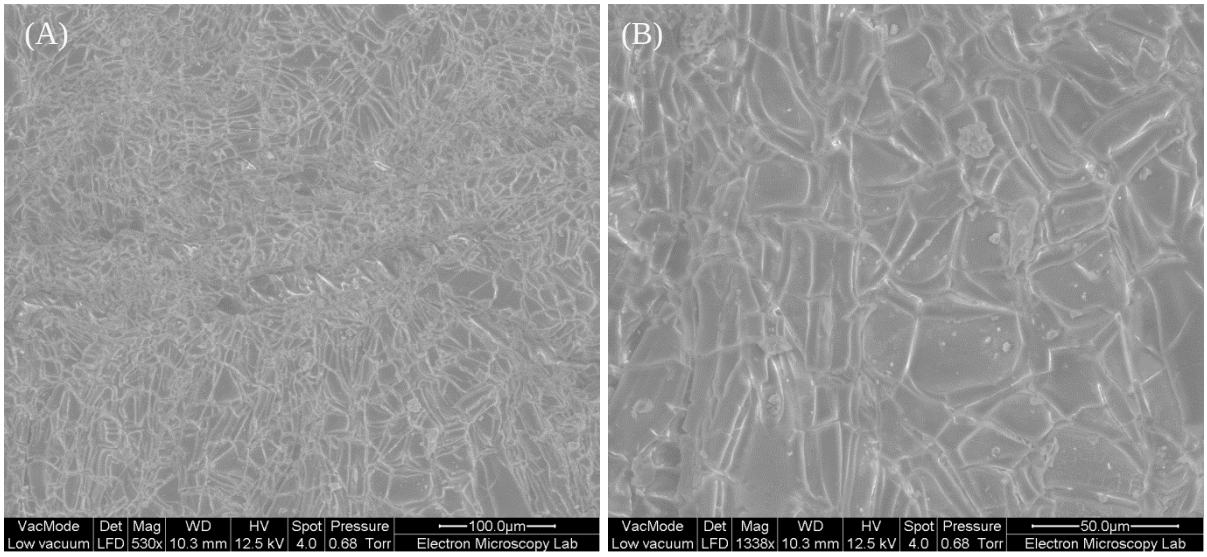


**Figure 2. 25 SEM images from the surface of raw bitumen that has been naturally aged for 4 weeks on the roof of Crowthorne House, UK. (A) 530 × magnification (B) 1338 × magnification**

**Table 2. 10 Magnification of the SEM images in Figure 2.25**

| Microscope Image (Figure 2.25) | Magnification (×) |
|---|---|
| **A** | 530 |
| **B** | 1338 |

At 530 x magnification it is possible to see that small platelets have formed on the exposed surface of the naturally aged bitumen. These are similar to those seen in the UV aged sample however they present smaller platelets with and more rounded edges. These cracks could be an artefact of the thermal cycling of the environment. At 1338 × magnification, small particles of matter are visible. These are likely to be pollen grains that have drifted onto the sample surface from the surrounding area.

## Summary

The results presented in this chapter show that there are chemical changes occurring in raw bitumen upon ageing with the E-RTFO test, within a UV chamber and with natural ageing conditions on the roof of TRL, Crowthorne.

The extended rolling thin film oven test has induced oxidation within raw bitumen. This has been confirmed by ATR-IR spectroscopy. It is possible to observe and quantify the increase in the carbonyl, C-O and sulfoxide functional groups. A 300% increase in carbonyl absorbance band area (1735-1659 $cm^{-1}$) was measured in the ATR spectra of the aged bitumen.

Gel permeation chromatography of these samples shows an increase in the molecular weight of the molecules within the bitumen composition as it ages in the E-RTFO test. This is consistent with an increase in oxygen containing molecules within the bitumen.

The scanning electron microscopy of the E-RTFOT aged samples shows a very smooth microstructure which is unchanging throughout the thermal ageing.

DRIFT spectroscopy has been used to analyse the surface of the UV aged bitumen and has been used to measure an increase in the presence of a carbonyl absorbance band. This band is presenting as a first derivative absorbance band as a result in the changing structure of the surface layers upon UV ageing and hence changes in refractive index.

The growth of the measureable carbonyl and sulfoxide groups begins after approximately 96 hours of UV exposure in the UV chamber. The increase in the integrated absorbance band area of these oxidation product functional groups correlates with a decrease in the integrated absorbance band area of the alkane C-H absorbance bands. This could be indicating a decrease in alkane C-H bonding as a result of the oxygen containing functional groups and of the formation of unsaturated hydrocarbons.

The 3 week control sample, which was not exposed to UV light, did not develop any oxidation product absorbance bands and it can be concluded that the thermal energy experienced by the sample while being held at 60 ˚C is not enough to initiate a measureable amount of oxidation. A temperature of 60 ˚C is rarely experienced in the UK, therefore, it could be speculated that the temperatures experienced in the UK are not enough to initiate oxidation of the bitumen alone; however, in combination with the UV light exposure, oxidation can occur.

The UV aged bitumen has developed a skin on the surface after exposure to UV light. The presence of a broad C-O absorbance band in the DRIFT spectra indicates that there is an increase in hydrogen bonding and intermolecular forces. The increase in these forces indicates that the bitumen at the surface is self-assembling and creating a rigid molecular network in the form of a surface skin which protests the bulk from further exposure.

The 3 week control sample that experienced thermal ageing in the UV chamber but covered from the UV light did not develop this skin. This indicates that the UV light is an initiator for the surface oxidation.

The bitumen skin has been visualised with SEM at high magnifications. The SEM images show small platelets covering the surface of the UV exposed surface.

The same skin and cracked plates are seen on the surface of the naturally aged samples with SEM. They can be attributed to the micro-cracking starting on the surface of the bitumen.

Gel Permeation Chromatography shows no significant change in the number or weight average molecular weights in the UV or the naturally aged samples. This is the opposite effect to that seen in the E-RTFO test. However, the conditions for the ageing are very different. The E-RTFO test experiences higher temperatures (163˚C) and constant movement and air flow. The UV chamber experiences a lower temperature (60˚C) and is static, therefore only the surface layers are being exposed to oxygen and UV light and once the skin has formed

there is little oxidation occurring within the bulk bitumen. This explains why there is a dramatic increase in the DRIFT spectra, indicating oxidation, whereas the GPC shows little change. The same is true for the natural ageing; the bitumen is experiencing even lower temperatures (average 10˚C) and lower levels of UV exposure.

The DRIFT spectroscopy from the naturally aged bitumen experiment has measured an increase in the carbonyl absorbance band area and the intensity of the 1700 $cm^{-1}$ absorbance band. This result indicates that the DRIFT spectroscopy can be used to monitor the chemical changes that occur within the 4 weeks of the natural ageing experiment.

The testing of the mechanical properties of these aged bitumen samples will allow for the quantification of the increase in brittleness of the bitumen as a result of the different ageing mechanisms and this aspect will be explored in the following chapter.

# References


[1] EN, BS. "12607-1: Bitumen and bituminous binders- Determination of the resistance to hardening under the influence of heat and air, RTFOT method". (2007) British Standards Institution.

[2] J. Reed and D. Whiteoak, The Shell Bitumen Handbook, 5th Edition, Thomas Telford Publishing, London, 2003, ISBN: 0-7277-3220-X.

[3] D. Gershkoff, A38 Pervious Mecadax Trial 1984: Binder Rheology before and after artificial hardening, Transport and Road Research Laboratory, Dept. Transport, Unpublished Work, 1984.

[4] M. R. Nivitha, E. Prasad and J. M. Krishnan, Ageing in modified bitumen using FTIR spectroscopy, *Int. J. Pavement Eng.*, **17**(7), 2015, 1-13.

[5] R. E. Robertson, Chemical properties or asphalt and their relationship to pavement performance, *Strategic Highway Research Program*, Washington D.C, 1991.

[6] J. C. Petersen and R. Glaser, Asphalt oxidative mechanisms and the role of oxidation products on age hardening revisited, *Road Mater. Pavement*, **12,** 2011, 795-819.

[7] D. A. Skoog, *Principles of Instrumental Analysis*, Thompson Brooks/Cole, Belmont California, 2006.

[8] The Asphalt Institute, *Introduction to Asphalt,* Manual Series No. 5, 8th Ed., Shell Bitumen, Maryland USA, 1986.

[9] F. Deygout, Volatile emissions from hot bitumen storage tanks, *Environ. Prog. Sustain.*, **30**(1), 2011, 102-112.

[10] C. Mathieu, L. Khouchaf and A. Kadoun, Exploring the high pressure SEM, *Modern Research and Educational Topics in Microscopy,* 2007.

[11] T. Yi-Qui, W. Jia-Ni, F. Zhong-Liang and Z. Xing-Ye, Influence and mechanism of ultraviolet ageing on bitumen performance, 26th Southern African Transport Conference, Pretoria South Africa, 2007, 726-735.

[12] T. Telford, *The Shell Bitumen Industrial Handbook,* 1995.

[13] G. D. Airey, in *ICE manual of Construction Materials: Volume I/II: Fundamentals and theory; Concrete; Asphalts in road construction; Masonry,* ed. Mike Forde, ICE institution of Civil Engineering, 2009, eISBN: 978-07277-4048-9.

[14] Perkin Elmer Technical Note, Reflection Measurements in IR spectroscopy, R. Spragg, Perkin Elmer Inc. Seer Green, UK, https://www.perkinelmer.com/CMSResources/Images/44-153348TCH_reflection-Measurements.pdf ACCESSED 30.05.2018 17:12.

[15] M. Gorman, The evidence from infrared spectroscopy for hydrogen bonding: A case history of the correlation and interpretation of data, *J. Chem. Educ.*, **34**(6), 1957, 304.

[16] W. Zeng, S. Wu, J. Wen and Z. Chen, The temperature effects in ageing index of asphalt during UV ageing process, Constr. Build Mater., 93,2015, 1125-1131.

[17] M. Lopes, D. Zhao, E. Chailleux, M. Kane, T. Gabet, C. Petiteau and J. Soares, Characterisation of ageing processes on the asphalt mixture surface, Road Mater. Pavement, 15(3), 2014, 477-487.

[18] S. Wu, L. Pang, L. Mo, J. Qui, G. Zhu and Y. Xiao, UV and thermal ageing of pure bitumen-comparison between laboratory simulation and natural exposure ageing, *Road Mater. Pavement*, EATA, 2008, 103-113.

[19] J. C. Petersen and H. Plancher, Quantification determination of carboxylic acids by selective chemical reactions and differential infra-red spectrometry, *Analytical Chemistry,* **53,** 1981, 786-789.

# Chapter 3

## Artificial and natural ageing of bitumen- Mechanical property testing

The chemical analysis which was reported in Chapter 2 has identified a degree of chemical oxidation within the bitumen that had been aged in the E-RTFO test, the UV chamber and also naturally. It is now of interest to determine the mechanical effect that these chemical changes have had on the physical properties of the bitumen.

The mechanical properties of bitumen can be related to the intermolecular interactions and structuring within the bitumen composition. There are two methods of age hardening that can occur within bitumen; oxidative hardening and organisational hardening. The first has been described in Chapters 1 and 2, and involves the increase in aromaticity and oxygen content within the bitumen composition. The increase in electron density and polar, oxygen-containing groups increases the amount and strength of intermolecular interactions that are possible and therefore increases the viscosity.[1] The chemical ageing is irreversible. By contrast the organisational hardening is reversible. Organisational hardening is the result of the intermolecular interactions between the polar groups and the electron dense groups within the bitumen. In this way the molecules are able to organise and stack themselves into a composition that is stable and immobile. The agglomerates formed from this arrangement are sometimes termed colloids or micelles however the use of these terms is somewhat misleading as the structures formed within bitumen are different to the structures that a surface or colloidal chemist might describe as a colloid or a micelle.[2,3] The molecular organisation is susceptible to rearrangement with the energy supplied from high temperatures and physical stresses, such as trafficking. The highly interacting molecular network becomes very rigid and cannot heal or deform elastically. This means that the bitumen and asphalt are more likely to crack under the stress of trafficking.

There are standardised mechanical tests that are used regularly in industry which allow a highways company, such as Highways England in the UK, to determine the physical characteristics of the bitumen being used on their road network. The most commonly used are

the Penetration point, Softening point and, less commonly, the Vialit pendulum test. These tests are used to measure the stiffness, viscosity and cohesion of the bitumen, respectively.

The viscosity of the bitumen is also measured in order to characterise the bitumen being utilised within road surfaces. There are two standardised tests that allow for the measurement of bitumen viscosity, the dynamic viscosity,[4] and the kinematic viscosity[5] tests. They both involve measuring the time that it takes for a volume of bitumen to travel through a capillary tube.

This chapter outlines the mechanical tests have been carried out on the bitumen samples that have been aged artificially and naturally and the results are presented in this chapter.

## 3.1 Mechanical testing methodology

### *3.1.1 Penetration point test*

The penetration point test has been carried using the British Standard method EN 1426:2015.[6] This method involves heating and pouring raw bitumen into standardised sample tins. The tins have a 55 mm diameter and a 35 mm depth. This is then cooled for at least 1 hour and is then placed into a water bath, set to 25 ˚C, for 1 hour to allow the sample to equilibrate in temperature. The sample is then placed underneath a standardised needle with a 100 g weight attached. The needle is brought down to touch the surface of the bitumen which just breaks the surface tension of the bitumen. The needle is then released and allowed to drop into the bitumen for 5 seconds. The distance that the needle travels in this time is recorded in $1/10^{th}$ millimetre units. This is repeated 3 times in 3 different locations on the bitumen surface, at least 1 cm apart, and the average penetration point is calculated.

### *3.1.2 Softening point test*

The softening point test described in the British Standard EN 1427:2015 [7] requires two discs of bitumen to be formed within standardised steel rings. These are poured and cooled for at least 1 hour before being placed into the softening point cradle which is then held in a water bath at 5 ˚C. At the start of the test a steel ball is placed on the top of each of the bitumen discs (Figure 3.1 A) and the water bath is heated at a rate of 5˚C per minute while stirring to ensure efficient heat distribution.

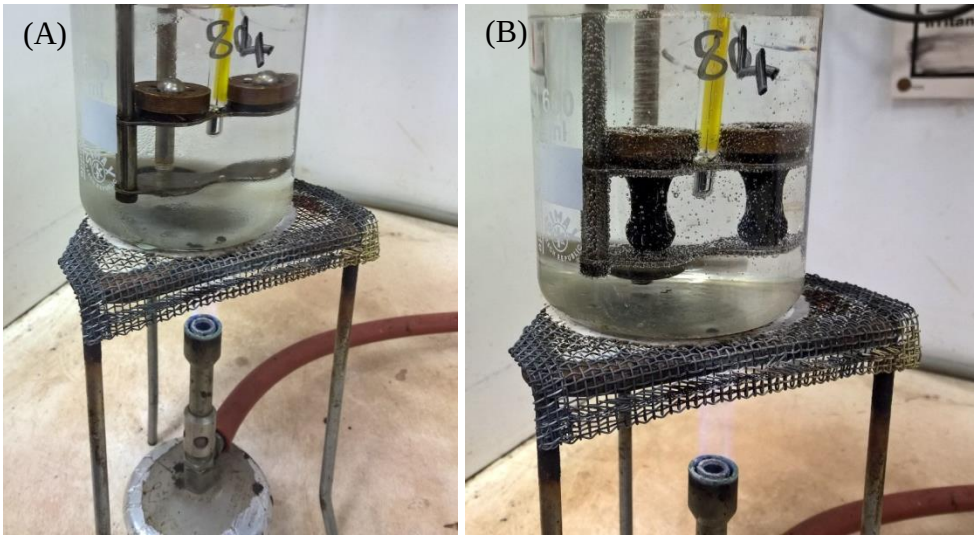


**Figure 3. 1 Photographs indicating the softening point test experimental set up at the start of the test (A) and the end point (B)**

The temperature of the water bath is heated until the two steel balls reach the bottom of the cradle which is approx. 2.5 cm away from the starting position (Figure 3.1 B). The temperature of the water bath at this point is recorded as the softening point.

### *3.1.3 Vialit Pendulum test*

The pendulum test has been standardised and is described within the British Standard EN 13588:2008.[8] It is started by preparing steel block sample holders with bitumen. The steel blocks are heated in an oven for at least an hour to ensure the bitumen does not cool too quickly when placed, with a scalpel on to the sample holder. A top steel block is then placed on top of the bitumen sample and any excess bitumen is carefully cut away.

(a)

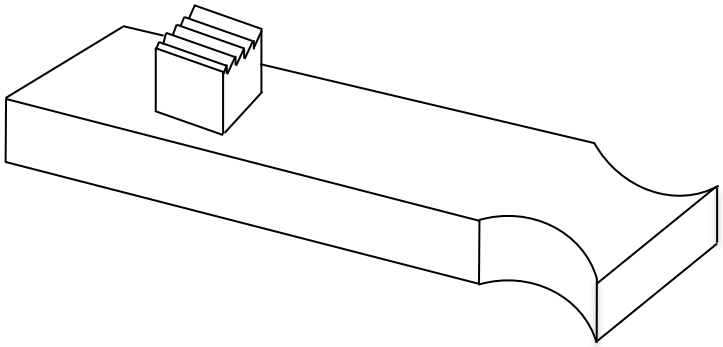

**Figure 3. 2 Diagram representation of the sample holder for the Vialit Pendulum test (a). Bitumen is placed onto the grooved surface of the bottom cube, and then the top cube is pressed onto the bitumen.**

Six of these samples are then placed into a water bath which is being held at the required test temperature. The samples are then allowed to equilibrate for 1.5 hours. After this time the samples are removed, one at a time, and placed into the pendulum test apparatus. The pendulum is released and hits the top steel block and the bitumen between the two blocks is broken. The angle that the pendulum swings after contact with the block is recorded. The top block that was removed by the pendulum is overturned and placed onto a clean sample holder and the pendulum is swung again and the second angle recorded. These two angles are used to calculate the energy required to break the bitumen and therefore, calculate the cohesion within the bitumen.

### *3.1.4 Intrinsic viscosity*

The intrinsic viscosity can be defined as the measure of the effect of a solute on the viscosity of a solution. This has been measured here in combination with Gel Permeation Chromatography (GPC) separation.

This technique works by eluting a sample through a GPC column to separate a solution based upon molecular weight of its components. This procedure has been described in more detail in Chapter 1.2.5. The GPC is then coupled to an intrinsic viscosity measurement device. This measurement is carried out using two capillary tubes. One carries a pure solvent and is used to provide a reference for the experiment. A second tube, with equal dimensions, carries the sample solution that has been prepared in the same solvent as the reference. The tubes are fitted with two light scattering detectors at a distance of 3 cm apart. The light scattering detector can identify the moment that the sample reaches the first detector, and can then measure the time that the solution takes to reach the second detector. This elution time can be used to calculate the intrinsic viscosity of the sample solution, in comparison to the blank solvent elution time. The diagram in Figure 3.3 shows a pictorial representation of this experiment.

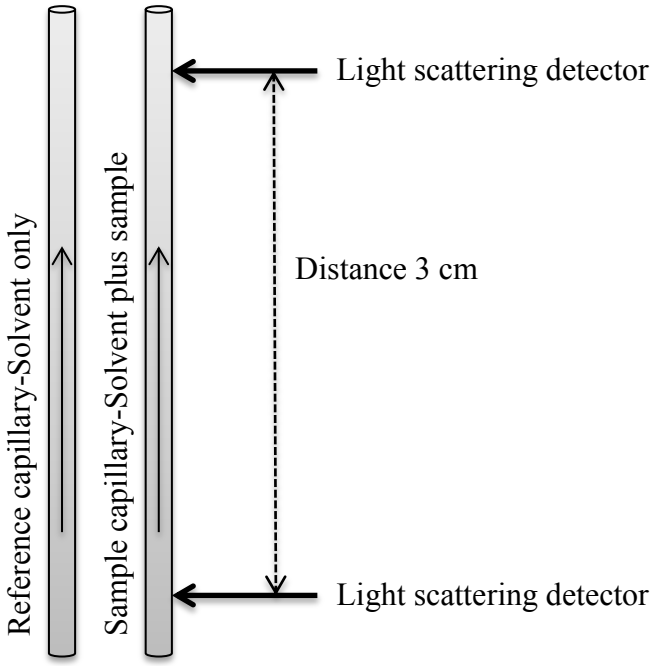


**Figure 3. 3 Diagram displaying the intrinsic viscosity measurements carried out using a reference and a sample capillary tubes and light scattering detectors.**

The raw bitumen samples that have been aged in the E-RTFO test, the UV chamber and naturally (experimental ageing parameters outlined in Chapter 2) were dissolved in analytical grade THF (2 mg/mL) with a butylate hydroxytoluene (BHT) stabiliser, and run using the same solvent as a mobile phase. The samples were analysed using a Malvern Panalytical OMNISEC Resolve and Reveal GPC system, fitted with a differential refractometer, light scattering detectors and a balanced capillary bridge viscometer. The solvent eluted through two Viscotek T6000 columns in series. Data was analysed using the OMNISEC V10.31 software. The author acknowledges Tahkur Singh Babra for help in carrying out the intrinsic viscosity analysis and in processing and the data obtained.

## 3.2 Extended Rolling Thin Film Oven test-Mechanical test results

The bitumen that was aged in the E-RTFO test displayed an increase in the carbonyl, carboxylic and sulphoxide absorbance bands in the ATR spectra (Chapter 2.1). This, alongside an increase in molecular weight measured *via* GPC is indicative of an increase in the oxygen content of the bitumen. The mechanical testing allows for the physical effect of these chemical changes to be determined.

The short-term, spurt, ageing mechanism is known to increase the viscosity of the bitumen as it reacts with oxygen at high temperatures.[1] The decomposition of hydroperoxide groups increases the aromaticity and the electron density of the asphaltene molecules, leading to an

increase in interactions between molecules and therefore increasing viscosity. This short-term ageing occurs during the RTFO test, a test in which the conditions are similar to that of short-term ageing of bitumen while in transit to the road surface.

The penetration and the softening point test results for the E-RTFO test bitumen can be found in Figure 3.4. The penetration is measured in $1/10^{th}$ mm units and the softening point is displayed in degrees centigrade.

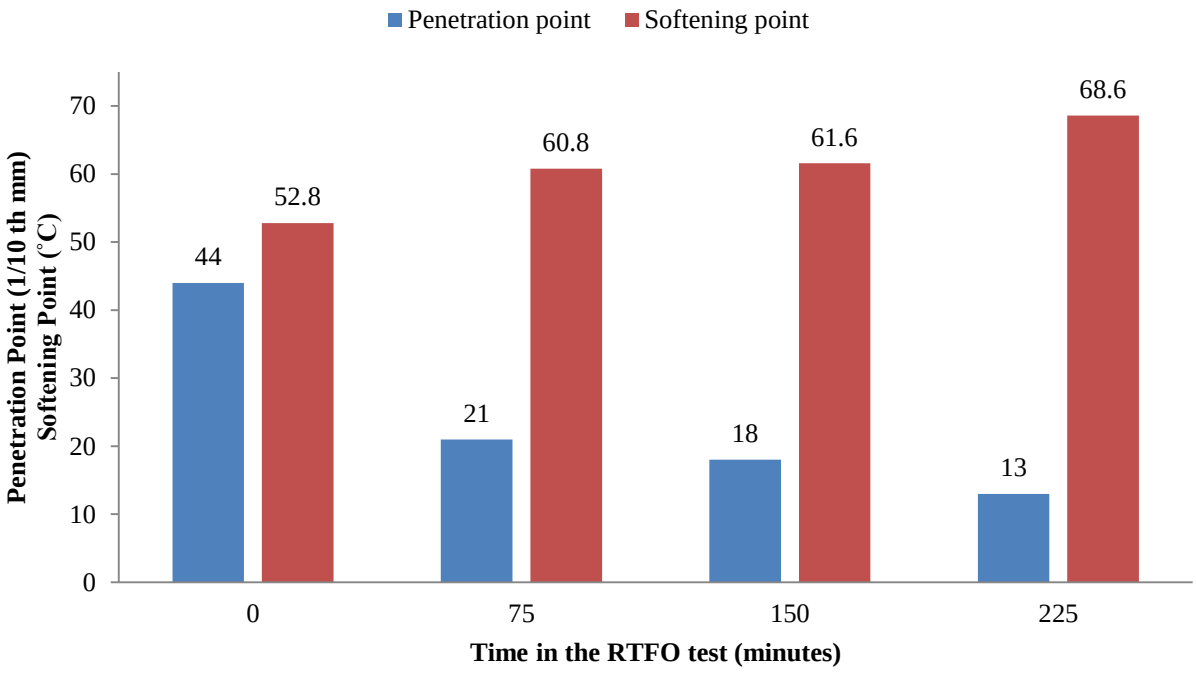


**Figure 3. 4 Penetration and Softening point results for the raw bitumen that has been aged in the E-RTFO test for 0-225 minutes**

There is a very dramatic drop in the penetration point results between the unaged bitumen and the bitumen after 75 minutes in the rolling thin film oven. The drop in penetration point indicates that after ageing the bitumen is becoming stiffer and it is increasingly difficult for the needle to penetrate into the bitumen. After 225 minutes in the E-RTFO test the penetration point of the bitumen has decreased by 70% of its original, unaged value.

The softening point, on the other hand, shows an increase in temperature as the sample is aged. As the softening point is the temperature of the water bath when the steel ball reaches the bottom of the cradle, the temperature at which this is achieved can give an indication as to the viscosity. The increase in temperature of the softening point, as the time in the rolling thin film oven increases, means that the bitumen is more viscous at lower temperatures. Bitumen

with high viscosity is less likely to be able to flow and 'heal' any micro-cracks that may occur throughout the asphalt service life, leading to crack propagation within the asphalt.[9]

The cohesion of the bitumen is a measure of how well the bitumen can bind with itself. There are two ways that an asphalt surface can fret; a loss of adhesion with the bitumen and the aggregates, or as a result of a loss of cohesion within the bitumen.[10] The Vialit pendulum test allows for the cohesion of the bitumen to be measured and therefore can give an indication of the bitumen's probability to undergo fretting in a road surface. The Vialit pendulum test is carried out at a range of different temperatures, which allows for a temperature profile to be produced for the bitumen. The British Standard for this test states that the temperature range must be extended until the cohesion falls below 0.4 J/cm$^2$.

The results for the pendulum test of the E-RTFO test aged raw bitumen can be found in Figure 3.5. Each point is an average of 6 samples at each temperature and the error bars are the 95% limits for the data sets.

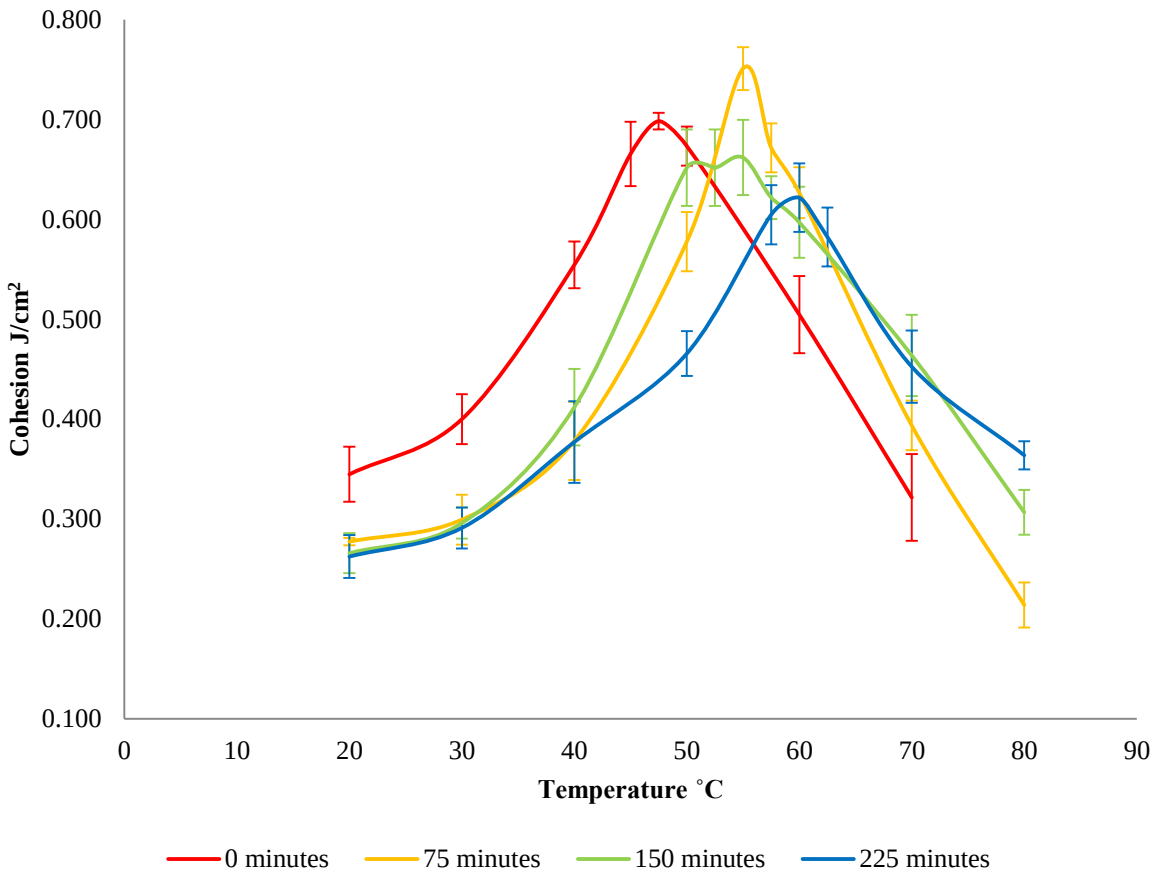


**Figure 3. 5 Vialit pendulum test results for the raw bitumen that has been aged in the E-RTFO test for 0-225 minutes**

Vialit Pendulum test results present as a curve which increases to a peak at the maximum cohesion and then drops off as the temperature increases. The maximum cohesion of these temperature profiles must be within a 5 ˚C temperature range to confirm the temperature of maximum cohesion. This curve can be explained by the intermolecular forces that are occurring within the bitumen. As the temperature rises from 20 ˚C there is an increase in energy to the bitumen hydrocarbon system which allows the molecules to align and stack in a manner that increases the intermolecular forces between the molecules, creating an increase in cohesion. As the temperature rises above its maximum cohesion the thermal energy results in a breakdown in these intermolecular forces and the molecular matrix re-assembles causing a decrease in viscosity which leads to a reduction in cohesion.[11]

The results from the raw bitumen aged in the E-RTFO test show an interesting profile change as the bitumen is aged. The maximum cohesion is seen to increase between 0-75 minutes. It then decreases as the ageing time increases. As the standard test length for the RTFO test is 75 minutes and this is said to replicate the short-term, in-transit ageing experienced by the bitumen prior to being laid, this result would misleadingly suggest that the short-term ageing increases the cohesion of the bitumen and would not show that cohesion *decreases* after 75 minutes.

It is interesting to note the temperature of the maximum cohesion measured. For all samples the temperature of the maximum cohesion increases as the ageing time increases. The result follows the same trend as the softening point which increases as the ageing time increases.

**Table 3. 1 Maximum cohesion and the temperature of the maximum cohesion for the bitumen aged in the E-RTFO test measured with the Vialit pendulum test**

| Time in E-RTFO test (minutes) | Maximum Cohesion (J $cm^{-2}$) | Temperature of maximum cohesion (˚C) |
|---|---|---|
| **0** | 0.698 | 47.5 |
| **75** | 0.751 | 55 |
| **150** | 0.662 | 55 |
| **225** | 0.622 | 60 |

The cohesion results at the lower temperatures are of interest when analysing bitumen that is to be used in roads in a country such as the UK which rarely experiences temperatures above

20-25 ˚C. By investigating the cohesion results measured at 20 ˚C independently, it is possible to see that there is a decrease in cohesion from 0.4 to 0.263 J/cm$^2$ after 75 minutes in the RTFO test. This is a 34% loss in cohesion and as the 75 minutes of the RTFO test is said to represent the short-term, in-transit oxidation, this oxidation is enough to cause an initial decrease in cohesion at the start of the road surface life.[12]

The intrinsic viscosity measurements presented in Figure 3.6 have been collected using the experimental parameters outlined above (3.1.4). The error bars within Figure 3.6 are the 95% confidence limits for two runs.

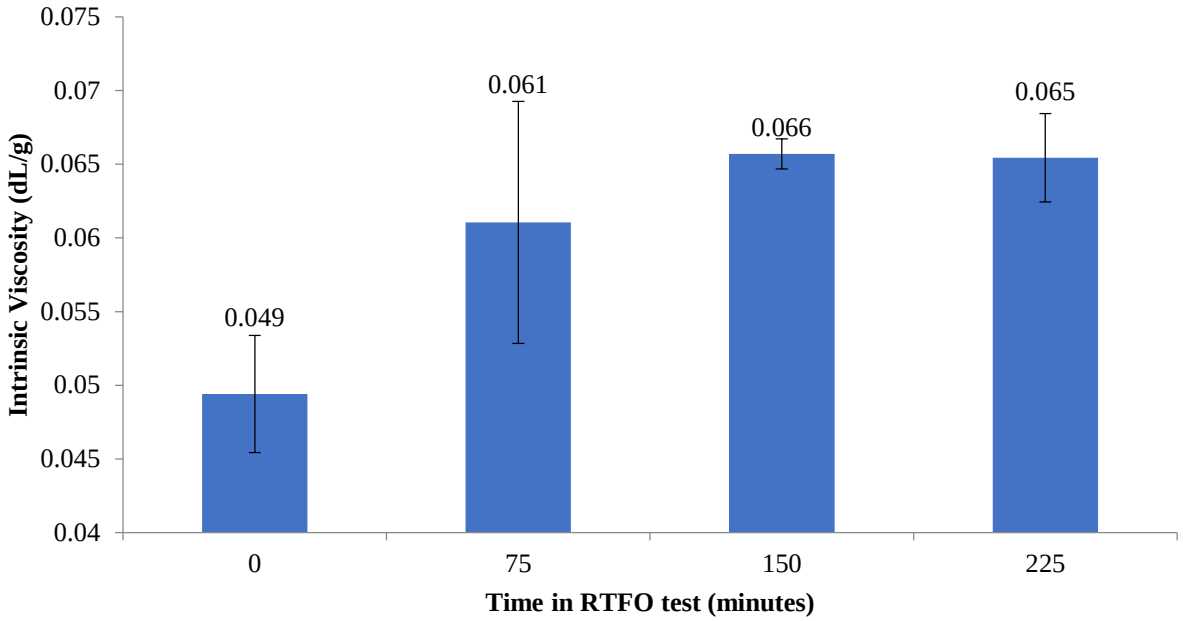


**Figure 3. 6 Intrinsic Viscosity results for the bitumen that has been aged in the E-RTFO test**

It is possible to see an overall 33% increase in the intrinsic viscosity of the bitumen that has been aged in the E-RTFO test for 225 minutes. The error bar on the average value for the intrinsic viscosity measurement of the 75 minute RTFO test aged bitumen is large and overlaps with all measurements. However, excluding this value, the trend shows an increase which levels to a plateau. This is similar to the result presented by Robertson *et al.*[11] Repeating this experiment would increase the reliability of this conclusion and unfortunately as a result of the time scale of this project this was not achievable in this work.

## 3.3 Ultra-Violet Light enhanced ageing-Mechanical test results

The spectroscopic results from the UV aged raw bitumen also indicated an increase in the oxidation product absorbance bands after ageing (Chapter 2.2 Figure 2.9). The formation of a brittle 'skin' was detected after 1 week of ageing and these experiments indicated that it was only the surface of the bitumen that was being oxidised as a result of the UV light exposure.

The nature of the penetration point tests requires the bitumen to be placed into standardised metal tins of specific dimensions (outlined in Section 3.1). In this case the UV aged bitumen samples needed to be heated and poured into the penetration point tins. This then dissolved the skin and the oxidised surface was integrated into the bulk of the bitumen. As a result the mechanical testing results are not representative of the properties of the surface of the sample which was exposed to UV light.

As a result of this, the experiment was altered and repeated using a different procedure for sample preparation. The raw bitumen was poured into the penetration point tins prior to the UV ageing. This allowed the skin to form on the surface of the bitumen, as seen before, and the penetration point was taken from the surface of these new samples. By making this change the skin was allowed to remain on the surface and was not integrated into the bulk, therefore a more reliable representation of the brittleness of this skin was measured. The results of both of these experiments are compared in Figure 3.7.

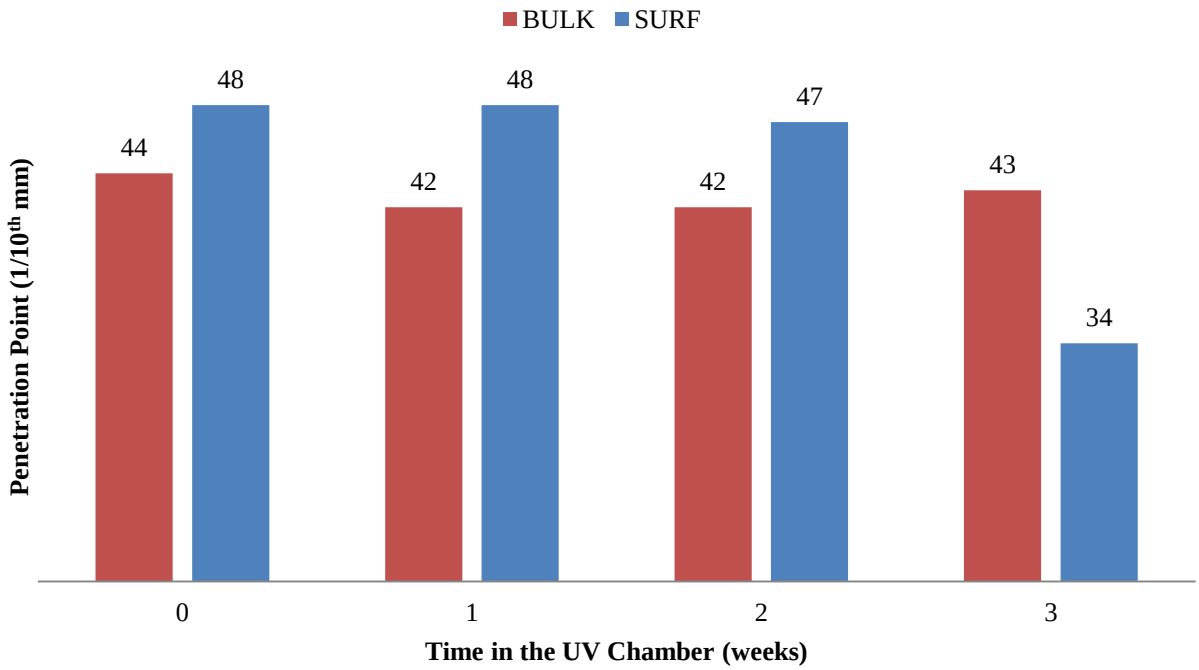


**Figure 3. 7 Penetration and Softening point results from the raw bitumen samples that have been aged in the UV chamber for 0-3 weeks with mixing (BULK) and without mixing (SURF)**

As predicted the bulk results show very little change in the penetration point. There is only a 4% decrease between the unaged bitumen and the bitumen after 1 week of ageing. The penetration point then increases at 3 weeks of UV ageing, which suggests that the change in penetration point for these samples is not outside of the error of the test. When the surface is oxidised and the oxidised skin is not mixed into the bulk the surface penetration does show a decrease with increasing ageing time. The overall penetration drops from 43 to 34 ($1/10^{th}$ mm) after the 3 weeks of UV exposure which is a 29% decrease in penetration. By comparing these results and combining them with the chemical information from the DRIFT spectroscopy, (Chapter 2.2), it seems very likely that the UV exposure of the bitumen oxidises the surface layer only. This creates a brittle skin on the surface and this skin then protects the bulk bitumen from further oxidation. This brittle skin is made from a combination of molecular stacking of the bitumen asphaltene molecules, with strong intermolecular interactions holding the network together. When this is heated the molecular framework breaks down resulting in a less viscous material.[11]

In order to measure the softening point of the bitumen it is necessary to heat the sample. The softening point rings were then be prepared using the bulk bitumen mixture. The results of this test for the UV aged bitumen can be found in Figure 3.8.

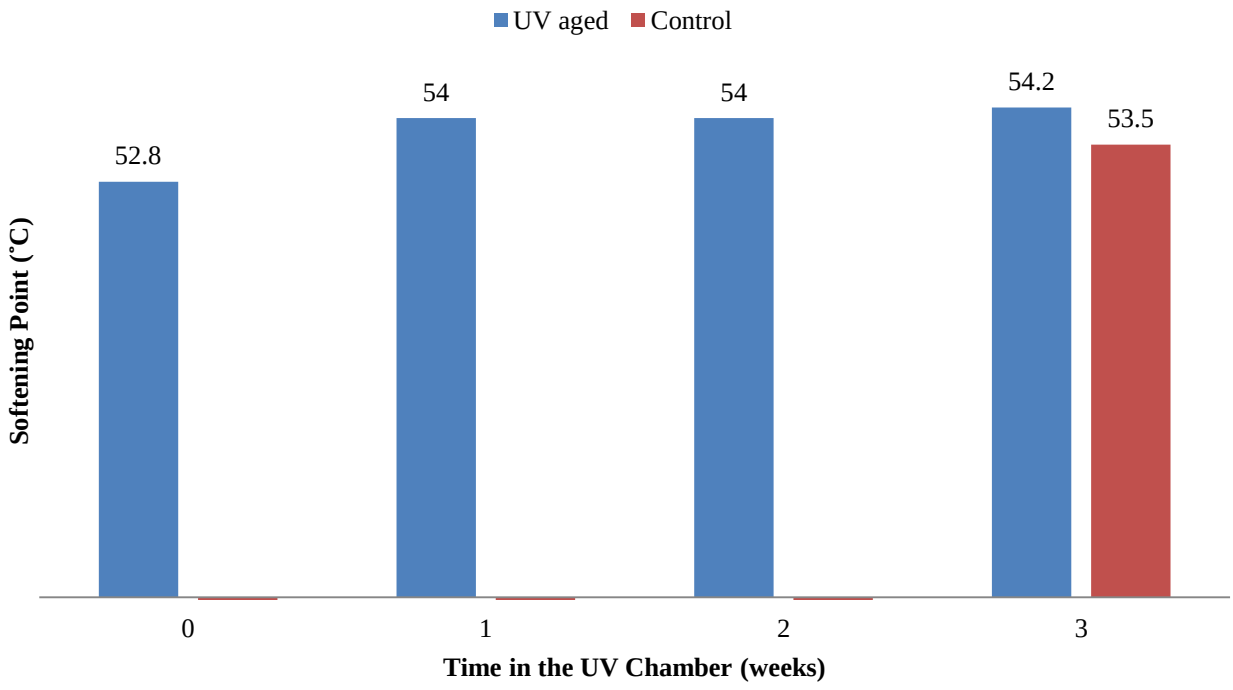


**Figure 3. 8 Softening point results of the raw bitumen that has been aged in the UV chamber for 0-3 weeks**

The softening point of the bitumen shows only a very small change, (3% increase) throughout the 3 weeks of UV ageing. This is to be expected and mirrors what was seen in the penetration point test of the bulk mixture. The bitumen has been oxidised on the surface however there has been little, reliably measureable change in mechanical properties of the bulk of the bitumen. Interestingly, the softening point value for the control sample is within range of the UV exposed samples (53.5 ˚C). The control sample was exposed to only thermal ageing within the UV chamber for 3 weeks. Therefore this result supports the hypothesis that the conditions in the UV chamber are not inducing measurable physical or chemical change within the bulk bitumen even though they clearly cause significant oxidation at the surface of the bitumen.

The Vialit pendulum test has been carried out and the results for these samples are quite variable. In a similar manner to the penetration point and softening point tests, the bitumen needs to be heated and mixed in order to prepare the steel blocks for the pendulum testing. This then incorporates the surface bitumen into the bulk. Therefore the results from the Vialit pendulum test are not representative of the surface ageing that has occurred.

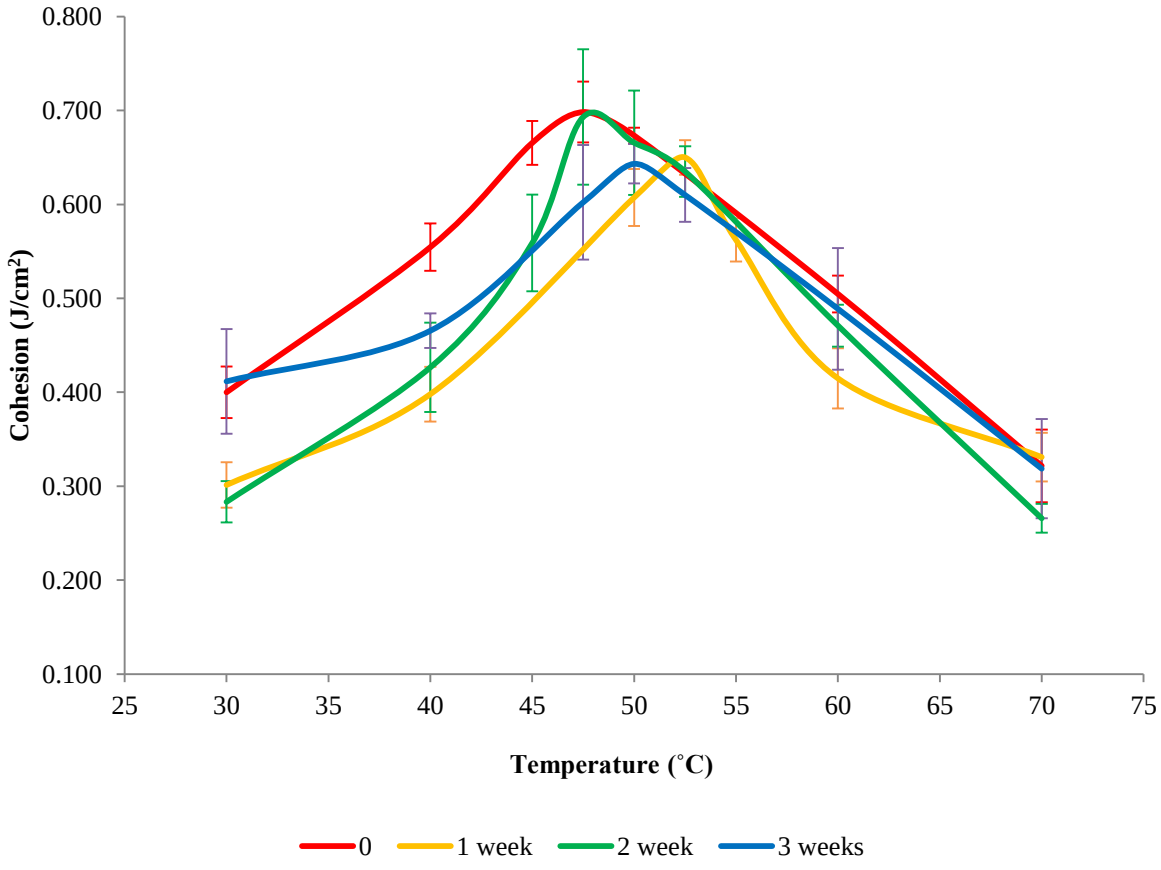


**Figure 3. 9 Vialit pendulum test results for the raw bitumen that has been aged in the UV chamber for 0-3 weeks**

There is a very small decrease in the overall maximum cohesion between 0 and 3 weeks in the UV chamber from 0.693 to 0.643 J/cm$^2$ (7% decrease) and the temperature of the maximum cohesion measurement shifts from 47.5 to 50 ˚C. The error bars are presented in Figure 3.9 are the 95% confidence limits and there are many areas within Figure 3.9 that show these error bars overlapping. As a result of this it would be difficult to state with certainty that any of these measured differences are real. Therefore these tests results should not be regarded as representative of a real change within the bitumen. The maximum cohesion and the temperature of this maximum cohesion are outlined in Table 3.2.

**Table 3. 2 Maximum cohesion and the temperature of the maximum cohesion for the bitumen aged by the UV chamber measured using the Vialit pendulum test**

| Time in UV chamber (weeks) | Maximum Cohesion (J/cm$^2$) | Temperature of Maximum Cohesion (˚C) |
|---|---|---|
| **0** | 0.698 | 47.5 |
| **1** | 0.650 | 52.5 |
| **2** | 0.693 | 47.5 |
| **3** | 0.643 | 50.0 |

The data listed in Table 3.2 highlights the variability of the measured maximum cohesion. The variation in this measurement means that no decrease in the maximum cohesion, or the temperature at which the maximum cohesion is reached, can be detected.

These results allow a similar conclusion to be drawn as from the penetration and softening point tests. The oxidation has produced a skin on the surface of the bitumen, which has protected the bulk bitumen. These mechanical tests are a measure of the bulk bitumen properties; therefore they are less sensitive to smaller changes that have occurred on the surface layers of the bitumen.

The intrinsic viscosity of the UV aged bitumen was analysed using the parameters outlined above (3.1.4).

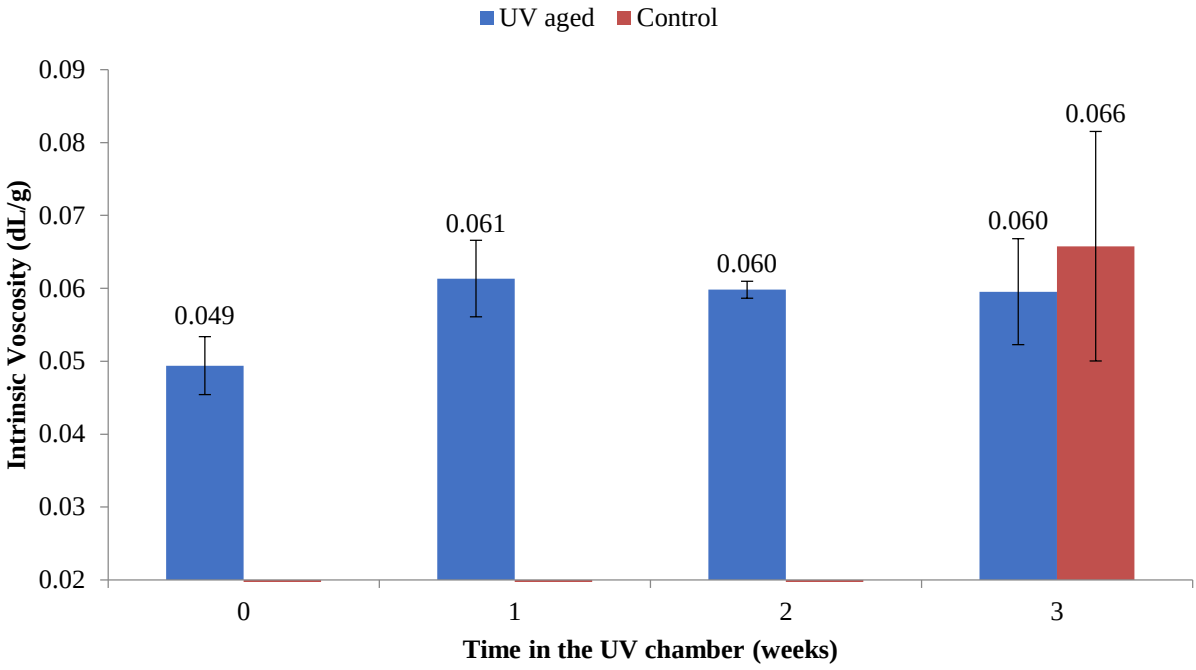


**Figure 3. 10 Intrinsic viscosity measurements for the UV aged bitumen and the control sample**

The intrinsic viscosity shows a slight increase between 0-3 weeks however the error bars are overlapping which indicates that the trend is unreliable. It is interesting to note that the 3 week control appears to have a higher intrinsic viscosity than the unaged sample (34% increase). However, the error bar for this average value is very large indicating that there is much variability associated with this value and that no reliable conclusion can be drawn regarding the intrinsic viscosities of the UV-aged and unaged samples.

The initial results from this experiment show very little trend in viscosity changes, which supports the GPC findings (Chapter 2.2) that there is not a sufficient change in the chemistry of the bulk sample upon ageing in the UV chamber to initiate measureable change in viscosity. These conclusions could be supported by a repeat of this viscosity analysis which was outside of the time scale for this research.

## 3.4 Naturally aged bitumen-Mechanical test results

Upon analysis of the results from the UV aged bitumen it is concluded that the thermal conditions, compared to the E-RTFO test, are less harsh and that the UV exposure in the UV chamber only affects a very thin surface layer which has produced a skin on the surface which protected the bulk from further oxidation. It is known that the natural conditions that the

bitumen sample were exposed to on the roof of TRL are even less 'harsh' than the UV chamber, with lower temperatures and less UV exposure.

It is therefore hypothesised that there will be little to no reliable mechanical data measureable within the naturally aged bitumen. The skin formed by the UV exposure of the natural sunlight will protect the bulk bitumen from further oxidation and mechanical changes and the temperatures experienced by these naturally-aged samples would be unlikely to cause significant changes to the mechanical properties of the bulk samples on this short time scale.

It could also be the case that the classic mechanical property tests used here are not sensitive enough to detect the slight changes that may occur in the UV and naturally aged bitumen samples. Therefore only the intrinsic viscosity has been measured for the naturally aged bitumen samples.

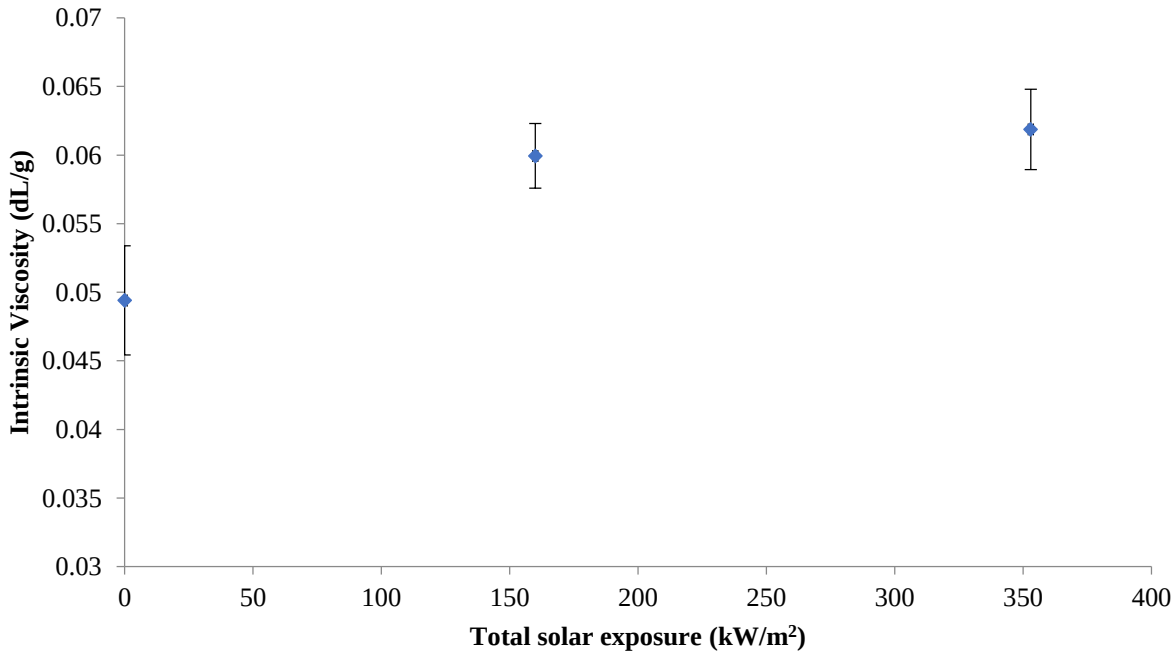


**Figure 3. 11 Intrinsic viscosity measurements for the bitumen that has been aged naturally for 0-4 weeks on the roof at Crowthorne House**

The intrinsic viscosity measured for the naturally aged bitumen shows a gradual increase as the total solar exposure increases. This gradual increase appears to plateau as the bitumen ages although the error bars overlap slightly. An increase in viscosity as a result of natural conditions can be attributed to the second stage of the ageing (long-term) outlined by Petersen *et al.*[1] . This mechanism is much slower that the spurt reaction seen in the RTFO test and forms a number of different oxygen containing functional groups. The formation of these

oxidation product absorbance bands have been seen in the DRIFT spectra from the surface of the naturally aged bitumen samples (Chapter 2.3). The increase in oxygen within the bitumen composition has caused an increase in polarity of the asphaltene molecules which leads to an increase in interactions within the molecules and therefore an increase in the viscosity. More repeats would be required to determine the reliability of this conclusion.

## Summary

The mechanical tests on the E-RTFO test aged bitumen show a decrease in penetration point and an increase in softening point. This shows that there is an increase in stiffness and an increase in viscosity. There is also a measureable decrease in maximum cohesion measured with the Vialit pendulum test. This confirms that the viscosity is increasing. It is concluded that the bitumen cohesion decreases as a result of this increased viscosity. The intrinsic viscosity measurements have also confirmed an increase in viscosity as the time in the E-RTFO test increases. It is possible that under these ageing conditions the bitumen has become highly viscous, and therefore would be more likely to incur cracking and fracturing if this bitumen was present within an asphalt road surface. The physical change is recorded with all mechanical tests; therefore it is the case that the change in viscosity is as a result of the chemical change that has occurred within the bitumen composition.

The penetration point, softening point and the Vialit pendulum tests have not been able to measure a reliable trend in mechanical properties of the bitumen that has been aged in the UV chamber. The oxidation has been localised on the surface of the bitumen and a brittle surface skin has formed.

The property of the surface skin of the UV aged bitumen has been measured using the penetration point test and a dramatic decrease in penetration was measured. This highlights the physical change occurring on the surface. However, the oxidation only affects the first 4-5 μm and the bulk is unaffected.[13]

Once the bitumen surface skin is heated and blended into the bulk the mechanical property test results are inconclusive. This indicates that the brittleness of the surface skin that formed upon UV exposure was a result of physical interactions between the thin oxidised layers at the surface.

The intrinsic viscosity measurement of the bitumen aged in the UV chamber also shows no reliable trend in viscosity change. This test is a more advanced measure of viscosity than the

classic mechanical tests. A problem with the intrinsic viscosity measurement is that it is carried out in solution. The weak intermolecular interactions being formed between molecules on the UV oxidised surface will almost certainly be broken down when the sample is dissolved, reducing the viscosity and meaning that this test cannot give reliable data on the properties of the surface layer. This is similar to the effect of the heating and blending of the bitumen, which would break down the intermolecular interactions between the bitumen molecules.

The problem with all of these classic tests of mechanical properties is that they require a large amount of bitumen and therefore assume that a sample is relatively homogenous. They are not so suitable for heterogeneous samples such as those produced in this work where oxidation only of a thin layer has occurred. In order to gain a further insight into the physical changes occurring on the surface of the bitumen more testing could be carried out in which a very thin film of bitumen is aged in the UV chamber and the viscosity of this very small samples is then measured. This would require considerable modification of the mechanical property test and was beyond the scope of the current project.

The increase in the intrinsic viscosity of the bitumen that has been aged naturally highlights a decrease in the flow of the bitumen. This will ultimately reduce the bitumen's ability to heal and recover from the mechanical stresses of traffic loading. In turn this makes the bitumen more likely to fracture and lead to failure mechanisms such as fretting or cracking.

Chemical and mechanical changes can be monitored for raw bitumen as it is aged; however, the chemical and physical composition of raw bitumen is much less complex than that of asphalt. Therefore the next step for this project is to analyse asphalt concrete with diffuse reflectance spectroscopy and the above mechanical tests to identify if the DRIFT technique can identify similar changes in asphalt to those obtained in this work for the bitumen and to determine whether or not any correlations between spectroscopic and mechanical testing for asphalt samples can be obtained. This work is reported in the subsequent chapters of this thesis.

## References


[1] J. C. Petersen and R. Glaser, Asphalt oxidative mechanisms and the role of oxidation products on age hardening revisited, Road Mater. Pavement, 12, 2011, 795-819.

[2] P. Redelius, The structure of asphaltenes in bitumen, *Road Mater. Pav. Des.,* **7,** 2006, 143-162.

[3] J. L. Creek, Freedon of action in the state of asphaltenes: Escape from conventional wisdom, *Energy and Fuels,* **19,** 2005, 1212-1224.

[4] British Standard, EN 12596:2007, Bitumen and bituminous binders- Determination of dynamic viscosity by vacuum capillary.

[5] British Standard EN 12595:2007, Bitumen and bituminous binders- Determination of kinematic viscosity.

[6] British Standard EN 1426:2015, Bitumen and bituminous binders- Determination of needle penetration.

[7] British Standard EN 1427:2015, Bitumen and bituminous binders- Determination of the softening point- Ring and Ball method.

[8] British Standard EN 13588:2008, Bitumen and bituminous binders- Determination of cohesion of bituminous binders with pendulum test.

[9] C. Li, S. Wu, G. Tao and Y. Xiao, Initial self-healing temperatures of asphalt mastics based on flow behaviour index, *Materials,* **11**(6), 2018, 917.

[10] H. Bahia, R. Moraes and R. Velasquez, presented in part at the 5th Eurasphalt and Eurobitume Congress, June, 2012.

[11] R. E. Robertson, Chemical properties of asphalts and their relationship to pavement performance, Strategic Highway Research Program, Washington, DC, 1991, Research Paper

[12] J. Reed and D. Whiteoak, The Shell Bitumen Handbook, 5th Edition, Thomas Telford Publishing, London, 2003, ISBN: 0-7277-3220-X.

[13] W. Zeng, S. Wu, L. Pang, H. Chen, J. Hu and Y. Sun, Research on ultra violet (UV) ageing depth of asphalt, *Constr., Build., Mater.,* **160,** 2018, 620-627.

# Chapter 4

## Artificial ageing of asphalt- Ultra-Violet light

Following the study of the ageing of the bitumen the next step for this project was to determine if similar changes could be detected in asphalt samples. Asphalt samples are more complex than raw bitumen as a result of the addition of filler and aggregates to make up the asphalt mixture. The presence of these materials will have an effect on the infrared spectra collected from the samples. It is therefore necessary to be able to identify the chemical changes occurring as a result of the oxidation of the bitumen component of the asphalt in IR spectra alongside the absorbance bands that correspond to the fillers.

Asphalt samples were produced using a 10 mm Stone Mastic Asphalt (SMA) mixture from United Asphalt. Bitumen was mixed with carbonate filler and 10-mm stone aggregates. This was then weighed into 4 kg samples which were then compressed with an industrial pavement roller (Benford, WPH roller) into a wooden mould with 200 x 200 x 50 mm dimensions. The bitumen content was approximately 6% and the asphalt contained an approximate void content of 12%. The asphalt slabs were made in accordance with the British Standard EN 13108-1:2006.[1]

This asphalt was aged using the UV chamber built by engineers at TRL used previously for the UV-ageing on bitumen samples (see Chapter 2.2). The chamber is maintained at an internal temperature of 60 ˚C while exposing the asphalt to UV light with a maximum wavelength of 368 nm. The slab was aged between 0-4 weeks and diffuse reflectance spectroscopy was used to map the asphalt throughout the ageing experiment to monitor any chemical changes that occur.

This mapping involves placing an asphalt slab into an x, y table built at TRL. The table can move in x and y directions, and the spectrometer is fixed at the centre and the co-ordinate location of the focal point can be recorded.

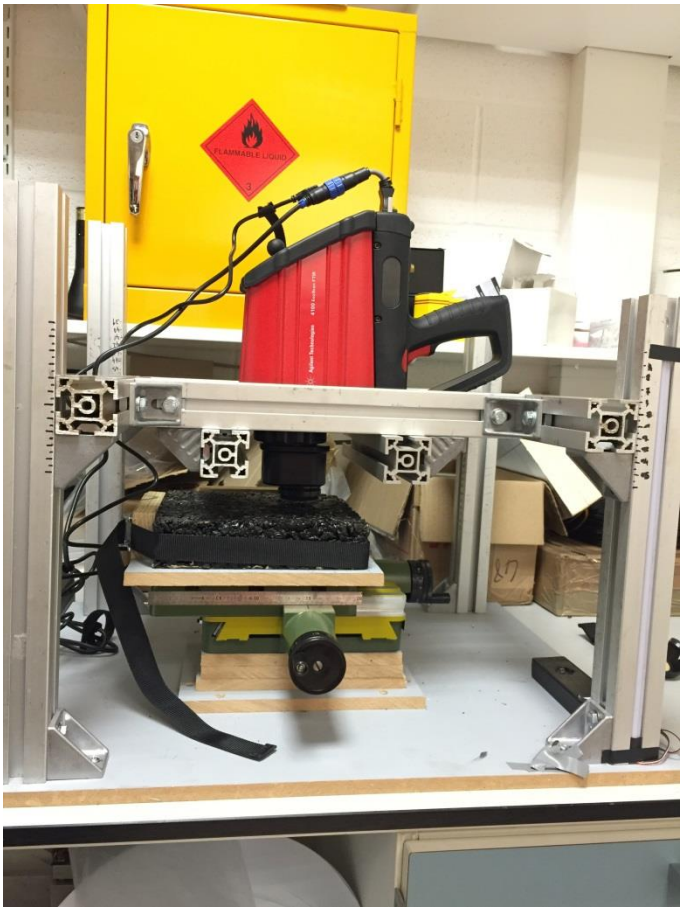


**Figure 4. 1 Photograph of the x,y table at the Transport Research Laboratory, with the ExoScan 4100 handheld spectrometer in position.**

A number of Diffuse Reflectance Infrared Fourier Transform (DRIFT) spectra have been collected from different coordinates and the same coordinates have been returned to after ageing. This type of experiment allows a clearer comparison between DRIFT spectra that are collected from the same point on the same sample, removing any errors from internal variation across the surface of the asphalt.

## 4.1 Diffuse Reflectance Infrared spectroscopic analysis

### *4.1.1 4 week UV aged asphalt- mapping*

Figure 4.2 shows a photograph of the co-ordinates that were used to collect DRIFT spectra from the asphalt slab used in the 4 week UV ageing experiment. The unaged sample spectra were collected from these coordinates and the slab was placed into the UV chamber. At weekly intervals the sample was removed and spectra were then taken at the same co-ordinate locations and the asphalt was placed back into the chamber. This was repeated for 4 weeks.

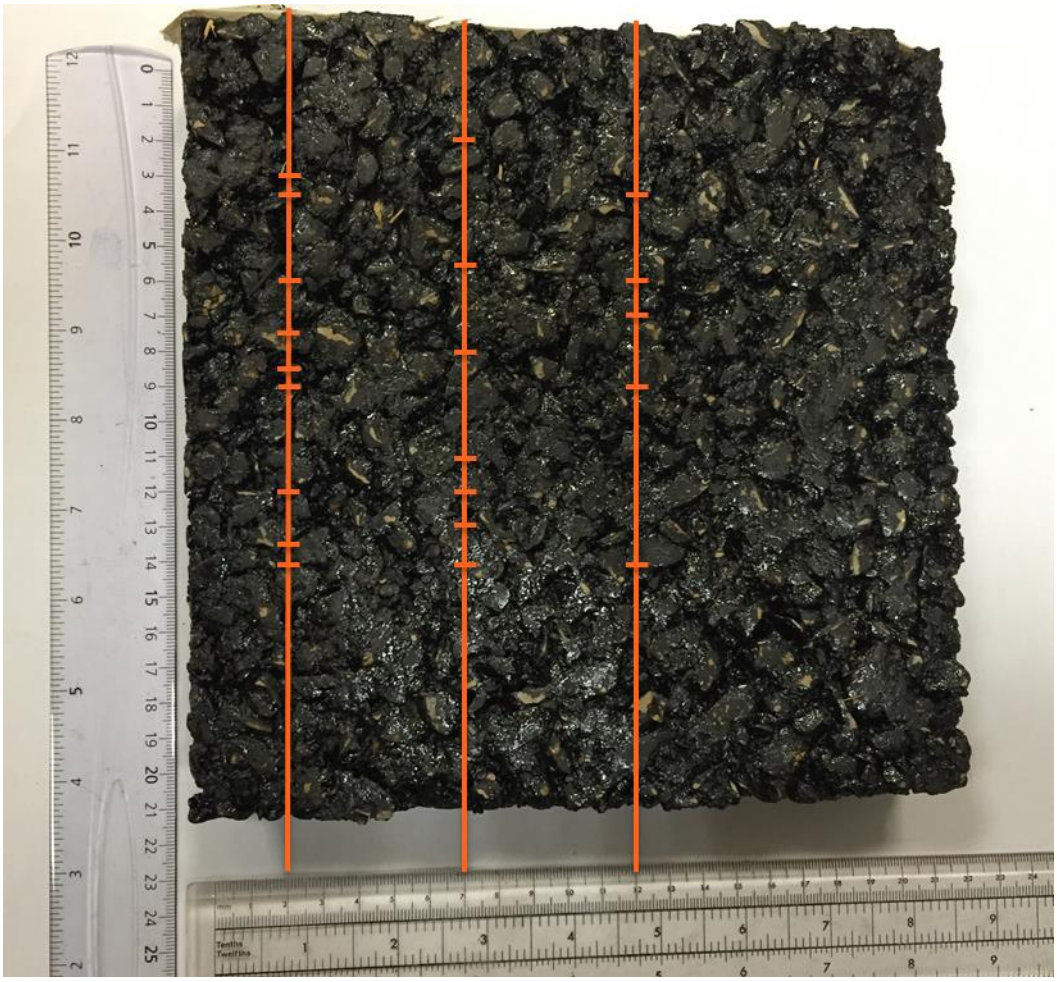

**Figure 4. 2 Photograph of the DRIFT spectra location points on the UV-aged asphalt map experiment**

The diffuse reflectance spectra from these locations look slightly different to the reflectance spectra from the raw bitumen. There is a number of new absorbance bands that can be attributed to the carbonate filler and aggregates used to create the bulk asphalt.

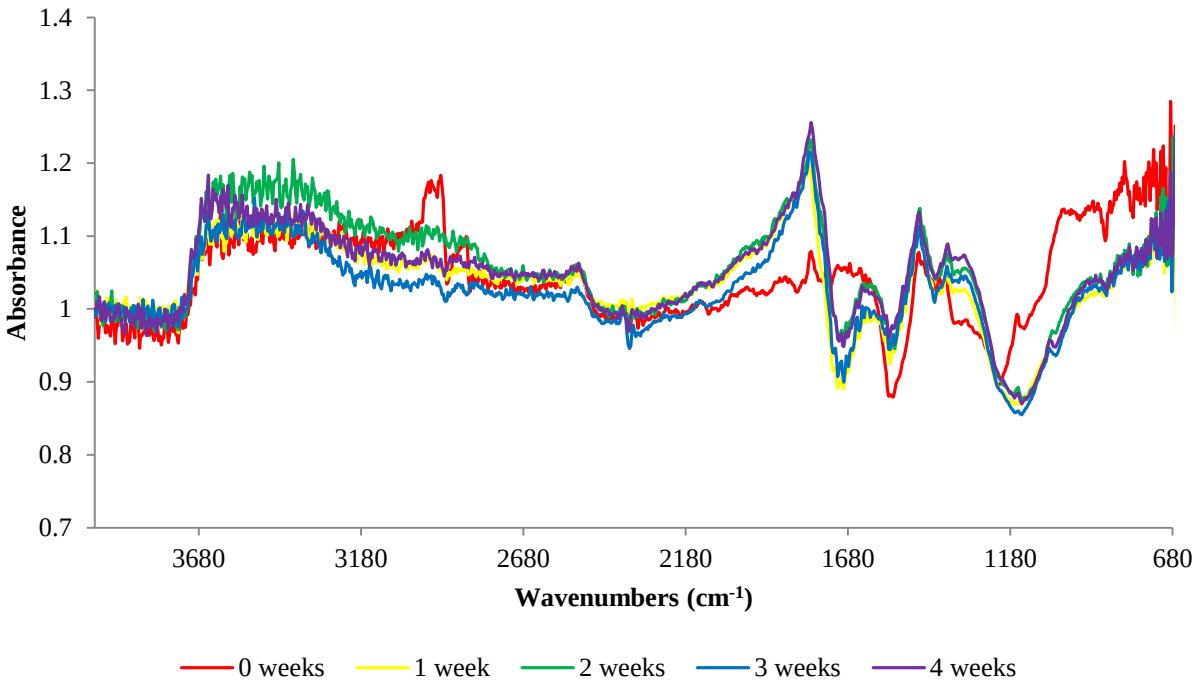


**Figure 4. 3 DRIFT spectra from the surface of the asphalt samples aged in the UV chamber for 0-4 weeks**

It is possible to see in the DRIFT spectra in Figure 4.3, the presence of the absorbance bands for the hydrocarbon bitumen C-H bonds stretching. The C-$H_2$ bending modes can also be seen, however these overlap with an absorbance band at 1543 $cm^{-1}$. It is also possible to see an $SiO_2$ bond at 1159 $cm^{-1}$.

**Table 4. 1 Absorbance bands present in the DRIFT spectra of the UV-aged asphalt samples**

| Absorbance band ($cm^{-1}$) | Bond Assignment |
|---|---|
| **2922, 2848** | C-H (stretch) |
| **2510** | $CO_3^{2-}$ (combination 1543 +883) |
| **1755** | $CO_3^{2-}$ (overtone 883) |
| **1692** | C=O (stretch) |
| **1543** | $CO_3^{2-}$ (asym stretch) |
| **1461, 1371** | C-$H_2$ (bend) |
| **1159** | Si-O (stretch) |
| **1144** | C-O (stretch) |
| **883** | $CO_3^{2-}$ (in plane bend) |

The carbonate absorbance bands can be confirmed by taking a reference spectrum of the calcium carbonate filler alone. The ExoScan 4100 spectrometer has been used to collect spectra of calcium carbonate in both ATR and DRIFT detection modes for comparison.

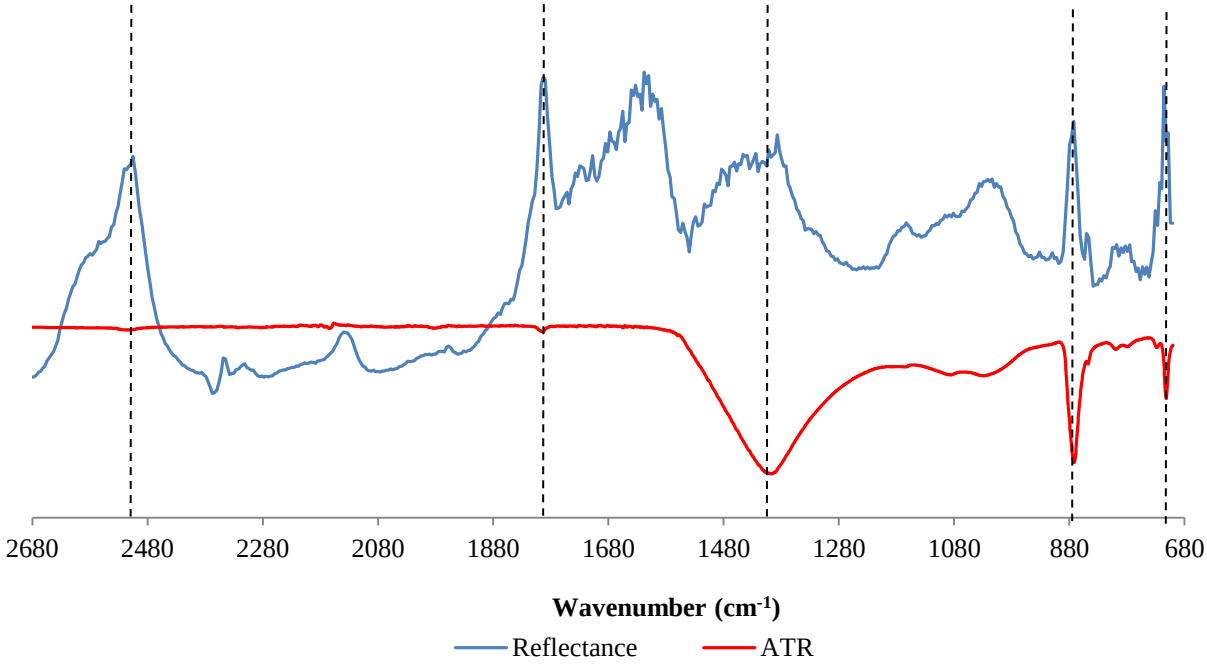


**Figure 4. 4 ATR and reflectance-FTIR spectra of calcium carbonate between wavenumbers 2680-680 $cm^{-1}$**

The ATR and DRIFT spectra shown in Figure 4.4 show a clear similarity in the absorbance bands that are arising within the IR spectra of calcium carbonate. The bands can be assigned to specific vibrations within the carbonate ion. The structure displayed in Figure 4.5 shows the bonding within a calcium carbonate molecule. The calcium ion is ionically bonded to a carbonate ion *via* two of the three oxygen atoms. This gives rise to two long C-$O^-$ bonds with a third C=O double bond. This molecule is stabilised by the resonance of electrons between all three bonds.[2]

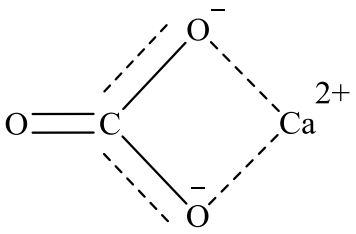


**Figure 4. 5 Mode of coordination of $Ca^{2+}$ and $CO_3^{2-}$ ions in calcium carbonate**

There are three fundamental absorbance bands that occur within calcium carbonate when irradiated with infrared light that have been recorded in these spectra; the asymmetric stretch, and the in plane and out of plane bends of the $CO_3^{2-}$ ion.[3,4]

**Table 4. 2 Absorbance bands from Figure 4.4 that correspond to calcium carbonate and their bond assignment**

| Absorbance band ($cm^{-1}$) | Bond Assignment |
|---|---|
| **2512** | Combination (1793 +711) |
| **1793** | Overtone (871) |
| **1396** | Asymmetric stretch |
| **871** | In plane bend |
| **711** | Out of plan bend |

The most dominant absorbance bands in the ATR spectrum correspond to the asymmetric stretch of the $CO_3^{2-}$ bond and the sharp absorbance bands at 871 and 711 $cm^{-1}$ which can be attributed to the in and out of plane bends. The in-plane bend at 871 $cm^{-1}$ has shifted slightly in this spectrum compared to the spectra of the asphalt in Figure 4.3 where this bond is absorbing at 883 $cm^{-1}$, however, this is still within the range for the in-plane bend absorbance. There are three other very strong absorbance bands in the diffuse reflectance spectra that are very weak in the ATR. These include the combination and overtone absorbance of the carbonate vibrations at 2512 and 1793 $cm^{-1}$ respectively.

Overtones and combination absorbance bands can be explained with simple quantum theory of the absorbance of infrared light by a bond. The energy gap between vibrational energy levels (E) is determined by the masses of the atoms and the force constants of the chemical bonds within a molecule or ion. When a molecule is irradiated with infrared light which has a frequency that matches the vibrational transition i.e. the energy gap between two energy levels, the IR light is absorbed. The ground state ($\nu$ =0) is the lowest energy state and the fundamental transition occurs when the molecule is exited to the first energy level ($\nu$ =1). Figure 4.6 is a diagrammatic representation of the possible vibrational transitions and overtones within a harmonic oscillator. Harmonic oscillation leads to energy gaps between energy levels that are equal.[5]

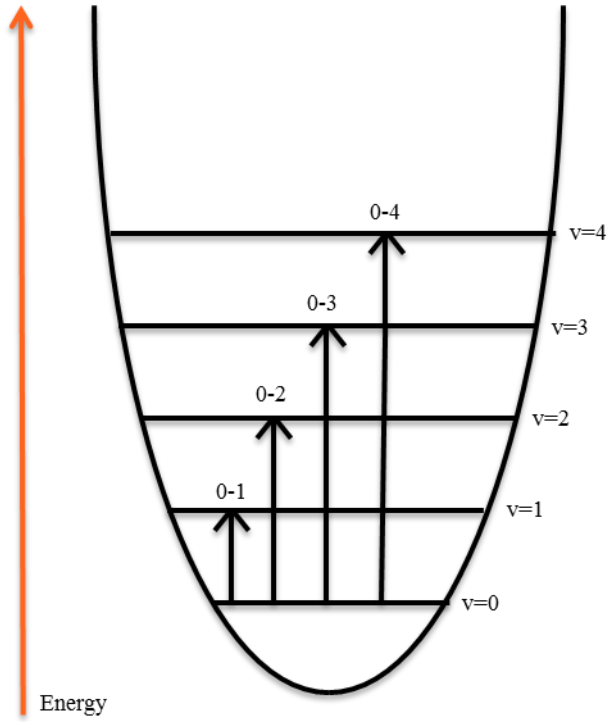


**Figure 4. 6 Potential Energy Diagram representing the vibrational overtone transitions possible within a harmonic oscillator**

Overtones occur when the molecule or ion is excited to an energy level that is greater than 1. The first overtone is the transition from ν = 0-2 and leads to and absorbance band at $\nu_1$ x 2 wavenumbers.[6] The second overtone involves the transition from 0-3 and would absorb energy equal to $\nu_1$ x 3 wavenumbers, assuming that the molecule or ion vibrates harmonically. In fact the observed overtone absorption bands do not occur at *exactly* $\nu_1$ x 2 and $\nu_1$ x 3 etc. because in reality molecules are anharmonic oscillators. Anharmonic oscillators are different to harmonic oscillators such that the restoring force of the oscillation is not linearly related to the displacement. This leads to energy gaps being uneven, increasingly more so at higher energy levels.[5] Combination absorbance bands occur when two fundamental vibrations (for example, $\nu_1$ and $\nu_2$) are excited at the same time, absorbing $\nu_1 + \nu_2$ energy.

There is also an absorbance band within the diffuse reflectance spectrum of the carbonate (Figure 4.4) that has first derivative properties between the wavenumbers 1750-1480 $cm^{-1}$ with a maximum absorbance value at 1640 $cm^{-1}$ and a minimum at 1539 $cm^{-1}$. This could be attributed to a first derivative absorbance band with a centre at approximately 1580 $cm^{-1}$. An absorbance at this wavenumber could correspond with a combination of the in and out of plane bending modes (871+711 $cm^{-1}$). The absorbance band at 1543 $cm^{-1}$ in the spectra of the asphalt (Figure 4.3) can be now assigned to this first derivative, combination absorbance band

as opposed to the asymmetric stretch which would be absorbing at a lower wavenumber at approximately 1460 $cm^{-1}$ and overlapping with the C-$H_2$ bending modes.

It is now possible to confidently assign the absorbance bands in the DRIFT spectra from the surface of the UV aged asphalt, Figure 4.3. The small sharp absorbance band at 1755 $cm^{-1}$ can be assigned to the first carbonate $CO_3^{2-}$ overtone of the in plane bending mode at 871 $cm^{-1}$. This overlaps with a carbonyl absorbance band which is seen in the DRIFT spectra after ageing in the UV chamber.

The carbonyl absorbance band is presenting as a first derivative as seen previously within the DRIFT spectra from the UV-aged raw bitumen. It is also possible that the surface characteristics are changing as a result of the UV light exposure, as seen before with the formation of the surface skin on the UV aged bitumen (Chapter 2.2). This would be altering the refractive index of the sample surface, leading to a change in the scattering and the absorbance of the infrared light by the sample.[7]

It is now possible to attempt to quantify the intensity of the absorbance band of this carbonyl functional group. This has been done in two ways; by integrating the area underneath the absorbance band and by recording the absorbance intensity at a specific wavenumber.

The absorbance band area has been measured between the wavenumbers 1826-1763 $cm^{-1}$ which is the higher wavenumber section of the first derivative carbonyl band. Only half of this first derivative absorbance band has been integrated here. If the absorbance band is a true first derivative, in theory the area across the entire wavelength will be equal to 0 as a result of the positive and negative directions of the wave feature.

The results of the area integration for each spectra from each coordinate analysed on the asphalt sample can be found in Figure 4.7. The spider graph displays the x, y co-ordinates, where the spectrum was collected, around the circumference of the chart and the absorbance band area measured from this spectrum is recorded on the radial axis.

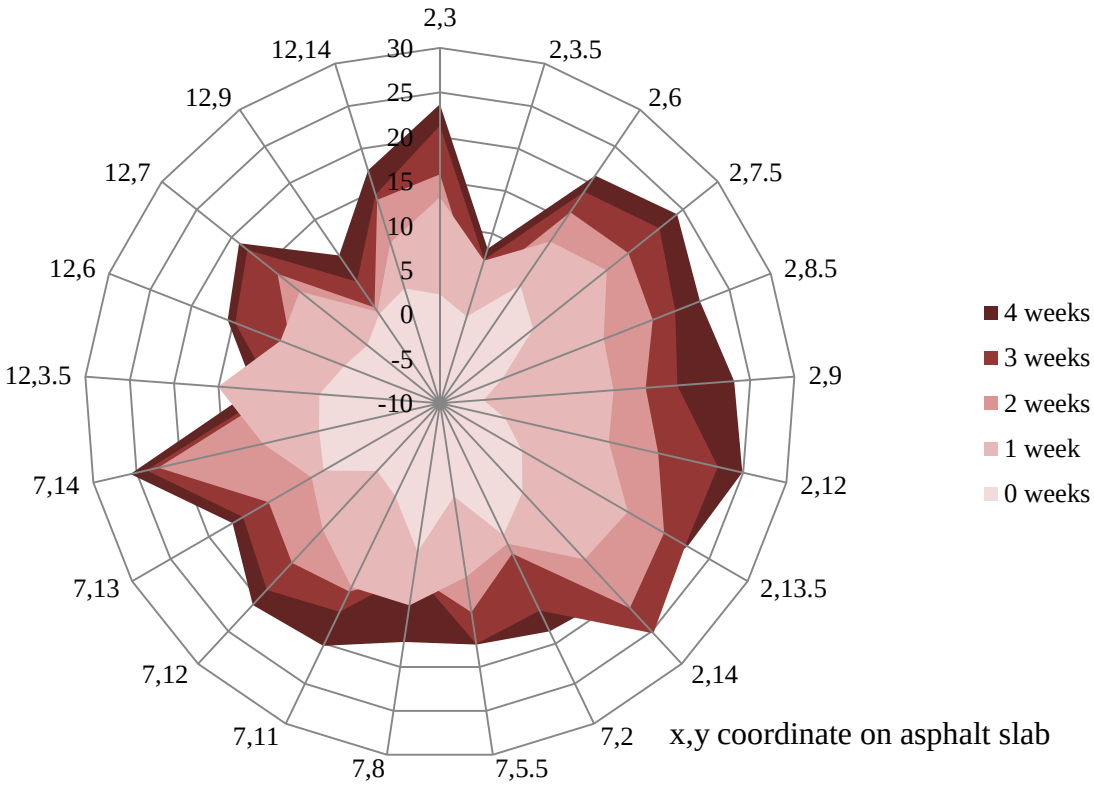


**Figure 4. 7 Spider-graph of the absorbance band areas from each coordinate location on the surface of the asphalt slab that has been aged for 0-4 weeks. The radial axis shows the integrated absorbance band area and the shaded areas represent an amount of UV ageing**

It is possible to see an increase between the unaged (0 weeks) and the 1 week UV-aged sample for all locations on the asphalt map. The measured absorbance band areas become more variable for some of the locations on the asphalt after this time, however, for the majority of the sites there is gradual increase in absorbance band area as the time in the UV chamber increases.

In order to identify the extent of this variability, the average absorbance band area calculated using each spectral location measurement has been calculated. This average calculation allows every absorbance band area to be taken into account and error bars can be calculated to visualise the variability of the measurements at each time point.

The average absorbance of the band between 1826 and 1763 $cm^{-1}$ has been calculated from all 24 absorbance band areas measured from all DRIFT spectra from each location at each age. The results for this and the 95% confidence limits for these averages can be found in Figure 4.8.

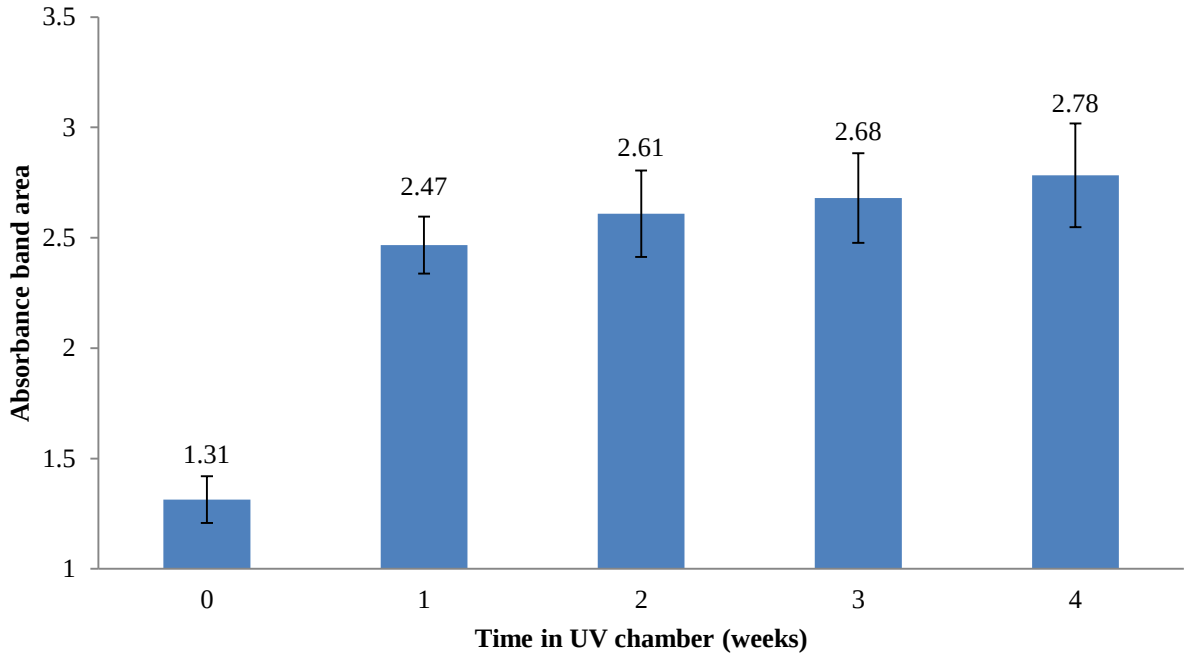


**Figure 4. 8 Average absorbance band areas from DRIFT spectra collected from 24 different co-ordinate locations on the surface of the asphalt slab that has been aged in the UV chamber for 0-4 weeks**

The average absorbance band area has increased between 0 and 1 week of UV ageing (87 %). This is an indication that there are carbonyl functional groups being created within this first week of ageing. This corresponds to the result seen for the UV-aged bitumen samples (Chapter 2.2). The area of this absorbance band increases less dramatically after this first week of ageing and the chart displays an average increase which, as a result of overlapping error bars for the older samples, could be a plateau. The size of the error bars allows a confident conclusion to be drawn that between 0-1 weeks of the UV ageing, there is an oxidation of the surface bitumen. It is noteworthy that a similar plateau trend has been recorded in the literature. [8,9,10] There is then no significant increase in oxidation and the absorbance band area does not change dramatically. This could indicate that the bitumen on the surface of the asphalt has become completely oxidised, or as close to completely oxidised as the conditions allow. There may be un-oxidised sites within the bitumen composition that require a higher temperature or a more intense UV light irradiation for oxidation to occur.

It is possible to visualise the change in the absorbance band at 1700 $cm^{-1}$ however when the maximum value is recorded the change appears to indicate a decrease in the absorbance band intensity. This however is a misleading result as it suggests that the band is reducing in intensity, when visually the band is increasing. Therefore the data in Figure 4.9 shows the

*difference* in absorbance intensity measured at 1700 $cm^{-1}$ from the DRIFT spectra of the unaged and UV aged samples (Figure 4.3).

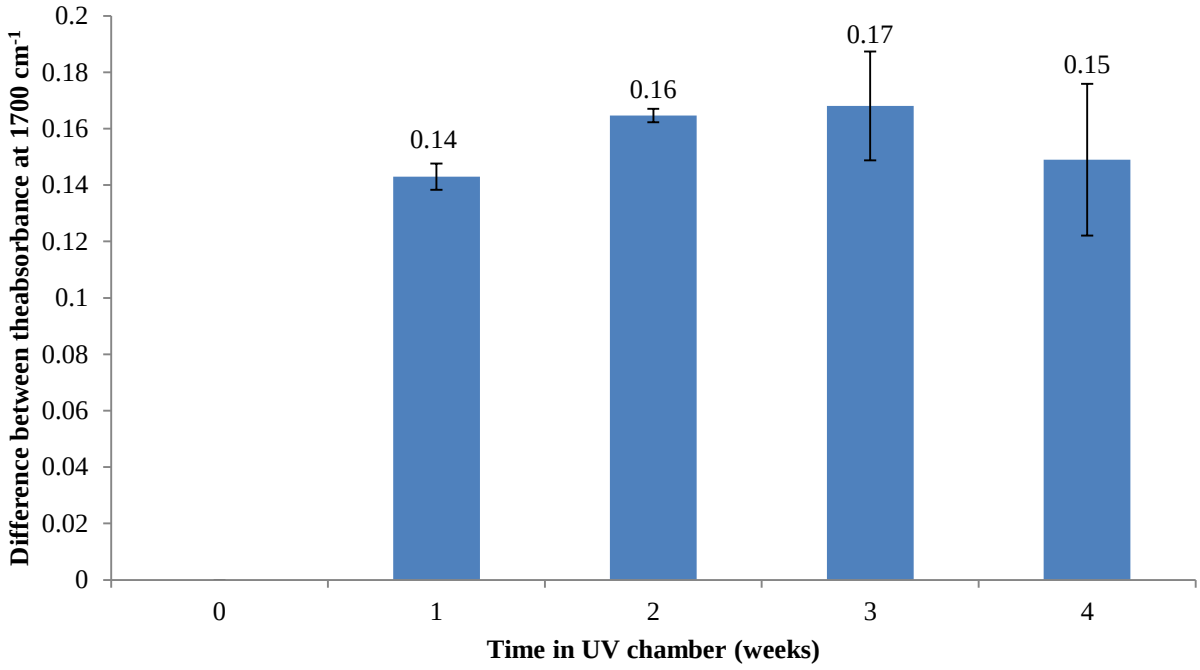


**Figure 4. 9Difference in absorbance values at 1700 $cm^{-1}$ from the DRIFT spectra from the surface of the asphalt that has been aged in the UV chamber for 0-4 weeks compared to the absorbance at 1700 $cm^{-1}$ of the unaged asphalt**

This graph indicates an increase in the amount of carbonyl group between 0-1 weeks and then this does not change significantly after this. This plateau is similar to what was seen for the spectra from the surface of the UV aged raw bitumen (see Chapter 2.2). In the case of the bitumen, a brittle skin was formed which protected the bulk bitumen from further oxidation. This could be the case here where the surface layers of the bitumen coating the asphalt surface has become oxidised. These asphalt samples have not been exposed to any mechanical agitation and therefore the lower layers of the bitumen are being protected. In reality the asphalt road surfaces are exposed to trafficking and therefore this brittle skin would likely be eroded. This would expose the lower layers of bitumen allowing this bitumen to be oxidised.

## 4.2 Scanning Electron Microscopy and elemental analysis

Scanning Electron Microscopy (SEM) has been carried out on the 1 and 4 week UV-aged asphalt samples in order to determine whether the surface characteristics change upon ageing with UV light.

An aggregate sub-sample was collected from the surface of an unaged asphalt slab and also from the 4 week UV aged sample and then placed onto a carbon SEM tab. These sub-samples were then placed into the sample holder and the chamber was brought to a vacuum of 0.68 Torr. A light microscope has also been used to collect images from the surface of the aggregate used for the SEM visualisation (Figure 4.10).

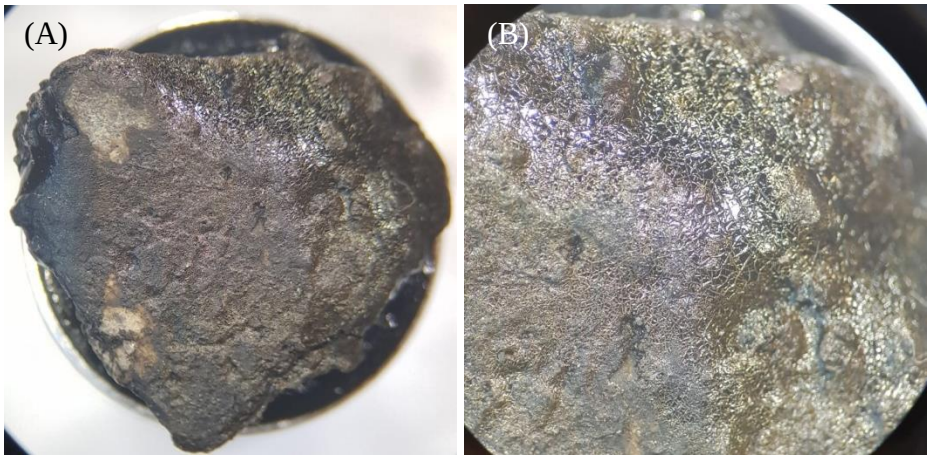


**Figure 4. 10 Photograph of the aggregate sub sample collected from the 4 week UV-aged asphalt slab, at two different magnifications in a light microscope**

Under the light microscope it is possible to see the some areas that are dull and some that are shiny on the surface of the UV aged asphalt aggregate subsample (Figure 4.10). It is also possible to see some exposed aggregate through the bitumen layer. The shiny area appears to have small cracks on the surface which can be seen more clearly by utilising the scanning electron microscope (see Figure 4,11).

**Table 4. 3 Magnifications of the SEM images presented in Figure 4.11**

| Microscope Image (Figure 4.10) | Magnification (×) |
|---|---|
| **A** | 72 |
| **B** | 300 |
| **C** | 530 |

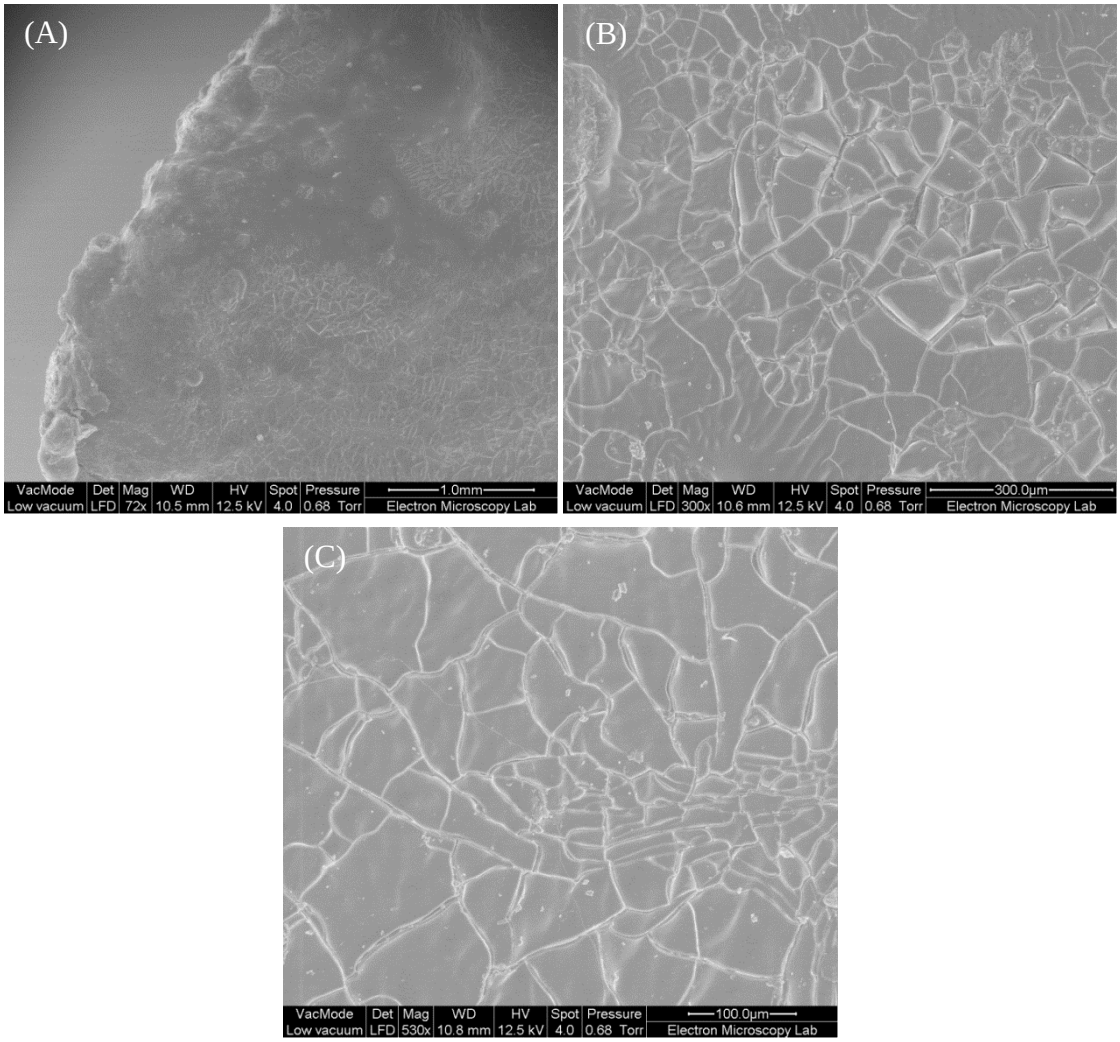


**Figure 4. 11 SEM images from the surface of an aggregate that has been pulled from the surface of the 4 week UV-aged asphalt slab**

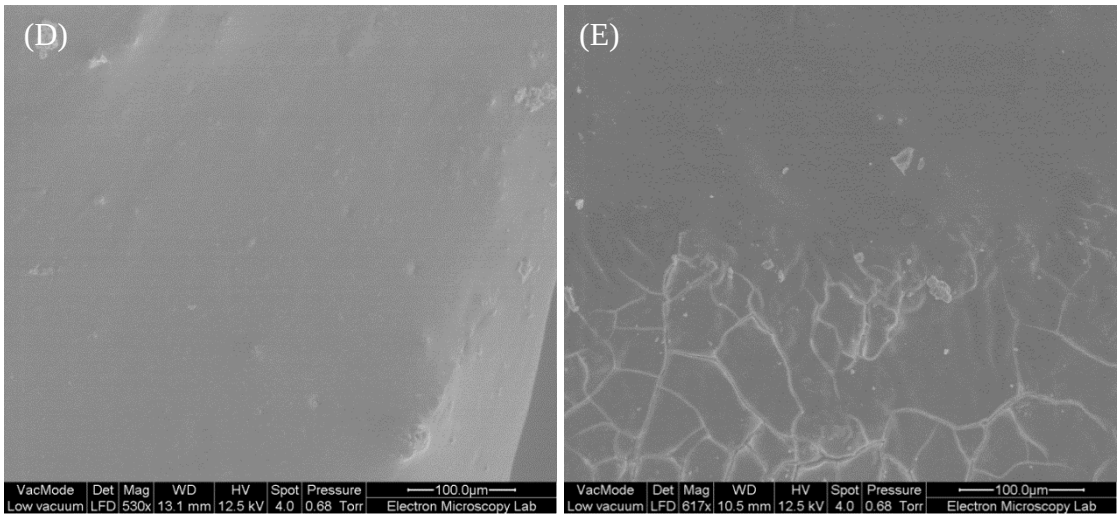


**Figure 4. 12 SEM images from the surface of a subsample of the unaged (D) and the 1 week UV-aged asphalt sample (E)**

**Table 4. 4 Magnification details of the SEM images in Figure 4.12**

| Microscope Image (Figure 4.12) | Magnification (×) |
|---|---|
| **D** | 530 |
| **E** | 617 |

Under the high magnification of the scanning electron microscope the cracks are much more prominent. There are areas of micro cracking on the surface of the UV-aged asphalt. This is the same phenomenon seen previously (Chapter 2.2) in the SEM images from the surface of the UV-aged bitumen. This is not seen across the entire surface of the aggregate that has been analysed and there are areas where the cracking is less defined than these sharp edged platelets. It is also noteworthy that these platelets were not identified on the surface of an unaged asphalt sample (Figure 4.12 D). However, the micro-cracks can be seen after a short time in the UV chamber (1 week, Figure 4.12 E) and could be the initiation of larger cracks within the asphalt. The asphalt used in this experiment has not been exposed to any mechanical stress or agitation however these cracks indicate weakness within the bitumen which most certainly would be exacerbated by trafficking.

The area shown in Figure 4.12 (E) highlights a divide between cracked and un-cracked bitumen on the 1 week UV aged asphalt. This may be indicative of how cracking may propagate across the sample moving from cracked to un-cracked areas. Top down crack propagation is a term used when a road surface begins to crack from the surface of the asphalt. This phenomenon has been identified and there are a number of possible causes including the age hardening of the bitumen and high thermal stress at the surface.[11]

The elemental analysis of the surface of the 4 week UV aged asphalt shown in Figure 4.10 (A and B) has been carried out and a number of different elements were detected. Carbon was the most dominant element in the sample area measured, as expected for bitumen which is hydrocarbon based. The EDX detector also picked up atoms of calcium, oxygen and silicon which can be attributed to the calcium carbonate filler, which was mixed with the bitumen during asphalt production, and the siliceous, stone aggregates. Other elements detected were magnesium, potassium and iron. The fillers used to bulk the bitumen when constructing road surfaces need to be low cost and are typically sourced from a quarry that is close to the road site or asphalt production plant, in order to keep the costs low. There is little in the way of purification of these mineral aggregates or fillers and therefore the carbonate filler used is not

solely calcium carbonate and could also include magnesium carbonate. The granite aggregate used to form the bulk of the asphalt has a composition of mainly $SiO_2$; however, potassium and iron are also present in the granite. They can be found in the form of a wide range of minerals.[12]

## 4.3 Infrared microscopy of UV aged asphalt

Infrared microscopic analysis was carried out on the asphalt slab that had been subjected to 4 weeks ageing in the UV chamber. This analysis aimed to detect changes in the IR spectra collected from the bitumen located at the surface of the sample and to probe further into the bulk of the sample by means of taking a cross section. This could give an indication of the depth of penetration of the UV light and also the degree of oxidation that occurs within the bulk of the asphalt. The asphalt slab was cut using a CUTROCK machine with a diamond embedded cutting blade. The photographs in Figure 4.13 display the sample preparation for the microscopy experiment.

**Figure 4. 13 Photograph outlining the sample preparation of the asphalt slabs for infrared microscopy. Red box indicates an example of the area being mapped by the IR microscope**

The infrared microscope has been used to collect images of the asphalt, to take controlled point spectra from specific areas on the surface of the sample and also to create ChemiMaps. A ChemiMap is an image of a sample that has been created by taking an infrared spectrum within each pixel of the image area. The parameters used throughout spectra and image collection were 32 scans per pixel, 8 cm resolution and a 25 μm pixel size.

The image in Figure 4.14 shows the visible-light image survey from a section of the cross section surface of the UV-aged asphalt sample. As a result of the instrument optics the top of the asphalt slab (that had been exposed to the UV ageing) is seen at the bottom of this image. The image is dark in colour and there is little detail that can be picked out. It is important to note that there is a large dark section on the right hand side which correlates to a void section where the camera becomes out of focus due to the difference in distance from the focal point. The scale shows that the area of this image is 3.649 mm x 6.149 mm. The red box highlights the area that was used to create the following ChemiMaps.

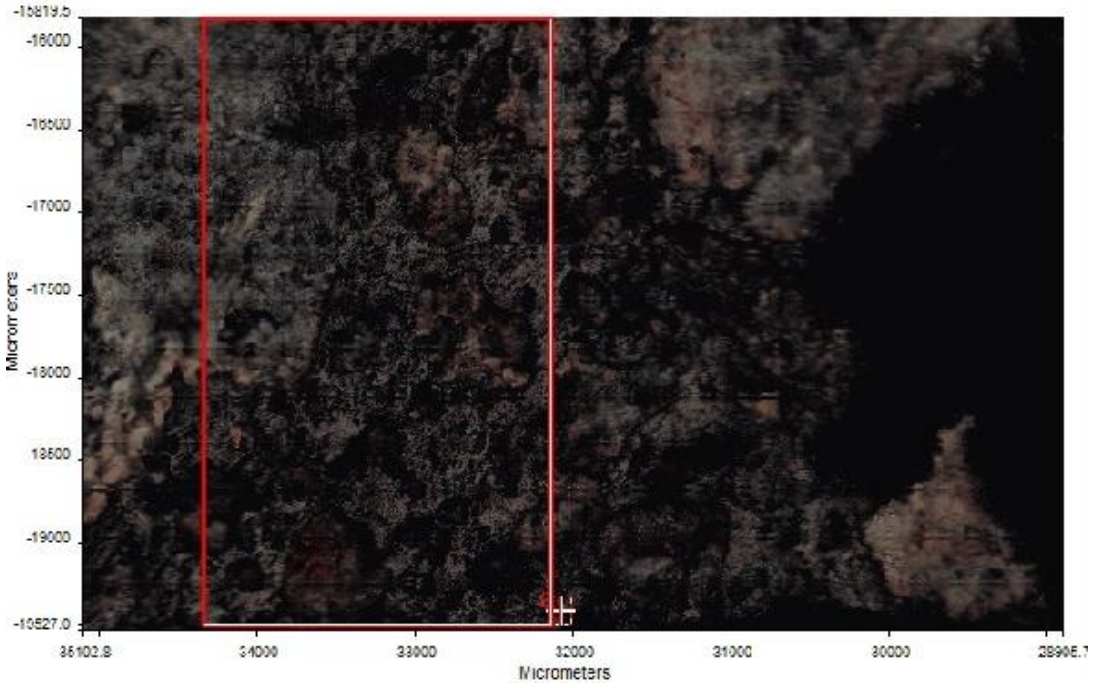


**Figure 4. 14 Microscope image from the asphalt slab that has been aged in the UV chamber for 4 weeks**

The ChemiMaps are useful when analysing a dark sample such as asphalt as it is possible to manipulate the colour scheme and highlight the areas with similar chemical composition. Thus areas which may have a similar dark colour may nonetheless have different reflectivity to infrared light at different wavelengths and this may be observed by using the infrared microscope.

The average absorbance image shown in Figure 4.15 has been created by calculating the average absorbance of the whole infrared spectrum (4000-680 $cm^{-1}$) in each pixel and displaying the values along a colour scale. The areas of red and white have a high average absorbance compared to the green and blue regions for example. This image highlights the

presence of the aggregates within the bitumen binder as having a high average absorbance while the bitumen has higher reflectance.

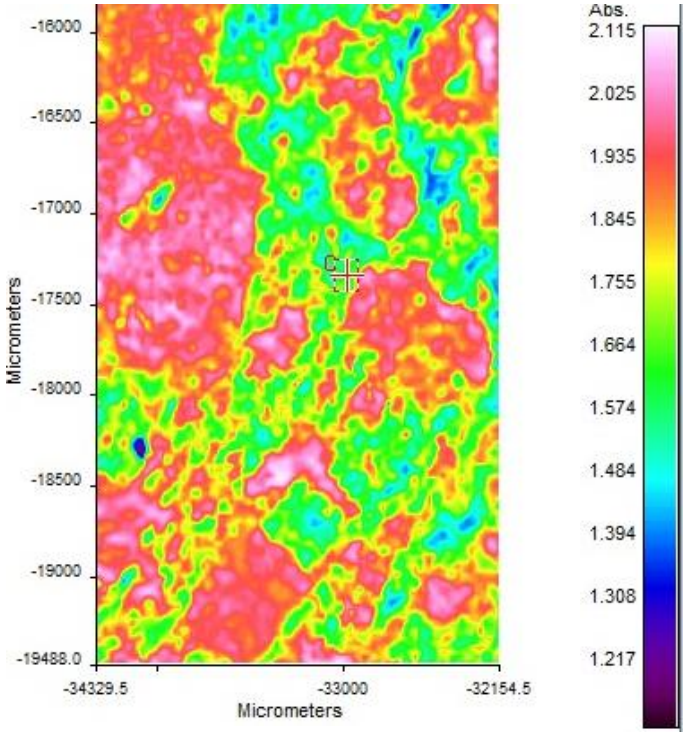


**Figure 4. 15 ChemiMap of the asphalt sample that has been aged in the UV chamber for 4 weeks, area highlighted in Figure 4.14**

It is possible in the 'Spectrum' software to view each spectrum that was collected at each pixel of a ChemiMap and highlight specific absorbance bands of interest. By integrating the absorbance band area between specific wavelengths the software is able to produce an image that indicates the pixels that contain spectra with a high area and a low area along a gradient colour scale. It is then possible to view areas where a specific functional group, or absorbance band, is dominant. In this way specific chemical entities across the surface of the sample may be mapped.

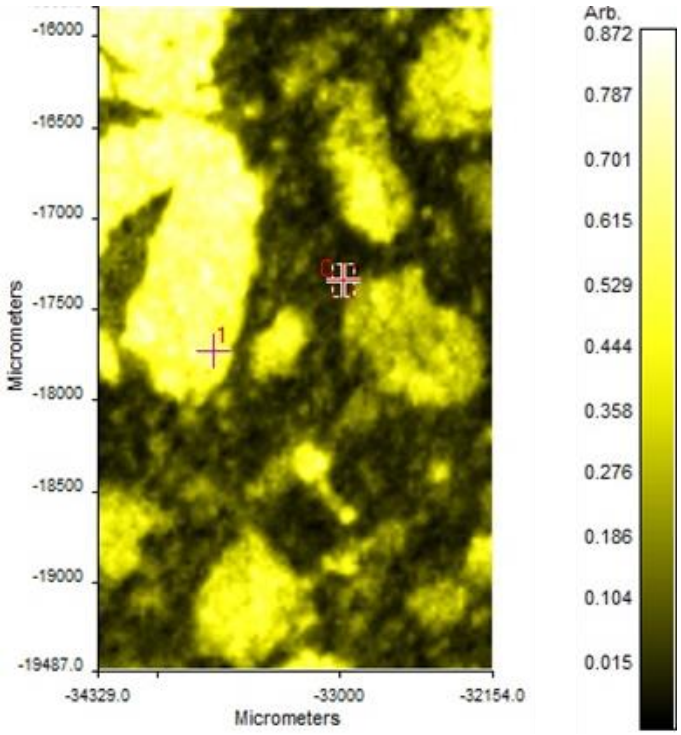


**Figure 4. 16 ChemiMap produced by integrating the area between wavenumbers 1306-916 $cm^{-1}$**

The ChemiMap in Figure 4.16 has been created by integrating the area underneath the absorbance band between wavenumbers 1306-916 $cm^{-1}$ which corresponds to a strong silicate absorbance. This is found in the siliceous aggregate and therefore the ChemiMap shows lighter areas that correspond to the aggregate sections of the asphalt, with high silicate content.

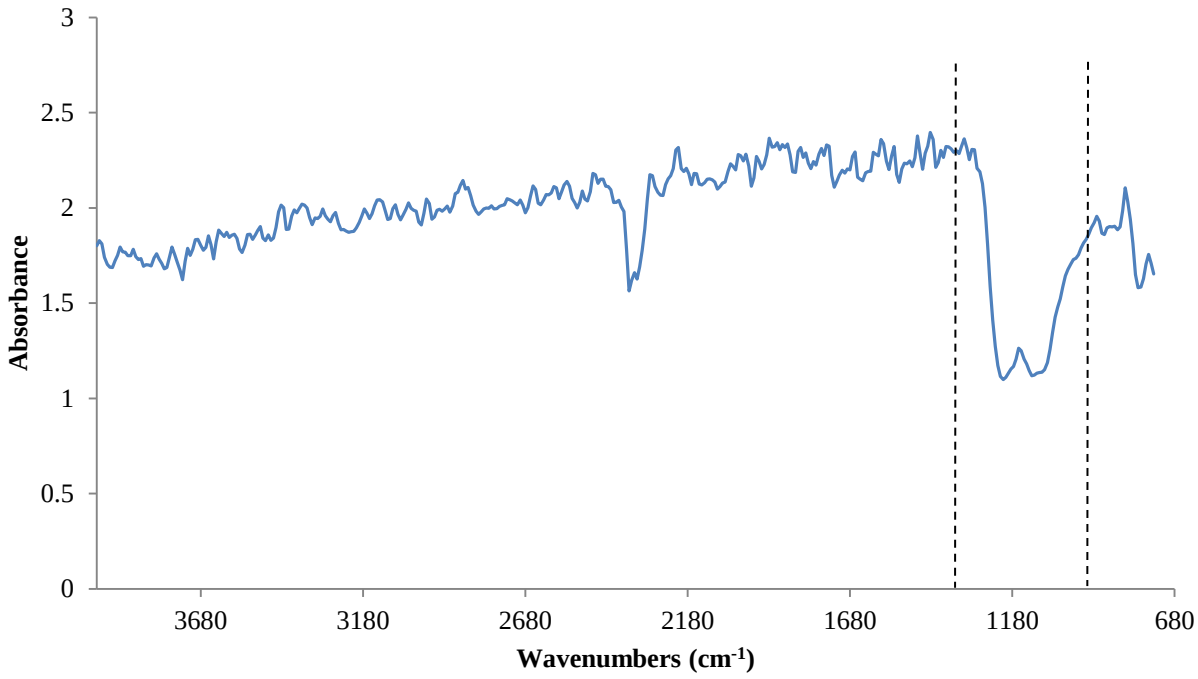


**Figure 4. 17 Reflectance spectrum used to create the ChemiMap in Figure 4.16**

Figure 4.17 is an example of a spectrum taken from one of the aggregate pixels. The strong Si-$O_2$ absorbance band used to produce the ChemiMap is clear in the spectrum. The absorbance band at 2360 $cm^{-1}$ can be attributed to carbon dioxide in the air. As the distance between the sample and the detector is greater than that for the handheld spectrometer, the spectra are more influenced by changes in the atmosphere. It is not possible to update the background spectrum while a ChemiMap is being taken therefore the carbon dioxide peak is expected.

When analysing road surfaces, this silicate absorbance band (1306-916 $cm^{-1}$) could be used as an indicator for identifying spectra that have been taken from aggregates as opposed to bituminous material. This is important information for those monitoring road surfaces. If the aim is to monitor ageing of bitumen in the road surface then a quick method for identifying areas where aggregates or fillers are present would allow those unwanted spectra to be discounted. More spectroscopic analysis would be needed here in order to include the wide variety of aggregate types that are used on the road network. This would allow for an infrared spectral database of different aggregates to be compared and accessible depending upon the road being analysed with this technique.

It would therefore also be beneficial to identify an absorbance band that would indicate the areas of bituminous hydrocarbons. The ChemiMap shown in Figure 4.18 has been produced

using the integrated area beneath the absorbance band between the wavenumbers 2857-2789 $cm^{-1}$.

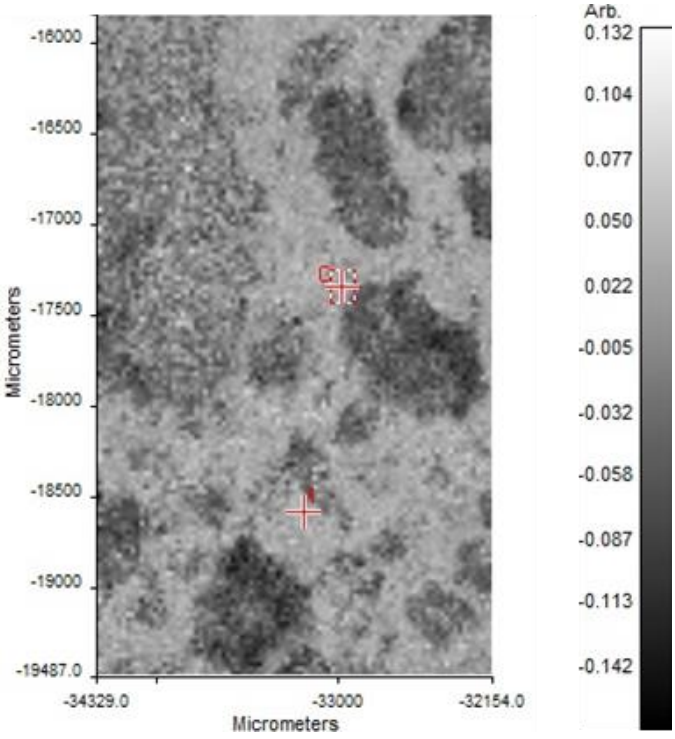


**Figure 4. 18 ChemiMap from the surface of the UV-aged asphalt created using the absorbance band area between the wavenumbers 2957-2789 $cm^{-1}$**

Although the C-H absorbance bands at wavenumbers 2922 and 2848 $cm^{-1}$ are very weak in the IR spectra (see Figure 4.19) a ChemiMap has been produced which clearly shows areas where the bitumen content at the sample surface is higher. By mapping the band between 2975 and 2789 $cm^{-1}$ it is possible to see that the bitumen is identifiable between the aggregates. This may be seen by comparing the positions of the bright areas in Figure 4.16 (aggregate) and Figure 4.17 (bitumen). Areas where the aggregate peaks are more intense correspond to those where the bitumen peaks are less intense and vice versa. Figure 4.19 shows a reflectance spectrum from an area of bitumen between the aggregates.

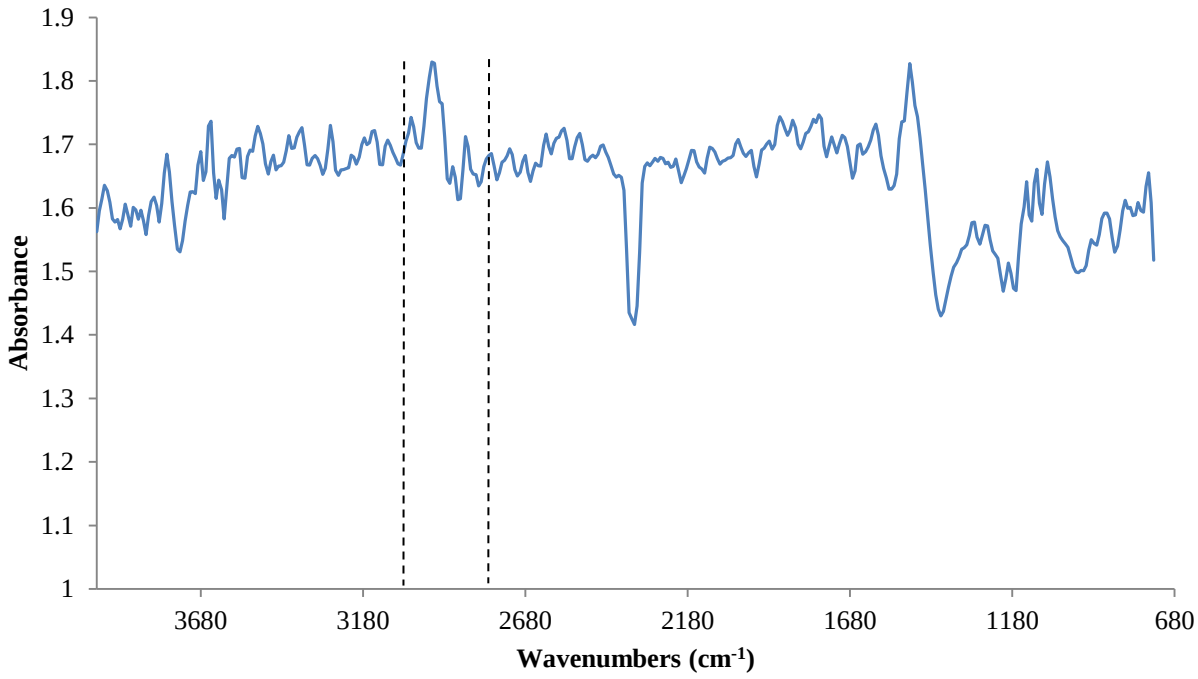


**Figure 4. 19 Reflectance spectrum used to create the ChemiMap in Figure 4.18**

The signal to noise ratio is lower in spectra recorded using the IR microscope than in DRIFT spectra recorded with the handheld spectrometer as the path length is higher and less IR light is directed towards the detector after interaction with the sample. However the clear intensity differences in the ChemiMaps in Figures 4.15 and 4.17 demonstrate that the spectra can differentiate between areas of aggregate and bitumen. The weak C-H absorbance band intensities in these reflectance spectra could be due to the fact that the bitumen is highly absorbing and little signal is being reflected and hence detected by the diffuse reflectance detector of the IR microscope.

In order to obtain a clearer picture of the chemical changes throughout the bulk of the asphalt, a higher number of scans need to be collected for each point spectrum. This will increase the signal to noise ratio and highlight the absorbance bands of functional groups.

The image in Figure 4.20 has been taken from the surface of a cross section of the UV-aged asphalt prepared as shown in Figure 4.13. The bottom of the picture is the surface of the asphalt that has been exposed to the UV light and the bulk of the asphalt is shown in the rest of the image. It is possible to see a number of pieces of aggregate in the image and the bitumen can be seen in between these. The aim of this experiment was to collect point spectra from the bituminous material through the bulk of the sample to see if there are any changes in

the spectra and to see if any oxidation has occurred in the bulk of the sample rather than just on the surface.

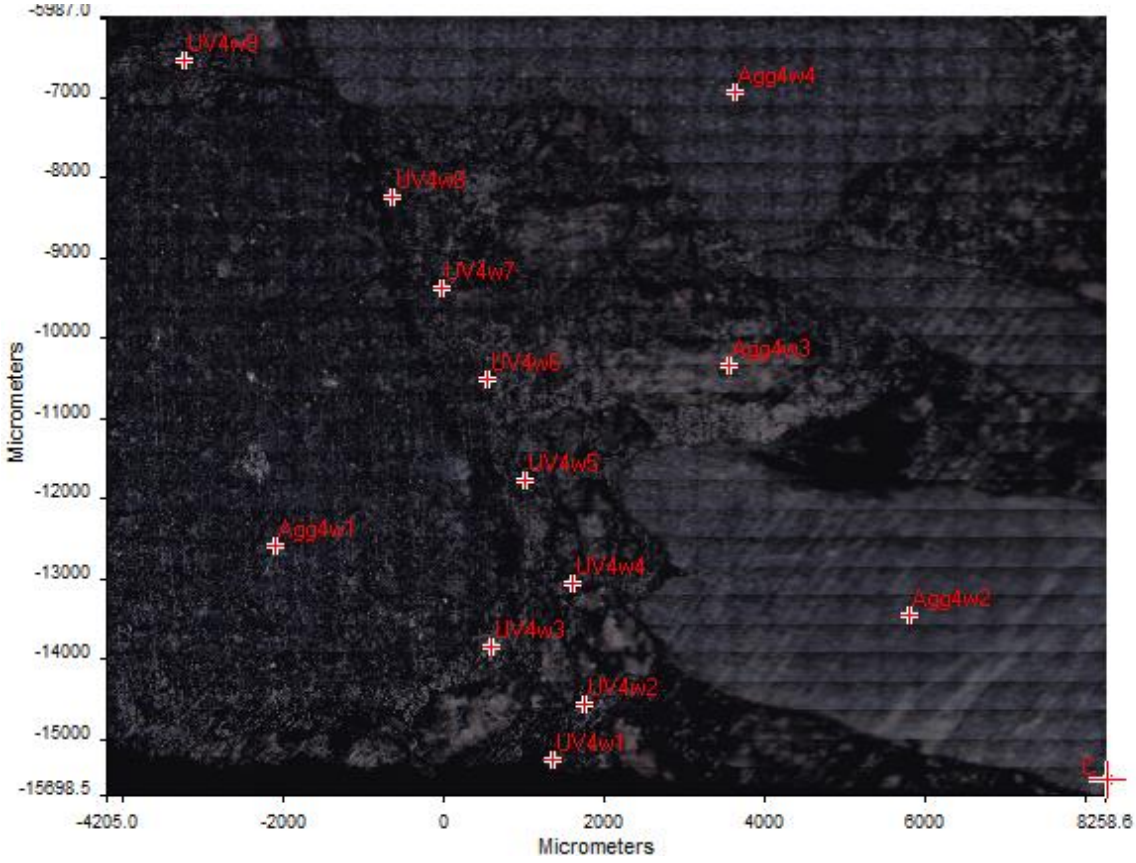


**Figure 4. 20 Infrared microscope image from the cross section surface of the 4 week UV-aged asphalt**

The image shown in Figure 4.20 indicates the locations at which the point spectra were collected and is labelled with the spectrum name. A number of spectra have been collected from the aggregates for a comparison between the bitumen and the aggregates. The point spectra collected are an average of 132 spectra at 2 $cm^{-1}$ resolution.

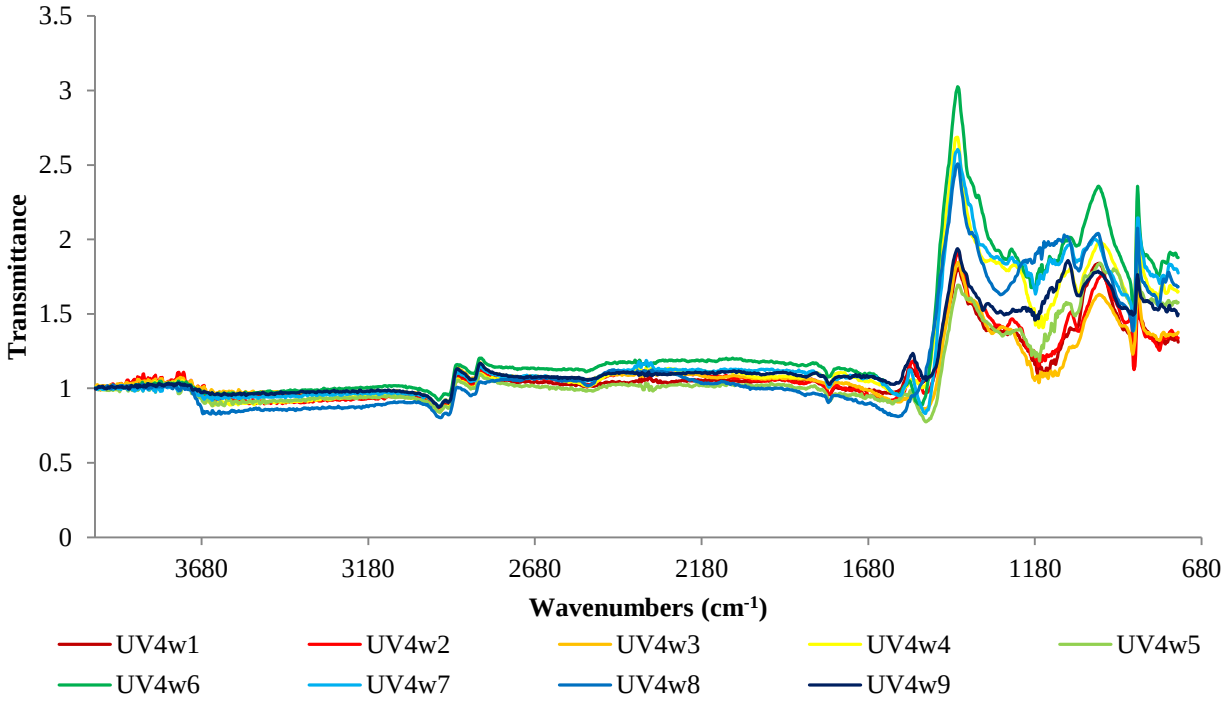


**Figure 4. 21 Reflectance spectra from the cross section surface of the 4 week UV-aged asphalt slab, collected from the markers shown in Figure 4.20**

The spectra shown in Figure 4.21 have a much better signal to noise ratio than those in Figure 4.17 and Figure 4.19. It is possible to clearly assign the C-H stretching modes of the bitumen (2904, 2848 $cm^{-1}$), along with a strong fundamental $CO_3^{2-}$ asymmetric stretch (1418 $cm^{-1}$) and out of plane bend (874 $cm^{-1}$).

There is no trend between the absorbance band intensity at 1700 $cm^{-1}$ and the location of the point spectra through the bulk. This suggests that no measurable chemical changes have occurred within the bulk of the sample on exposure to UV light. This is not surprising. The UV light is not expected to penetrate very far into the sample (no more than 4-5 μm at most).[13] Moreover, in a similar manner to the UV-aged bitumen (Chapter 2.2) the UV exposure has produced a surface skin, which acts to prevent further oxidation throughout the bulk. It could be speculated however that in a trafficked road the wearing away of the cracked surface layer by trafficking would then expose the lower layers and oxidation can then occur. Further work would be needed in order to determine the validity of this hypothesis.

The scanning electron micrographs of the UV-aged bitumen showed that the platelets on the surface skin were approximately 2 μm thick. The resolution of the IR microscope is not as high as the SEM with a pixel size of 25 μm; therefore the IR microscope does not have good

enough resolution to investigate this surface layer at this level of precision of the cross section sample.

The aggregates are clear in the microscope image from the cross section and point spectra have been taken from these to compare to the bitumen. The reflectance spectra have been collected using the same parameters as the bitumen point spectra.

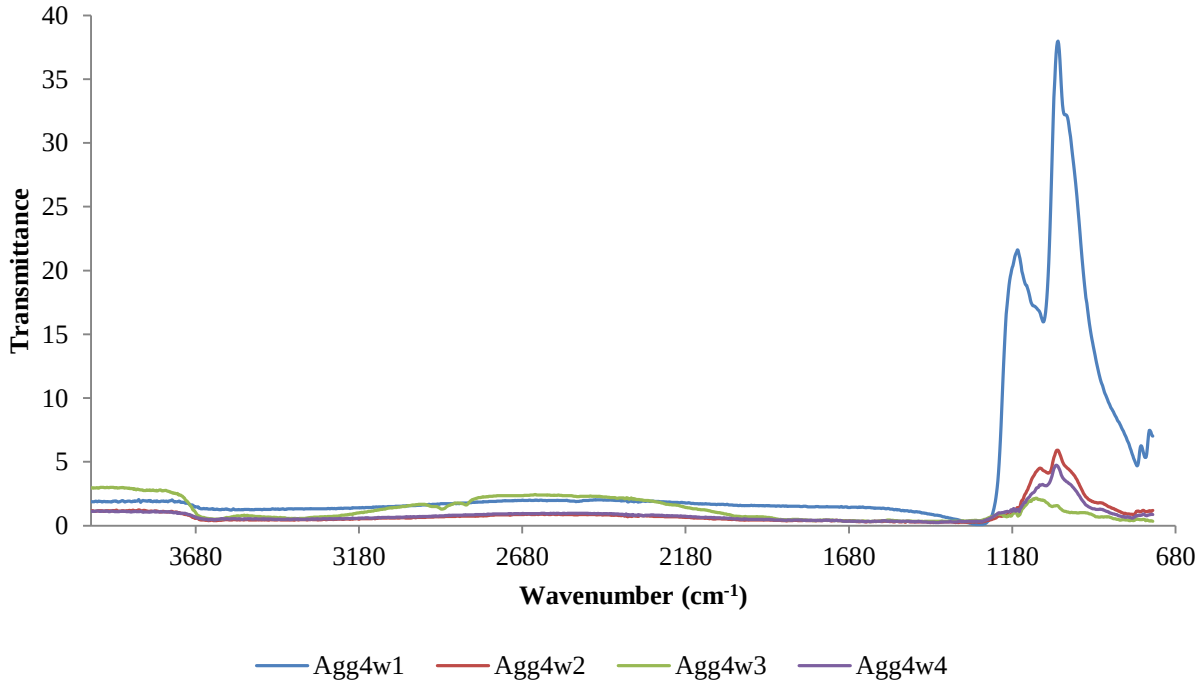


**Figure 4. 22 Reflectance spectra from the aggregates present in the cross section surface of the 4 week UV-aged asphalt collected from the markers shown in Figure 4.20**

The main absorbance bands arising in the DRIFT spectra from the aggregate sections occur at the low wavenumber range between 1270 and 680 $cm^{-1}$. Within the spectrum from Agg4w1 four absorbance bands can be identified with varying intensities and overlap. The bands can be seen at 790, 1010, 1036 and 1174 $cm^{-1}$ and correspond to the asymmetric stretching modes of the silicates.[14] The aggregate used to create this asphalt is therefore a siliceous granite material. The lack of spectral information outside of the silicate absorbance bands indicates that there will be little conflict between the siliceous aggregates and the bitumen hydrocarbons and their oxidation products.

## Summary

The aim for this chapter was to identify the feasibility of diffuse reflectance infrared spectroscopy for the detection of oxidation product absorbance bands in the spectra.

It has been possible to identify the absorbance bands that correspond to the carbonate fillers and siliceous aggregates within the DRIFT spectra from the surface of asphalt. It is also possible to see a new absorbance band occurring after 1 week of artificial ageing in the UV chamber which is separate from the carbonate bands. This absorbance band can be attributed to a carbonyl functional group within the bitumen at 1692 $cm^{-1}$.

This absorbance band is seen as a first derivative, in the spectra of the UV-aged raw bitumen spectra. The first derivative is similar to that seen in the spectra from the UV-aged bitumen (Chapter 2.2). This is possibly as a result of the shiny surface of the UV-aged asphalt and the absorbance band being a mixture of specular and diffuse reflectance or a change in surface structure leading to a change in refractive index of the surface of the bitumen.

This absorbance band can be quantified and the results show a steep increase in intensity between 0-1 week and after this there is a plateau as the concentration of the carbonyl functional group does not change between weeks 1-4.

The light and scanning electron microscopy experiments have provided enhanced visual information on the surface of the asphalt samples. Within the SEM images it is possible to see small micro-cracking on the UV exposed bitumen that coats a surface aggregate. This replicates what was seen on the surface of the UV-aged bitumen. This micro-cracking could be an initial cause of more significant cracking of the road surface. The surface bitumen could become cracked and brittle by UV exposure and hence incorporate weaknesses within the structure of the bitumen. By adding the mechanical agitation of trafficking, the road surface is weakened on a micro-level and the cracks begin to propagate. The weakened surface is then likely to erode away as a result of the trafficking and expose the lower layers of bitumen to oxidation and eventually expose the aggregates below.

IR-microscopy has identified wavenumber regions that could be useful in differentiating between spectra from aggregate and bituminous material. ChemiMaps with a good contrast between the aggregate and bitumen have been produced. The DRIFT spectra throughout the bulk have been measured and show no real trend throughout the bulk. Indicating that, as expected, exposure to UV light only causes oxidation at the sample surface.

## References


[1] British Standard EN 13108-1:2006, Bituminous mixtures, Asphalt Concrete.

[2] PubChem Open Chemistry Database, Carbonate Ion, Compound Summary for CID 19660 https://pubchem.ncbi.nlm.nih.gov/compound/carbonate#section=Top ACCESSED 21.05.2018 14:46.

[3] J. Godleman, M. Almond and W. Matthews, An infrared micro spectroscopic study of plasters and pigments from the Neolithic site of Bestansur, Iraq, *J. Archaeol. Sci: Reports,* **7**, 2016, 195-204.

[4] E. Anderson, M. J. Almond, W. Matthews, Elemental and spectroscopic characterization of plasters from Fatih Mosque-Istanbul (Turkey) by combined micro-Ramen, FTIR and EDXRF techniques, *Spectrochim. Acta A*, **133**, 2014, 326-334.

[5] N. Colthup, L. H. Daly and S. E. Wiberley, *Introduction to infrared and ramen spectroscopy,* Elsevier Science and Technology, London, 1975, EBOOK ISBN: 9780323161602.

[6] B. Stuart, *Infrared Spectroscopy: Fundamentals and Applications,* John Wiley and Sons Ltd, 2004, ISBN 9780470854280.

[7] Perkin Elmer Technical Note, Richard Spragg, PerkinElmer. Inc, Seer Green, UK, Reflection Measurements in IR Spectroscopy, https://www.perkinelmer.com/CMSResources/Images/44-153348TCH_reflection-Measurements.pdf ACCESSED 21.05.2018 15:25.

[8] V. Mouillet, F. Farcas and S. Besson, Ageing by UV radiation of an elastomer modified bitumen, *Fuel,* **87,** 2008, 2408-2419.

[9] F. Durrieu, F. Farcas and V. Mouillet, The influence of UV ageing of a Styrene/Butadiene/Styrene modified bitumen: Comparison between laboratory and on site ageing, *Fuel,* **86,** 2007, 1446-1451.

[10] M. Lopes, D. Zhao, E. Chailleux, M. Kane, T. Gabet, C. Petiteau and J. Soares, Characterisation of ageing processes on the asphalt mixture surface, *Road Mater. Pavement,* **15** (3), 2014, 477-487.

[11] D. Harmelink, S. Shuler and T. Aschenbrener, Top-down cracking in asphalt pavements: Causes, Effects and Cures, *J. Transp. Eng.*, **134,** 2008.

[12] H. Blatt and R. J. Tracey, *Petrology: Ingenuous, Sedimentary and Metamorphic,* 2nd Ed, Freeman, ISBN: 0716724383.

[13] W. Zeng, S. Wu, L. Pang, H. Chen, J. Hu, Y. Sun and Z. Chen, Research on ultra violet (UV) ageing depths of asphalts, *Constr. Build. Mater.*, **160,** 2018, 620-627.

[14] M. A. Karakassides, D. Gournis and D. Petridis, An infrared reflectance study of Si-O vibrations in thermally treated alkali-saturated montmorillonites, *Clay Minerals*, **34,** 1999, 429-438.

# Chapter 5

## Natural ageing of asphalt

This chapter reports the results of ageing asphalt samples with exposure to natural conditions, which replicates those experienced by live road surfaces. These conditions differ to those in the UV chamber as the asphalt will experience lower temperatures and temperature cycling, rainfall, and variable UV exposure. The introduction of these other external factors may have an effect on the ageing of the asphalt and the reduction in temperature and UV intensity may slow the oxidation of the asphalt surface.

This experiment is important to the titular aim of this project. If natural ageing conditions can produce oxidation products on the surface of the asphalt that are measurable with DRIFT spectroscopy, alongside a decrease in physical performance of the asphalt, then it could be possible that diffuse reflectance infra-red spectroscopy can be utilised as a surveying technique for live roads.

A number of the asphalt slabs, prepared as described in Chapter 1-Part 2, were placed onto the roof of TRL headquarters at Crowthorne House, and then exposed to the natural conditions of the UK weather. A number of weather parameters have been monitored throughout the duration of the experiment and DRIFT spectra have been collected from the asphalt surface. There is currently no standardised test that can be used to analyse asphalt in order to determine the fretting potential. Therefore, the current method for testing the mechanical property of a road involves recovering the bitumen from a core from an asphalt road surface and testing the mechanical properties of the bitumen using the penetration point, softening point and Vialit pendulum test. These have been carried out in this project as described in Chapter 3.1.

The visual characteristics of the aged asphalt surfaces have been analysed with light and scanning electron microscopy.

In this chapter the natural ageing experiment will be outlined and the spectroscopic, microscopic and mechanical property testing results will be presented, along with the weather data analysis.

## 5.1 Natural ageing experimental methodology

The natural ageing of the asphalt samples has been carried out over two different time scales. One asphalt slab was mapped by taking DRIFT spectra from specific co-ordinates on the surface of the slab as described previously for the UV aged asphalt map (Chapter 4.1.1). The slab was then placed onto the roof of TRL, Crowthorne House, in order to be exposed to natural conditions. At weekly intervals the slab was removed and DRIFT spectra were taken from the same co-ordinates. This was continued for 8 weeks, between the 19th April 2017 and the 14th June 2017.

Figure 5.1 shows the locations of the DRIFT spectra coordinates upon the surface of the asphalt.

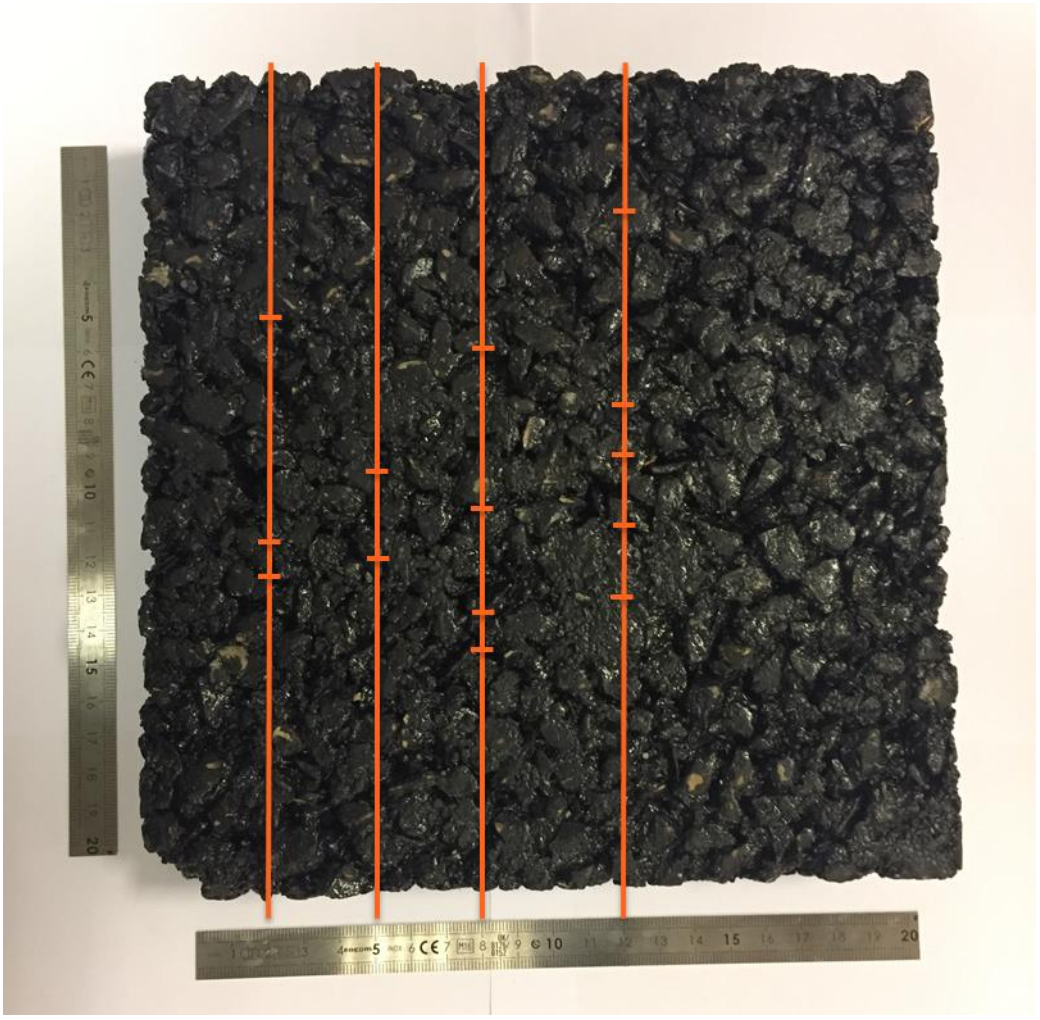

**Figure 5. 1 Photograph of the asphalt slab used for the natural ageing map experiment including the 14 locations of the DRIFT spectra**

Eleven other asphalt slabs were placed onto the roof in August 2015 and have been allowed to age for 30 months with 'time point' samples being removed at approximately 3 month

intervals. This experiment will more reliably replicate the ageing of an un-trafficked road surface over the course of 2.5 years. Table 5.1 outlines the dates that the 30 month natural aged asphalt samples have been aged on the roof of Crowthorne House.

**Table 5. 1 List of the dates that the naturally aged asphalt samples were placed onto and take from the roof, and the total solar exposure that they experienced throughout that time**

| Time naturally aged (months) | Date placed onto roof | Date taken off roof |
|---|---|---|
| **1** | 01.04.2017 | 02.05.2017 |
| **3** | 27.08.2015 | 27.11.2015 |
| **5** | 01.04.2017 | 01.09.2017 |
| **7** | 27.08.2015 | 18.03.2016 |
| **9** | 27.08.2015 | 25.05.2016 |
| **12** | 27.08.2015 | 27.08.2016 |
| **15** | 27.08.2015 | 27.11.2016 |
| **18** | 27.08.2015 | 27.02.2017 |
| **21** | 27.08.2015 | 26.05.2017 |
| **24** | 27.08.2015 | 27.08.2017 |
| **30** | 27.08.2015 | 27.02.2018 |

DRIFT spectra have been collected from the surface of each time point sample. The raw bitumen has then been recovered from the asphalt sample using the method outlined in the British Standard EN 13074 2:2011.[1] This standard describes the binder recovery process which begins by 'breaking' the asphalt slab. In this project this involved heating the asphalt slab in a RAMoven Sanyo commercial microwave oven for 2 minutes and pulling the slab into smaller chunks by hand while wearing heat proof gloves. This asphalt mixture was left to cool, and then placed into a metal bottle with 1500 mL of dichloromethane (DCM). The container was stoppered and allowed to roll on a bottle roller for 45 minutes and then left to settle for 10 minutes. After this time the bitumen should be dissolved into the DCM and the aggregates were then filtered off using a 6 μm filter. This solution was then poured into three

500 mL, twist cap containers and placed into a Centurion Scientific K3 Series centrifuge. The solutions were centrifuged at 15000 m $s^{-2}$, 4000 rpm for 18 minutes in order to separate the calcium carbonate filler from the bitumen in the solvent. Following this separation the solvent was then evaporated from the bitumen with the use of a rotary evaporator. The solution was added gradually into a round bottom flask being heated to 120 ˚C by an oil bath, under a vacuum of 850 mbar. Once all of the solution had been added to the round bottom flask the pressure is reduced to 13 mbar and the temperature increased to 155 ˚C. This new set of conditions was used until the bubbling inside the round bottom flask has ceased then they were continued for a further 15 minutes. The bitumen was then cooled for 1 hour and is then ready for further testing.

The mechanical properties of the recovered bitumen were then measured using the penetration point, softening point and Vialit pendulum tests (methodologies described in Chapter 3.1).

## 5.2 Weather data analysis

The weather parameters measured by the weather station at Crowthorne House were the UV exposure, temperature, humidity, rainfall, pressure and wind speed and direction. The literature has identified that the temperature, UV exposure and the presence of rainwater are three of the main environmental factors that contribute to the age hardening and failure of asphalt road surfaces.[2] Therefore these parameters were looked at in more detail for the duration of the, long-term, naturally aged asphalt experiment.

The solar exposure ($W/m^2$) was recorded every 15 minutes for 24 hours a day throughout the experiment, starting from the 14$^{th}$ September 2015. This data can be presented in many ways. Every 15 minutes the UV monitor records a data point, all of which can be summed for the day, month or year of natural ageing. This has been carried out for each month of the experiment and has been plotted in Figure 5.2.

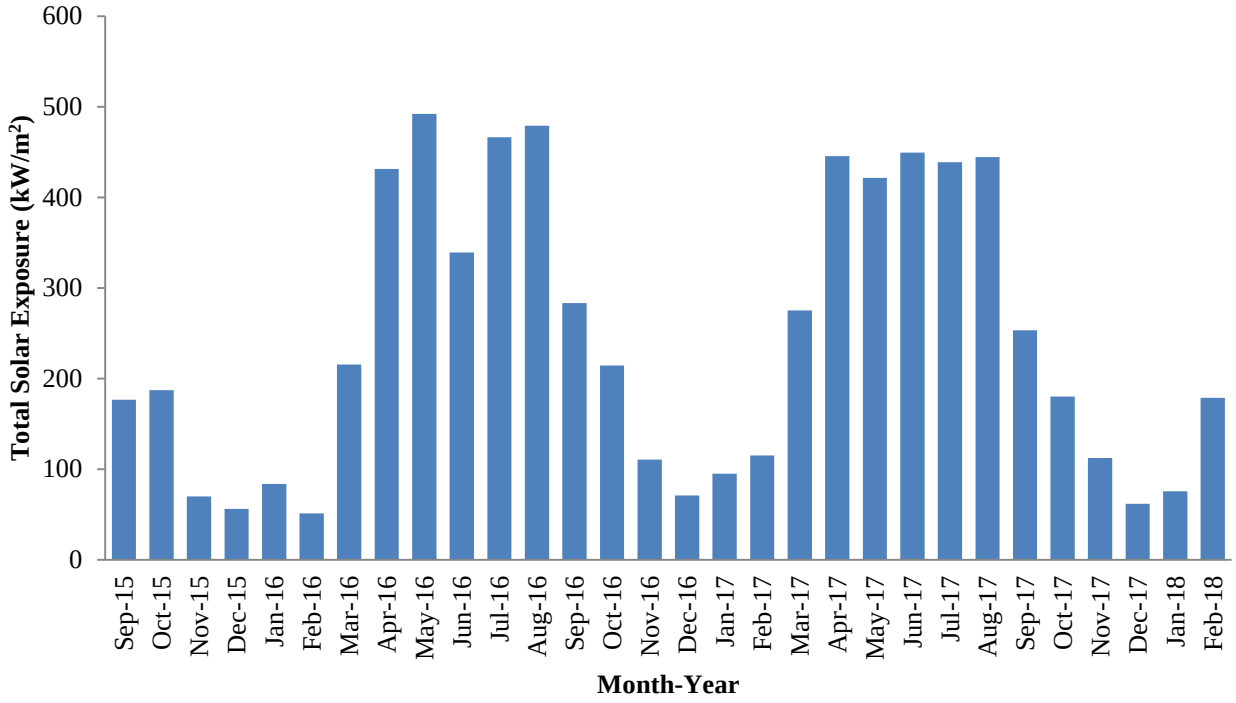


**Figure 5. 2 Column graph containing the total solar exposure measured throughout each month of the natural ageing experiment**

The variable nature of the solar exposure throughout the year is highlighted in the chart in Figure 5.2. This is to be expected as the seasons change, the days shorten in the winter and there is less solar energy reaching the earth. In the summer months, days lengthen and total solar intensity increases. This cyclisation means that the solar exposure intensity that the asphalt road surfaces experiences is variable and this is one of the reasons why a standardised UV enhanced ageing method is very difficult to develop.

Another variable and contributing factor to the oxidation of the surface of asphalt is the temperature. The temperature has also been recorded every 15 minutes of the ageing experiment, and the maximum, minimum and average temperatures for each month throughout the ageing experiment have been plotted into the column graph in Figure 5.3.

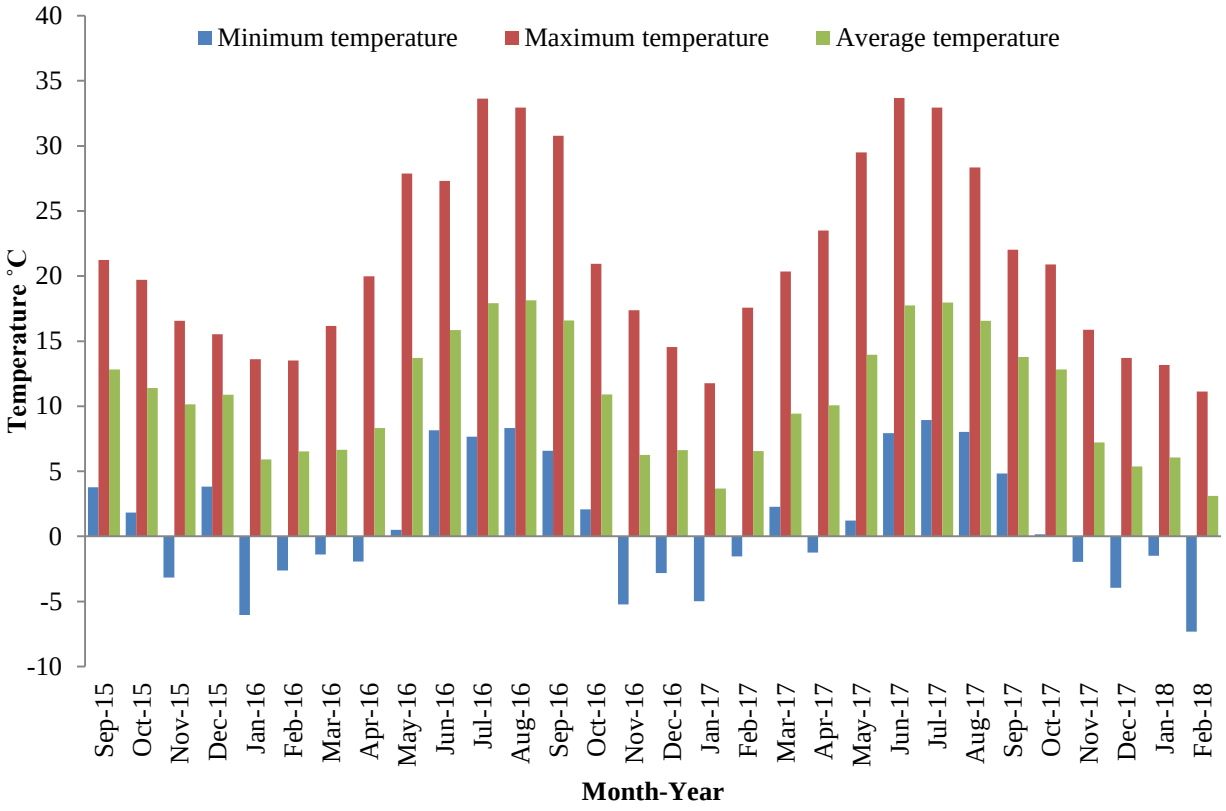


**Figure 5. 3 Column graph containing the minimum, maximum and average temperatures recorded each month for the duration of the naturally aged asphalt experiment**

The temperature column graph (Figure 5.3) shows an approximate sinusoidal wave being produced as the temperature increases and decreases throughout the years. The temperatures that have been recorded range from 33.68 ˚C (June-2017) to -7.33 ˚C (Feb-2018). By comparing the data from the temperature and UV exposure graphs it is possible to see that the UV and the temperatures are the highest between the months of May-August. This combination of higher temperatures and more intense UV light exposure would be more likely to initiate oxidation of bitumen.[3] The temperatures reaching below 0 ˚C within the winter months could indicate that the bitumen becomes brittle making it less able to withstand the mechanical stresses of the traffic. At these low temperatures the less-polar component of the bitumen composition begins to stack and align adding further rigidity to the bitumen, leading to cracking and fracturing.[4]

The rainfall (mm) has also been recorded at 15 minute intervals and this has been totalled for each month of the natural ageing experiment. Figure 5.4 contains this data.

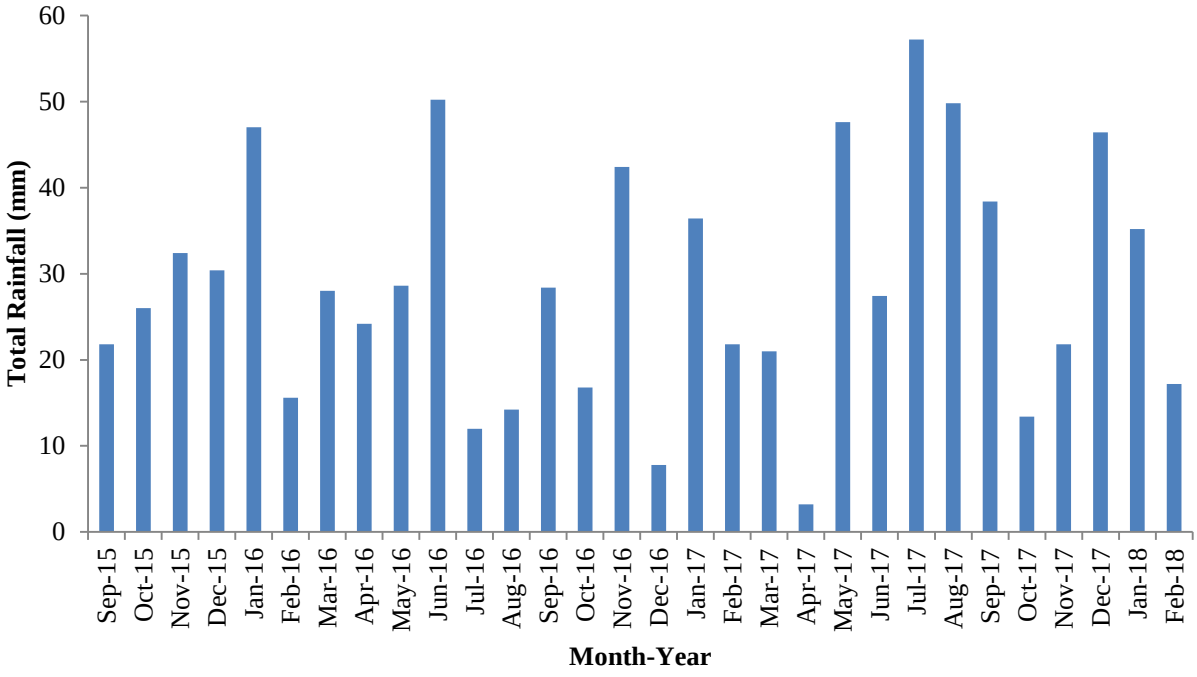


**Figure 5. 4 Column chart displaying the total rainfall each month throughout the duration of the naturally aged experiment**

It is interesting to note that during the period of the experiment the summer months are also the wettest months with June 2016 and July 2017 having the highest total rainfall over the 2.5 year experiment. The two years recorded throughout this project were unusually rainy in the summer, and dry in the winter months. As the presence of water is known to affect the oxidation of bitumen[5] it is possible to assume that the majority of the oxidation will have happened during the summer months of the experiment as a result of the increased temperature, UV exposure and rainfall.

## 5.3 Spectroscopic analysis of naturally aged asphalt

The following section contains the spectroscopic analysis of the 8 week naturally aged asphalt map experiment and the 30 month, long-term, naturally aged experiment. The 8 week sample was mapped (as described in Chapter 4) and the DRIFT spectra were collected from the same slab every week. The 30 week asphalt ageing experiment involved a number of different slabs, one for each time point. This allows mechanical property testing to be carried out at each time point. Scanning electron, infrared and light microscopy has been carried out on an unaged and the 30 month aged asphalt slab.

### *5.3.1 8 week naturally aged asphalt*

The 8 week natural ageing experiment was carried out between 19th April and the 14th June 2017. The total solar exposure has been calculated for each week in this time period and the results can be seen below.

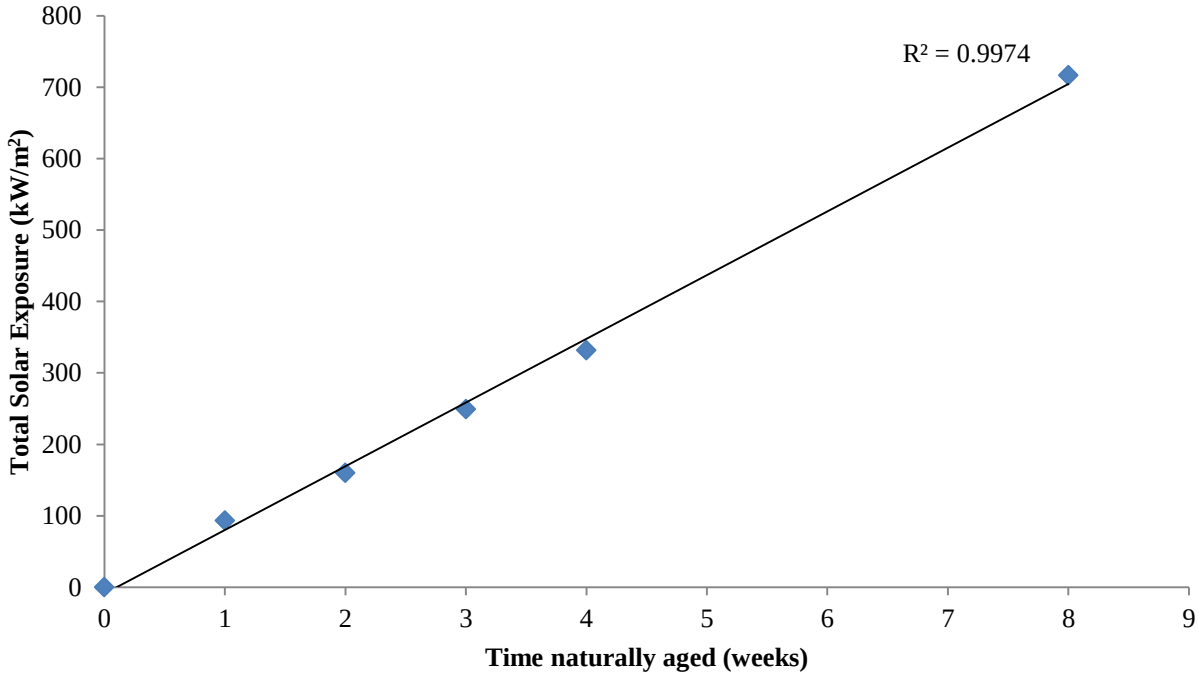


**Figure 5. 5 Total solar exposure experienced by the asphalt slabs that have been naturally aged for 0-8 weeks**

There is a very consistent increase in the total solar exposure measured through the 8 week time period. This could, in theory, create a consistent increase in the measureable characteristics of oxidative ageing of the sample. The maximum temperature experienced during this experiment was 27.42 ˚C; the minimum was -1.25 ˚C with an average of 10.32 ˚C. The total rainfall for this 8 week period was 67.8 mm.

The spectra obtained from the naturally aged asphalt contain a number of similar features as the spectra from the UV aged asphalt (Figure 4.2). The spectra have been displayed with a legend of the total solar exposure experienced by the asphalt during the experiment.

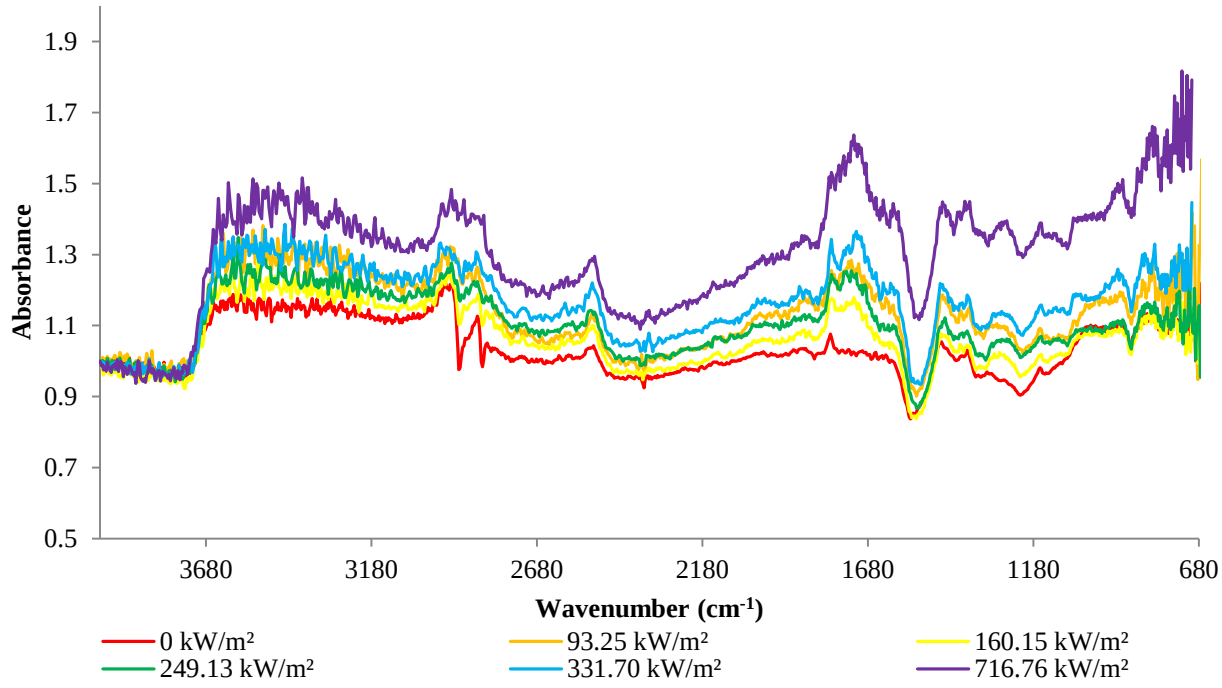


**Figure 5. 6 DRIFT spectra from the (2, 5) coordinate on the surface of the naturally aged asphalt that has been aged for the on the roof at Crowthorne House for 8 weeks**

It is possible to identify the C-H stretching modes at 2911 and 2844 $cm^{-1}$. The carbonate absorbance bands are very clear at 2479, 1815, 1532 and 883 $cm^{-1}$. These absorbance bands have been tabulated and assigned previously in Chapter 4.1.1. There is an increase in an absorbance band arising between the wavenumbers 1770-1615 $cm^{-1}$ in the aged samples. This can be assigned to the absorbance of a carbonyl functional group. This feature can be attributed to a change as a result of ageing as there is a large difference between this absorbance band in the spectra from the unaged (0 $kW/m^2$) and 8 week aged sample (716.76 $kW/m^2$).

The naturally aged asphalt has been mapped and analysed at a number of different coordinates therefore it is possible to look at the spectral change in terms of carbonyl absorbance band growth at a number of different x,y coordinates on the surface of the slab. The radar graph in Figure 5.7 shows the absorbance band area (1767-1617 $cm^{-1}$) calculated for each coordinate at each time point sample. The x, y coordinate is shown in the circumference of the chart and the absorbance band area is plotted on the radial axis representative of the spectra from that coordinate.

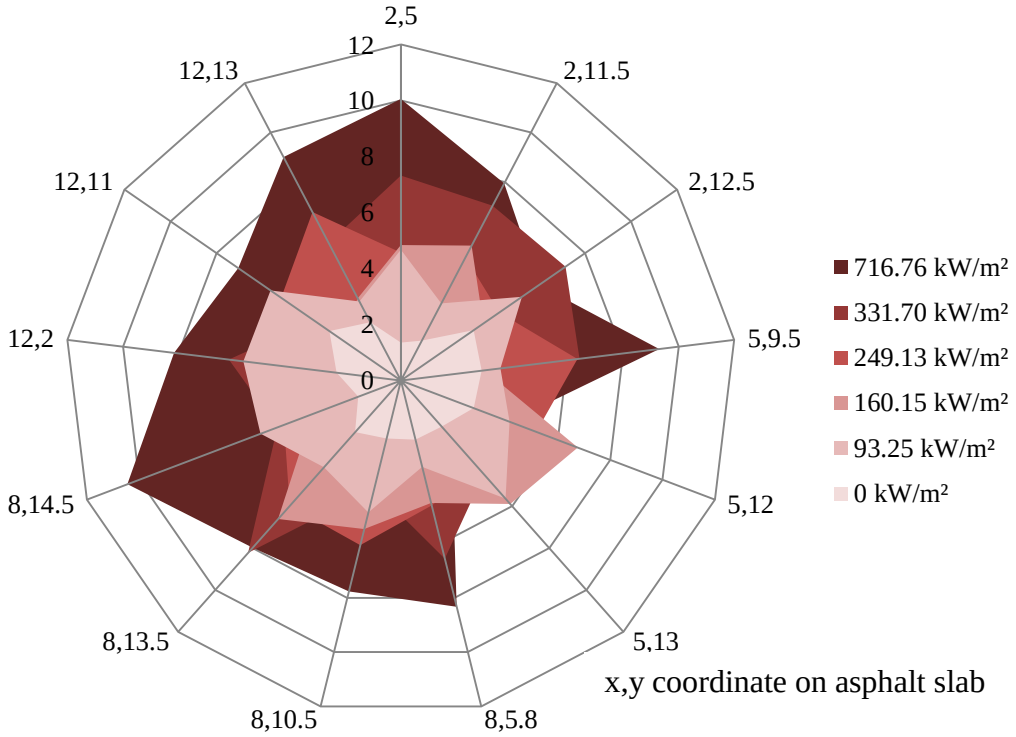


**Figure 5. 7 Radar graph for the carbonyl absorbance band area (1767-1617 cm) measured from the DRIFT spectra collected from the surface coordinates of the 8 week naturally aged asphalt map. The radial axis indicates the spectral positions and the shaded areas indicates the amount of solar exposure**

It is possible to see an increase in the absorbance band area between the 0 and 1 week (0-93.25 kW/m$^2$) time points on the roof, for all coordinates. As seen previously with the ageing map produced from samples held in the UV chamber, (Chapter 4.1.1) there is an increase in variability after this time point. A method to identify the degree of this variability is to calculate the average absorbance band area for all spectra collected at each time point and to calculate error bars. This has been carried out and the results can be found in Figure 5.8.

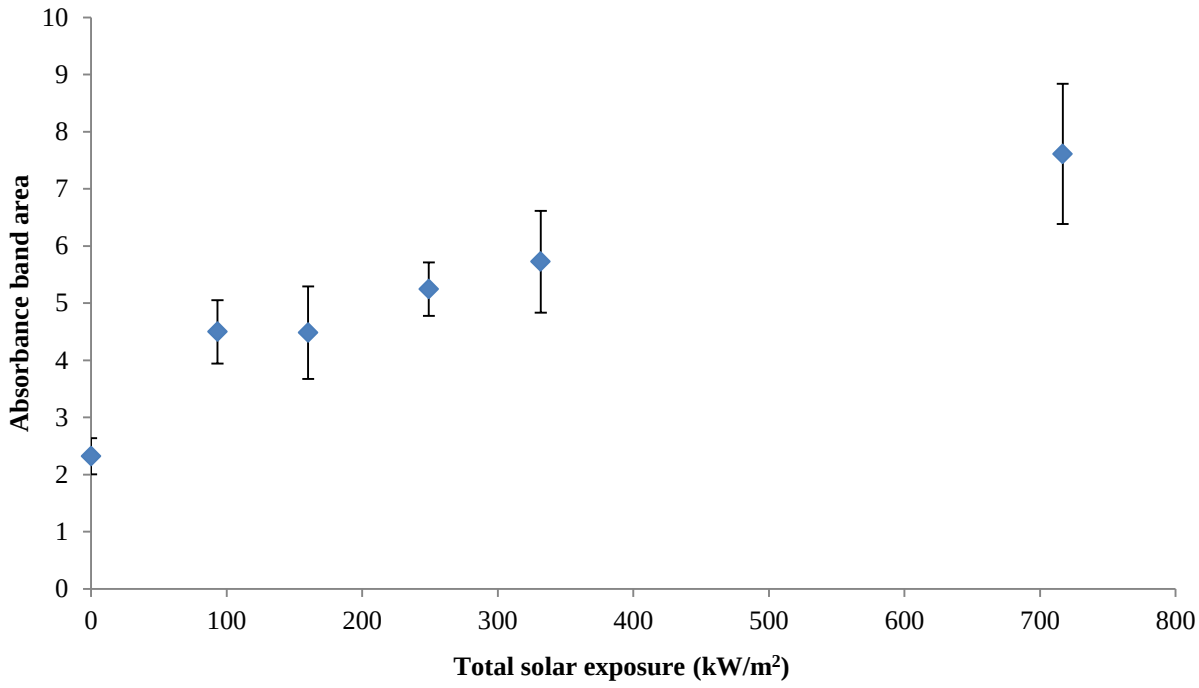


**Figure 5. 8 Average absorbance band area (1767-1617 $cm^{-1}$) from the DRIFT spectra collected from the 8 week naturally aged asphalt mapping experiment.**

The average carbonyl absorbance band area increases linearly as the total solar exposure increases. This suggests strongly that the solar exposure is a contributing factor to the oxidation of the surface of the asphalt. The error bars presented are the 95 % confidence limits for all spectra collected at each time point. There is a slight increase in the size of the error bars for each value as the natural ageing time increases, which indicates that the spectra have a lower signal to noise ratio as the samples become older.

The changes in intensity of the carbonyl absorbance band have also been quantified by recording the absorbance at 1700 $cm^{-1}$ and plotting the intensity against the total solar exposure experienced by the sample. The results of this quantification can be found in Figure 5.9.

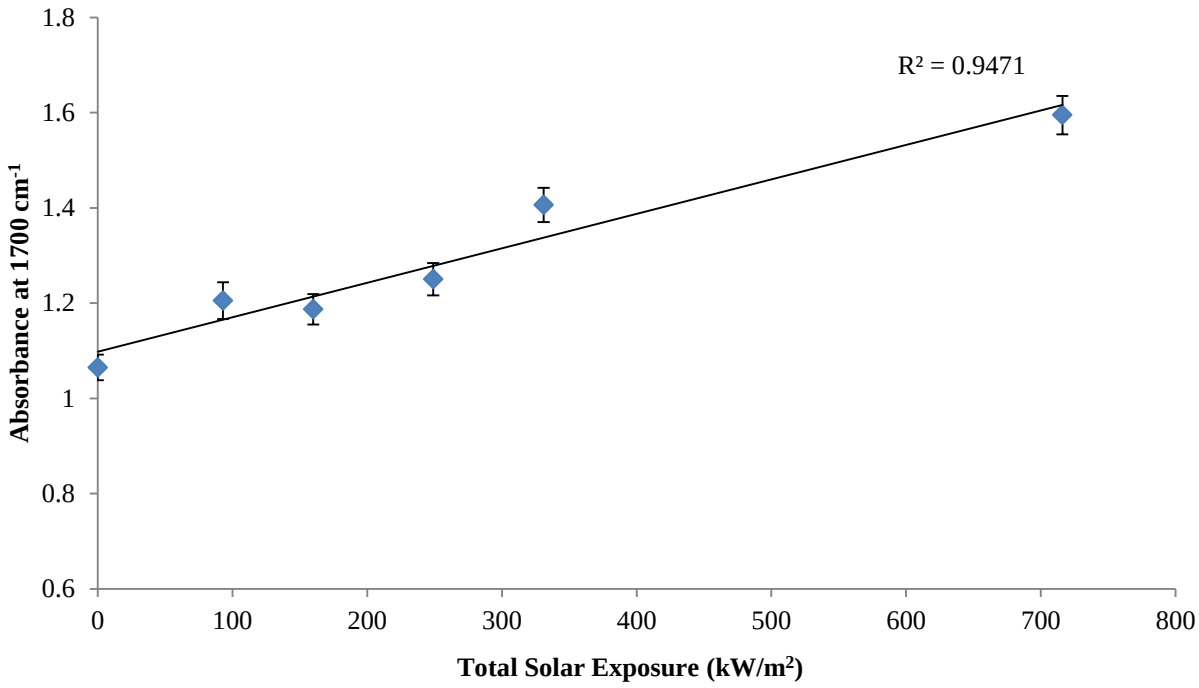


**Figure 5. 9 Absorbance at 1700 $cm^{-1}$ measured from the DRIFT spectra from the surface of the asphalt samples that have been naturally aged for 0-8 weeks**

The absorbance measured at 1700 $cm^{-1}$ shows a gradual linear increase (+56 %) as the sample is aged naturally for 8 weeks. This trend correlates well with the increase in solar exposure. This data analysis technique has produced a linear trend line with small error bars, giving the result reliability.

8 weeks is not a very long period of time in the life span of a road surface therefore the data collected from the 30 month ageing experiment must be carefully investigated to see if this trend continues.

### *5.3.2 30 month naturally aged asphalt*

The 30 month natural ageing experiment was carried out between the 27th August 2015 and the 27th February 2018. Table 5 presented in Section 5.2 lists the dates that these samples were removed. Figure 5.10 contains the total solar exposure experienced by each asphalt sample throughout its ageing on the roof. The results have been calculated by summing every UV-intensity reading for the time that the asphalt slabs were on the roof.

It is worth noting that the 1 month and 5 month samples had a different start date to all other samples. The 1 month sample was placed onto the roof between the 1st April and the 2nd May 2017. It experienced a greater solar exposure within these 4 weeks than the 3 month sample

which was aged between the 27th August and the 27th November 2015. The 5 month sample was placed onto the roof between the 1st April and the 1st September 2017 and therefore has a greater solar exposure than the 7 and 9 month samples that experienced only winter and spring.

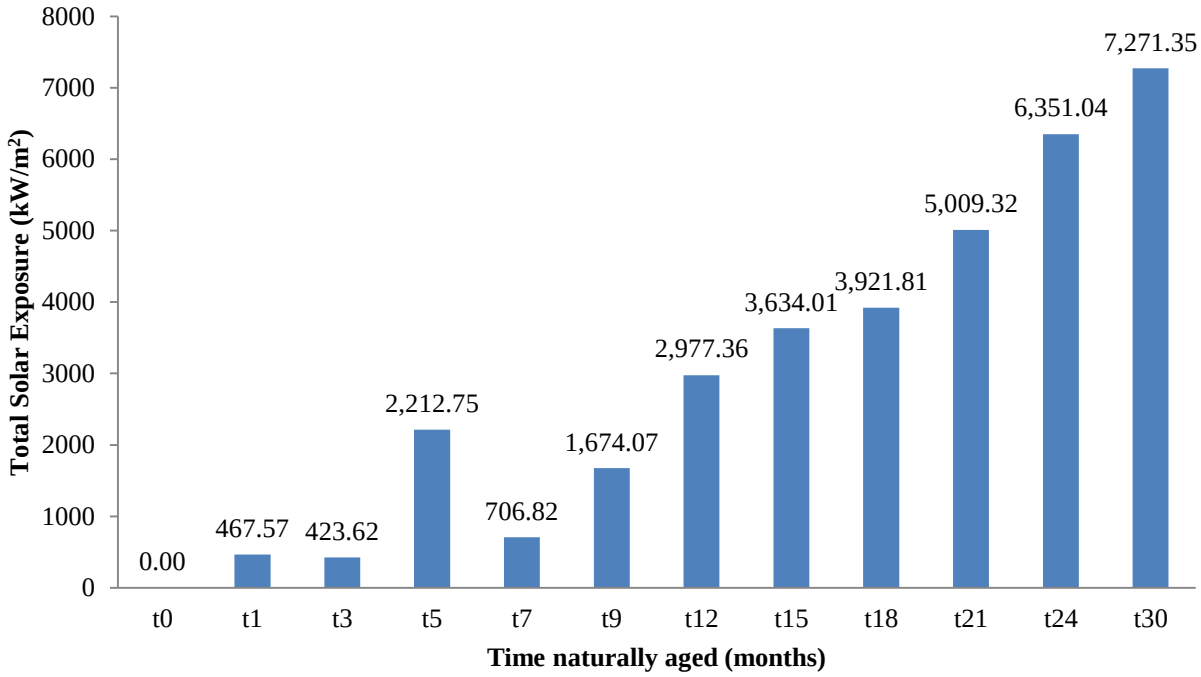


**Figure 5. 10 Total Solar Exposure experienced by the asphalt samples that have been aged naturally on the roof of Crowthorne House**

Apart from these anomalies in the time line the total solar exposure for every other sample increases as the time on the roof increases. Taking into account this variation in the UV exposure, recording the data in terms of months of exposure is unreliable. If the solar exposure is the initiating factor for oxidation, as opposed to time itself, then any data collected from these samples should be displayed in terms of the solar exposure and not the length of time on the roof.

As seen before with the 8 week experiment, there is a gradual increase in the total solar exposure of the asphalt slabs. Based upon the linear result of carbonyl absorbance band area and intensity at 1700 $cm^{-1}$ from the 8 week experiment, the increase in carbonyl absorbance band measured may be expected to increase linearly with solar exposure. The DRIFT spectra from the surface can be found in Figure 5.11.

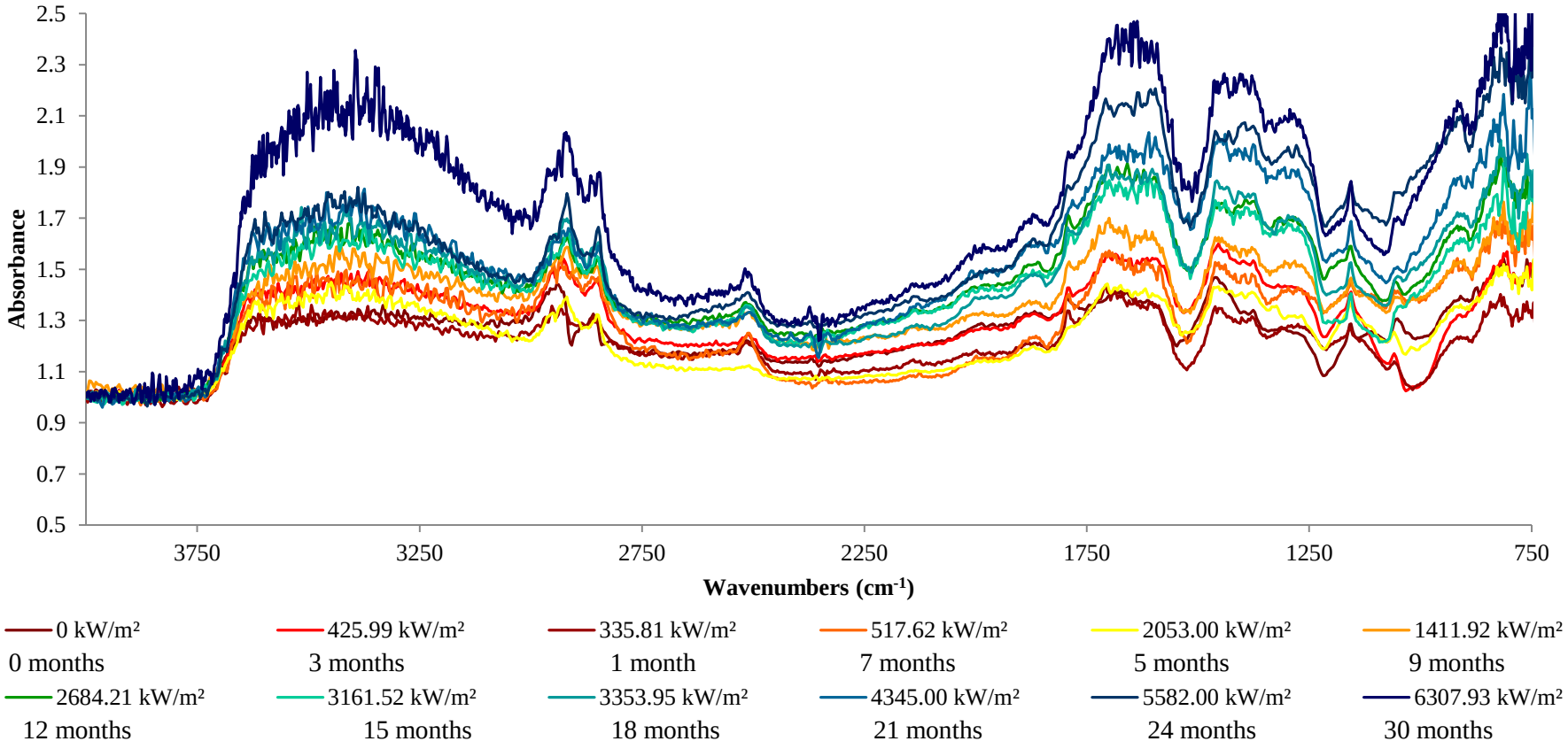


**Figure 5. 11 DRIFT spectra from the surface of the asphalt samples that have been naturally aged on the roof of Crowthorne House for 0-30 months together with the total solar exposure of each sample.**

As with the UV aged asphalt, the absorbance bands that correspond to the carbonate filler and the siliceous aggregates can be identified, alongside the hydrocarbon bitumen. Table 5.2 lists these bands and gives their bond assignment.

**Table 5. 2 Absorbance bands present in the DRIFT spectra of the naturally aged asphalt (Figure 5.11) and their bond assignment**

| Absorbance band ($cm^{-1}$) | Bond Assignment |
|---|---|
| **2920, 2842** | C-H (stretch) |
| **2520** | $CO_3^{2-}$ (combination) |
| **1791** | $CO_3^{2-}$ (overtone) |
| **1653** | C=O (stretch) |
| **1517** | $CO_3^{2-}$ (asym stretch) |
| **1219** | C-O (stretch) |
| **1155** | Si-O (stretch) |

The absorbance bands appear in similar locations to those seen in the UV aged asphalt spectra. However, the main difference between the samples is the formation of the carbonyl absorbance band. In the DRIFT spectra of the UV aged asphalt, the carbonyl presented as a first derivative. This is not the case for the naturally aged asphalt. It is possible to see the growth of an absorbance band between the wavenumbers 1778 and 1550 $cm^{-1}$ which is presenting as a 'normal' band which indicates there is something different about the surface characteristics of the naturally aged asphalt compared to the artificially UV aged asphalt. The first derivative nature of the carbonyl absorbance band in the DRIFT spectra from the UV aged asphalt was a result of the change in absorbance across the wavenumber range 1923-1632 $cm^{-1}$ and occurred because of a change in refractive index of the surface. As absorbance is proportional to refractive index it can be said that because of this change in absorbance band characteristic, there is a difference in refractive index of the bitumen on the surface of the asphalt after natural ageing. The surface of naturally aged asphalt is more dull and grey than the UV aged asphalt which would lead to more diffuse reflectance from the surface and less specular reflectance. The surface characteristics will be explored in more detail later in this chapter.

As this project is aiming to produce a traffic speed detection method the rapid nature of single wavelength analysis makes it a much more favourable technique. In this case the single wavelength quantification has been focused on here. This involved measuring the absorbance band height. It is observable in Figure 5.11 that the 'base line' for the spectra seems to increase as the total solar exposure. The area between 2780 and 1810 $cm^{-1}$ is considered the baseline in these spectra. Therefore another method for measuring the height of this absorbance band is to determine the difference between the apex of the absorbance band (1700 $cm^{-1}$) and this base line (1845 $cm^{-1}$ for example). Both of these quantification methods can be found below.

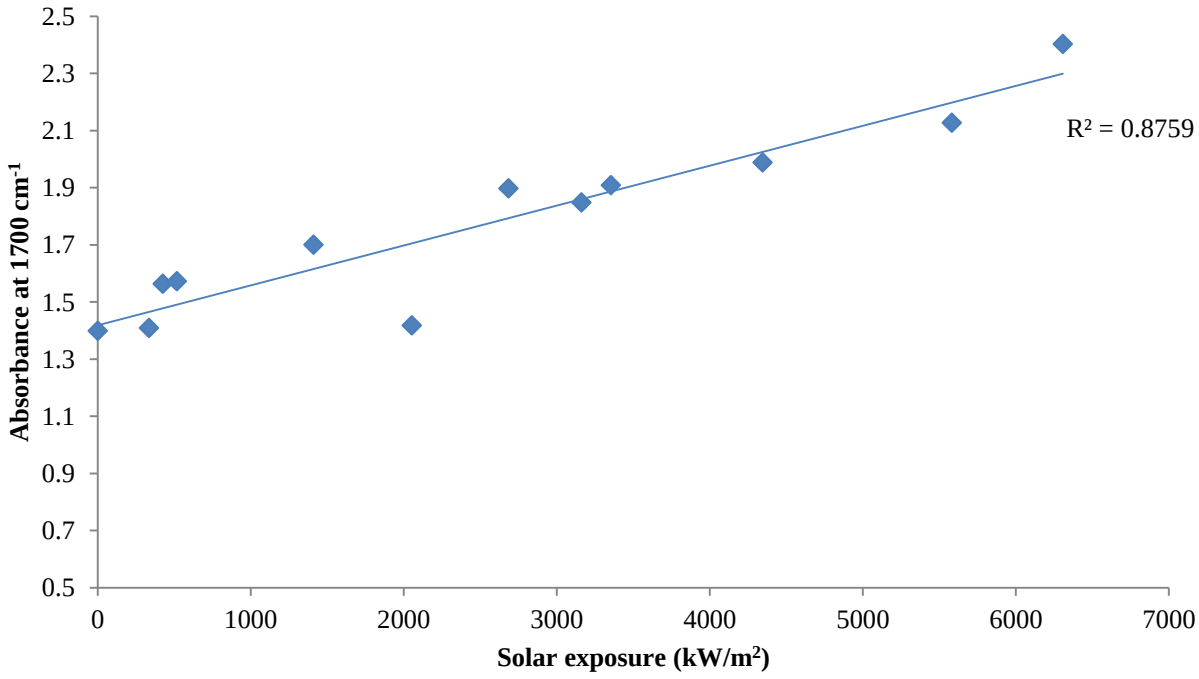


**Figure 5. 12 Absorbance at 1700 $cm^{-1}$ from the DRIFT spectra from the surface of the asphalt slabs that have been aged naturally on the roof of Crowthorne House**

The change in the absorbance at 1700 $cm^{-1}$ increases linearly with increasing solar exposure.

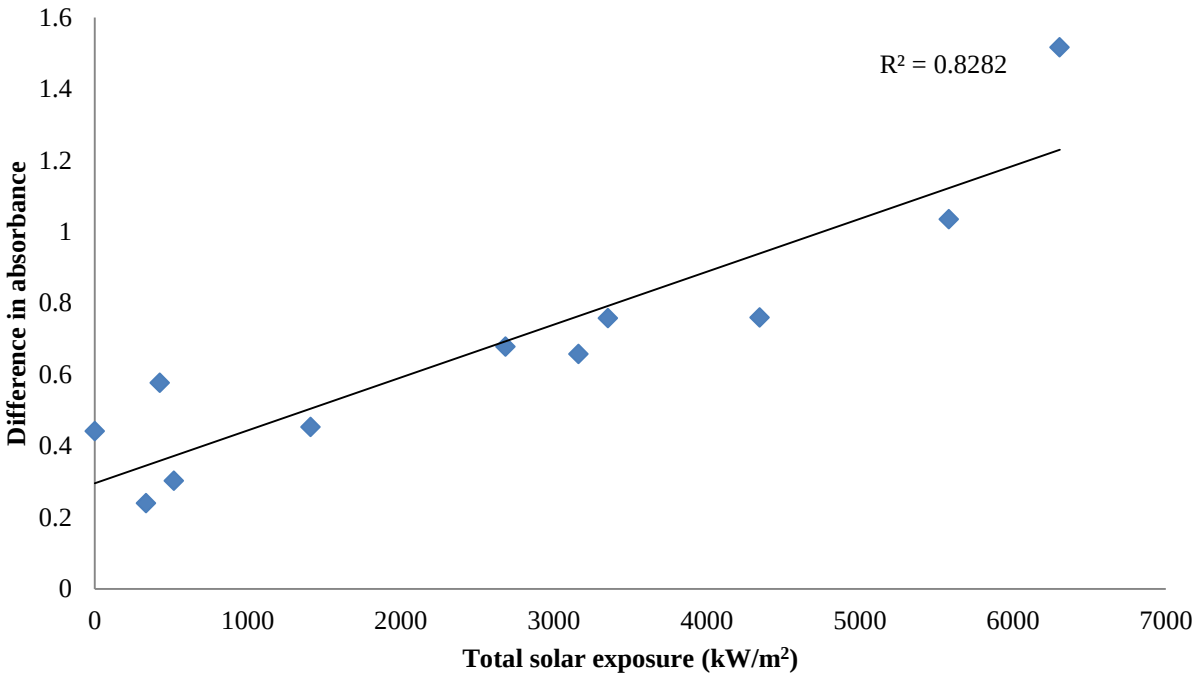


**Figure 5. 13 Difference in absorbance measured at 1700 and 1845 $cm^{-1}$ recorded from the DRIFT spectra in Figure 5.11**

It is possible to see that the difference in the absorbance band height between 1700 and 1845 $cm^{-1}$ is also a linear trend with increasing solar exposure. This confirms that the absorbance band at 1700 $cm^{-1}$ is increasing, and therefore the presence of carbonyl functional groups within the bitumen surface is increasing.

There is some variability within the straight line trend shown in Figure 5.12 and Figure 5.13 and this is because of the reduced signal to noise ratio around 1700 $cm^{-1}$ in the DRIFT spectra from the naturally aged asphalt (Figure 5.11). The presence of noise in the spectra could be a result of a small amount of water on the surface of the asphalt. All spectra presented in Figure 5.11 were collected from samples when they appeared to be dry. However, traces of moisture may well have been present as the samples were not handled in a moisture-free atmosphere. Moreover, it is known that calcium carbonate is hygroscopic; meaning the calcium carbonate filler in the samples can absorb water from the atmosphere on to its surface.[6] This could be an explanation for the presence of water absorption bands in the DRIFT spectra from the surface of dry asphalt samples that have been naturally aged, and therefore previously exposed to water in the form of rain and dew. An experiment has been devised to determine if the presence of water on the surface of calcium carbonate can be proven. This is important as the

presence of calcium carbonate as filler in asphalt road surfaces could be the reason for this interference in the absorption spectrum.

Thermal Gravimetric Analysis (TGA) has been utilised here to determine the presence of water in a seemingly dry sample of calcium carbonate. TGA involves heating a sample while continuously measuring the weight loss while being subjected to a controlled temperature gradient.[7] TGA can be used to determine the effect of factors such as crystallinity, molecular weight and the orientation of molecules on thermal stability and the loss of volatiles.[8] In this experiment three samples of calcium carbonate from Sigma Aldrich were used. The first (a) was untreated; the second (b) was placed into a desiccator for 24 hours and allowed to dry completely and the third (c) was wetted by a few drops of water and allowed to air dry for 2 days. Each sample was then placed into a TGA Q50 instrument and the weight of the sample was monitored while the temperature increased from 25-200 ˚C at a rate of 5 ˚C per minute. The data from this experiment was processed with the TA Universal Analysis Version 4.7A and Microsoft Excel. As this experiment aimed to look for the loss of water, this temperature range was appropriate due to the boiling point of water being 100 ˚C. This experiment aimed to prove that after exposure to water the sample contains the same amount of water on its surface than if it was air dried, and that both of these samples contain more water than the samples dried in the desiccator.

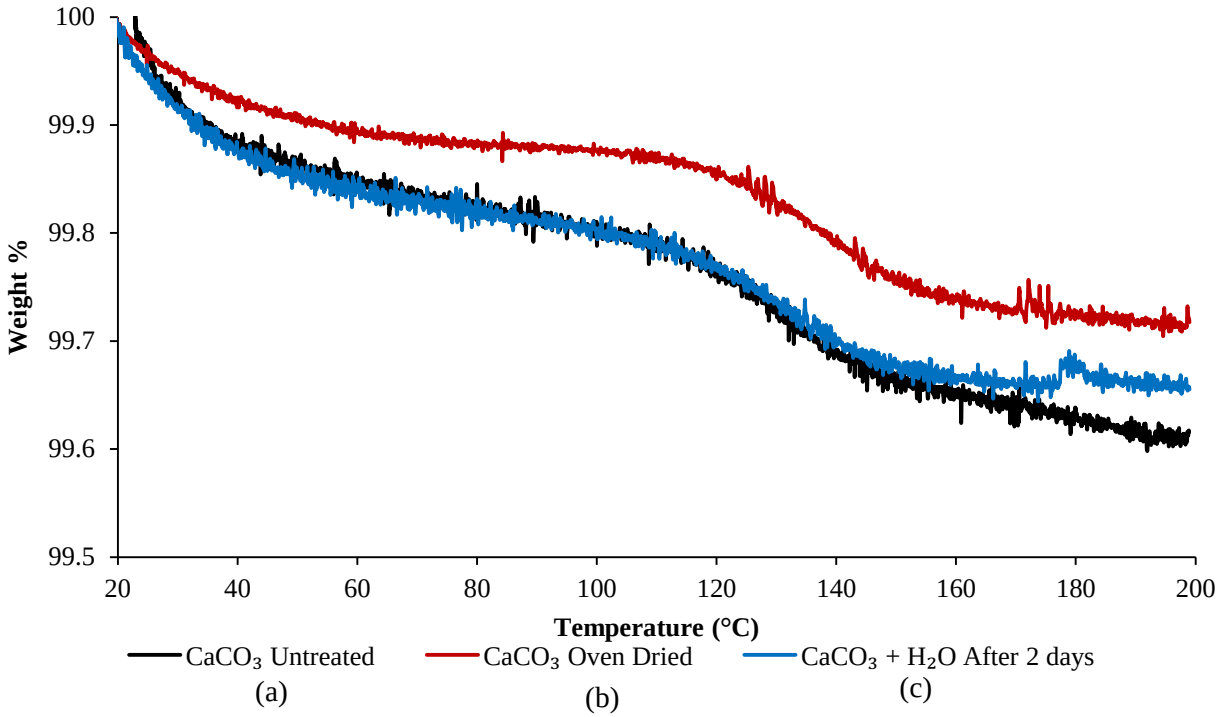


**Figure 5. 14 Thermal Gravimetric Analysis of calcium carbonate samples that are (a) untreated, (b) dried in a desiccator for 24 hours and (c) placed into water and allowed to air dry for 2 days**

The TGA results are presented as % weight loss versus temperature of the system. The red line in Figure 5.14 represents the carbonate that was placed into a desiccator overnight which would have dried the sample. The blue and black lines represent the wetted and the untreated samples respectively. There is a slight but measureable drop between the dried and the wet and untreated samples. One important feature of this graph is the similarity between the untreated and the wetted samples. The fact that these samples lose weight between the temperatures 106-153 ˚C, and the dried sample does not, indicates that there is water present within the carbonate structure that is not removed completely by evaporation at room temperature. It is therefore sensible to assign the noise within the wavenumber ranges 3700-3071 $cm^{-1}$ and 1713-1597 $cm^{-1}$ to the bending and stretching modes of water that is present upon the hygroscopic calcium carbonate filler and aggregates.

Water is an unavoidable contaminant that may be present on the road surface. Although it's effect on the spectra could be reduced by only collecting data from the roads that are dry, or at least two days after rainy weather. The data presented above (Figure 5.11 and Figure 5.14) shows that it is very unlikely that a completely dry road surface would ever be encountered.

## 5.4 Road surface contamination analysis

Water is not the only material that may interfere with the infra-red spectrum of a road surface. The unpredictability of the live road surface environment allows for many other contaminants to be present on the road surface. It is therefore necessary to identify a number of different potential road surface contaminants, to analyse them with infra-red spectroscopy and to determine if they will interfere with the ageing analysis.

The contaminants analysed in this project were fluids that could possibly leak from moving cars and other vehicles. Table 5.3 lists the details of the vehicle fluids used and their main chemical components.

**Table 5. 3 Possible road surface contaminants to be analysed by ATR for their chemical signatures**

| Contaminant | Brand | Composition |
|---|---|---|
| **Power Steering Fluid** | Comma | Petroleum Distillates-Oil |
| **Antifreeze** | Car Plan Blue Star | Ethanediol |
| **Engine Oil** | Mobil Super 1000$x_i$ 15w-40 | Hydrocarbon oil |
| **Transmission Fluid** | Halfords | Alkyl Acetamide |
| **Brake and Clutch Fluid** | Mobil DOT 4 ESP | Glycol Ether |
| **Screen wash** | ASDA | Anionic Surfactants <0.1% |
| **Petrol** | Sigma-Aldrich | Petroleum Ether |

These contaminants can be grouped based upon their chemical composition. For example the power steering fluid, engine oil and petrol, are all hydrocarbon, oil-based. The chemical composition of the bitumen is also oil-based and this could present an issue when analysing road surfaces. Figure 5.15 contains the ATR spectra of these oil-based contaminants and a spectrum of a 40/60 bitumen sample as a comparison. Petroleum ether has been included to represent a possible petrol spill on the road surface. As a result of the health and safety protocols at the University of Reading, petrol or diesel was not permitted as a sample into the laboratory. Samples were analysed by dropping a small amount of the liquid onto the diamond ATR crystal of a Perkin Elmer Spectrum 100 FTIR. The samples were analysed through a wavenumber range from 680-4000 $cm^{-1}$ and the spectra shown are an average of 16 total scans.

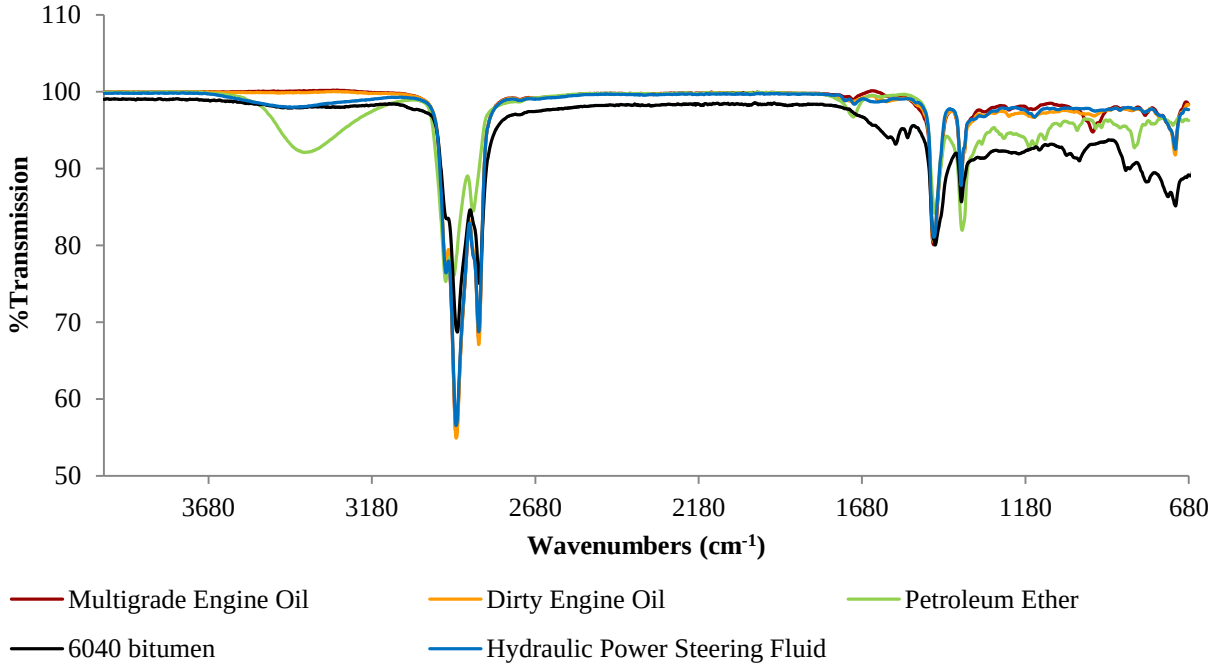


**Figure 5. 15 ATR spectra for a number of hydrocarbon based road surface contaminants**

The strongest absorbance bands in all spectra correspond to the C-H stretch at 2925 and 2835 $cm^{-1}$ and the C-$H_3$ bending modes at 1462 and 1378 $cm^{-1}$. This is as expected as all samples have a hydrocarbon composition. If the C-H absorbance bands are to be used as a marker to prove the spectra are being collected from bitumen, in a traffic speed device, then the presence of these types of contaminants on the road surface could make it difficult to differentiate between the spectra collected from the bitumen and the contaminant. The spectrum from the petroleum ether contains a broad absorbance band between the wavenumbers 3525 and 3150 $cm^{-1}$ which is due to the presence of water in the sample.

The remaining contaminants, the brake and clutch fluid, antifreeze and screen wash, all have a water-based composition which makes the spectra quite different to those of the hydrocarbon based samples.

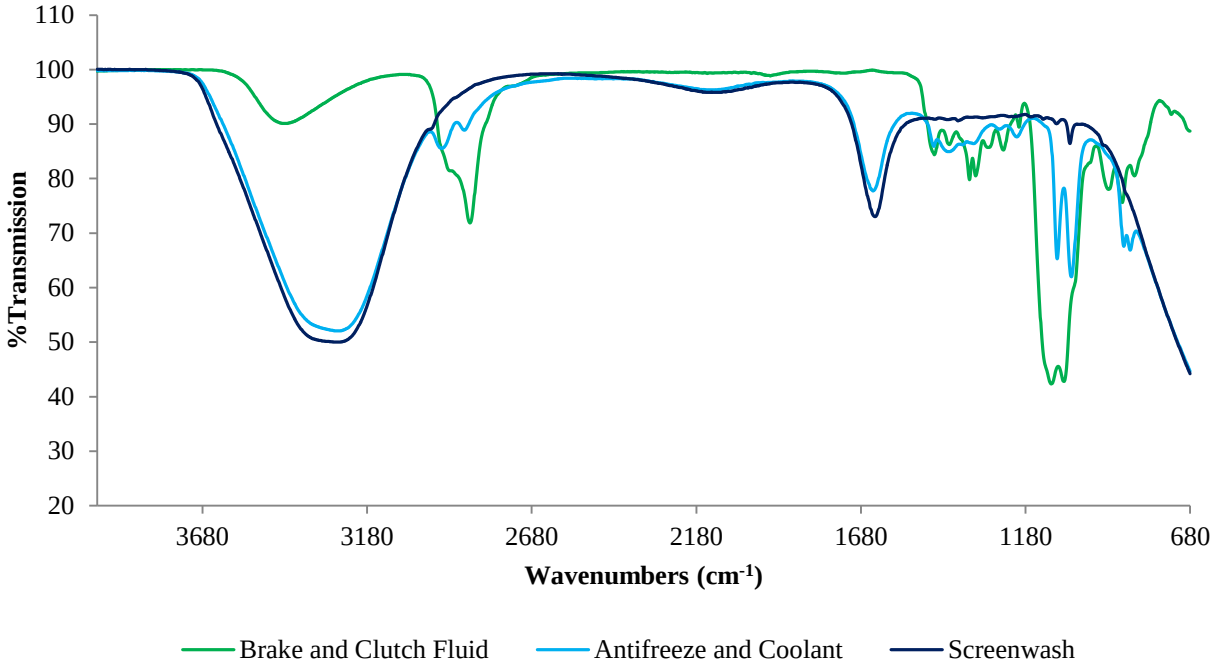


**Figure 5. 16 ATR spectra of three common, water based fluids used in cars that could be possible contaminants on a road surface**

The spectra from the anti-freeze and the screen wash have very strong and broad absorbance bands between the wavenumbers 3743-2879 $cm^{-1}$ and 1781-1540 $cm^{-1}$. These correspond to the bending and stretching of the H-O-H bonds within water, and are broad as a result of hydrogen bonding within the water. There is little other spectral detail in these spectra as the other ingredients are possibly inorganic surfactants.

There are some weak hydrocarbon C-$H_3$ bending and stretching modes present within the spectra of the brake and clutch fluid. One of the main ingredients of the brake and clutch fluid is quoted as glycol ethers.[9] Specific structures of glycol ether are not always quoted on the commercial bottles as a mixture of different molecular weight and structure of glycol ethers may be used. Diethylene glycol and diethylene glycol monoethyl ether have been identified as commonly used glycol ethers in brake fluid.[10]

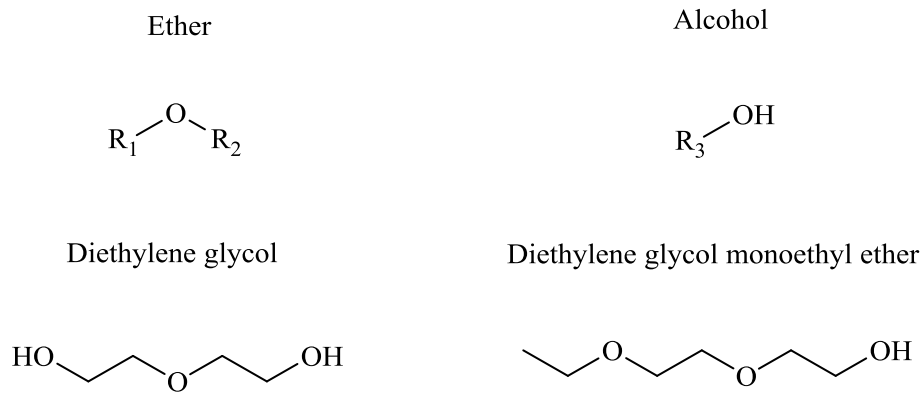


**Figure 5. 17 Chemical structure of an Ether linkage, and alcohol functional group, Diethylene glycol and Diethylene glycol mono ethyl ether**

These compounds contain C-H, O-H and C-O functional groups. The presence of these bonds can be confirmed by the ATR spectra collected. There is a strong absorbance band at 1097 $cm^{-1}$ in the brake and clutch fluid spectra, which almost certainly corresponds to the C-O stretching mode of the ethers present in the fluid. This absorbance band is split at the apex which suggests there are different C-O functional group positions within the ether structure, and the change in their position in the chain changes the shift of the absorbance frequency.

As previously mentioned water is a contaminant that can interfere with the infra-red spectrum of a road surface. The weather is an uncontrollable parameter and this project needs to include an investigation into the effects of rain water on the infra-red spectrum of the road surface when the traffic speed, vehicle mounted device is developed.

As part of the 8 week mapping experiment (Section 5.3.1), the 4 week naturally aged sample was collected from the roof on a rainy day. A spectrum was taken from the surface while the surface was still wet and is shown in Figure 5.18.

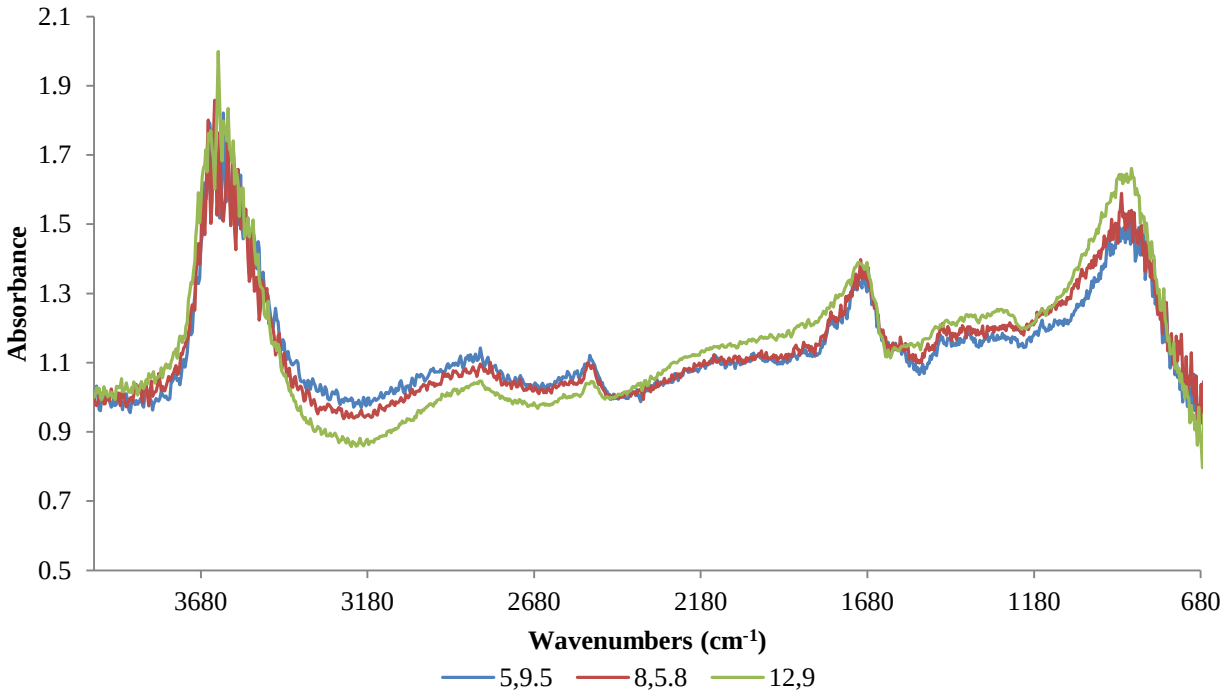


**Figure 5. 18 DRIFT spectra from three, (x,y) coordinate locations, (5,9.5), (8.5.8) and (12,9) on the wet surface of the asphalt that has been aged for 4 weeks**

The absorbance bands that correspond to the bending and stretching modes of the water are the most dominant in the DRIFT spectrum from the surface of the wet asphalt in Figure 5.18 It is possible to also see the carbonate absorbance bands at 2516 $cm^{-1}$ and a sharp shoulder at 1804 $cm^{-1}$.

**Table 5. 4 Absorbance bands and their assignment from the DRIFT spectra from the surface of the wet 4 week naturally aged asphalt**

| Absorbance Band ($cm^{-1}$) | Bond Assignment |
|---|---|
| **3390- 3840** | O-H (stretch) |
| **2515** | $CO_3^{2-}$ (combination) |
| **1804** | $CO_3^{2-}$ (overtone) |
| **1595** | H-O-H (bend) |

It is no longer possible to see C-H stretching modes between the wavenumbers 2900-2800 $cm^{-1}$. It is also impossible to use this data for the identification of oxidation products, especially the carbonyl function group which absorbs between the wavenumbers 1650-1750

$cm^{-1}$. If this technique is to be used to analyse live road surfaces this result suggests that the survey must only be carried out in dry conditions, or a few days after raining, in order to obtain more reliable indicators of oxidation reactions. Further experimental work could be carried out here to identify the length of time that needs to be left after it has been raining in order to start collecting reliable infrared spectra from a road surface.

## 5.5 Scanning Electron Microscopy and elemental analysis

Scanning electron microscopy (SEM) has been carried out on the surface of the 30 month naturally aged asphalt slab. An aggregate chip was removed from the surface of the asphalt and placed onto the carbon SEM tab which was inserted into the low vacuum SEM chamber.

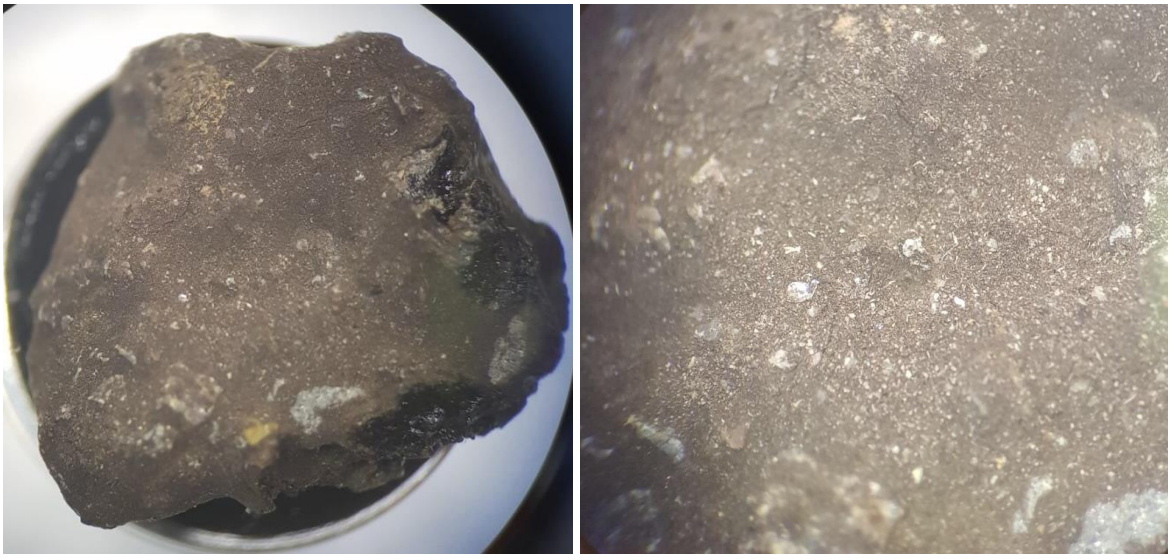

**Figure 5. 19 Photograph of the aggregate subsample from the surface of the 30 month naturally aged asphalt slab at two different magnifications in a light microscope**

The images from the light microscope (Figure 5.19) show an aggregate subsample taken from the surface of the naturally aged asphalt slab. It is possible to see the aggregate surface underneath the bituminous binder. The bitumen covering the aggregate is no longer black and shiny and has become dull and grey with some areas that look like dirt present on the surface. Higher magnification images have been taken with the scanning electron microscope to enhance the surface structure.

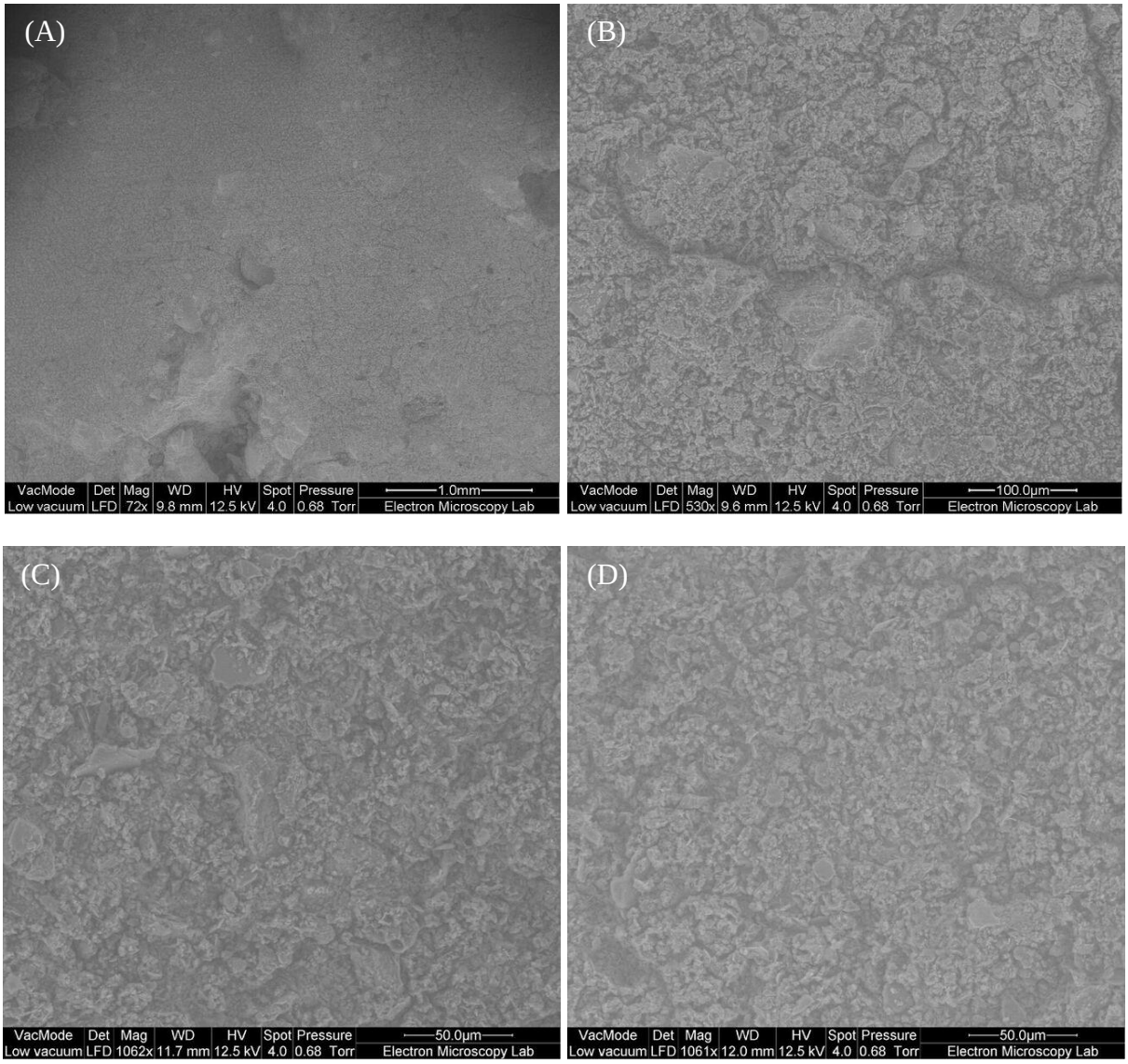


**Figure 5. 20 SEM images from the surface of an aggregate pulled from the surface of the 30 month (6307.93 kW/m$^2$) naturally aged asphalt slab**

**Table 5. 5 Magnifications of the SEM images presented in Figure 5.20**

| Microscope Image (Figure 5.20) | Magnification (×) |
|---|---|
| **A** | 72 |
| **B** | 530 |
| **C** | 1062 |
| **D** | 1061 |

The images from the surface of the naturally aged asphalt do not contain the same 'platelet' cracking as seen in the UV aged asphalt samples (Chapter 4.2). The surface of the naturally aged sample is a lot less homogenous with many different shapes and structures present on the surface.

It is possible to see in Figure 5.20 B that a crack has formed on the surface of the asphalt sub-sample. This is thicker than the cracks seen in the UV aged asphalt between the platelets (Chapter 4.2) and could be a result of the bitumen becoming more brittle as the natural exposure increases. A crack such as this would be exacerbated by the mechanical agitation of trafficking and could lead to deeper cracks, wearing away of the bitumen or fretting of these aggregates.

Scanning electron microscopy images were taken of the carbonate filler that was recovered from one of the asphalt slabs created for this project. This was carried out in order to examine the nature of the electron microscope images of this filler and hence to determine to what extent the carbonate filler influences the nature of the surface of the asphalt. The images can be seen below.

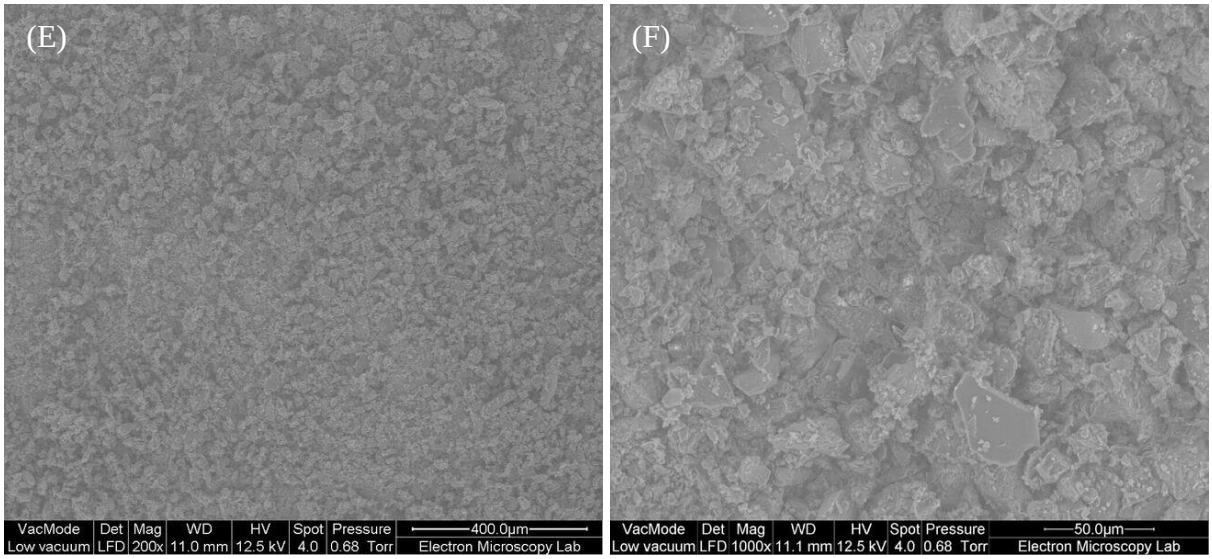


**Figure 5. 21 SEM images of calcium carbonate filler that has been recovered from an asphalt slab *via* the binder recovery process[1]**

**Table 5. 6 Magnifications of the SEM images in Figure 5.21**

| Microscope image (Figure 5.21) | Magnification (×) |
|---|---|
| **E** | 200 |
| **F** | 1000 |

The carbonate filler appears to have a similar surface structure to the naturally aged asphalt except that it is slightly more uniform. This suggests that the images from the naturally aged asphalt slabs indicate the presence of some carbonate filler at the surface, however there are more contaminants present on the surface of the asphalt. Visually, naturally aged asphalt is a lot less shiny and black compared to the UV aged asphalt. It is clear to see this in a real world situation where a newly laid road is very dark black in colour whereas, after a few weeks the road becomes muted and grey. However, visual examination does not show the changes in microstructure that have been highlighted by experiments utilising the light microscope and SEM reported here.

The light microscope and SEM images show that there is a coating of dirt and particulate matter on the surface of the asphalt sub-sample (Figure 5.19 and Figure 5.20). This could be deposited on the surface *via* air or rain contamination. Upon closer inspection of the particular matter a number of spherical particles became visible.

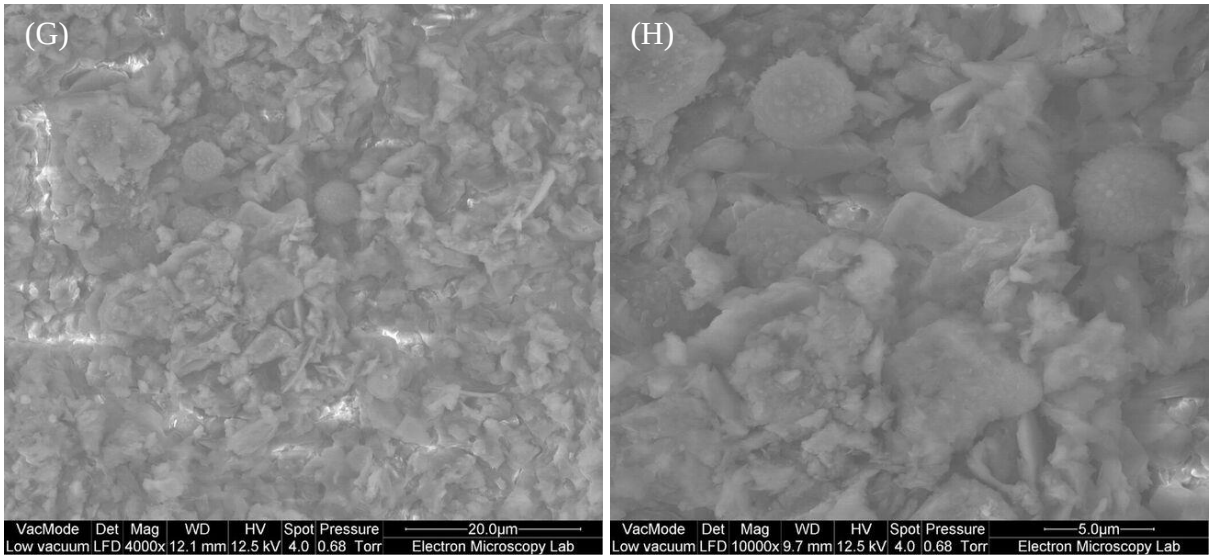


**Figure 5. 22 SEM images of spherical particulates present on the surface of the naturally aged asphalt sub sample.**

**Table 5. 7 Magnifications of the SEM images in Figure 5.22**

| Microscope Image (Figure 5.22) | Magnification (×) |
|---|---|
| **G** | 4000 |
| **H** | 10000 |

These spherical structures are likely to be pollen particles. As the samples are naturally aged on the roof it is possible that pollen can be carried in the air and deposited onto the surface of asphalt. They are approximately 5 μm in diameter. The spherical and spiked shape is similar in structure to that of Dandelion or Ragweed pollen.[11,12,13] Both dandelion and ragweed are common weeds in the UK.

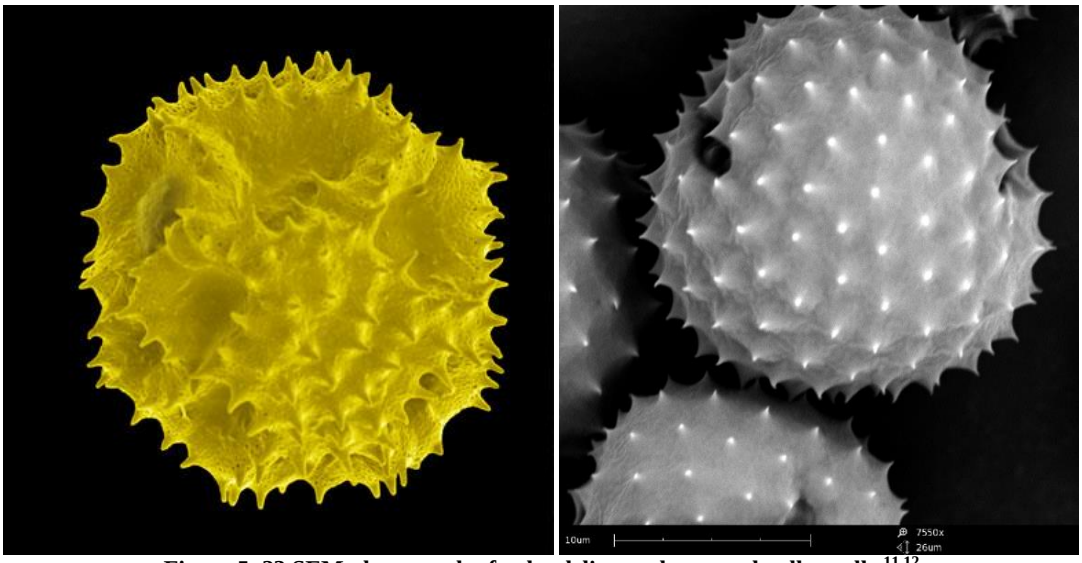


**Figure 5. 23 SEM photograph of a dandelion and ragweed pollen cells.[11,12]**

However, the presence of the pollen is sparse and does not appear to be affecting the DRIFT spectra; therefore it is a natural contaminant that can be ignored.

## 5.6 Infrared Microscopy

The infra-red microscopy analysis has been carried out on the cross section surface of the asphalt slab. An artefact of the optics of the microscope means that the bottom of the image in Figure 5.24 is the top of the asphalt and the bulk moves towards the top of the image. The red markers indicate the location of the point infra-red spectra on the bitumen (Nat301-7) and the aggregates (Agg301-4).

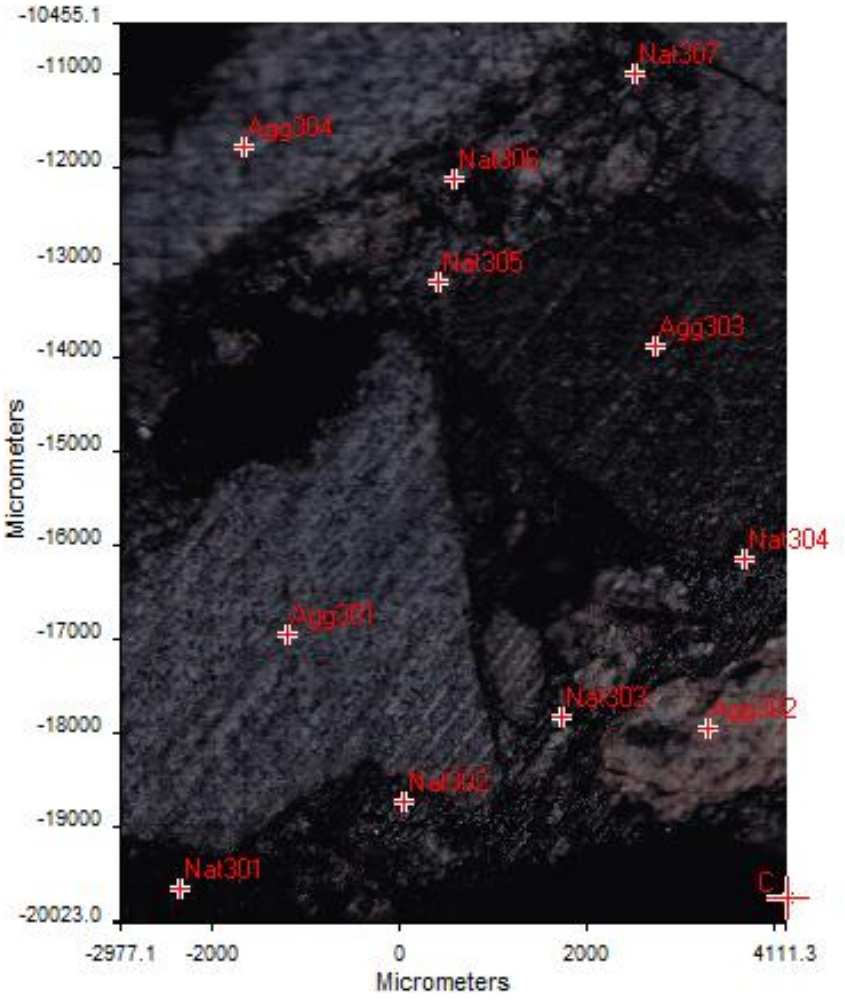


**Figure 5. 24 Infra-red microscope image from the cross section of the 30 month naturally aged asphalt slab.**

The point spectra have been collected from locations throughout the bulk of the asphalt, starting at the surface (Nat301) to approximately 9 mm into the bulk of the asphalt (Nat307). The aim of this experiment was to monitor any changes that may occur within the bulk of the asphalt sample, compared to the surface. The spectra collected were an average of 132 scans with a 2 $cm^{-1}$ resolution and can be found in Figure 5.25.

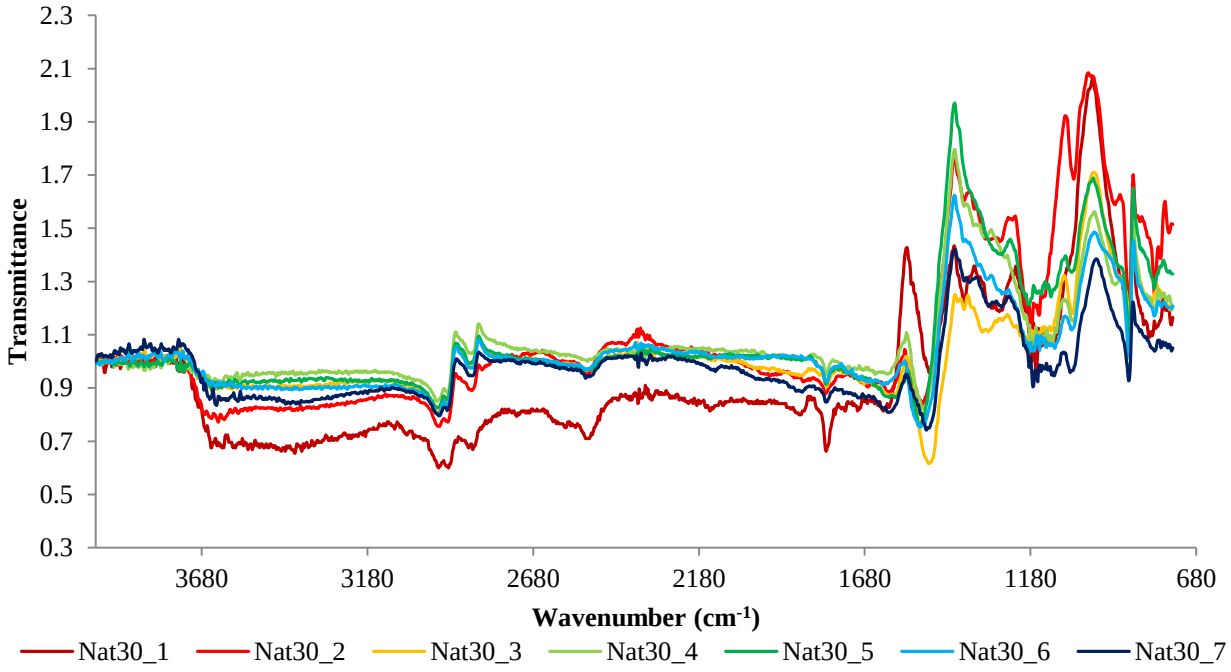


**Figure 5. 25 Reflectance spectra from the cross section surface of the 30 month naturally aged asphalt collected from the markers shown in Figure 5.24.**

There are a number of different features that can be assigned to the hydrocarbon bitumen but also the carbonate filler used to bulk out the bitumen.

As seen previously with the IR microscopy of the UV aged asphalt (Chapter 4.3), there is no trend between the absorbance band intensity at 1700 $cm^{-1}$ and the location of the point spectra through the bulk. It is possible that there is not a measureable amount of oxidation products being produced within the bulk as the oxidation is occurring on the very surface of the asphalt, which was exposed to the natural ageing conditions. As the UV penetration is only into the first 4-5 μm[14] the IR microscope does not have a high enough spatial resolution to analyse this small distance.

Figure 5.26 contains the spectra collected from the aggregates present within the bulk of the asphalt sample that has been analysed with the infrared microscope.

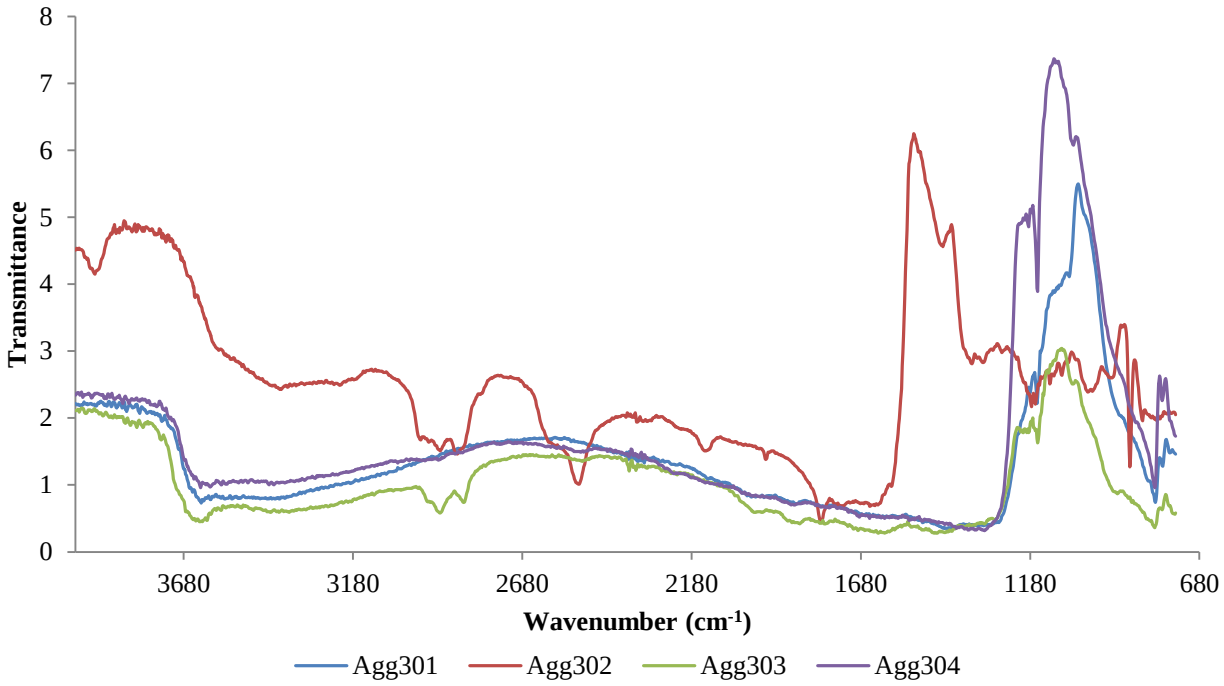


**Figure 5. 26 Reflectance spectra from the aggregates from the cross section of the 30 month naturally aged asphalt, collected from the markers shown in Figure 5.24.**

The spectra shown in Figure 5.26 have been taken from 4 different aggregate stones present through the cross section of the naturally aged asphalt, (Figure 5.24). It is possible to see two different types of aggregate, siliceous granite (Agg301, 3 and 4) and a limestone/carbonate (Agg302). The spectra from the siliceous granite contain a large absorbance band between the wavenumbers 1300-800 $cm^{-1}$ that correspond to an $SiO_2$ stretch, whereas the carbonate aggregate has a large absorbance band at 1530 $cm^{-1}$ which corresponds to the fundamental $CO_3^{2-}$ asymmetric stretch. By identifying the carbonate aggregate spectra it is possible to confidently assign some of the carbonate absorbance bands in the reflectance spectra from the bitumen sections (Figure 5.25). The large fundamental stretch can be seen in Figure 5.25 at approximately 1560 $cm^{-1}$. There is also a sharp, negative absorbance band at 1800 $cm^{-1}$ in the spectrum of the carbonate aggregate and also the bituminous binder. This highlights the lack of absorbance bands that correspond to the carbonyl as it would arise between these two carbonate absorbance's; however, there are no absorbance bands present. This indicates that any carbonyl absorbance bands that are present upon the surface of the aggregate correspond to the bitumen and not an aggregate or carbonate filler absorbance band.

## 5.7 Mechanical property testing

As there is not yet a standardised test method for determining the fretting potential of asphalt as a whole, the bitumen must be recovered from the asphalt. The mechanical properties of live road surfaces are measured in industry by collecting cores from a stretch of road to be analysed and recovering the bitumen *via* the binder recovery process.[1] Following binder recovery, mechanical property tests are then carried out on the bitumen. These tests include the penetration point, softening point and, less commonly, the Vialit pendulum test and have been outlined in more detail in Chapter 3.1

Such a procedure has been carried out on the asphalt slabs that have been naturally aged in this experiment. The results are presented in terms of the total solar exposure which ranges between 0-7271.35 kW/m$^2$.

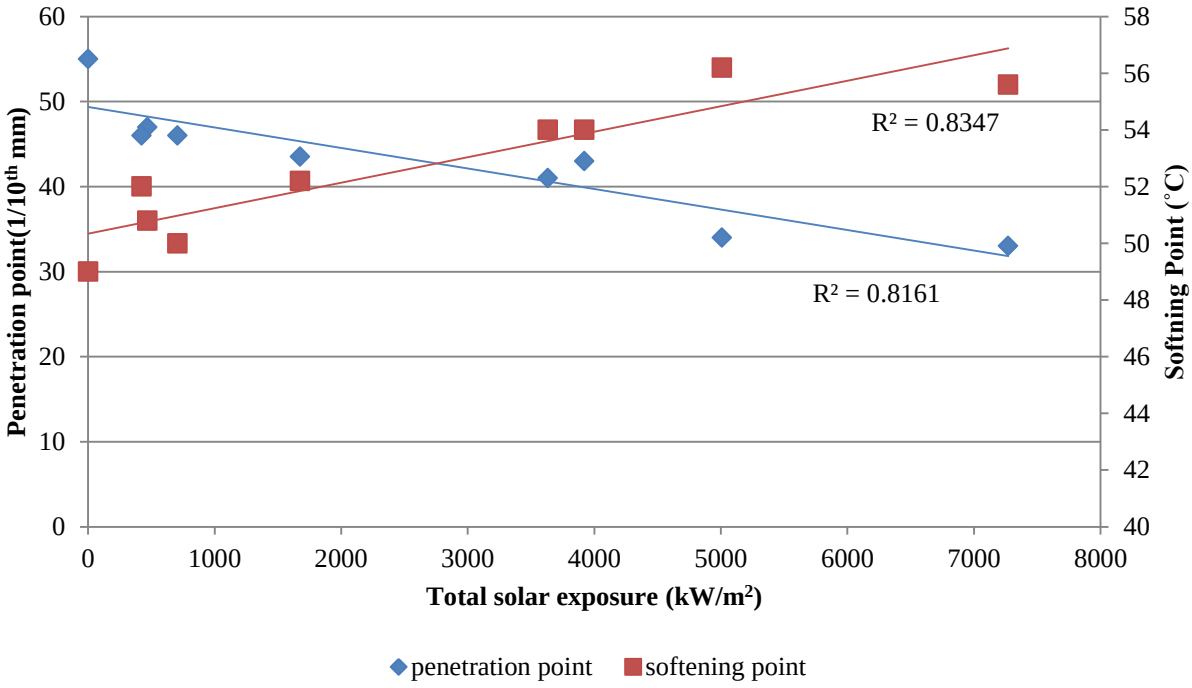


**Figure 5. 27 Penetration and softening point of the raw bitumen recovered from the naturally aged asphalt slabs**

The penetration and softening point test results show a decrease in penetration point (40%) and an increase in softening point (24%) as the sample is aged and the total solar exposure increases. This is the trend that would be expected for the bitumen as it is aged. It is also the trend that has been consistent throughout the ageing experiments.

It was suggested in Chapters 2.2 and 2.3 that the majority of the oxidative ageing is occurring in the bitumen on the surface of the asphalt. However, these results presented here suggest

that there is a physical change occurring also within the bulk of the asphalt which leads to an overall, measureable physical property change.

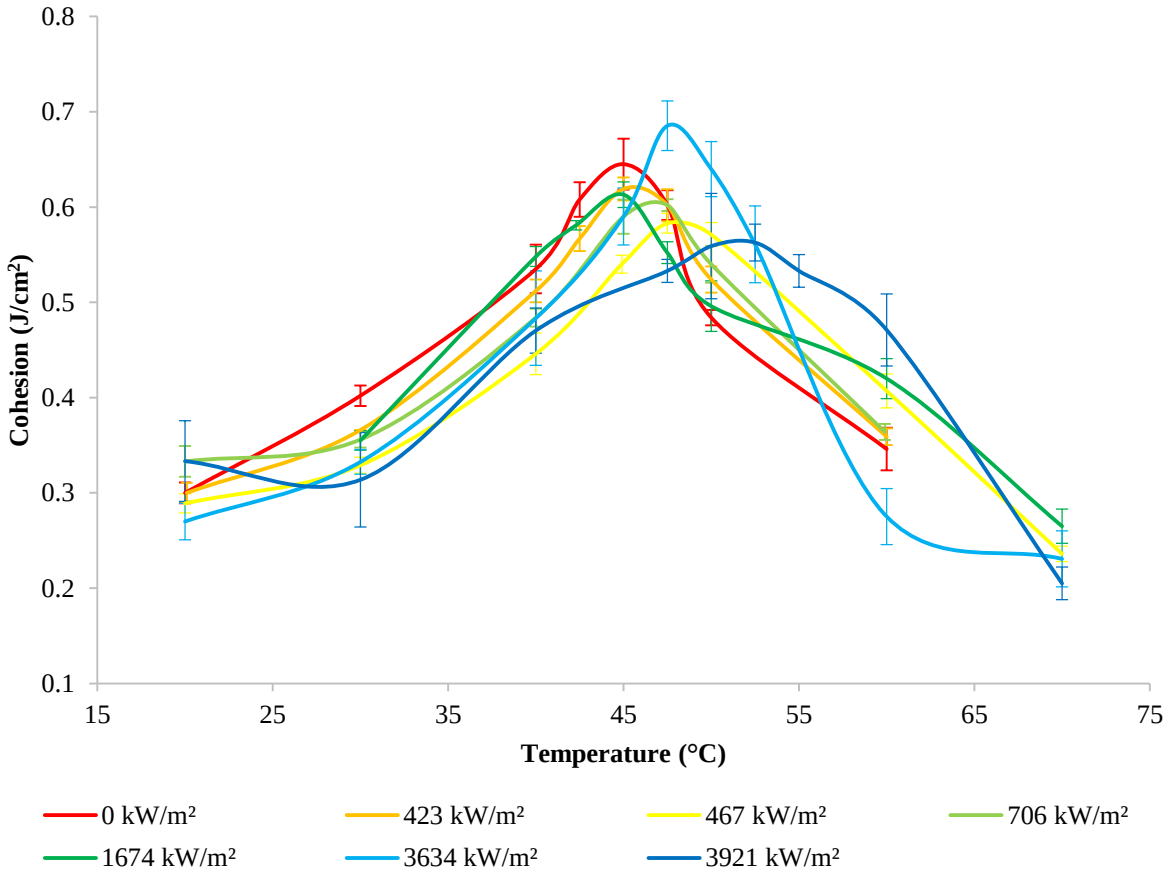


**Figure 5. 28 Vialit pendulum test results of the raw bitumen that has been recovered from the asphalt samples that have been aged naturally on the roof between 0-18 months**

The pendulum test result profiles for the naturally aged bitumen follow the same pattern as for the E-RTFO test aged bitumen, (Chapter 3.2). The error bars on the Vialit pendulum test graph (Figure 5.28) are the 95% confidence limits for the 6 samples that were analysed at each temperature. There is an increase in cohesion as the temperature is raised from 20 ˚C to around 40-50 ˚C, and then the cohesion drops as the temperature is raised further. There are a number of different profiles in Figure 5.28 and it is difficult to determine any definite trends. The information that is potentially of interest is the maximum cohesion recorded and the temperature of this maximum cohesion.

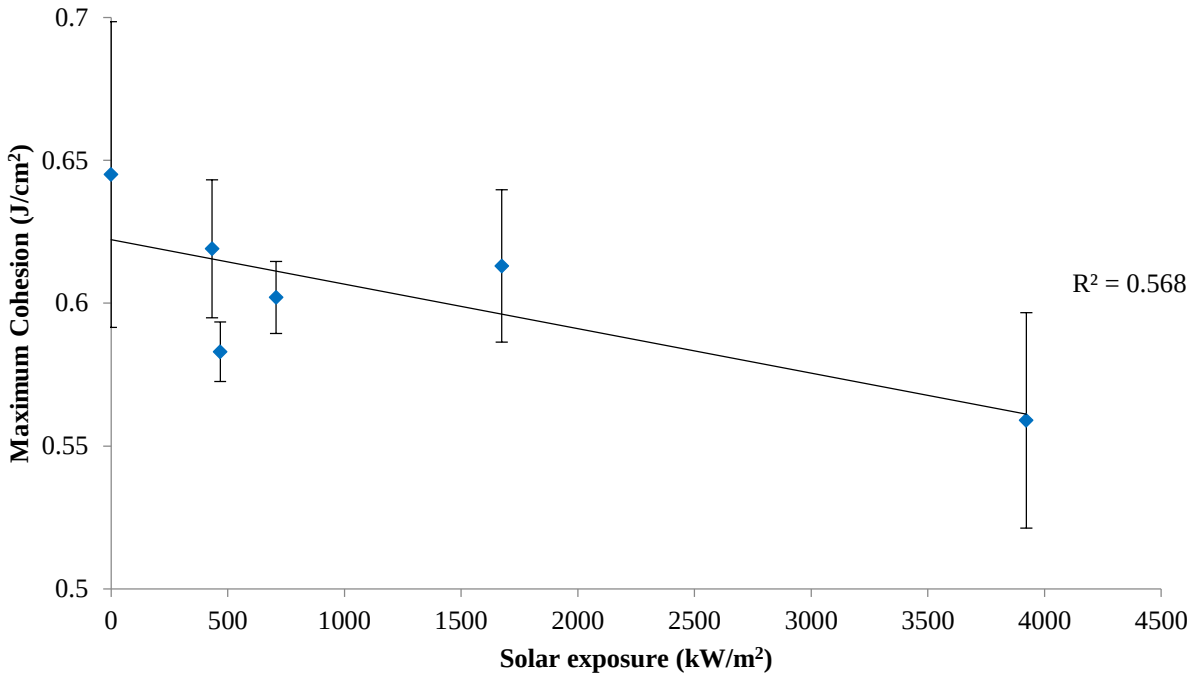


**Figure 5. 29 Scatter chart of the maximum cohesion recorded by the Vialit pendulum test for the bitumen recovered from the naturally aged asphalt samples.**

There is an overall decrease (- 13 %) in the maximum cohesion recorded at 0 and 3921 kW/m$^2$. However the trend between these two solar exposure values is much more variable with large error bars. From the data shown in Figure 5.29 it is possible to conclude that while the average maximum cohesion decreases as the solar exposure increases, the reduction in the maximum cohesion does not follow a stable, linear trend. However the fact that the maximum cohesion does decrease with increasing solar exposure suggests that solar exposure is contributing to the ageing process of the asphalt.

**Table 5. 8 Temperature of maximum cohesion measured with the Vialit pendulum test for the bitumen that was recovered from the naturally aged asphalt slabs**

| Total Solar Exposure (kW/m$^2$) | Temperature of Maximum Cohesion (˚C) |
|---|---|
| **0** | 45 |
| **423.6** | 45 |
| **467.6** | 47.5 |
| **706.8** | 47.5 |
| **1674.0** | 45 |
| **3634.0** | 47.5 |
| **3921.8** | 52.5 |

Likewise, the data given in Table 5.8 shows that the temperature of maximum cohesion increases as the solar exposure increases. However, the changes are not clearly defined as it is not easy to see any particular trend in the data as solar exposure increases. This may be because the majority of the oxidation is occurring on the surface of the asphalt and these mechanical tests require the binder to be recovered from the asphalt. This process involves dissolving the bitumen into DCM and as a result of this the bulk bitumen, which has not been exposed to the natural weathering conditions, is mixed with the bitumen from the surface. Any oxidised bitumen from the surface has now been 'diluted' by the bulk bitumen. It could be the case that the Vialit pendulum test is not sensitive enough to detect a clear trend in the measured properties whereas the penetration and softening point tests are.

In light of this result it is essential that future work should be focussed on developing a mechanical test that can measure the deterioration of the surface of asphalt, and that the results from such a test could be used to determine the potential for fretting. Any further spectra that are collected can then be reliably linked to fretting potential.

## Summary

The results presented in this chapter allow a number of conclusions to be drawn.

The weather data collected highlights that the months between May-August are the hottest and have the most total UV exposure. In the years studied these also happened to be the wettest months. These conditions provide the optimum conditions for the oxidation of bitumen.

The 8-week naturally aged asphalt experiment (Chapter 5.3.1) shows a linear increase between the carbonyl absorbance band area and the absorbance at 1700 $cm^{-1}$ in the DRIFT spectra of the surface as the total solar exposure increases.

When this experiment is extended to 30 months, (Chapter 5.3.2) the measured absorbance at a fixed wavenumber (1700 $cm^{-1}$) increases as the total solar exposure increases. The increase in the height of this absorbance band indicates that the amount of carbonyl present in the bitumen at the surface of the asphalt is increasing with increasing solar exposure.

As this project is directed at producing a method that can be used on a vehicle travelling at traffic speed; intensity measured at a single wavelength data collection method such as the single wavelength analysis presented here could be of great use to the Transport Research Laboratory and Highways England in developing such a method. The data collection would be rapid and the use of multiple, single wavelength diodes could provide more data in order to calculate indices and ratios and also to indicate spectra that are contaminated and therefore not reliable.

The SEM of the naturally aged asphalt showed a higher number of contaminants present on the sample surface. These can be identified as dirt and pollen from plant matter that has been deposited by rainfall and air pollution, with the help of scanning electron microscopy. However, it was felt that these would have little bearing on the ageing of the sample. It is possible that contaminants such as water, oil based vehicle fluids and water based vehicle fluids may make some surface infra-red measurements more difficult to interpret and interfere with oxidation product absorbance bands identification. Therefore, visual road surface analysis should be carried out alongside or prior to, the spectroscopic analysis.

The scanning electron microscopy analysis also identified the presence of cracks developing on the surface of the bitumen. The surface structure no longer contained small platelet cracks but it does seem to be covered in a layer of natural contaminants that could be attributed to

dirt and pollen or plant matter. The development of larger cracks on the surface could be an indication of early failure and a point of weakness in the road surface.

The mechanical testing of the bitumen recovered from the naturally aged 30 month slabs recorded a decrease in penetration point and an increase in softening point: trends that are representative of the bitumen becoming more brittle and viscous at ambient temperatures.

The results of the Vialit pendulum test however contains a higher amount of error, therefore is less sensitive and the results from this test are less conclusive. There is, however, evidence that cohesion decreases as solar exposure increases. This lack of sensitivity may be because the bulk bitumen dilutes the oxidised surface bitumen making it difficult for the Vialit pendulum test to distinguish between the samples.

Collection of 64 infra-red spectra at 4 $cm^{-1}$ resolution can take between 30-60 seconds, depending upon the quality of the signal being received which is not a suitable time frame for a traffic speed data collection. Therefore a link should be explored between a number of different absorbance bands and their relation to the quality of the asphalt road surface. In this way a single-point infra-red method could possibly be developed for traffic-speed measurements.

## References


[1] British Standard EN 13074 2:2011, Bitumen and bituminous binders- Recovery of binder from bituminous emulsion or cut-back or fluxed bituminous binders. Stabilisation after recovery by evaporation.

[2] J. Zhang, A. K. Apeagyei, G. D. Airey and J. R. A. Grenfell, Influence of aggregate mineralogical composition on water resistance of aggregate-bitumen adhesion, Int. J. Adhe. Adhe., 62, 2015, 45-54.

[3] W. Zeng, S. Wu, J. Wen and Z. Chen, The temperature effects in ageing index of asphalt during UV ageing process, Constr. Build Mater., 93,2015, 1125-1131.

[4] R. E. Robertson, Chemical properties of asphalts and their relationship to pavement performance, Strategic Highway Research Program, Washington, DC, 1991, Research Paper

[5] J. A. H. Noguera, H. A. R. Quintana and W. D. F. Gomez, The influence of water on the oxidation of asphalt cements, Const. Build. Mater., 71, 2014, 451-455.

[6] ASCOM Carbonate and Chemicals manufacturing, Materials Safety Data Sheet, Calcium Carbonate, https://www.accm.com.eg/pdf/ACM_MSDS.pdf, ACCESSED 07.07.2018, 12:40

[7] P. Haines, P. G. Laye, S. B. Warrington, R. Heal, D. M. Price and R. Wilson, *Principles of Thermal Analysis and Calorimetry,* Royal Society of Chemistry, Cambridge, 2002, ISBN 0854046100.

[8] T. R. Crompton, *Thermal Methods of Polymer Analysis,* Smithers Rapra Publishing, United Kingdom, 2013, EBOOK ISBN 9781847356635.

[9] Mobil Brake Fluid DOT 4 ESP, Material Safety Data Sheet, Exxon Mobil, http://www.my-sds.co.uk/Admin/ViewDocument.aspx?ID=4db141e9-6443-42de-aa63-d8d68d55d2ef&primaryReportId=0, ACCESSED 07.07.2018, 13:03 .

[10] D. Stoye, "*Solvents", Ullmann's Encyclopaedia of Industrial Chemistry,* Weinheim: Wiley-VCH, 2005.

[11] Morphological characteristics of pollen, Radbound University Nijmegen, http://www.vcbio.science.ru.nl/en/virtuallessons/pollenmorphology/ ACCESSED 11.06.2018, 11:22.

[12] H. Lin, Z. Qu and J. C. Metedith, Pressure sensitive micro particle adhesion through biomimicry of the pollen-stigma interaction, *Soft Matter,* **12,** 2016, 2965.

[13] Nanoscience Instruments SEM gallery, https://www.nanoscience.com/products/sem/why-phenom-sem/gallery/, ACCESSED 11.06.2018, 12:01.

[14] W. Zeng, S. Wu, L. Pang, H. Chen, J. Hu, Y. Sun and Z. Chen, Research on Ultra Violet (UV) ageing depth of asphalts, *Constr. Build. Mater.*, **160,** 2018, 620-627.

# Chapter 6

## Spectroscopic analysis of road cores and live roads

The research presented in the previous chapters of this thesis has developed the use of diffuse reflectance infrared (DRIFT) spectroscopy for the analysis of asphalt that has been aged artificially and naturally. The results have led to the conclusion that oxidation products can be observed and quantified using DRIFT spectroscopy. These experiments however have been carried out using the ExoScan 4100, handheld spectrometer to collect data from bitumen and asphalt samples only in the laboratory.

The next logical step for this research is to use the handheld spectrometer to analyse live road samples. A live road is one that is still currently in use and open to traffic. Collecting DRIFT spectra from asphalt samples that are on the road network, will allow for a database of spectra to be developed and analysis of this data could be carried out to determine the link between the chemical signature and mechanical condition of the road surface.

The data collection from real roads has been approached in two ways for this research. The first method involves collecting DRIFT spectra from the surface of cores that have been collected from live roads and brought to the lab. Road cores are collected by TRL as part of other research projects being carried out on the live road network. The ExoScan handheld spectrometer has been used to analyse the topmost surface of these cores that has been exposed to natural weathering conditions and trafficking throughout its service life.

The second method involves taking the ExoScan outside the laboratory and collecting data from live roads. A trolley was designed by the engineers at TRL which supported the ExoScan at the correct focal distance from the road surface. The trolley was designed to be able to be pushed along a stretch of road and to collect DRIFT spectra at periodic locations.

## 6.1 Spectroscopic analysis of road cores

A number of cores from a variety of roads have been collected by the Transport Research Laboratory and some of these have been analysed with the ExoScan handheld spectrometer. The cores are cylindrical sections of the road taken at 90 degrees to the road surface, cut using a hydraulic coring rig. The collection of road core allows analysts to monitor and test thee different layers of the road, from the surface to the subgrade. The DRIFT spectra have been collected from the topmost surface of the collected cores, which has been exposed to the traffic and the environmental conditions.

Table 6.1 outlines the road that the cores have been collected from, how many cores have been analysed and the total number of spectra collected.

**Table 6. 1 Outline of the cores that have been analysed at the Transport Research Laboratory, their location and the number of cores form each site**

| Road location | Number of Cores | Total number of spectra collected from all cores |
|---|---|---|
| **M32** | 21 | 110 |
| **A264** | 10 | 74 |
| **A14** | 20 | 119 |
| **Scottish Cores** | 11 | 79 |

The DRIFT spectra collected from the cores listed in Table 6.1 have been plotted in the following figures (Figures 6.1-3). All spectra from each road have been plotted on the same spectra in grey, and the average of these spectra has been plotted in black.

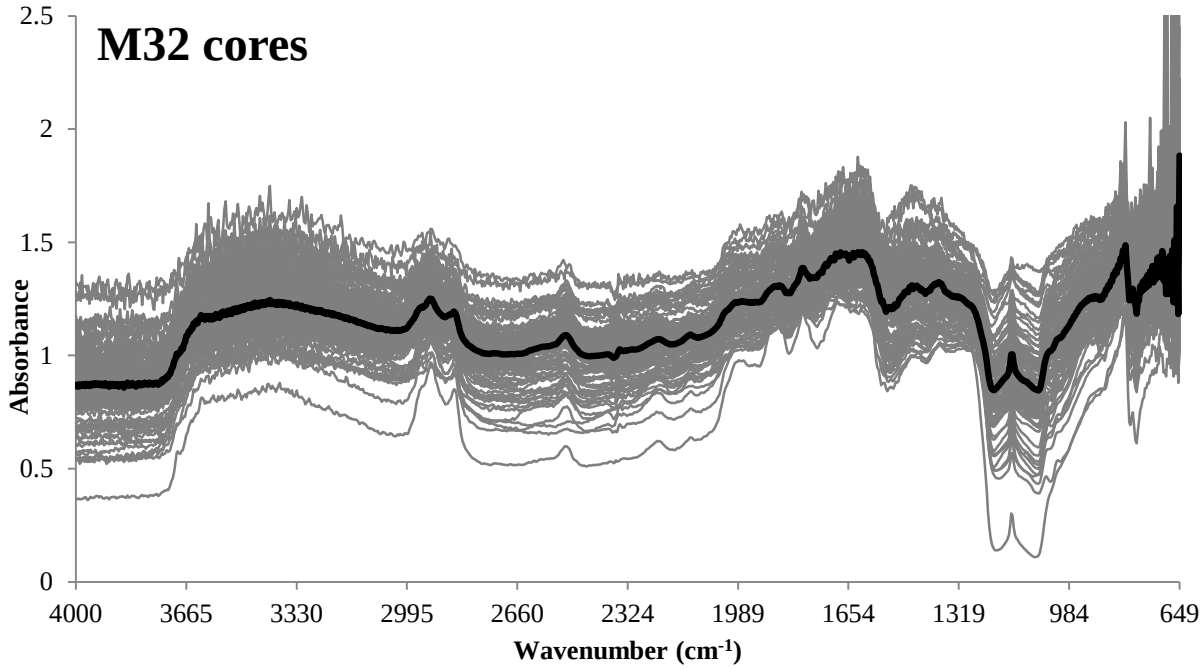


**Figure 6. 1 DRIFT spectra from the surface of cores collected from the M32**

110 individual spectra were collected from the cores sampled from the M32. The spectra from the M32 contain many of the absorbance bands seen in the naturally aged asphalt spectra (Chapter 5). The carbonate and silicate absorbance bands (2520, 1790, 1530, and 1150 $cm^{-1}$) are prominent in all 110 spectra collected from the different cores from the M32 road surface. This spectrum highlights the internal variation of a road surface. The difference in reflectivity can be seen between the samples with the 'baseline' absorbance at 4000 $cm^{-1}$ varying from approximately 1.35 to 0.35.

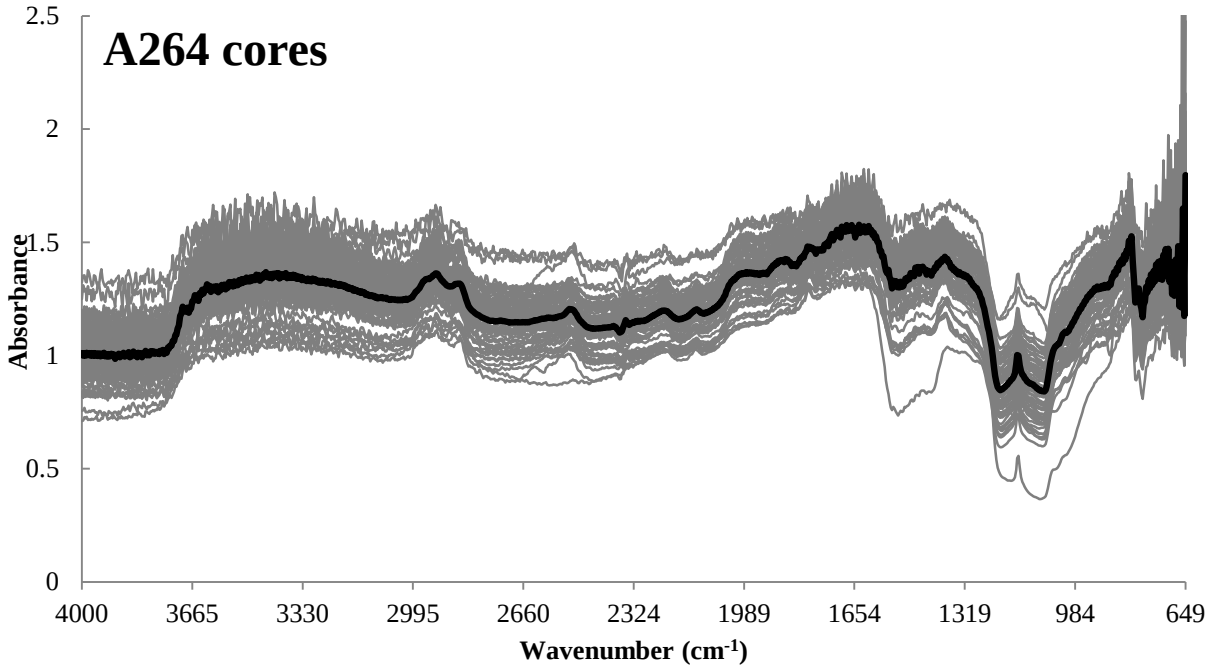


**Figure 6. 2 DRIFT spectra from the surface of a number of cores collected from the A264**

The spectra from the A264 cores contain a strong silicate absorbance band between the wavenumbers 1345-945 $cm^{-1}$. This is indicative of siliceous aggregates, granite and sand for example, present in this asphalt road surface. There are also some absorbance bands that correlate to carbonate, (2250, 1790, 1540, 1150 $cm^{-1}$) which are indicative of carbonate fillers and limestone aggregates. Each spectrum however is very similar in shape and contains the same absorbance bands. The differences arise again in the value of the 'baseline' of the spectra. The variation in this 'baseline' can be seen at 4000 $cm^{-1}$. This is indicative of a difference in overall infrared reflectivity of the sample, which may itself be indicative of ageing.

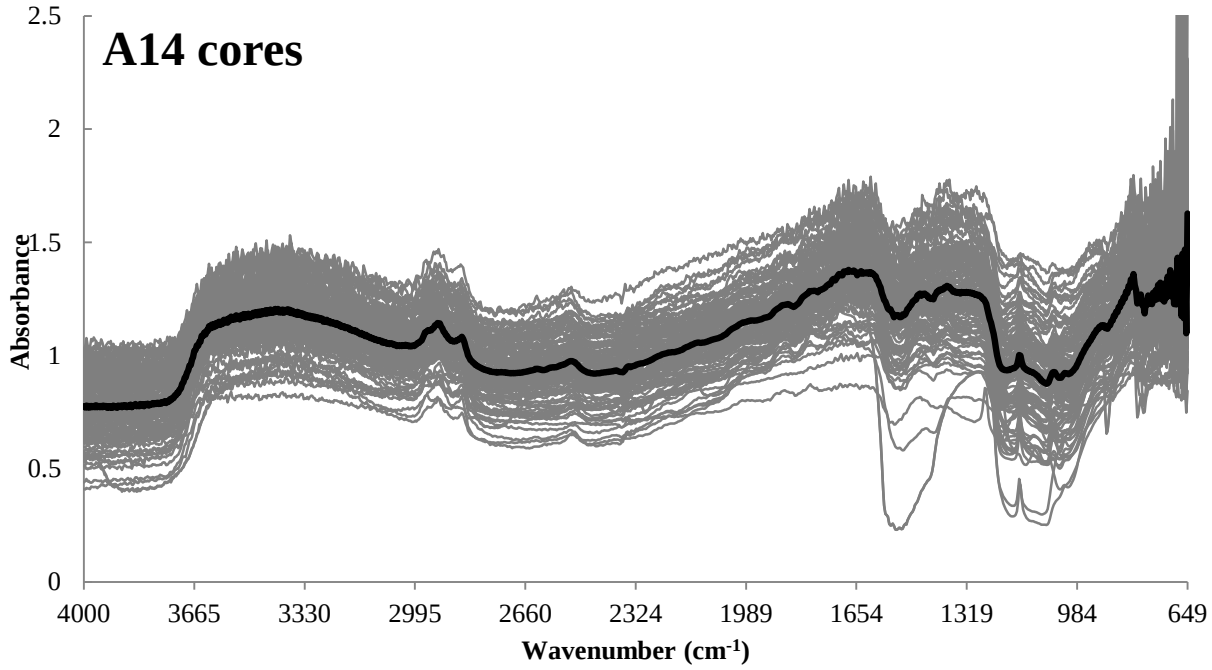


**Figure 6. 3 DRIFT spectra collected from the surface of a number of cores from the A14**

The spectra from the A14 cores show a similar signature to the A264 cores however there are a number of spectra that are quite different to the majority. There is a very strong absorbance band at approximately 1510 $cm^{-1}$ in some of the spectra. This corresponds to an absorbance band of the carbonate (Chapter 4). The difference in spectra highlights the local variation within the same road. Depending upon the location of the spectrum collection on the surface of the sample depends on what components will absorb and the spectra collected can be very different. For example if the spectrometer is focused on a piece of aggregate, the spectra collected will look very different to a spectrum that has been collected from bitumen.

Taking the average spectrum of all locations means that some spectral features are lost or reduced. The spectrum of the A14 cores in Figure 6.3 highlights the danger of taking multiple spectra from a stretch of road and averaging them all. For example the spectra collected that have strong aggregate absorbance bands present could indicate that there is exposed aggregate at that location, which could be an indication of loss of adhesion between the bitumen and aggregate and therefore an area where there is potential for fretting.

The spectra collected from the above cores are interesting and contain information about different road surfaces and their components. It is reassuring that there are a number of similar absorbance bands arising in all spectra with some variation in intensity in specific places. There is limited detail that can be obtained from these cores in terms of ageing and

oxidation over time as the age and condition of the roads that these cores have been taken from is unknown. It would therefore be difficult to reliably compare them.

There were, however, available at the Transport Research Laboratory a number of Scottish cores where the ages were known. A road site in Scotland has been monitored for a different project by TRL and therefore the age of the road when each core was collected is known. Samples were collected at 0, 2.9, 3.2 and 5.4 years of service life. This means that the chemical change over time can be measured using the DRIFT spectra collected.

Figure 6.4 contains the average spectra from each core.

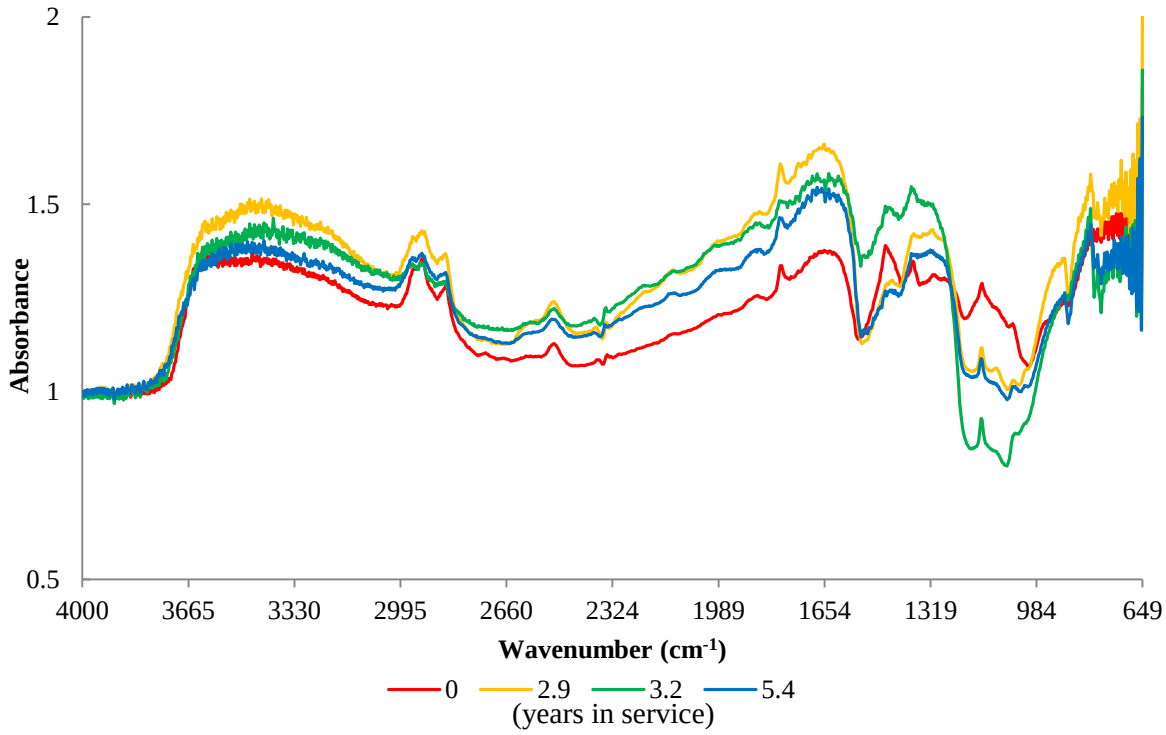


**Figure 6. 4 Normalised DRIFT spectra from the surface of Scottish cores that have been naturally aged for 0, 2.9, 3.2 and 5.4 years**

The spectra from the Scottish cores contain absorbance bands that can be assigned to the C-H stretching (2950, 2880 $cm^{-1}$) and the carbonate filler and siliceous aggregates (2510, 1790, 1530, 1160 $cm^{-1}$). It is interesting to note the similarity of these spectra to the spectra collected from the naturally aged asphalt (Figure 5.12). There is also a visible increase in the slope of the spectrum between the wavenumbers 2700-1530 $cm^{-1}$. These spectra can be analysed using the quantification technique outlined in the previous chapters for ageing asphalt, (Chapters 4 and 5). The absorbance value at 1700 $cm^{-1}$ has been recorded and plotted

in Figure 6.5 along with the absorbance value at 1700 $cm^{-1}$ from the DRIFT spectra from the naturally aged asphalt experiment outlined in Chapter 5.

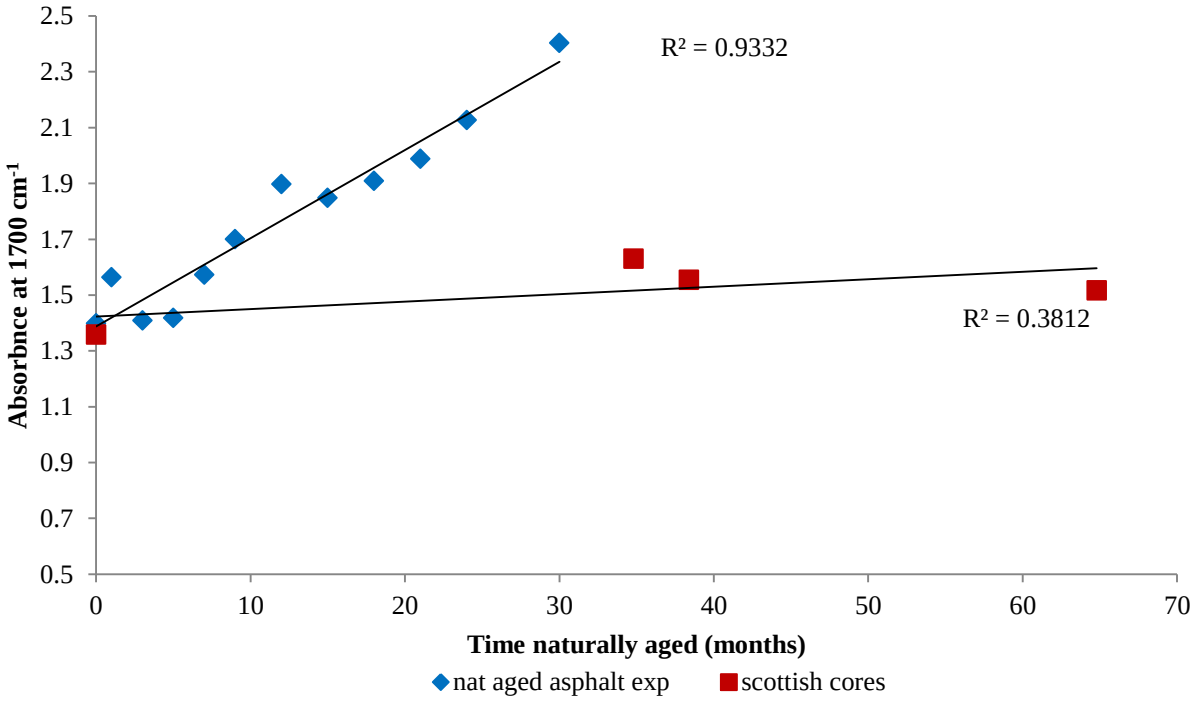


**Figure 6. 5 Absorbance value measured from the spectra collected from the surface of the Scottish cores (red) and the naturally aged asphalt experiment samples (Chapter 5) (blue)**

The Scottish cores (red) show a linear increase of 12% in the absorbance value measured at 1700 $cm^{-1}$ however this trend has a lower regression coefficient ($R^2$) than that of the naturally aged asphalt experiment (blue). The change in absorbance at 1700 $cm^{-1}$ is much lower for the Scottish cores than for the asphalt that was naturally aged in Crowthorne which saw a 72% increase in absorbance. There is a very dramatic difference in the steepness of these linear trend lines for each data set. It could be speculated that the 30 months chosen for the naturally aged asphalt experiment (August 2015-May 2018) have provided conditions that initiate oxidation more readily. For example there could have been a higher solar exposure, temperature and rainfall in Crowthorne throughout this time than in Scotland throughout the service life of the experimental cores. It is impossible however to know that this is the case as the weather data and the time that the cores were collected for the Scottish cores is not known. It is also worth noting that the Scottish cores have been collected from road sites that have been trafficked whereas the natural cores (Chapter 5) have not had any trafficking. This could be another reason for the difference in trend of absorbance at 1700 $cm^{-1}$. It is quite likely that oxidation products accompany a physical deterioration in the road surface. As such trafficking may physically remove this damaged surface, thereby removing the oxidised layer. Ideally

more research should be carried out on trafficked and non-trafficked samples to investigate this point further.

This experimental data is further evidence that highlights the fact that the time that the samples have been exposed to natural conditions is not the only factor affecting the amount of oxidation products on the asphalt surface, and in the case of the live roads, the change in oxidation products measured may not be a linear relationship with time.

## 6.2 Spectroscopic analysis of live roads

The spectroscopic analysis of the road cores has provided information about the appearance of DRIFT spectra of samples from genuine roads which have been trafficked. The next step is to take the ExoScan handheld spectrometer outside of the laboratory and to collect spectra from real live road surfaces. A trolley has been built by Andrew Hannay at the Transport Research Laboratory (Figure 6.6) which supports the spectrometer at its optimum focal distance from the asphalt. The spectrometer can be controlled using a PDA computer attachment that connects *via* Bluetooth to the spectrometer and spectra can be collected and saved to this device.

**Figure 6. 6 Photograph of data collection from South Road, Crowthorne, with the ExoScan 4100 and the trolley built at TRL**

The first experiment with this trolley was carried out in the car park of Crowthorne House, TRL headquarters. Spectra were collected every 1 metre for 16 metres. This was repeated three times with two different spectral resolutions, (1 and 64 $cm^{-1}$). The higher number of spectra that are collected and averaged at each location increases the signal to noise ratio,

making the resultant spectra clearer with less noise. However, the increase in the number of spectra collected at each location means a longer the time spent at each location. In order to develop this into a traffic speed method the time for data collection needs to be as rapid as possible and a balance needs to be found between spectral quality and data collection time. The spectra shown in Figure 6.7 have been collected using 64 scans per spectrum. The second set of data (Figure 6.8) contains spectra that have been recorded with only one scan per spectrum.

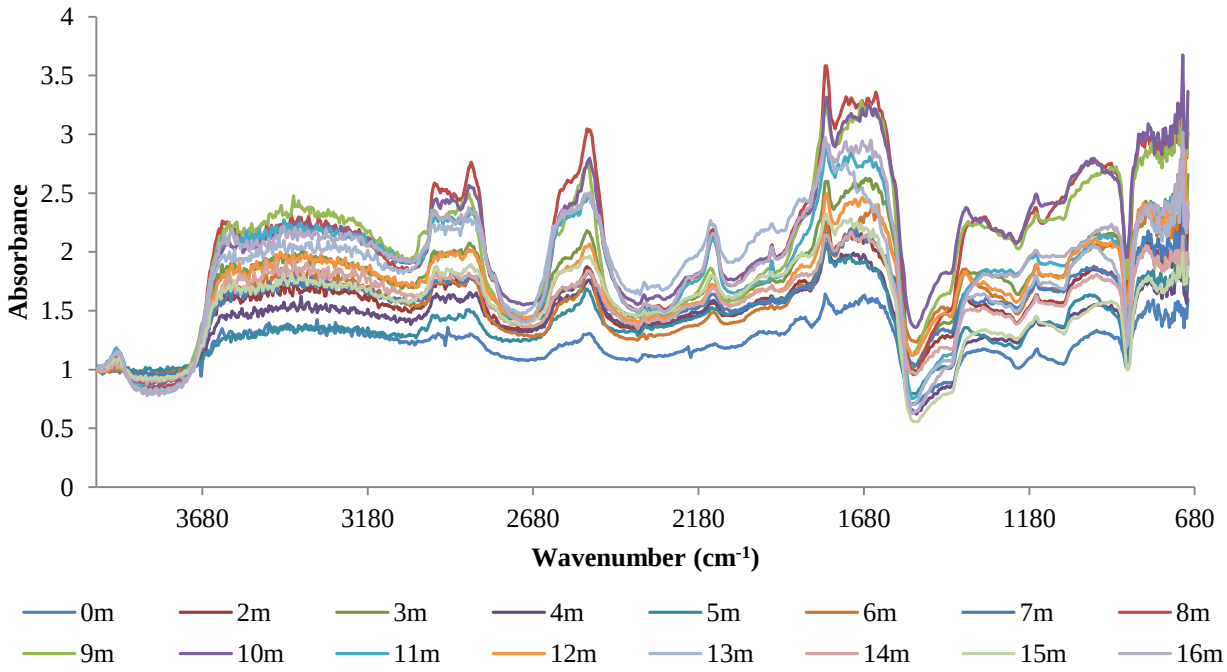


**Figure 6. 7 DRIFT spectra from a 16 metre stretch of the TRL car park, taken at 1 metre intervals, with 64 scans, 4 $cm^{-1}$ resolution being taken at each location.**

The spectra shown in Figure 6.7 contain a number of absorbance bands that correspond to carbonate (2520, 1790, 1532, 1155, 887 $cm^{-1}$). The car park surface structure was very open and coarse, and with a large amount of exposed aggregate. The exposed aggregate is likely the cause of the carbonate absorbance bands being dominant in the spectra. Without knowing the age of the car park surface, this data is not easily comparable to the other data collected. However this experiment has identified that the trolley is able to collect spectroscopic data from the road surface and this can be used to identify absorbance bands of the components in the asphalt.

It is interesting to note the variability in intensity of the carbonyl absorbance band region, between the wavenumbers 1760-1570 $cm^{-1}$. This is the area where the quantification has been carried out for monitoring the increase in carbonyl functional groups within the aged samples

(Chapters 4 and 5). A large amount of data collection is required to be able to determine to what extent the difference in peak intensity in this area is a result of local variability compared to changes in the physical condition of the road surface.

One of the issues faced when taking measurements using the trolley is the speed that the trolley can be moved to collect data. The time taken to collect 64 scans for each spectrum is between 20 and 60 seconds and therefore the trolley and spectrometer must be static for this period of time at each data point. By collecting a lower number of scans it would be possible to speed this collection time up. The spectra shown in Figure 6.8 are single scan measurements at each location.

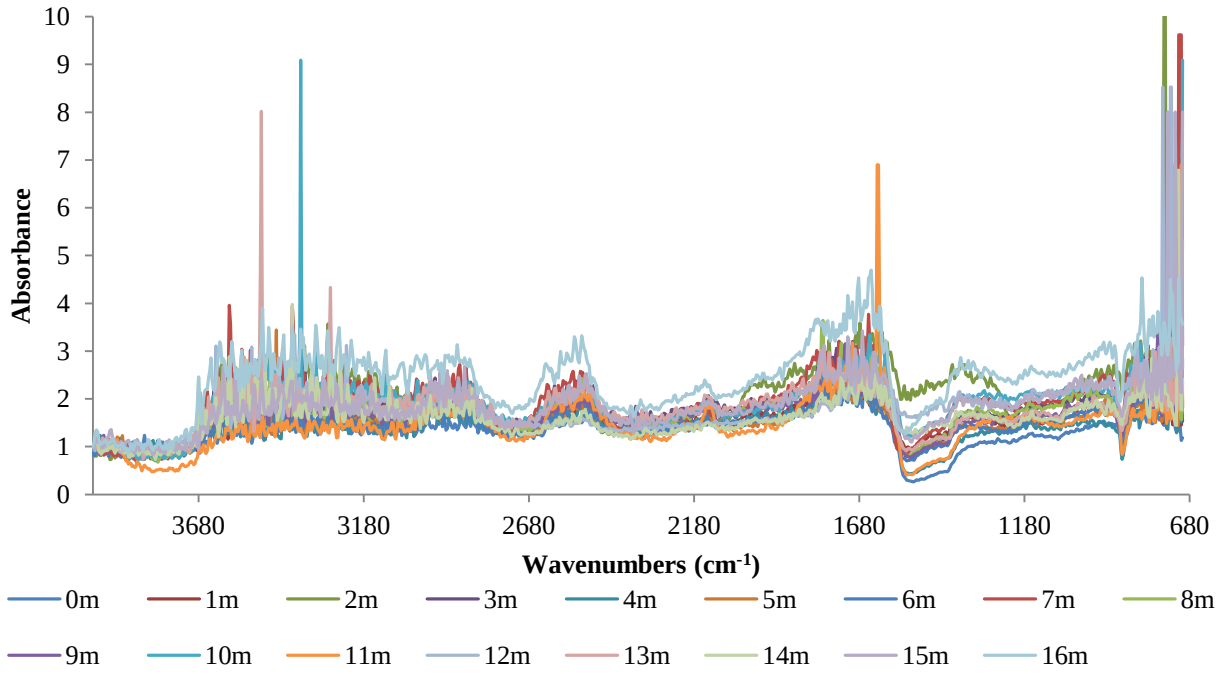


**Figure 6. 8 DRIFT spectra taken form a 16 meter stretch of the TRL car park taken at 1 meter intervals, with 1 scan at each location and 4 cm-1 resolution**

The DRIFT spectra presented in Figure 6.8 highlight the dangers of collecting a very low number of spectra per location. There is a very low signal to noise ratio and therefore it is very difficult to identify absorbance bands and measure their intensities reliably. There is a large amount of noise present in the wavenumber ranges between 3680-3120 and 1830-1570 $cm^{-1}$. This noise corresponds to regions where the absorption of water vapour in the air is strong and has been seen to be reduced when a higher number of scans are used. Unfortunately the carbonyl oxidation product absorbance band absorbs within the latter

wavenumber range and therefore it would be unreliable to attempt to use single scan spectra to determine the degree of oxidation by measuring the intensity of any band in this region.

However, the rapid collection of a single scan could be utilised at traffic speed. A moving survey vehicle could drive a stretch of road collecting a spectral data point every few metres which would probably appear rather like the single scans presented in Figure 6.8. It would, however, be possible to calculate an average spectrum of a limited area of the road surface with these single scans. The spectrum shown in Figure 6.9 is the average spectra calculated from the 16 single scan spectra collected from the 16 metre stretch of the TRL car park.

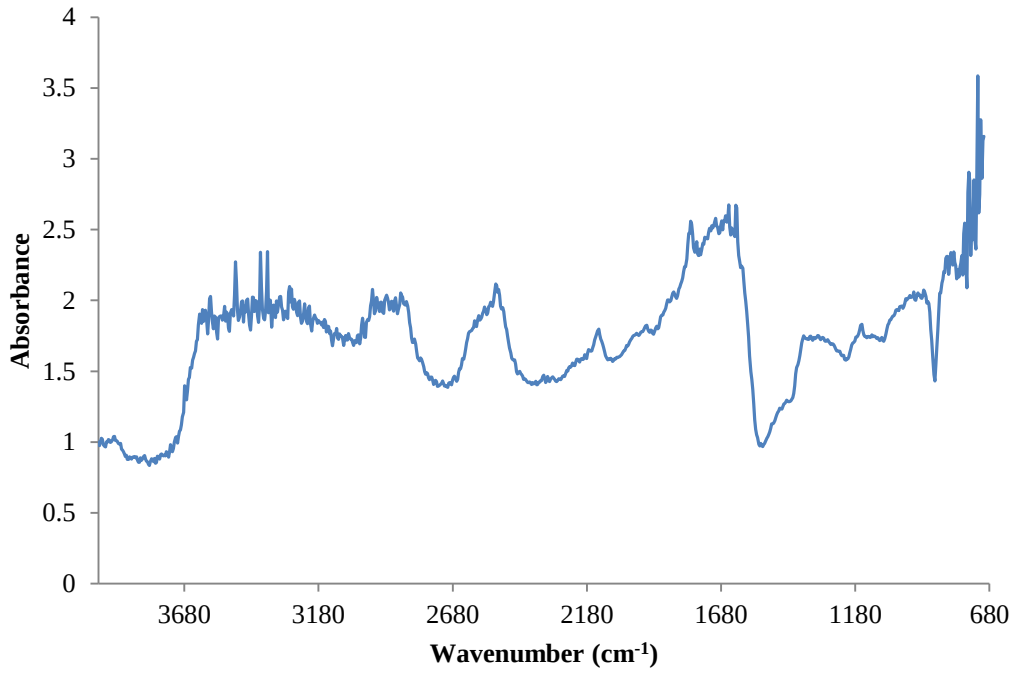


**Figure 6. 9 Average infrared spectrum calculated by averaging every 1 scan spectrum collected from the 16 metre stretch of the car park at Crowthorne House, shown in Figure 6.8**

A surprising amount of detail is obtainable from the average spectrum of the single scans. The signal to noise ratio has been dramatically increased and absorbance bands that correspond to carbonate aggregates are identifiable, (2510, 2130, 1790, 1530, 883 $cm^{-1}$). This is a positive result as it allows a reasonable quality spectrum to be produced from a number of single IR scans across a stretch of road. It must be noted; however, that large amount of data analysis and further data collection will be required in order to be able to reliably obtain a physical and chemical link from real road surfaces in this way.

The trolley was then used to analyse a stretch of road in Crowthorne called Wooden Hill (Figure 6.10). The spectra have been collected using the following parameters- 4 $cm^{-1}$ resolution, 64 scans.

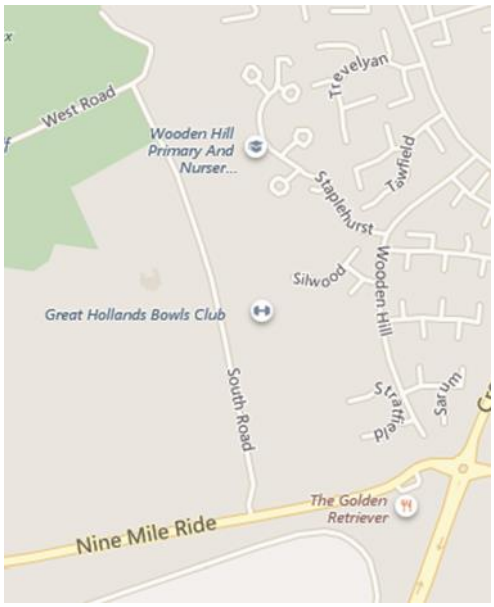


**Figure 6. 10 Bing Maps-Location of Wooden Hill in Crowthorne, UK**

Wooden Hill is a residential road leading to houses with no through road access; therefore it is lightly trafficked. As a result of this some spectra were able to be collected as the roads surface was in good condition. A 20 metre stretch of road was analysed with one spectrum being collected each metre. The results of this data collection can be found in Figure 6.11 (grey) with an average spectrum being calculated and plotted in black.

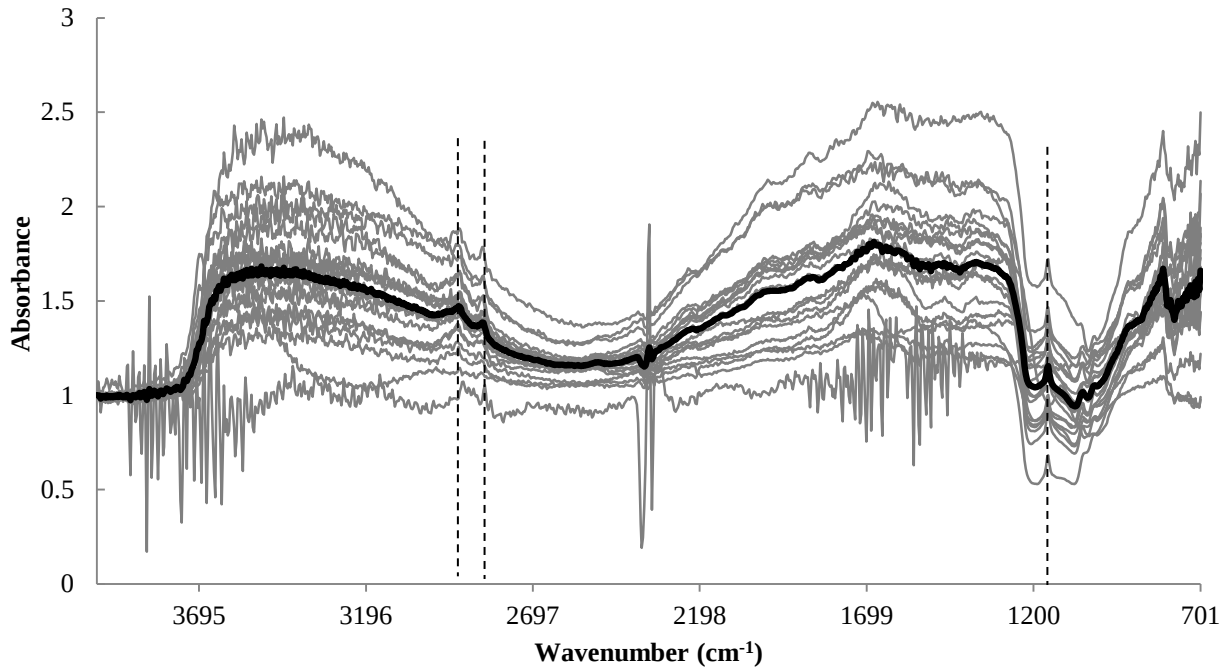


**Figure 6. 11 DRIFT spectra taken at 1 metre intervals along a 20 metre stretch of Wooden Hill road in Crowthorne**

The average spectrum shown in Figure 6.11 demonstrates the strong benefits of averaging the spectra collected along a stretch of road. It is possible to see one particularly noisy spectrum that is clearly affected by the carbon dioxide and water vapour in the air, however, the effect that this spectrum has had on the average is very little and the average spectrum has a good signal to noise ratio in the areas that correspond to water vapour and carbon dioxide absorptions. The average spectrum contains absorbance bands corresponding to the C-H of hydrocarbon bitumen and also the Si-O stretch of aggregates.

South Road was a second location that was used to collect some DRIFT spectra. South Road is located close to TRL headquarters, just off of Nine Mile Ride (Figure 6.10).

South Road has an extremely open texture with a high void content on the surface. South road leads to a golf club and a crematorium and therefore is trafficked more intensely than Wooden Hill and is made from a different type of asphalt material that has a larger texture depth. This made the collection of DRIFT spectra extremely difficult as the asphalt surface was not smooth enough for the ExoScan to successfully collect spectra at all points. No reliable spectra were collected on this occasion and therefore have not been presented in this report. This experiment highlights the difficulty of data collection from asphalt road surfaces. The ExoScan has been designed with a specific focal point at a set distance therefore the spectrometer will struggle to collect data outside of this focal point range. When designing

this technology to be at traffic speed there would need to be considerations regarding the focal ranges of the infrared light and the detectors.

## Summary

While much of the work presented in this chapter is speculative, there are a number of conclusions that can be drawn that are both positive and negative;

Good quality spectra are able to be collected from road cores and live roads that have been exposed to genuine road surface conditions. The carbonate and silicate absorbance bands of the aggregates can be identified confidently.

Collecting good quality spectra requires a high scan count to achieve a good signal to noise ratio, which takes time requiring the spectrometer to be static. However, good quality spectra can also be produced from single scans collected along a stretch of road which are then averaged.

Care must be taken when averaging multiple spectra from a stretch of road as there might be localised detail that is being missed. Many more spectra need to be collected in this way from roads with varying conditions in order to determine the effect of this averaging in more detail.

A change in reflectivity can also be seen in the un-normalised spectra. This base reflectivity of infrared light might be an indicator of ageing, and is therefore worth investigating in the future work.

It has not been determined reliably within this work whether the change in oxidation products can be identified in the DRIFT spectra from ‘real’ road surfaces. Much more data collection on road surfaces with known condition and age is required to make this assignment confidently. The eroding of the bitumen from the surface of the asphalt surface might be the reason for this lack of carbonyl absorbance band. The oxidation of the surface layers would increase the viscosity, and repeated trafficking would wear this more brittle layer away. This means that the carbonyl absorbance band detected is less intense than if the oxidised bitumen remained on the surface.

# Conclusions and further work

The research presented within this thesis allows for a number of conclusions to be drawn:

### *Artificially aged bitumen-E-RTFO test*

The literature review carried out for this project identified the lack of research using diffuse reflectance infrared spectroscopy for the analysis of bitumen oxidation in asphalt.

The investigation was started by looking into the artificial and natural ageing of bitumen. This involved the E-RTFO test, UV light exposure and natural ageing of the bitumen samples on the roof of Crowthorne House.

The E-RTFO test oxidised the raw bitumen and oxidation products were detected using ATR-FTIR. Carbonyl, C-O and sulfoxide absorbance bands were identified and quantified from the ATR spectra. An increase in the integrated absorbance band area and absorbance at 1700 $cm^{-1}$ were measured as time in the E-RTFO increased.

The GPC results from the thermally aged bitumen showed an increased in molecular weight that corresponded to an increase in oxygen within the bitumen composition.

The mechanical properties of the E-RTFO test aged bitumen were measured and showed an increase in viscosity of the bitumen as it was aged. The penetration point decreased (-70 %), the softening point increased (+30 %), the maximum cohesion decreased (- 34 %) and the intrinsic viscosity of the samples increased (33 %) as time in the RTFO increased.

### *Artificially aged bitumen-UV light exposure*

The UV-aged bitumen has been analysed using DRIFT spectroscopy. The reflectance spectra collected from the surface of the UV aged bitumen contained absorbance bands that correspond to the carbonyl, C-O and sulfoxide functional groups. The C-O band is very broad which is indicative of some intermolecular hydrogen bonding. The carbonyl absorbance band presents as a first derivative. This band was initially detected between 72-96 hours of UV ageing. The presence of first derivative absorbance bands in reflectance spectra is indicative of a surface structure property giving rise to specular reflectance and of refractive index change.

Upon UV exposure a brittle skin was formed on the surface of the bitumen. The brittle skin was measured with the penetration point test and results proved that the skin was much more difficult to penetrate (-29 % penetration point) as the sample was exposed to a longer time in the UV chamber. The skin was also analysed with SEM and small cracks forming platelets, were visible on the surface of the UV exposed bitumen. The formation of this skin could be attributed to molecular stacking of the oxidised asphaltene molecules within the bitumen composition.

The UV aged bitumen samples needed to be heated in order to prepare the samples for the mechanical property tests. This heating meant that the surface skin was melted and mixed into the bulk. The mechanical test results were then inconclusive, with no reliable change being measured between samples. This suggests that the thermal energy being applied to the bitumen has broken down the intermolecular interactions occurring within the oxidised bitumen on the surface, and therefore reversing any viscosity changes.

The GPC, softening point, Vialit pendulum test and the intrinsic viscosity results of the UV aged bitumen are also inconclusive with no reliable change being measured. This could again be a result of the intermolecular forces being broken down as the surface sample is heated, mixed and dissolved into solution.

The ageing effects of UV exposure is localised on the surface of the bitumen as a result of the UV light only penetrating the first 4.5 μm of the sample.[1] There is also the possibility that singlet oxygen is an initiator of the UV initiated oxidation and this species can only be formed on the surface, where there is exposure to molecular oxygen and UV light.

***Naturally aged bitumen***

Similar chemical and mechanical test results have been obtained for the raw bitumen samples that have been aged naturally as for those that were aged artificially. DRIFT spectroscopy detected carbonyl, C-O and sulfoxide absorbance bands; the C-O band is broad, indicating molecular interactions within the bitumen composition. A skin also develops on the surface which is similar to that seen on the artificially UV-aged bitumen. The presence of this skin and the increase in oxidation product functional groups in the DRIFT spectra prove that the bitumen has been oxidised by the natural weather conditions, and that these conditions have induced a physical change in the surface structure and molecular network of bitumen hydrocarbon molecules.

SEM of the naturally aged surface indicated the same micro-cracks forming on the surface as in the artificially UV-aged bitumen, with small platelet features being produced.

GPC results showed no definitive change in molecular weight of the bitumen composition and intrinsic viscosity is seen to increase as the sample is aged. This could be a result of the molecular stacking and intermolecular interactions holding together the brittle, oxidised surface skin being broken down as the bitumen is dissolved into solution. However repeats of this experiment are required in order to support this result.

***Artificially aged asphalt-UV light exposure***

The DRIFT spectra collected from artificially UV-aged asphalt have been used to identify the absorbance bands from the carbonate filler and the siliceous aggregates. Upon exposure to UV light the reflectance spectra have also been used to identify oxidation products. The carbonyl, C-O and sulfoxide absorbance bands have been identified and the changes in the carbonyl absorbance band have been quantified as the sample is aged. The increase is steep during the first week of exposure in the UV chamber and following this time the absorbance is seen to plateau. This could be an indication of the surface becoming completely oxidised or reaching the maximum level of oxidation under the conditions of the experiment.

The carbonyl absorbance band also presents as a first derivative in the reflectance spectra from the asphalt. The surface was analysed with SEM (530 x) and micro-cracking platelet formation was observed. It is also possible to see some of these cracks with a light microscope suggesting that the cracks are able to propagate into larger cracks that are visible at lower magnifications.

Infrared microscopy of a cross section of UV-aged asphalt has identified different absorbance bands that could be used to differentiate between spectra that have been collected from aggregates from those collected from bitumen. The infrared microscope does not work at a small enough spatial resolution to differentiate between the oxidised surface layers and the bulk bitumen below. To achieve a better spatial resolution experiments using an infrared microscope with a much brighter Synchrotron source, such as the Diamond Light Source, could have been carried out. Such experiments were unfortunately impossible on the time scale of this project.

### *Naturally aged asphalt*

The conditions used for the natural ageing of asphalt showed that throughout the 3 years recorded for this project (2015-2018), the summer months (May-Aug) had the highest temperature, rainfall and UV light exposure. The DRIFT spectra collected from the surface of the naturally aged asphalt showed a linear trend in the absorbance measured at 1700 $cm^{-1}$ and the total solar exposure.

The quantification of the carbonyl absorbance band from the DRIFT spectra collected from the surface of the naturally aged asphalt has identified an increase as the total solar exposure increases. This has been carried out using single wavelength analysis at 1700 $cm^{-1}$. Single wavelength analysis is a rapid method for quantifying absorbance bands and could be an efficient traffic speed detection method. By comparing the difference between two single wavelengths could increase the reliability of the size of the absorbance band by allowing comparison to a 'baseline'.

The analysis of the surface of the naturally aged asphalt showed a large amount of surface contamination. This could be sediment from rain water evaporation and pollen from nearby plants. Cracks were also visible in the bitumen regions on the surface of the naturally aged asphalt, which could be the result of micro-cracks propagating into larger cracks on the surface of the asphalt.

Mechanical property testing on the bitumen that was recovered from the naturally aged asphalt slabs was carried out. The tests measured a 40 % decrease in penetration point, a 13 % rise in softening point and a 13 % decrease in maximum cohesion after the 30 months of natural ageing. However the last of these values is unreliable and should be supported by further mechanical testing of the asphalt. These tests require the bitumen to be recovered from the asphalt sample and therefore might be misleading with regard to the surface structure of asphalt and the likelihood of the surface of an asphalt sample to fret.

### *Real road analysis-Cores and live roads*

The analysis of real road surfaces has been carried out using a trolley built specifically to hold the ExoScan handheld spectrometer at the appropriate distance from the road surface. Spectra were collected that contain similar absorbance bands to those collected in the laboratory based experiments. Carbonate and silicate absorbance band have been identified. The spectra collected highlight the internal variability of the same road surface.

Data collection was carried out on the car park of the Transport Research Laboratory, at different scan rates and a big difference in signal to noise was recorded with 64 scans, giving good quality spectra at each location while 1 scan gave very poor spectra with a low signal to noise ratio. The averaging of these 16, 1 scan spectra produced a very good quality spectrum, however, repetition of this type of averaging is required in order to determine the effect of the averaging on localised differences. This point needs to be considered when moving forward towards collecting data from roads at traffic speed.

A series of Scottish cores were collected at known stages within the life span of the road and therefore could be analysed for a chemical change with age more reliably. However, simply measuring the time that a sample has been aged does not give a full picture of the exposure conditions such as total solar exposure and trafficking. This was highlighted in the results obtained from naturally aged asphalt which were presented in Chapter 5, where ageing was related to the total solar exposure and not the total time of ageing. Another difference between the lab based experiments and the experiments on cores from real roads is the effect of trafficking on the asphalt. The lower change in absorbance at 1700 $cm^{-1}$ could be as a result of trafficking eroding the brittle, oxidised bitumen on the surface of the asphalt.

### *Future work*

Further work for this project could involve collecting many more spectra from roads that have a known age and of varying condition. This needs to be done extensively, and it is imperative that the age is known. The ‘age’ of the road would include details about when the road was first laid, along with any rejuvenation and resurfacing works that have been carried out on the road throughout its service life. This would allow analysts at TRL to identify a chemical change in the spectra that can correlate to physical condition or age of the road surface.

Collection of spectra from roads that are in a poor physical condition will allow these to be compared to newer road surfaces. This comparison would allow the analyst to identify the chemical markers that are consistent with a poor road condition.

Once a database of spectra has been collected, data analysis needs to be carried out in order to try and correlate the mechanical properties of the asphalt to the chemical signature. This could be done with single wavelength analysis, intensity ratios of two or more fixed wavenumbers and calculation of indices, or baseline reflectivity measurements.

Single wavelength diodes could be used to target specific wavenumbers and can be used to collect absorbance data from the road surface for specific functional groups. By comparing this absorbance data to the condition of the road, a potential failure marker could be developed. If such an experiment is successful it then needs to be trialled extensively at traffic speed to ensure the reliability of data collection and the accuracy of the results.

A mechanical test needs to be developed that will measure the fretting potential of the asphalt. This test could be a variation of a shear test,[2] which works by measuring the force required to shear the surface layers from the lower layers, or a pull off test which measures the force required to pull an aggregate from the surface.[3] Both of these methods have different issues that make them unsuitable therefore development of a suitable test that is reliable and represents the type of failure that the asphalt road surface would experience.

## References

[1] W. Zeng, S. Wu, L. Pang, H. Chen, J. Hu and Y. Sun, Research on ultra violet (UV) ageing depths of asphalts, *Constr., Build Mater.,* **160,** 2018, 620-627.

[2] British Standard 1377-7 (1990). Methods of test for soils for civil engineering purposes – Part 7: Shear strength tests (total stress), BSI, London.

[3] J. Zhang, A. K. Apeagyei, J. Grenfell and G. D. Airey, Experimental study of moisture sensitivity of aggregate-bitumen bonding strength using a new pull-off test, in the *8th RILEM International Symposium on Testing and Characterisation of Sustainable and Innovative Bituminous Materials*, RILEM Book Series 11, DOI 10.1007/978-94-017-7342-3_58.